Deciphering of flavescence dorée phytoplasma adhesion to cells of its insect vector

Francesca Canuto

THÈSE PRÉSENTÉE

POUR OBTENIR LE GRADE DE

DOCTEUR DE

L'UNIVERSITÉ DE BORDEAUX

ÉCOLE DOCTORALE SCIENCES DE LA VIE ET DE LA SANTÉ

SPÉCIALITÉ MICROBIOLOGIE - IMMUNOLOGIE

Par Francesca CANUTO

Décryptage de l'adhésion du phytoplasme de la flavescence dorée aux cellules de son insecte vecteur

Sous la direction de : Xavier FOISSAC

Soutenue le 07/12/2023

Membres du jury :

Mme BÉBÉAR Cécile, Professeur-PH à l'Université de Bordeaux	Présidente du jury
Mme BRAULT Véronique, Directrice de Recherche, INRAE Colmar	Rapporteur
Mme MARZACHì Cristina, Directrice de Recherche, IPSP-CNR Turin	Rapporteur
M. SAUVION Nicolas, Ingénieur de Recherche, INRAE PHI-CIRAD Montpellier	Examinateur
M. FOISSAC Xavier, Directeur de Recherche, INRAE Bordeaux	Directeur de thèse

Remerciements & Ringraziamenti

Remerciements & Ringraziamenti

Je tiens à remercier Madame le Docteur Véronique Brault pour avoir accepté le rôle de rapporteur de ma thèse. Merci encore pour les conseils donnés au cours de mon comité de mi-thèse qui ont énormément aidé au déroulement et à l'avancement de ce projet.

Ringrazio la Dottoressa Cristina Marzachì per aver accettato di prendere parte alla mia commissione di Tesi di Dottorato e di valutare il mio manoscritto e il mio lavoro.

Merci beaucoup Madame le Professeur Cécile Bébéar et Monsieur le Docteur Nicolas Sauvion pour avoir accepté de faire partie de mon jury de thèse et d'évaluer mon travail.

Un grand merci à Stéphane Claverol de la plateforme Bordeaux Protéome pour son assistance technique dans le cadre des analyses de spectrométrie de masse effectuées au cours de ce projet.

Je tiens à remercier, du fond de mon cœur, les deux mentors qui m'ont accompagnée dans ce parcours de thèse, Xavier et Nathalie. Xavier, merci pour avoir dédié autant de ton temps et de ton énergie à ce projet et à mon parcours de doctorante. Ton intégrité et ta façon de voir les choses seront toujours une inspiration pour moi. Nathalie, merci pour tout. J'ai énormément apprécié échanger avec toi, et j'espère avoir appris au moins un peu de ta façon de travailler. Ta rigueur et ta passion sont pour moi un exemple à suivre et à viser.

Un grand merci à toute l'équipe Molli pour l'accueil et pour avoir toujours mis de la bonne ambiance dans ce qui est censé être juste un lieu de travail. Ça n'aurait jamais été pareil sans votre présence. Pour n'oublier personne, je parcours encore une fois ces couloirs où j'ai mis longtemps à m'orienter.

Je commence donc par remercier les vraies cheffes, Annie, Isa, Sonia et Laurence pour les fous rires en pause-café aussi bien que pour votre professionnalité.

Merci à Sybille, MPi, Christophe, Sylvie, pour le soutien et les échanges autant professionnels que personnels. Un grand merci à Laure pour ta disponibilité et ton support (intellectuel et matériel) dans la relation compliquée entre la biochimie et moi. Merci à Alain, Marielle, Thierry, Denny, Laure, Pascal, Sophie, Enora et Sandrine. Une pensée pour Sandra, Emilie et Mathilde aussi, qui sont maintenant parties rejoindre d'autres chanceuses équipes.

Je passe maintenant là, « o buro' » où tout a commencé. Je vais faire court car sinon l'un va chialer et l'autre va être gêné mais merci Arthur et Bastien pour avoir été là. C'était grave cool.

Je descends les escaliers une dernière fois pour remercier Fabi et Le Juj pour toutes les conneries, les bonne nouvelles et les galères que nous avons partagées pendant ces années. Il ne sera jamais plus 15h sans que je pense à vous et sans regretter un petit peu le fait que vous ne soyez pas là pour « bitcher » avec moi le temps d'une pause.

Et il ne faut pas oublier nos cinq petits derniers, Marie, Julien, Patrick, Yorick et Julien (oui, encore). « On aurait pu être des frères » mais, comme il dit Juj, « on n'est que… ». En vrai, merci pour tous les bons moments passés ensemble.

Merci à notre chef d'équipe, Pascal. Merci à Carole pour ta gentillesse et le cœur que tu mets dans tout ce que tu fais (ça se voit de très loin!).

Un mot à part pour GG, l'une de meilleures personnes que j'ai rencontrée sur ma route. Je te souhaite tout le mieux pour le futur et j'espère que nos chemins pourront se recroiser même en dehors du bureau qui m'a si bien accueilli pendant la deuxième partie de ma thèse. Merci pour tout.

Je passe à la laverie pour faire un bisou à Martine, qui cache sous l'écorce un cœur fondant. A bientôt, dans les Pyrénées!

C'est au coin café que je retrouve ma team Tupperware® préféré. Merci Claire et Yoyo pour tous les moments (et les recettes) partagés, autant que pour tout le reste.

And last but not least, merci à deux ex-molli qui gardent toujours un petit bout de mon cœur, Gab et Toto (on va pas se mentir, surtout Gab!).

Comment oublier la petite Schlo! C'était un plaisir de te connaitre et de te voir un peu grandir. Je te souhaite tout le mieux pour la suite!

Merci à Gaëlle pour toutes les magnifiques illustrations dont tu m'as fait cadeau. Je suis sûre que ton talent et ta gentillesse vont t'amener là où tu désires.

Merci à Loïse pour la grimpette, la psychanalyse et tous les sourires partagés.

Merci à Ninon pour ta folie et ta tendresse.

Merci à Paola pour les bières, les discussions et pour les après-midi avec les pieds dans l'océan.

Beaucoup des gens mentionné ci-dessus mérite bien plus des mots pour décrire l'importance de leur présence pendant ces trois incroyables années. Et je vais les trouver, au bon moment, avec quelques bières dans le corps pour repousser les larmes.

Bon, ok, on va quand même rajouter quelques mots pour Arthur, car dès le début il a été une présence fondamentale dans mon quotidien. Les moments que nous avons partagés font partie de mes meilleurs souvenirs de cette période à Bordeaux. Tu as connu aussi bien mes moments d'enthousiasme que mes démons et j'ai vite arrêté de compter les fois où j'ai pensé « heureusement qu'il est là! ». Donc, merci pour avoir été là jusqu'ici et merci d'avance pour les jours à venir.

Merci à Monique, Marielle et le petit tornade Marin. Je laisse un peu de mes racines ici avec vous, où je me sens chez moi même a mille kilomètres de là d'où je viens.

Grazie ai miei Amici, per la certezza che sanno essere anche quando siamo lontani e per quella sensazione da mattina di Natale che mi prende ogni volta che abbiamo la fortuna di re-incontrarci in qualche parte di mondo.

Grazie alla Ceci, grande acquisto di questa campagna, che sono certa mi accompagnerà ancora per un bel pezzo in questo viaggio.

Grazie ad Antonio per questi anni di supporto, Amore e ragù. E per tutto quello che ne rimarrà.

Dulcis in fundo, grazie dal profondo del cuore a Irene, Bruno, Marco e Alessandra.
Per prendersi cura, da sempre, della mia felicità.
Per aver supportato (e sopportato) la mia lontananza di questi anni.
Per avermi accolto ad ogni ritorno con un grande sorriso e le braccia aperte, ricominciando tutto come se ci fossimo lasciati il giorno prima.
Siete il mio porto sicuro, la mia buona ragione per tornare a Casa.

Table des matières

***Résumé**: Décryptage de l'adhésion du phytoplasme de la flavescence dorée aux cellules de son insecte vecteur* 5

***Summary**: Deciphering flavescence dorée phytoplasma adhesion to its insect vector cells* 8

Formations suivies 9

List of publications 10

List of communications 11

List of abbreviations 12

Reagents 14

Genes 15

Species 16

List of Tables and Figures 17

Tables 17

Figures 17

General introduction 20

1. Discovery, characterization, cellular and molecular properties of phytoplasmas 21

1.1. Discovery and initial characterization of phytoplasmas 21

1.2. Phytoplasma classification 22

1.3. Transmission and prophylactic control of phytoplasma diseases 23

1.4. Phytoplasmas genome features 24

2. Flavescence dorée 27

2.1. Symptomatology 27

2.2. Surveillance and control 29

2.3. Epidemiology, ecology and genetic diversity of flavescence dorée phytoplasmas 29

3. Phytoplasma interaction with hosts 33

3.1. Phytoplasma interaction with plant host 34

3.2. Interaction of phytoplasmas with the insect host 36

4. Adhesion of bacteria to eukaryotic cells and entry 40

4.1. Membrane proteins of phytoplasmas and interaction with insect vectors 44

4.2. The pathogen-host interface as target to cope with vector-borne diseases 48

5. Aim of the work and experimental outline 51

Materials and Methods 53

1. Insect rearing, cell lines and bacteria 54

2. Identification of *E. variegatus* proteins interacting with VmpA 55

2.1. Purification of VmpA-*E. variegatus* proteins complexes on affinity column 55
2.2. Far-western blot analysis 56
2.3. Mass spectrometry analysis (nLC-MS/MS) 58
2.4. Database search and results processing 58
3. Setting up of a simplified system *ex vivo* 60
3.1. Cloning of *E. variegatus* CDS 60
3.2. RNA interference on Euva-11 cells, RNA extraction and mRNA analysis 61
3.3. Adhesion assays of VmpA-His_6-coated beads to Euva cells 61
3.4. Immunofluorescent staining and microscopic observations 62
4. Assessment of uk1_LRR expression on *E. variegatus* 63
5. Yeast Two-Hybrid 63
5.1. Bait clone preparation for yeast two-hybrid 63
5.2. Prey library preparation for yeast two-hybrid 64
5.3. Two-hybrid library screening using yeast mating 65
5.4. Rescue of the prey plasmid 66
5.5. Yeast colony PCR 68
5.6. Yeast transformation 69
5.7. Yeast proteins extraction 70
5.8. Western Blot analysis 71
5.9. Prey proteins sequences analysis 71
6. Statistical analysis 72
Chapter 1 - Looking for VmpA receptors in *Euscelidius variegatus* 73
1. Justification of the experimental strategy 74
2. Results 77
2.1. Selection of Euva proteins interacting with VmpA collected through affinity column 77
2.2. Selection of transmembrane Euva proteins interacting with VmpA using far-western blot interaction assay 78
2.3. RNAi knock-down gene expression on Euva cells 78
2.4. Simultaneous multiplexing RNAi on Euva cells 79
2.5. Adhesion assays to Euva cells of VmpA-coated beads 80
2.6. Characterization of the uk1_LRR gene 81
2.7. Assessment of uk1_LRR expression in *E. variegatus* 82
2.8. Far-western blot VmpA FD92 vs PGYA 83
2.9. Adhesion assays on Euva cells using VmpA_PGYA coated beads 83
Chapter 2 - Yeast Two-Hybrid 84
1. Justification of the experimental strategy 85

2. Results 86
2.1. Yeast Two-Hybrid 86
2.2. Rescue of the prey plasmids 87
2.3. Yeast retro transformation 88
2.4. Western blot and insert sequences analysis 88
Discussion 90
1. Looking for VmpA glycoprotein receptors in *Euscelidius variegatus* 92
2. Search for insect vector protein-VmpA interaction by yeast two-hybrid screening 99
Conclusions and perspectives 104
References 109
Annexes 126

Résumé

Décryptage de l'adhésion du phytoplasme de la flavescence dorée aux cellules de son insecte vecteur

La flavescence dorée (FD) est une maladie de la vigne provoquée par un phytoplasme transmis par la cicadelle *Scaphoideus titanus*. Elle affecte désormais de nombreuses régions viticoles en Europe du sud. Mieux comprendre l'interaction phytoplasme-insecte vecteur pourrait aider au développement de techniques innovantes pour contrôler les épidémies de FD. Le mécanisme de colonisation des tissus de l'insecte vecteur par le phytoplasme n'a pas encore été décrypté mais il a été démontré que la protéine de surface VmpA du phytoplasme FD est une adhésine qui intervient dans les étapes précoces d'adhésion aux cellules du vecteur. La protéine VmpA interagit avec les résidus N-acetyl-glucosamine et mannose portés par les glycoprotéines membranaires de l'insecte vecteur et ses variations de séquence sont corrélés à la capacité de vection par *S. titanus*. Dans ce contexte, l'objectif de mon projet de thèse était d'identifier les protéines d'insecte interagissant avec la VmpA.

Les protéines des cellules en culture de l'insecte vecteur *Euscelidius variegatus* (cellules Euva) interagissant *in vitro* avec la protéine recombinant VmpA-His_6 ont été identifiées par spectrométrie de masse. Treize protéines candidates ont été selectionnées en raison de leur proprietés d'interaction avec la VmpA, de la présence dans leur séquence de sites potentiels de N-glycosylation et de segments transmembranaires compatibles avec leur localisation à la surface des cellules. L'étape de validation de l'interaction avec la VmpA a consisté à mesurer l'effet de la baisse de l'expression de ces gènes provoquée par ARN interférence (RNAi) sur l'adhésion de billes fluorescentes recouvertes de VmpA aux cellules Euva. Cette technique de RNAi a été utilisée pour inhiber simultanément l'expression de douze gènes, tout en gardant un niveau d'inhibition comparable à celui obtenu dans le cadre de l'inhibition d'un seul gène. Lorsque l'expression de la protéine uk1_LRR était inhibée, les billes recouvertes de VmpA adhéraient significativement moins aux cellules Euva.

Cette protéine uk1_LRR est constituée de 4 domaines LRR (Leucine Rich Repeat) et les prédictions structurales indiquent qu'elle forme une structure en fer à cheval typique de protéines impliquées dans des interactions protéine-protéine. L'expression de uk1_LRR a été mesurée par PCR en temps réel chez des insectes *E. variegatus* infectés ou non-infectés par le phytoplasme FD. L'expression de uk1_LRR est restait stable chez les insectes non infectés et chez les insectes infectés une augmentation de son expression a été constatée 7 jours après le début de l'acquisition de phytoplasmes ainsi qu'à 28 jours, probablement suite à une re-ingestion *de novo* du phytoplasme transmis à la fève durant la latence. Des insectes sains ont été disséqués pour évaluer l'expression de

la protéine uk1_LRR dans differents organs par PCR en temps réel: le gène uk1_LRR était 6 fois plus exprimé dans les intestins par rapport aux glandes salivaires et 18 fois plus par rapport aux ovaires. Ces résultats sont compatibles avec une possible implication de la protéine uk1_LRR dans les étapes précoces de l'interaction entre le phytoplasme FD et son insecte vecteur, notamment, dans les phases suivant l'ingestion de la sève infectée.

La technique du double hybride chez la levure *Saccharomyces cerevisiae* a été utilisée pour visualiser d'éventuelles interactions entre la VmpA et l'ensemble des protéines de l'insecte vecteur *E. variegatus*. Aucun résultat positif d'interaction n'a été obtenu.

En conclusion, les travaux effectués dans le cadre de ma thèse ont amené à l'identification d'une protéine contenant des domaines LRR impliquée dans l'adhésion de la VmpA du phytoplasme de la flavescence dorée aux cellules en culture de l'insecte vecteur *E. variegatus*. Le rôle de cette protéine dans la transmission du phytoplasme aux plantes et dans la spécificité de vection reste à confirmer.

Mots clés: phytoplasmes, insectes vecteurs, interaction protéine-protéine, RNAi, microbiologie cellulaire

Summary

Deciphering flavescence dorée phytoplasma adhesion to its insect vector cells

Flavescence dorée is an epidemic grapevine disease associated with a phytoplasma infection and affecting viticultural areas throughout Southern Europe. The phytoplasma is transmitted among *Vitis* by its leafhopper vector *Scaphoideus titanus*. A better understanding of the interaction between the phytoplasma and its vector could help in the development of new strategies to reduce disease spread in the vineyard. The flavescence dorée phytoplasma (FDp) adhesion to the midgut epithelium cells of its insect vector is partly mediated by the Variable Membrane Protein A (VmpA), an adhesin which shows lectin properties. Morevover, VmpA sequence variation is correlated to the vector competence towards different phytoplasmas genotypes. The aim of this work was to identify proteins of the FDp experimental vector *E. variegatus* interacting with VmpA.

For that purpose, we identified *E. variegatus* cells proteins interacting with recombinant VmpA-His_6 by mass spectrometry analysis of VmpA-*E. variegatus* protein complexes formed upon *in vitro* interaction assays. Thirteen candidate proteins possessing potential N-glycosylation sites and predicted transmembrane domains were selected. To assess their impact in VmpA binding, we reduced the expression of the candidate genes on *E. variegatus* cells in culture by dsRNA-mediated RNAi. We optimised RNAi protocol to simultaneously inhibit twelve genes in *E. variegatus* cultured cells with a satisfying efficiency. The effect of candidate gene knockdown on VmpA binding was measured by the capacity of VmpA-coated fluorescent beads to bind *E. variegatus* cells. The decrease in the expression of an unknown transmembrane protein with Leucine Rich Repeat domains (uk1_LRR) was correlated with the decreased adhesion of VmpA-beads to *E. variegatus* cells. Uk1_LRR expression levels evaluated in infected insects throughout the infection slightly increased following ingestion of phytoplasmas meanwhile it was stable in non-infected insects. Moreover, the uk1_LRR was more expressed in digestive tubes than in salivary glands of *E. variegatus*, suggesting the possible implication of this protein in early stages of the infection by the phytoplasma.

A double yeast hybrid assay was set up in order to explore the potential protein-protein interactions occurring between VmpA and *E. variegatus* through heterologous expression in yeast cells. No interaction was evidenced through this technique.

In conclusion, our results suggest the implication of *E. variegatus* uk1_LRR in VmpA mediated adhesion of the phytoplasma to its insect vector cells. The role of uk1_LRR as VmpA receptor still need to be confirmed, as well as its implication in phytoplasma transmission and vector specificity.

Keywords: phytoplasmas, insect vectors, protein-protein interaction, RNAi, cellular microbiology

Formations suivies

Ethique de la recherche (18 mai 2021 - 15 juillet 2021) FUN MOOC plateforme en ligne (Université de Lyon)
12 heures enregistrées par: Sciences de la Vie et de la Santé.

Intégrité scientifique dans les métiers de la recherche (03 mars 2021) plateforme en ligne FUN mooc
15 heures enregistrées par: Sciences de la Vie et de la Santé.

Papirus-Parcours d'accompagnement pour publier et communiquer en science (janvier 2022) INRAE, formation permanente nationale
20 heures enregistrées par: Sciences de la Vie et de la Santé.

SBM - Cytométrie en flux « théorie » (12 janvier 2022) Immunoconcept
4 heures enregistrées par: Sciences de la Vie et de la Santé.

SBM - La technologie CRISPR-Cas9 (26 avril 2023) Institut Magendie
6 heures enregistrées par: Sciences de la Vie et de la Santé.

Statistiques fondamentales (06-10 mars 2023) INRAE Villenave d'Ornon
20 heures enregistrées par: Sciences de la Vie et de la Santé.

Statistiques multivariées (05-07 juin 2023) INRAE formation permanente Nouvelle-Aquitaine Bordeaux
20 heures enregistrées par: Sciences de la Vie et de la Santé.

Write your first paper step by step (28 février 2023) formation à distance
20 heures enregistrées par: Sciences de la Vie et de la Santé.

Opportunities of job after a PhD on international organizations (ONG) (07 juin 2022)
3 heures

Ecole d'été Biodiversité & Vecteurs (20 septembre 2022 - 23 septembre 2022) Key Initiative MUSE Risques Infectieux et Vecteurs, Montpellier
3 heures enregistrées par: Sciences de la Vie et de la Santé

Initiation à l'utilisation du microscope à epifluorescence AxioImager, Bordeaux Imaging Center (BIC, UAR 3420, France-BioImaging infrastructure)

Initiation à l'utilisation du microscope confocale, Bordeaux Imaging Center (BIC, UAR 3420, France-BioImaging infrastructure)

Analyse d'image – manipulation des stacks avec Fiji/imageJ, Bordeaux Imaging Center (BIC, UAR 3420, France-BioImaging infrastructure)

……

Élu doctorante Commission de Recherche UB (13 mai 2022 - 31 décembre 2023), Université de Bordeaux

List of publications

Arricau-Bouvery, N., Dubrana, MP., Canuto, F., Duret, S., Brocard, L., Claverol, S., Malembic-Maher, S. & Foissac, X. **Flavescence dorée phytoplasma enters insect cells by a clathrin-mediated endocytosis allowing infection of its insect vector**. Sci Rep **13**, 2211 (2023).https://doi.org/10.1038/s41598-023-29341-1

Canuto, F., Arricau-Bouvery, N., Duret, S, Dubrana, MP., Beven, L., Garcion, C., Brocard, L., Claverol, S., Malembic-Maher, S. & Foissac, X. **Identification of a "flavescence doree" phytoplasma VmpA candidate receptor in the experimental insect vector, *Euscelidius variegatus*.** Phytopathogenic Mollicutes **13**, 13-14 (2023). doi: 10.5958/2249-4677.2023.00007.5

Canuto, F., Duret, S., Dubrana, MP., Claverol, S., Malembic-Maher, S., Foissac, X. & Arricau-Bouvery, N. **A knockdown gene approach identifies an insect vector membrane protein with Leucin Rich Repeats as one of the receptors for the VmpA adhesin of flavescence dorée phytoplasma.** Front Cell Infect Microbiol. Nov 6;13:1289100 (2023). doi: 10.3389/ fcimb.2023.1289100. PMID: 38029232; PMCID: PMC10662966

List of communications

May 2023 – **5th Meeting of the International Phytoplasmologist Working Group** (IPWG) (Muscat, Sultanate of Oman) with the oral presentation "Identification of a Flavescence dorée phytoplasma VmpA candidate receptor in the experimental insect vector *Euscelidius variegatus*"

April 2022 – **Journée Scientifique de l'École Doctoral SVS** (Bordeaux) with the poster "First steps towards the identification of potential receptors to Flavescence dorée phytoplasmas in the experimental leafhopper host *Euscelidius variegatus*"

November 2021 – **XXIII Biennial Congress of the International Organisation for Mycoplasmology** (IOM) with the online oral presentation "First steps towards the identification of potential receptors to flavescence dorée phytoplasmas VmpA in the experimental leafhopper vector *Euscelidius variegatus*"

March 2021: online oral presentation "Deciphering of Flavescence Dorée phytoplasmas adhesion to cells of its insect vector" for the **network Biologie Adaptative des Pucerons et Organismes Associés** (BAPOA)

March 2021 and May 2022: oral presentations "Deciphering of flavescence dorée phytoplasma adhesion to cells of its insect vector" for the "**Séminaires scientifiques de l'unité UMR 1332 Biologie du Fruit et Pathologie**"

List of abbreviations

List of abbreviations

16Sr: 16S ribosomal gene

AAP: acquisition access period

AD: activation domain

AYp: aster yellow phytoplasma

AY-WB: aster yellow witches broom

BD: binding domain

bp: base pair

Ca. P.: "*Candidatus* Phytoplasma"

cfu: colony-forming unit

CYp: chrysanthemum yellows phytoplasma ("*Ca. P. asteris*")

dsRNA: double strand RNA

Euva cells: *Euscelidius variegatus* cells in culture

FD: flavescence dorée disease

FD92: Flavescence dorée phytoplasma strain FD92

FDp: Flavescence dorée phytoplasma(s)

GFP: green fluorescent protein

GlcNAc: N-acetylglucosamine

GNA: Galanthus Nivalis Lectin

GY: grapevine yellows

His: histidine

IAP: inoculation access period

Leu: leucine

LCA: Lens Culinaris lectin

LC-MS/MS: Liquid Chromatography coupled to tandem Mass Spectrometry

LEL: Lycopersicon Esculentum lectin

LP: latency period

LRR: leucine-rich repeat

Man: mannose

MLOs: mycoplasma-like organisms

MM: microvillar membrane

Ni-NTA column: Nickel-nitrilotriacetic acid agarose column

NLS: nuclear localization signal

NxS/T: amino acidic motif (N: asparagine; x: any amino acid but proline; S/T: serine or threonine)

OYp: onion yellow phytoplasma ("*Ca. P. asteris*")

PGY: Palatinate grapevine yellows

PGYA: Palatinate Grapevine Yellows strain A

PM: perithrophic membrane

PMM: erimicrovillar membrane

PMUs: potential mobile units

RdRP: RNA-dependent RNA Polymerase

RI: ribonuclease inhibitor

RISC: RNA-induced silencing complex

RNAi: RNA interference

SD: Synthetic Defined medium for *Saccharomyces cerevisiae*

SDS-PAGE: Sodium Dodecyl Sulphate - PolyAcrylamide Gel Electrophoresis

siRNA: small interference RNA

SNP: single nucleotide polymorphism

TEM: transmission electron microscopy

Trp: tryptophan

TSA: Transcriptome Shotgun Assembly

T3SS: type III secretion system

UAS : upstream activating sequences

VmpA: Variable membrane protein A

Y2H: Yeast double hybrid

Reagents

ACN: ammonium bicarbonate 50% acetonitrile

BSA: bovine serum albumin

DAPI: 4',6-diamidino-2-phenylindole

DOC: sodium deoxycholate

EDTA: Ethylenediaminetetraacetic acid

EGTA: ethylene glycol-bis(β-aminoethyl ether)-N,N,N’,N’-tetraacetic acid)

Hepes: HCOOH: formic acid

HRP: horseradish peroxidase

KCl: Potassium chloride

NaCl: Sodium chloride

NH_4HCO_3: ammonium bicarbonate

MES: 2-(N-morpholino)ethanesulfonic acid

$MgCl_2$: Magnesium chloride

PBS: phosphate buffer saline

Genes

CD36-like: lysosome membrane protein CD36-like

cueball: LDL-like protein cueball

draper: protein draper isoform X1

EF1: elongation factor 1

EGFR: epidermal growth factor receptor

Endo: endoplasmin

Fasciclin: transforming growth factor-beta-induced protein ig-h3-like

GST: glutathione S-transferase

HERC4: HERC4-like E3 ubiquitin-protein ligase

Na/Ca exchanger: sodium/calcium exchanger 3-like isoform X1

tubβ: tubulin beta

Tuf: Elongation factor Tu

uk1_LRR: uncharacterized protein containing LRR domains_1 (identification via interpro)

uk2_TLR: uncharacterized protein containing LRR domains_2

uk3: uncharacterized protein_3

Wengen: Tumor necrosis factor (TNF) wengen

Species

C. haematoceps: Circulifer haematoceps

E. variegatus: Euscelidius variegatus

N. lugens: Nilaparvata lugens

M. quadrilineatus: Macrosteles quadrilineatus

S. citri: Spiroplasma citri

S. titanus: Scaphoideus titanus

X. fastidiosa: *Xylella fastidiosa*

O. alni: Oncopsis alni

List of Tables and Figures

Tables

Table 1. List of named *Candidatus* Phytoplasma species and their correspondent group.

Table 2. List of primers and plasmids used in this study.

Table 3. Repartition of Euva proteins that interacted with VmpA-His_6 in relation to their KEEG classification.

Table 4. Repartition of Euva proteins extracted with the buffer Rx Triton 1% + DOC 0.1% and that interacted with VmpA-His_6.

Table 5. Characteristics of the Euva proteins selected for adhesion assays.

Table 6. Homologs of uk1_LRR in NCBI databases using Blast and domains found with InterPro.

Table 7. Adhesion of the VmpA-His_6_PGYA and VmpA-His_6_FD92 coated beads to the Euva-11 cells in presence of dsRNA of uk1_LRR gene and GFP as control (raw values).

Table 8. Summary of the five mating experiences performed using Y2H Gold transformed with pGBKT7_VmpA as bait and Y187 transformed with pGADT7_cDNA_*E.variegatus* as preys.

Table 9. Prey sequences identified in the different clones obtained during mating experiments.

Table 10. Estimate molecular weight of the prey proteins contained in the clones tested in western blot for protein expression.

Table S1 (annex). Euva proteins that interact with VmpA-His_6 having TMHMM-predicted transmembrane segments and 'NxS/T' patterns.

Figures

Figure 1. Distribution of flavescence dorée.

Figure 2. Symptoms of grapevine Yellows (GY).

Figure 3. *S. titanus* and vineyard distribution in Europe.

Figure 4. Life cycle of *S. titanus.*

Figure 5. Sequence diversity of genes encoding Variable membrane proteins vmpA and vmpB and insect transmission.

Figure 6. Ecological cycle of flavescence dorée phytoplasmas.

Figure 7. Symptoms of phytoplasmas infection.

Figure 8. Acquisition of phytoplasmas and colonisation of their vector.

Figure 9. Schematic representation of N-linked glycosylation pathways in insects.

Figure 10. Acquisition transmission assays to propagate FD phytoplasma isolate FD92 in controlled conditions.

Figure 11. Schematic representation of pET28_VmpA-His_6.

Figure 12. Purification of VmpA-His_6_FD92.

Figure 13. Example of dot blot anti-VmpA on coated beads.

Figure 14. Protocol for the assessment of uk1_LRR expression in FD92-infected and non-infected *E. variegatus*.

Figure 15. Schematic representation of bait plasmid pGBKT7.

Figure 16. Schematic representation of SMART cDNA synthesis.

Figure 17. Schematic representation of prey plasmid.

Figure 18. A drop of culture after 16 hours of incubation observed at phase contrast microscope.

Figure 19. Schematic representation of RNAi machinery.

Figure 20. Proteins of Euva cells that interact with VmpA-His_6.

Figure 21. Interaction of VmpA-His_6 with Euva cell proteins *in vitro*.

Figure 22. Expression of candidate genes in Euva cells regards to the reference gene glutathione S-transferase and tubulin β.

Figure 23. Expression of the candidate genes in Euva cells regards to the reference gene glutathione S-transferase (RNAi multiplex).

Figure 24. Expression of the candidate genes in Euva cells regards to the reference gene glutathione S-transferase (off-target assessment).

Figure 25. Euva11 cells observed at the inversed microscope 3 days post transfection with uk1-LRR dsRNA.

Figure 26. Euva11 cells observed at the inversed microscope at 3 days post transfection (RNAi multiplex).

Figure 27. Adhesion of the VmpA-His_6-coated beads to the Euva-11 cells in presence of dsRNA of candidate genes and GFP as control.

Figure 28. Adhesion of the VmpA-His_6-coated beads to the Euva-11 cells in presence of dsRNA of uk1_LRR gene and GFP as control.

Figure 29. Adhesion of the VmpA-His_6-coated beads to the Euva-11 cells (RNAi multiplex).

Figure 30. Characterisation of uk1_LRR protein

Figure 31. Assessment of uk1_LRR expression in *E. variegatus*.

Figure 32. Far-western blot on Euva proteins incubated with VmpA-His_6 PGYA and VmpA-His_6 FD92.

Figure 33. Adhesion of the VmpA-His_6_PGYA and VmpA-His_6_FD92 coated beads to the Euva-11 cells in presence of dsRNA of uk1_LRR gene and GFP as control.

Figure 34. Double yeast hybrid principle.

Figure 35. Workflow of a classic double yeast hybrid assay.

Figure 36. Y2H Gold yeast strain transformed with prey plasmid alone.

Figure 37. Y2H Gold yeast strain transformed with prey plasmid and pGBKT7_VmpA.

Figure 38. Western blot anti-HA on yeast expressing prey proteins.

Figure 39. Flavescence dorée phytoplasma membrane proteins and their interaction with host cells.

General introduction

1. Discovery, characterization, cellular and molecular properties of phytoplasmas

1.1. Discovery and initial characterization of phytoplasmas

Before the discovery of phytoplasmas, the causal agents of many plant yellows were thought to be viruses. Indeed, it was not possible to cultivate the pathogens associated with the disease, and, like some plant viruses, they could be transmitted by sap-sucking hemipteran insects such as leafhoppers. In addition, extracts of diseased plants passed through 0.45 µm filters were retaining infectivity as they could be reinjected to insect vectors for transmission to plants.

Phytoplasmas have been observed for the first time by electron microscopy in 1967 in the sieve tubes of plants affected by yellowing, dwarfism or stem proliferations (Doi *et al.*, 1967). At that time, phytoplasmas were called mycoplasma-like organisms (MLOs) because of their morphological resemblance to human and animal mycoplasmas. Their phenotypic characteristics observed in ultrathin sections of infected plants phloem consists in pleiomorphic bodies of 100 to 800 nm surrounded by a single unit membrane devoid of rigid cell wall. In their publication, Doi and colleagues also mentioned a recent report that described the disappearance of plant symptoms and pleiomorphic bodies upon treatment of diseased plants with tetracyclines.

In 1969, Hirumi and Maramorosch confirmed that MLOs were present in the salivary glands of insect vectors carrying the aster yellows agent (Hirumi and Maramorosch, 1969).

In 1989, sequence comparison and phylogenetic analysis of the 16S rRNA gene of an of Aster Yellows (AY) MLO revealed that the AY MLOs should be tentatively placed in the class *Mollicute*s with mycoplasmas, ureaplasmas, spiroplasmas and acholeplasmas and could be more closely related to acholeplasmas (Lim and Sears, 1989). Lim and Sears confirmed the evolutionary relatedness of MLOs with acholeplasmas by determining that the AY MLO:

- uses UGA as a stop codon, like acholeplasmas but unlike mycoplasmas and spiroplasmas, as shown by the sequence of its ribosomal protein genes *rplB*, *rpsS*, *rplV* and *rpsC* (Lim and Sears, 1991).
- is more related to acholeplasmas than to mycoplasmas according to the phylogenetic analysis of its ribosomal protein genes *rplV* and *rpsC* (Lim and Sears, 1992).
- resembles acholeplasmas grown in the absence of sterols as they resist to digitonin that solubilizes membranes and precipitates cholesterol, and are sensitive to hypotonic salt solutions. The AY MLO could however be differentiated from acholeplasmas grown without sterols by its greater resistance to lysis in hypotonic sucrose solutions (Lim *et al.*, 1992).

Consequently, the term "phytoplasma" was adopted in 1994 by the Phytoplasma Working Team during the 10th Congress of the International Organization of Mycoplasmology held in Bordeaux, France. Since their discovery, phytoplasmas have been reported to be associated with thousands of different plant diseases affecting food crops, ornamental plants as well as timber and shade trees with a worldwide distribution (Rao *et al.*, 2018). Unlike most of the animal and human mycoplasmas, phytoplasmas have so far remained uncultivable in cell free media. This caused their characterisation, identification and classification as well as diagnostics to be limited, until the molecular techniques emerged during 1980s-1990s.

1.2. Phytoplasma classification

According to the official taxonomy implemented in the NCBI taxonomy browser, phytoplasmas are classified in the bacterial phylum *Mycoplasmatota* (formerly *Tenericutes*), in the class *Mollicutes*, order *Acholeplasmatales*, family *Acholeplasmataceae,* genus *"Candidatus* Phytoplasma" although the Bergey's manual for determinative bacteriology is placing this genus in a unnamed, *incertae sedis* family II (Gasparich *et al.*, 2020).

The first attempts to classify phytoplasmas into groups was based on the cross-reactivity of monoclonal and polyclonal antibodies and cross hybridizations of probes constituted by cloned phytoplasma specific DNA (Lee *et al.*, 2000). Then, the advent of polymerase chain reaction (PCR) boosted the design of both universal and group specific

Table 1. List of named* Candidatus *Phytoplasma species and their corresponding group (Wei and Zhao, 2022; Rodrigues Jardim et al., 2023)

Group	*"Ca.* Phytoplasma" specie(s)
16SrI	"*Ca*. Phytoplasma asteris" "*Ca*. Phytoplasma lycopersici" "*Ca*. Phytoplasma tritici"
16SrII	"*Ca*. Phytoplasma asiaticum" "*Ca*. Phytoplasma australasiaticum" "*Ca*. Phytoplasma bonamiae" "*Ca*. Phytoplasma citri" "*Ca*. Phytoplasma crotalariae" "*Ca*. Phytoplasma fabacearum" "*Ca*. Phytoplasma gossypii" "*Ca*. Phytoplasma planchoniae"
16SrIII	"*Ca*. Phytoplasma pruni"
16SrIV	"*Ca*. Phytoplasma palmae" "*Ca*. Phytoplasma cocostanzaniae"
16SrV	"*Ca*. Phytoplasma balanitae" "*Ca*. Phytoplasma rubi" "*Ca*. Phytoplasma ulmi" "*Ca*. Phytoplasma ziziphi"
16SrVI	"*Ca*. Phytoplasma sudamericanum" "*Ca*. Phytoplasma trifolii"
16SrVII	"*Ca*. Phytoplasma fraxini"
16SrVIII	"*Ca*. Phytoplasma luffae"
16SrIX	"*Ca*. Phytoplasma phoenicium"
16SrX	"*Ca*. Phytoplasma mali" "*Ca*. Phytoplasma prunorum" "*Ca*. Phytoplasma pyri" "*Ca*. Phytoplasma spartii"
16SrXI	"*Ca*. Phytoplasma cirsii" "*Ca*. Phytoplasma oryzae" "*Ca*. Phytoplasma sacchari"
16SrXII	"*Ca*. Phytoplasma australiense" "*Ca*. Phytoplasma convolvuli" "*Ca*. Phytoplasma fragariae" "*Ca*. Phytoplasma japonicum" "*Ca*. Phytoplasma solani"
16SrXIII	"*Ca*. Phytoplasma hispanicum" "*Ca*. Phytoplasma meliae"
16SrXIV	"*Ca*. Phytoplasma cynodontis"
16SrXV	"*Ca*. Phytoplasma brasiliense"
16SrXVI	"*Ca*. Phytoplasma graminis"
16SrXVII	"*Ca*. Phytoplasma caricae"
16SrXVIII	"*Ca*. Phytoplasma americanum"
16SrXIX	"*Ca*. Phytoplasma castaneae"
16SrXX	"*Ca*. Phytoplasma rhamni"
16SrXXI	"*Ca*. Phytoplasma pini"
16SrXXII	"*Ca*. Phytoplasma palmicola"
16SrXXV	"*Ca*. Phytoplasma melaleucae"
16SrXXIX	"*Ca*. Phytoplasma omanense"
16SrXXX	"*Ca*. Phytoplasma tamaricis"
16SrXXXI	"*Ca*. Phytoplasma costaricanum"
16SrXXXII	"*Ca*. Phytoplasma malaysianum"
16SrXXXIII	"*Ca*. Phytoplasma allocasuarinae"
16SrXXXVI	"*Ca*. Phytoplasma wodyetiae"
16SrXXXVII	"*Ca*. Phytoplasma stylosanthis"
16SrXXXVIII	"*Ca*. Phytoplasma noviguineense"
16SrXXXIX	"*Ca*. Phytoplasma dypsidis"

primers based on highly conserved regions of 16S ribosomal gene sequences, for the diagnostic and identification of phytoplasmas. A more precise classification has been possible by using restriction fragment length polymorphism (RFLP) and phylogenetic analyses, (Lee, 1993; Schneider *et al.*, 1993). Currently, the classification of phytoplasmas includes a total of 37 groups. Beside the description as a group, it is possible to declare "C*andidatus* Phytoplasma species" (**Table 1**). The rules to describe a new species were proposed by the IRPCM Phytoplasma/Spiroplasma Working Team-Phytoplasma Taxonomy Group in 2004 (The Irpcm Phytoplasma/Spiroplasma Working Team-Phytoplasma Taxonomy Group, 2004). These rules have recently been updated by new guidelines (Bertaccini *et al.*, 2022). These consist in:

- a minimum length of 16S rRNA sequence of 1500 bp
- the new phytoplasma species must share less than 98,65% of identity on the 16S rRNA sequence with previously established species

or

- if the 16S rRNA identity is higher than 98.65 %, at least two conserved housekeeping genes such as *groEL*, *tuf, rp, secA, secY* must be used to delineate the new species (MLSA approach).

A whole genome sequence coupled with the average nucleotide identity (ANI) method has also been proposed for "*Ca*. Phytoplasma species" delineation.

1.3. Transmission and prophylactic control of phytoplasma diseases

Phytoplasmas are restricted to the plant phloem sap and are transmitted by leafhoppers, planthoppers and psyllids (Weintraub and Beanland, 2006). They perform a persistent propagative cycle into their insect vectors where they have to invade and cross two main barriers, the midgut epithelium and salivary gland cells in which they multiply (Maillet and Gouranton, 1971). Thus, after their ingestion with infected sap, adhesion of phytoplasmas to apical surface of vector intestinal cells constitutes an initial and critical step in insect invasion. Once this first barrier is crossed, the adhesion of phytoplasmas to salivary gland cells is as well critical for transmission to the plant that is achieved upon injection of infected saliva.

A given phytoplasma has one or few insect vectors depending on the level of specificity of the interaction.

Phytoplasma diseases can also be propagated by grafting and vegetative propagation through the production of cuttings from phytoplasma-infected plant material in nurseries, through storage tubers, rhizomes, or bulbs (Lee *et al.*, 2000). The same authors reported that there are no substantial evidence for transmission of phytoplasmas through the seeds. This transmission pathway seems to be unlikely due to the lack of plant vascular direct connections to seeds and also because phytoplasma-infected plants do not usually produce viable seeds.

As there is no curative method against phytoplasmas, the control of phytoplasma-associated diseases relies on prophylactic measures based on diseases surveillance, elimination of infected plants in both production fields and nurseries, and insecticide treatments against the vector insects when adequate (Weintraub and Wilson, 2009).

1.4. Phytoplasmas genome features

The size of phytoplasma genome ranges from 530 to 1350 (kbp) as determined by pulse-field gel electrophoresis (Marcone *et al.*, 1999). It is constituted by one circular double stranded chromosomal DNA molecule except for "*Ca.* P. mali", "*Ca.* P. pruni" and "*Ca.* P. prunorum" that possess a linear chromosome (Kube *et al.*, 2008). In some species like "*Ca.* P. asteris", "*Ca.* P. australiense", "*Ca.* P. pruni", "*Ca.* P. trifolii" and "*Ca.* P. aurantifolia", small circular extrachromosomal plasmids of 3 to 5 kbp have been described, some of which could have a viral origin due to the similarity of their rolling-circle replicase with replicases of Geminiviruses (Rekab *et al.*, 1999; Nishigawa *et al.*, 2001; Oshima *et al.*, 2001). According to their sequences, phytoplasmas genomes are characterised by a low GC content ranging from 21 to 28 %, possess 2 ribosomal operons and 31 to 35 tRNAs (Kube *et al.*, 2012). The number of protein-coding genes varies from 481 for "*Ca*. P. mali" to 1126 for "*Ca.* P. australiense" strain OY-M (Kube *et al.*, 2012; Andersen *et al.*, 2013).

Compared to other mollicutes, phytoplasma genome reduction has led to a greater loss of metabolic genes. Phytoplasmas lack genes for F1F0 ATP synthases, enzymes of the pentose phosphate pathway, PTS systems for sugar import, enzymes for nucleotide synthesis

and for the post-translational maturation of lipoproteins (Oshima *et al.*, 2004). Surprisingly, "*Ca.* P. mali" lacks the enzymes for the lower, ATP-producing part of the glycolysis, which stops at the glycerol-3-P step and could serve for the synthesis of membrane phospholipids (Kube *et al.*, 2008). In counterpart, phytoplasma genomes encode for various P-type ATP synthase and ABC transporters suggesting their high dependence on host metabolism and their adaptation to an intracellular life in a nutrient-rich environment. Genes coding for proteins involved in DNA replication, transcription, translation and protein translocation are present, as well as a complete secretion system (Sec) which allows the insertion of transmembrane protein to the cell membrane as well as the release of effectors, proteins impacting hosts development and fitness. "*Ca.* P. mali" and the flavescence dorée phytoplasma possess an extended set of genes for homologous recombination, while "*Ca*. P. asteris" and "*Ca*. P. australiense" lack *rec*A, *rec*G, *rec*U, *ruv*A, *ruv*B and a gene for Holliday junction resolvase (Kube *et al.*, 2008; Debonneville *et al.*, 2022).

Despite the limited size of phytoplasma genomes, repeated sequences are present, a feature shared with other Mollicutes but with a peculiar organisation. In phytoplasmas, multicopy genes and transposon-like elements are organised in potential mobile units (PMUs) (Bai *et al.*, 2006) and some of these PMUs appear to be degenerated (Jomantiene *et al.*, 2007; Wei *et al.*, 2008). These regions, bordered by 330 bp long inverted-repeat, contain genes for replication and recombination as well as genes coding for transcription factors, membrane proteins and secreted effectors (Bai *et al.*, 2006). Indeed, data based on sequenced bacterial genomes revealed how genes involved in pathogenicity/virulence are likely to be derived from integration in the bacterial genome of transposons or phages and thus, spatially, are localised in specific genomic island named pathogenicity islands (PAIs) (Gal-Mor and Finlay, 2006). A comparative analysis of two strains of "*Ca.* P. asteris" genomes revealed the presence of PMUs accounting for 14-23% of chromosome (Bai *et al.*, 2006) and it has been estimated that, in general, their abundance explains nearly 80% of the variance in phytoplasmas genome size (Huang *et al.*, 2022). These repeated regions, also containing genes coding for effectors, could have a role in the adaptation of phytoplasmas to the different cellular environments and hosts they colonise. Indeed, in AY-WB PMU1 genes expression is upregulated during insect colonisation when compared to plants (Toruño *et al.*, 2010). At a larger scale, it is suggested that the regulation of PMUs expression could be a strategy to adapt to different

environments and their rearrangement might increase the chance for host shift and the occupation of new niches (Bai *et al.*, 2006) even if the plant host range is mainly limited by the feeding behaviour of the phytoplasma competent vectors. In addition, there are strong evidences that PMUs components have been exchanged during phytoplasma evolution (Chung *et al.*, 2013). In support of this scenario, it has been showed that Aster Yellows phytoplasma strain Witches' Broom (AY-WB) complete PMU1 can excise from chromosomes as an extrachromosomal circular form (Toruño *et al.*, 2010).

The complete genome of a strain of flavescence dorée phytoplasma (FDp) isolated in Switzerland has been published in 2022 (Debonneville *et al.*, 2022) and completed partial releases of the chromosome genetic map and draft genome of strain FD92 (Malembic-Maher *et al.*, 2008; Carle *et al.*, 2011). FDp strain CH has a circular chromosome of 654.223 bp with a G/C content of 21.7 %. Among major metabolic features CH genome encodes a complete glycolysis and pyruvate oxidation pathways, a malo-lactic enzyme, a lactate dehydrogenase, an incomplete pathway for fatty and amino acid biosynthesis, ABC transporters, a complete protein secretion system, a low number of putative secreted effectors, ATP-dependent zinc metalloproteases, a set of genes allowing homologous recombination as well as six genes with restriction endonuclease function. No PMUs like region has been identified but genes characteristic of the core set of these structures were found in single copy scattered on the circular genome.

The recent sequencing of the FD92 strain of FDp long of 647 kbp highlighted an unusual number of genes encoding ATP-dependent zinc proteases FtsH which have been previously linked to variations in the virulence of "*Ca.* P. mali" strains (Seemüller *et al.*, 2013). Eight complete *ftsH* genes have been identified in the FD92 genome (Carle *et al.*, 2011; Jollard *et al.*, 2020). In addition to *ftsH6*, which appeared to be the original bacterial ortholog, the other seven gene copies were clustering on a common distinct phylogenetic branch, suggesting intra-genome duplication of *ftsH* genes instead of acquisition of multiple copies through horizontal gene transfer. The expression of *ftsH* genes appeared to be modulated in a host-dependent manner. Two of the eight FtsH C-tails were predicted by Phobius software to be extracellular and, therefore, in direct contact with the host cellular content. As phytoplasmas cannot synthesize amino acids, these data suggest that phytoplasma FtsH could potentially

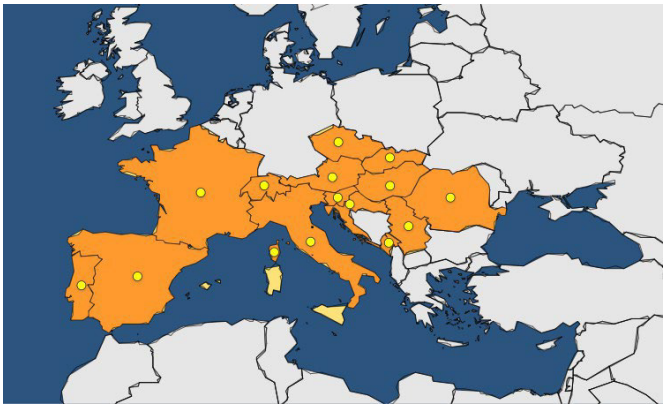

Figure 1. Distribution of flavescence dorée. Countries where the disease is present are Portugal, Spain, France, Italy, Switzerland, Austria, Slovenia, Croatia, Montenegro, Slovakia, Romania, Serbia, Czech Republic and Hungary (EPPO, 2023).

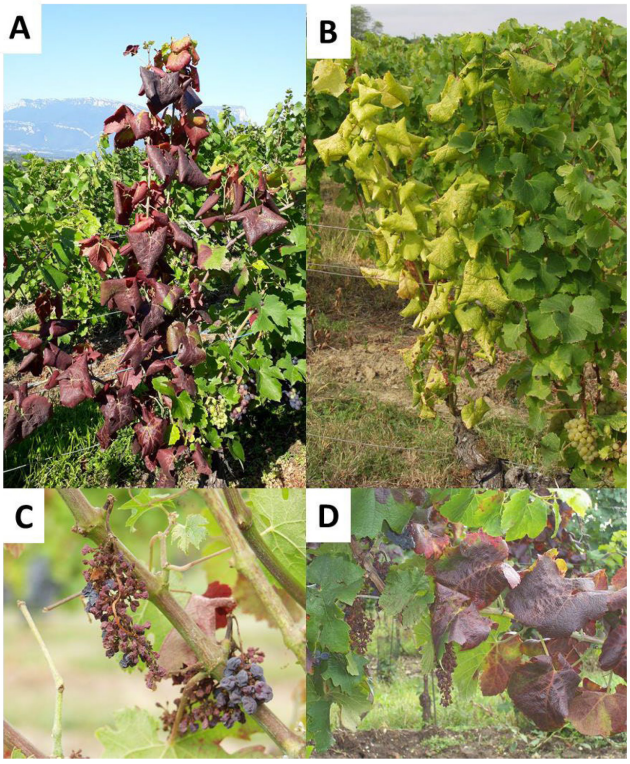

Figure 2. Symptoms of grapevine Yellows (GY). (A) flavescence dorée symptoms including leaves reddening and downwards roll on Gamay. (B) flavescence dorée symptoms including leaves yellowing and downwards rolling on Sémillon. (C) flavescence dorée symptoms on fruits of Cabernet-Sauvignon showing shrivelling and drying of grapes and incomplete lignification. (D) bois noir symptoms showing leaves reddening and downwards rolling, shrivelling of grapes and absence of lignification on red cultivar. (Photos, INRAE Bordeaux)

enhance recycling of phytoplasma cellular proteins and promote host protein degradation (Jollard *et al.*, 2020).

2. Flavescence dorée

2.1. Symptomatology

Flavescence Dorée (FD) is an epidemic grapevine disease classified in the category of Grapevine Yellows (GY). FD has been first reported in France in 1954 (Caudwell, 1957) and it has since spread to the viticultural areas of fourteen European countries (**Figure 1**), where it causes important yield losses and heavy management costs to winemaker industry (Jeger *et al.*, 2016). GY are associated with phytoplasmas belonging to the different taxonomic subgroups 16SrI, III, V, VII, XII that induce the same symptoms: discoloration such as reddening in red cultivars and yellowing in white cultivars, downward rolling of leaves, incomplete or no lignification of canes, shrivelling and drying of grapes and tendrils (**Figure 2**) (Boudon-Padieu, 2005; Constable, 2009). Diseased, FDp-infected grapevine can recover although the ability to recover depends on the cultivars (Caudwell, 1961; Osler *et al.*, 2004).

FD is associated with phytoplasmas belonging to the group 16rS V subgroups C and D (FDp) (Caudwell *et al.*, 1971; Davis and Dally, 2001). Phytoplasmas of both subgroups are transmitted from one grapevine plant to another by the leafhopper vector *Scaphoideus titanus* (Schvester *et al.*, 1961; Mori *et al.*, 2002).

Vitis varieties are characterised by variable susceptibility to FD such as disease incidence and severity of symptoms. As an example, the italian Barbera cultivar has shown to be highly susceptible to FDp, displaying severe symptoms correlated to high phytoplasma titres in symptomatic plants, meanwhile Nebbiolo cultivar showed almost no symptoms and plants were characterised by a lower titre of phytoplasma (Roggia *et al.*, 2014). Similarly, focusing on Bordeaux viticultural region, Cabernet Sauvignon (CS) is classified as a highly susceptible cultivar, meanwhile Merlot shows much less symptoms when infected with FDp. It has been shown that phytoplasmas in Merlot are restrained to a limited area in the plant, near the insect feeding site, and that phytoplasma loads were significantly lower when compared to CS, where phytoplasmas were found systemically throughout the plant (Eveillard

et al., 2016). Moreover, the variable susceptibility of these two cultivars reflects the susceptibility of their parents, the less susceptible Magdeleine noire des Charentes for Merlot and the high susceptible Sauvignon for CS. The common parent of Merlot and CS, Cabernet franc, showed an intermediate degree of susceptibility, suggesting the genetic heritability of susceptibility traits in *Vitis* cultivar to flavescence dorée phytoplasma. Less susceptible varieties were also associated with a lower vector survival on plants (Ripamonti *et al*, 2022a).

Results of greenhouses inoculations of 28 different *Vitis* varieties revealed a different degree of susceptibility among accessions. All varieties developed FD symptoms and their severity was correlated to the phytoplasma titre in plants measured by quantitative real time PCR (Eveillard *et al.*, 2016). Another study led on 14 grapevine cultivars typical of the piedmontese region (Italy) revealed a variable degree of susceptibility among varieties resulting in the less susceptibility of the cultivars named Moscato, Brachetto, Freisa and confirming the low susceptibility of Merlot to FD symptoms (Ripamonti *et al.*, 2021). Moscato and Brachetto are considered aromatic varieties due to the enhanced presence of aromatic compounds in their leaf and berries, which could act directly on phytoplasma plant colonisation or indirectly by decreasing the survival of the vectors on the plant. The vector acquisition efficiency depends both on the grapevine varieties and phytoplasma load although these two parameters are not always strictly correlated (Galetto *et al.*, 2016). Indeed, in the cited study, a higher percentage of exposed *S. titanus* acquired phytoplasma on susceptible varieties like Arneis, even when the phytoplasma titre characterising the plants was significantly lower than less susceptible cultivars, suggesting that vector acquisition efficiency drives the spread of disease, at least within the vineyard. Interestingly, comparative early transcriptomic profiling on grapevine exposed to infected and non-infected *S. titanus* suggested that FDp infection represses the defence responses induced by the insect feeding onto the grapevine cultivar Chardonnay (Bertazzon *et al.*, 2019).

Gone-wild *Vitis* and Rootstock such as *V. rupestris*, *V. berlandieri* and *V. riparia,* principal species used in rootstock breeding, were characterised by a wide range of phytoplasma titres while being symptomless (Eveillard *et al.*, 2016). The absence of symptoms is a difficulty for the surveillance of FD because such phytoplasma reservoirs constitute a source of inoculum for FD outbreaks in nearby vineyards (Lessio *et al.*, 2014).

2.2. Surveillance and control

Due to its epidemic potential, FDp is listed as a quarantine pest in Europe (A2 EPPO list, UE directive 2016/2031, Commission implementing regulation 2019/2072 and 2022/1630) and therefore is submitted to special regulations including

- planting of disease-free material
- annual monitoring of symptomatic plants in vineyard
- mandatory uprooting of infected plants from vineyard and nurseries
- mandatory insecticide treatments in preconized areas in order to decrease the vector populations.

The major difficulty in FD management is the detection of FDp in nurseries as the grapevine rootstocks are symptomless carriers that transmit FDp to the grafted susceptible cultivars (Caudwell *et al.*, 1994). Typical FD symptoms appears during the summer of the year following plant inoculation, constituting a source of inoculum for *S. titanus* in late spring-early summer prior to their detection during vineyard surveillance in August-September. Moreover, the coexistence of FD with Bois noir, another GY disease associated with "*Ca.* P. solani" and showing the same symptomatology can delay the detection of FD cases.

Multiplex real time PCR are routinely used to distinguish FDp from other GY-associated phytoplasmas such as the Bois noir agent (Hren *et al.*, 2007; Angelini *et al.*, 2007; Pelletier *et al.*, 2009). Once confirmed by molecular analysis, FDp infected grapes are uprooted and vineyards plot with more that 20 % infection are fully removed.

The hot-water treatment of 50°C during 45 minutes eliminates FDp from grapevine for planting (Caudwell *et al.*, 1997). Increase in the use of this treatment in nursery material in combination with an increased elimination of abandoned vineyards and gone-wild *Vitis* is predicted to better limit the spread and impact of FD (Jeger *et al.*, 2016).

2.3. Epidemiology, ecology and genetic diversity of flavescence dorée phytoplasmas

S. titanus, the natural vector of FDp in the vineyard compartment is an ampelophagous, univoltine, allochthonous leafhopper introduced at the beginning of 20th

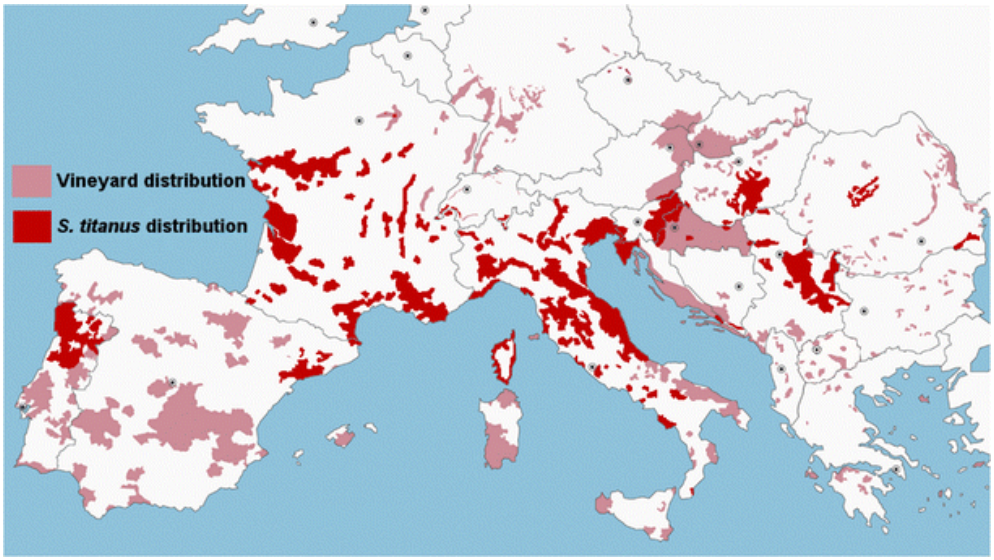

Figure 3. **S. titanus** ***and vineyard distribution in Europe (from Chuche and Thiéry, 2014).***

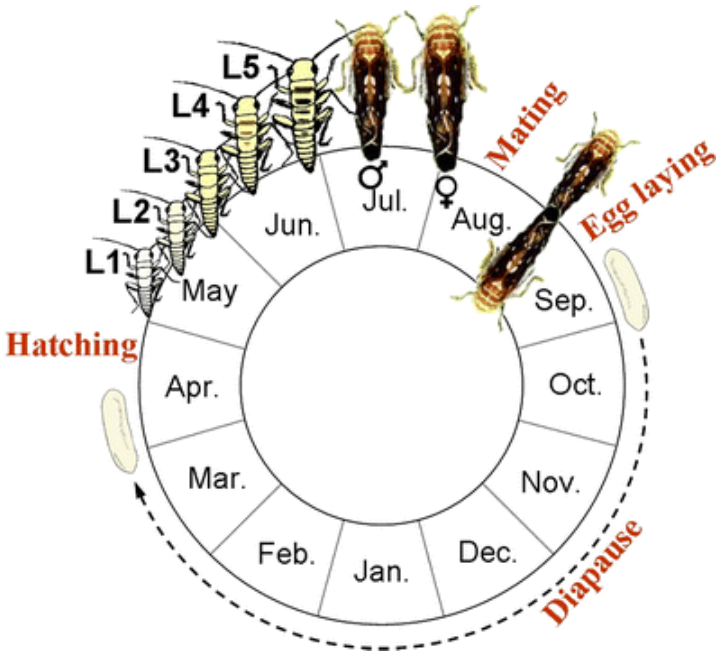

Figure 4. Life cycle of **S. titanus** *(from Chuche and Thiéry, 2014).*

century in Europe from North-America upon importation of American *Vitis* varieties to be used as rootstock in European vineyards to overcome the phylloxera crisis. The first report of its presence in Europe dates to 1958 in south western France and from there it rapidly spreads across the continent (Bonfils and Schvester, 1960; Chuche and Thiéry, 2014). European populations of *S. titanus* were found to have a limited diversity and therefore introductions from North-America have certainly sparsely occurred (Papura *et al.*, 2012). *S. titanus* is now present from Portugal to Romania and from Southern Italy to the Northeast of France and Hungary (**Figure 3**).

S. titanus life cycle, represented in **Figure 4**, is entirely accomplished on *Vitis* and has been rewieved in Chuche and Thiéry (2014). As already mentioned, *S. titanus* is a univoltine species, meaning it is characterised by only one brood of offspring per year. Eggs are laid from August to September inside the bark of wood vines and overwinter during 6-8 months. Hatching begins in late spring, and it depends on vineyard latitude, altitude and year as well as temperature, which affects beginning, dynamic and length of the hatching period. The adults emerge at beginning of summer after 5-8 weeks from the first nymphal instar stage. Females become mature after 6 days from emergence and only mate once meanwhile males can mate multiple times.

FD phytoplasma is acquired through feeding on an infected grapevine from the first larval stage, even though late nymphal instars acquire phytoplasma more efficiently. Phytoplasmas first multiply in filter chamber, foregut and midgut epithelial cells, then reach the hemolymph from where they colonise all organs but the Malpighian tubules, ovaries and testis as described for *Euscelidius variegatus*, the experimental vector of FDp (Lefol *et al.*, 1994). Once the salivary glands are colonised, usually after weeks, the insect remains infectious throughout its life.

Ecological and genetical insights on FD epidemiology have revealed the European origin of FDp (Malembic-Maher *et al.*, 2020). Whereas grapevine was thought to be the only plant host for FDp, phytoplasmas genetically related to FDp were detected during the 2000s in alders (*Alnus glutinosa*) and *Clematis vitalba* (Angelini *et al.*, 2001; Arnaud *et al.*, 2007; Filippin *et al.*, 2009).

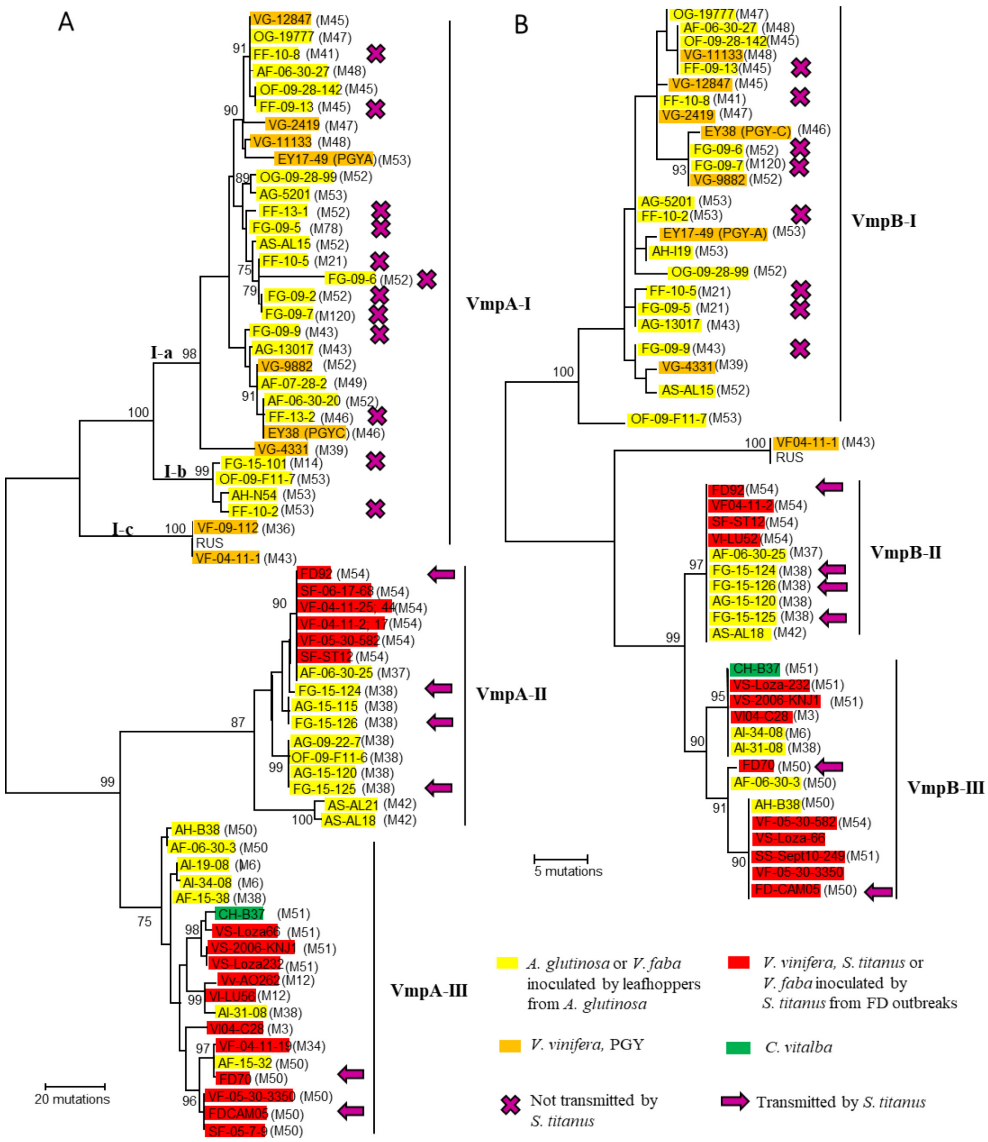

Figure 5. Sequence diversity of genes encoding Variable membrane proteins VmpA (A) and VmpB (B) and insect transmission according to Malembic-Maher* et al.*, 2020.

To better characterize these phytoplasmas, decipher their epidemiological cycles and their ability to initiate FD outbreaks, alders, clematis and leafhoppers have been collected in France, Italy, Germany, Serbia and Hungary from 1995 to 2011 in and around vineyards affected or not by FD outbreaks, as well as in non-viticultural areas. More than 80 % of the alders collected were found infected by phytoplasmas of the 16SrV-C group in all investigated areas and most of them were non-symptomatic. Results also revealed a high genetic diversity in alders with 127 *map* genotypes, some of which were also detected in FD outbreaks. In FD outbreaks, only 11 *map* genotypes were found to be clustered in three genetic groups, map-FD1, FD2 and FD3 as previously reported (Arnaud *et al.*, 2007). These data show the existence of a strong bottle-neck between alders and grapevine. The transmission assays to faba bean with the leafhoppers collected on alders indicated that the phytoplasma genotypes transmitted by the autochthonous alder Macropsinae leafhopper *Oncopsis alni* could not be acquired and transmitted by the Deltocephalinae *S. titanus*. On the contrary, phytoplasma genotypes transmitted by the autochthonous *Allygus* sp. Deltocephalinae leafhoppers and *Orientus ishidae*, a Deltocephalinae leafhopper originating from Asia, could be acquired and transmitted by *S. titanus* (Malembic-Maher *et al.*, 2020).

Interestingly, the variability of the adhesin-like genes *vmpA* and *vmpB* clearly discriminated three genetic clusters (**Figure 5**). Cluster Vmp-I grouped genotypes only transmitted by *O. alni*, while clusters Vmp-II and -III grouped genotypes transmitted by the Deltocephalinae leafhoppers and are epidemic in the vineyards. Phylogenetic analyses of the VmpA and VmpB repeated domains showed they evolved independently in cluster Vmp-I, whereas in clusters Vmp-II and–III they resulted of recent duplications. Latex beads coated with various ratio of VmpA of clusters II and I, showed that cluster II VmpA promoted enhanced adhesion to the Deltocephalinae *Euscelidius variegatus* epithelial cells and were better retained in both *E. variegatus* and *S. titanus* midguts (Malembic-Maher *et al.*, 2020). The authors therefore concluded that FDp originated from European alders and that their emergence as grapevine epidemic pathogens appeared restricted to some genetic variants possessing Vmp adhesins compatible with Deltocephalinae leafhoppers such as *S. titanus*. The ecological cycle of FDp is summarized in **Figure 6**. Once introduced in the vineyard compartment by occasional feeding of Deltocephalinae alder leafhoppers, these phytoplasma genotypes, compatible with *S. titanus* transmission and classified as vectotype II and III

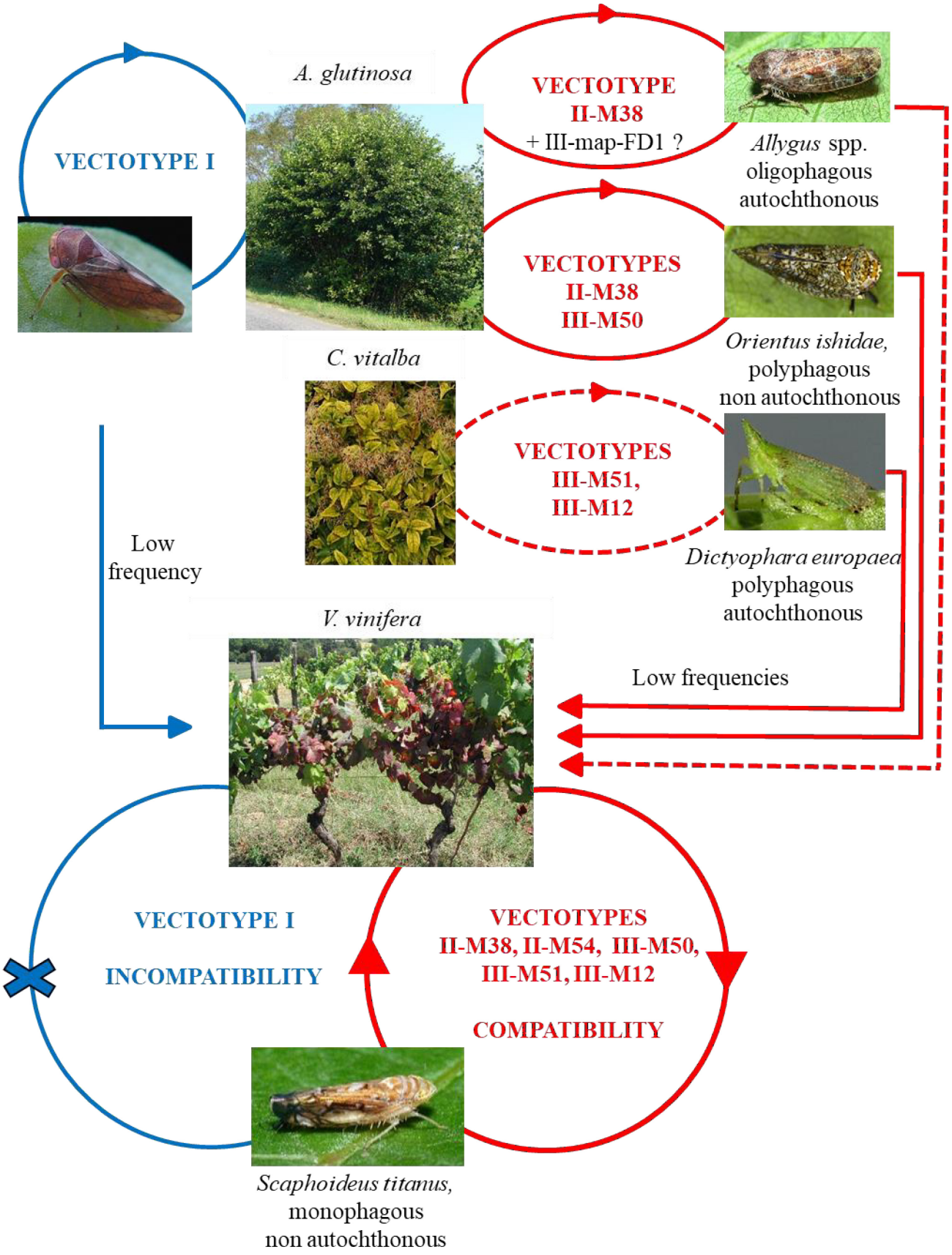

Figure 6. Ecological cycle of flavescence dorée phytoplasmas according to Malembic-Maher* et al.*, 2020

according to their vmp gene sequences of cluster vmpII and III, have gained an high epidemic potential in vineyards due to the abundance of the vector and its ampelophagous nature. Phytoplasmas of vectotype I can occasionally be detected in grapevine but they do not trigger FD outbreaks (Malembic-Maher *et al.*, 2020). These non-epidemic genotypes are classified as Palatinate grapevine yellows isolates (PGY) as they were initially found in South-western Germany with *O. alni* as a transfer vector (Maixner *et al.*, 2000). One third of *C. vitalba* were found infected in viticultural and non-viticultural areas in Italy, Hungary or Serbia, and in France in Burgundy with three *map* genotypes, all corresponding to genotypes associated to FD outbreaks (Malembic-Maher *et al.*, 2020). The only vector reported so far to transmit FDp from *C. vitalba* is the planthopper *Dictyophara europaea* that can experimentally transmit it to grapevine (Filippin *et al.*, 2009).

In France 85 % of the FD cases are associated with the genotype M54, 15 % with genotype M50, with very few cases of M38 and single nucleotide polymorphism (SNP) variants of M50 (Malembic-Maher *et al.*, 2020). In Balkan, M51 and M50 were predominent until M54 emerged and increased in frequency (Plavec *et al.*, 2019; Krstić *et al.*, 2022). In Italy, M54, M3, M6, M12 and M50 have so far been reported (Arnaud *et al.*, 2007; Rossi *et al.*, 2019a; Malembic-Maher *et al.*, 2020) but a recent report only detected the M54 genotype (Rigamonti *et al.*, 2023). In Veneto, the initial outbreaks were associated with two strains of 16SrV-C (FD-C, M3) and 16SrV-D (FD-D, M54) taxonomic subgroups, although only the 16SrV-D strain could be detected in *S. titanus* (Martini *et al.*, 1999). Transmission assays with *S. titanus* further confirmed a higher transmission efficiency for this FD-D strain (M54) (Mori *et al.*, 2002) However, when in competition in Madagascar periwinkle or in condition of mixed feeding acquisition by the experimental leafhopper vector *E. variegatus*, the FD-C (M12) strain outcompete FD-D (M54) (Rossi *et al.*, 2020; Rossi *et al.*, 2023).

Modeling studies (Bayesian spatial models) have allowed to gain some insights onto the epidemiology and the dispersal of FD at landscape scale (Adrakey *et al.*, 2022). The probability of FD infection depends both on the environment surrounding the vineyards and on the grapevine cultivar composition of the area. The probability of FD infection increases with proportions of forest, urban land and organic farming meanwhile it decreases with the proportion of vineyards. Semi-natural habitat can indeed harbors reservoir of FD

phytoplasmas such as gone wild *Vitis*. The proportion of susceptible cultivars in the area significantly increase the probability of FD infection too.

The dispersal ability of *S. titanus* adults is quite low, 25-30 meters outside the vineyard (Lessio and Alma, 2004), but individuals from populations hosted by gone-wild *Vitis* can migrate in a contiguous vineyard up to 330 meters, although 80% of them do not fly over 30 meters (Lessio *et al.*, 2014). Therefore, interregional dispersal of the vectors is likely to be linked to human activities such as the trade of vine cuttings. Nevertheless, some reports of long dispersal of *S. titanus* and FD cases probably due to the effect of the wind have been suggested (Steffek *et al.*, 2007).

Latest EFSA report includes perspective of spreading of FD. Based on *S. titanus* CLIMEX modelling study, vine-growing regions in east, central and northern Europe exempt of *S. titanus* up to this day, will provide in future years good climatic condition for its establishment. However, further establishment of *S. titanus* in northern regions will be limited by the lack of extensive grapevine productions and so by plant host distribution (Jeger *et al.*, 2016). It must be taken into account that the geographical areas suitable for grapevine cultivation are likely to change in reason of the loss of adapted climatic condition linked to climate change (reviewed in Droulia and Charalampopoulos, 2021). Warmer temperature and water deficit during grapevine-cropping season in southern Europe viticultural areas (*i.e*. south of France, south of Italy, Spain, Portugal and Greece) will result in a redistribution of vineyards towards those areas that today are considered too cold to cultivate grapevines.

3. Phytoplasma interaction with hosts

Phytoplasmas are trans-kingdom obligate parasites, capable to colonise both plant phloem and insect vectors. Phytoplasmas alter their gene expression during host switching. Microarray analysis led on "*Ca.* P. asteris" OY-M strain sampled in both plants and insects infected in controlled conditions, revealed that 246 genes (nearly 33% of the total gene number) coding for transporters, effectors and glycolytic genes, were differentially expressed in the two hosts possibly under the regulation of two different sigma transcription factors found in the genome of the phytoplasma (Oshima *et al.*, 2011).

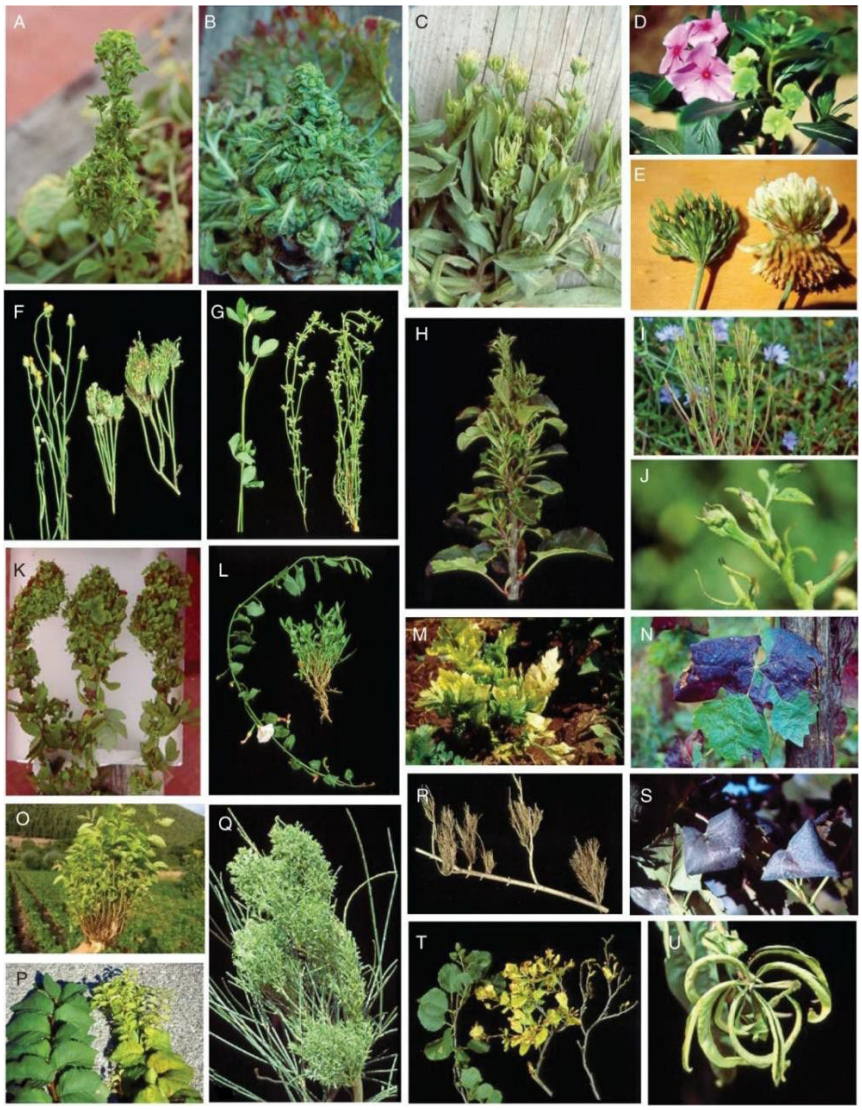

Figure 7. Symptoms of phyllody and virescence induced by aster yellows (16SrI) phytoplasmas in *Raphanus raphanistrum* (A), *Brassica oleracea* var. *capitate* (B), *Calendula officinale* (C), *Catharanthus roseus* (non-infected control on the left) (D) and *Trifolium repens* (non-infected control on the right) (E). (F) plants of *Crepis setosa* showing abnormal flowers from which numerous shoots proliferated (non-infected control on the left) associated with 16SrIX phytoplasma infections. (G) witches'-broom on 16SrII-phytoplasma infected *Medicago sativa* (non-infected control on the left). (H) Witches'-broom on apple caused by the apple proliferation agent '*Ca*. Phytoplasma mali'. (I) phyllody and proliferation symptoms on *Cichorium intybus* infected by a phytoplasma of the 16SrII group. Symptoms of flower abnormalities on tomato (J), stunting and proliferation on *Convolvulus arvensis* (non-infected control on the left) (L), yellowing on *Apium graveolens* (M), and grapevine yellows (N and S), all associated with stolbur (16SrXII) phytoplasma infections. (K) witches'-brooms on Rubus stunt (16SrV) phytoplasma-affected *Rubus fruticosus* (O and P) Elm yellows (16SrV) phytoplasma-infected *Ulmus minor* with witches'-brooms arising from a root (O) and at the tip of a twig (P) (non-infected control on the left). (Q) Witches'-brooms on *Spartium junceum* caused by '*Ca*. Phytoplasma spartii' and a 16SrV phytoplasma. (R) Witches'-brooms arising from a branch of *Rhamnus catharticus* associated with '*Ca*. Phytoplasma rhamni'. (T) Dieback and yellowing of *Alnus glutinosa* caused by the alder yellows (16SrV phytoplasma). (U) Symptoms of leaf rolling and curling on peach associated with European stone fruit yellows. (from Marcone, 2014)

In both plant and insect hosts, phytoplasmas are intra-cellular and all proteins secreted are therefore directly in contact with the host-cell machinery. Phytoplasma secreted proteins that have been demonstrated to act as effectors are TENGU, SAP11, SAP54 and SAP05 for "*Ca.* P. asteris" (Hoshi *et al.*, 2009; Sugio *et al.*, 2011a; MacLean *et al.*, 2014; Huang *et al.*, 2021), and PM19_00185, for "*Ca*. P. mali" (Strohmayer *et al.*, 2019). So far, only SAP11 and SAP54 have been shown to have a direct or indirect effect on insect vector populations (Sugio *et al.*, 2011a; MacLean *et al.*, 2014; Orlovskis and Hogenhout, 2016).

3.1. Phytoplasma interaction with plant host

Phytoplasmas inhabit the sieve tubes of the plant phloemian vascular system. Sieve cells are connected to one another by sieve plates characterized by small pores allowing the flow transport of nutrients and, in the case of an infected plant, of phytoplasmas that spread in this way systemically through the plant (Christensen *et al.*, 2004). Phytoplasma infection severely affects phloem function, resulting in the collapse of sieve elements following callose deposition and necrosis. Moreover, phytoplasma infection severely affects plant sugar transport and provokes the abnormal accumulation of sucrose and starch in the mature source leaves (Lepka *et al.*, 1999).

Phytoplasmas impair the hormone balance and development of host plants, causing a variety of symptoms. Most common plant symptoms of phytoplasma diseases consist in abnormal development of tissues and organs that includes virescence (abnormal presence of chlorophyll in floral organs which remain green), phyllody (development of floral parts into leafy structures), witches broom (proliferation of auxillary and axillary shoots), slender shoots (abnormal elongation of internodes), stunting (abnormally short internodes and small organs), flower sterility, discoloration of leaves and shoots, leaf curling or cupping, bunchy appearance at stem's ends (**Figure 7**) (Marcone, 2014). This acquired characters could also have an attractive role for insect vectors, which generally prefer young and green or yellowing tissues for feeding as well as laying eggs, leading to an increase spreading of phytoplasmas among host plants population (Hogenhout *et al.*, 2008). Furthermore, induced sterility of flowers or conversion of flowers to vegetative parts (phyllody) could delay reproductive shift and death,

increasing the vegetative growth phase of the plant and allowing the phytoplasma to live longer in its plant host.

The effector TENGU, a small protein of 38 amino acids, first identified in onion yellow phytoplasma, induces shorts internodes (dwarfism) and witches broom upon transient transfection in *Nicotiana benthamiana* (Hoshi *et al.*, 2009). Transgenic Arabidopsis plants expressing TENGU showed the same symptoms as well as defects in phyllotaxis and flower sterility. The transgenic plants were characterised by a significant downregulation of auxin-responsive genes, explaining the phenotype observed. Immuno-histochemical analysis revealed that TENGU was transported from phloem, where phytoplasmas were restrained, up to apical buds. Moreover, it has been showed that TENGU induces flower sterility in *Arabidopsis thaliana* by deregulating auxin response factor 6 and 8 (ARF6, ARF8) which are significantly down regulated both in transgenic and phytoplasma infected plants (Minato *et al.*, 2014). This deregulation leads to a decrease of jasmonic acid and auxin in transgenic buds, impairing hormonal signalling and thus, flower development. TENGU was also shown to suppress induced cell death (Wang *et al.*, 2018a) and to be processed by host proteases (Sugawara *et al.*, 2013).

The effector SAP11 impacts the development of the host plant and enhances its capacity to support reproduction of the insect vector through modulation of the jasmonate pathway (Sugio *et al.*, 2011a). SAP11 and its homologues were found to interact with specific transcription factors of the host (Sugio *et al.*, 2011a; Janik *et al.*, 2017; Wang *et al.*, 2018b; Chang *et al.*, 2018; Pecher *et al.*, 2019). Other reports indicated that SAP11 was also involved in interfering with the immune system and metabolic responses of the host plant (Lu *et al.*, 2014; Tan *et al.*, 2016). Importantly, immunolocalisation experiments showed that TENGU and SAP11 were found in plant tissues other than the phloem sieve tubes where phytoplasmas are confined, confirming that these effectors are secreted by phytoplasmas and then taken up by host sink tissues (Bai *et al.*, 2009; Hoshi *et al.*, 2009).

The effector SAP54 also known as PHYLLOGEN or PHYL1 induces spectacular transformations of floral parts into leaf-like organs through destabilization of MADS-box transcription factors of the host (MacLean *et al.*, 2011; MacLean *et al.*, 2014; Maejima *et al.*, 2014; Maejima *et al.*, 2015; Kitazawa *et al.*, 2017). SAP54 mediates degradation of MADS-domain transcription factor (MTF) by interacting with proteins of the RADIATION SENSITIVE23

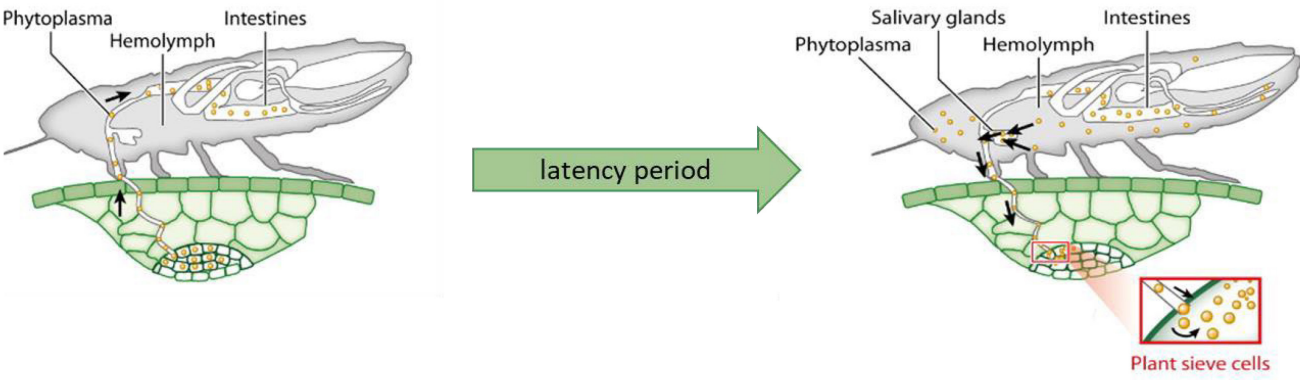

Figure 8. Acquisition of phytoplasmas and colonisation of their vector (adapted from *Sugio* et al.*, 2011b)*

(RAD23) family, eukaryotic proteins that shuttle substrates to the proteasome. Arabidopsis *rad23* mutants do not show conversion of flowers into leaf-like tissues in the presence of SAP54 and during phytoplasma infection, emphasizing the importance of RAD23 to the activity of SAP54. Remarkably, plants with SAP54-induced leaf-like flowers are more attractive for colonization by phytoplasma leafhopper vectors and this colonization preference is dependent on RAD23 (MacLean *et al.*, 2014; Orlovskis and Hogenhout, 2016).

The effector SAP05 of "*Ca.* P. asteris" binds plant SPL and GATA transcription factors and also to the plant ubiquitin receptor RPN10. Through this interaction, SAP05 mediates degradation of SPLs and GATAs via a process that hijacks RPN10, independent of substrate ubiquitination. The consequence is that SAP05 decouples plant developmental transitions and induces witches' broom symptoms (Huang et al., 2021).

3.2. Interaction of phytoplasmas with the insect host

Phytoplasmas are transmitted by leafhoppers (Cicadellidae), planthoppers (Fulgoroidea) and psyllids (Psyllidae) (Weintraub and Beanland, 2006) in a persistent-propagative manner (**Figure 8**). Phytoplasmas are acquired passively by the insect upon ingestion of sieve of an infected plant and multiplies within the insect tissues during host colonisation. Indeed, injection of tritiated thymidine in phytoplasma infected-*Euscelis lineolatus* abdomens followed by observation of ultrathin sections of the insects organs, revealed that phytoplasmas multiplication occurs both at the extracellular level (in hemolymph), as well as when phytoplasmas were inside the cells (in digestive tract and salivary glands) (Gouranton and Maillet, 1973). The feeding duration allowing to acquire a sufficient load of phytoplasma is called acquisition access period (AAP) and its duration depends on the insect-phytoplasma association considered. After their ingestion with infected sap, adhesion of phytoplasmas to apical surface of vector intestinal cells constitutes an initial and critical step in insect invasion. Then phytoplasmas have to cross a first barrier consisting in the midgut epithelium. During a latency period (LP) of few weeks, phytoplasmas enter in the circulatory system of the haemolymph finally reaching the salivary glands, the second insect barrier they have to cross. Once salivary gland cells are colonised, the insect become infective throughout its life. The transmission to healthy plants (inoculation access period, IAP)

is achieved upon injection of infected saliva while feeding in the sieve elements. Concerning FDp-*S. titanus* association, transmission assays performed in controlled conditions with newly emergent adults revealed that an AAP of 7 days followed by a LP of 7 days is sufficient to achieve FDp transmission to broadbeans, even though transmission efficiency reach its peak after 14 days of LP (Alma *et al.*, 2018). Moreover, phytoplasma loads measured in the insect increased with longer LP, confirming the phytoplasmas multiplication within the insect host. The study of spatiotemporal dynamics of onion yellow (OY) phytoplasma in its vector *Macrosteles striifrons* revealed that bacteria enter the midgut epithelium 7 days after the beginning of AAP (Koinuma *et al.*, 2020). Then, after 7-14 days of LP, phytoplasmas moved to visceral muscles surrounding the midgut and to hemocoel. After 14-21 days of LP, phytoplasmas enter into type III cells of salivary glands before colonising the insect brain, where evidences of their presence were observed after 34 days of LP.

3.2.1. Effect of phytoplasma colonization on insect vector population fitness

The impact of phytoplasma infection on insect vectors varies depending on the association considered. The leafhopper *Macrosteles quadrilineatus* is the vector of aster yellow phytoplasma (AYp). It has been found that females reared on plants infected with two different strains of AYp lived significantly longer and laid two times more eggs than females exposed to uninfected plants (Beanland *et al.*, 2000). *Dalbulus maidis* infected with the maize bushy stunt phytoplasma survived longer than non-exposed leafhoppers and the most remarkable increase in survival was for the insect population simultaneously exposed to two phytoplasma strains (Ebbert and Nault, 2001). On the contrary, *Scaphoideus titanus* exposed to FDp lived significantly less and produced less offsprings than insects fed on uninfected broad beans (Bressan *et al.*, 2005). The assessment of *S. titanus* female fecundity revealed that FDp infected insects had a reduced number of fully sized eggs when compared to uninfected females. Moreover, eggs showed a significant delay in hatching and the number of nymphs emerging from eggs laid by infected females was significantly lower comparing to non-exposed females (Bressan *et al.*, 2005).

The impact on vectors fitness could be direct or indirect through manipulation of plant physiology operated by phytoplasma effectors. We already mentioned the improved survival

and fecundity of *M. quadrilineatus* reared on AY-WB infected plants. It has been demonstrated that the same effects on insect fitness could be obtained by rearing insects on transgenic plants expressing the effector SAP11. This increase was correlated with a decrease of jasmonate production by the plant, a phytohormone involved in response to herbivory (Sugio *et al.*, 2011a). It was further shown that SAP11 binds to CINCINNATA-related TEOSINTE BRANCHED1, CYCLOIDEA, PROLIFERATING CELL FACTORS 1 and 2 transcription factors (CIN-TCPs), which physiologically regulates plant development and indirectly promotes jasmonate synthesis through the regulation of the expression of lipoxygenase LOX2, normally up-regulated upon insect exposure. Interestingly, not only AY-WB infected insects experienced increase fecundity on AY-WB plants. It has been found that even non-infected insects laid significantly more eggs once transferred to AY-WB infected plants, well before phytoplasma can infect and complete its cycle within the insect, demonstrating that the increased fecundity derived from the manipulation of the plant and not of the insect.

It has been demonstrated that apple trees infected with "*Ca.* P. mali" emitted higher amounts of β-caryophyllene, a sesquiterpene allomone that attracts newly emerged females of the vector *Cacopsylla picta* (Mayer *et al.*, 2008a; Mayer *et al.*, 2008b). This indirect manipulation of the insect behaviour can result in an increase in the number of transmitting vectors among the insect populations and could counteracts the fact that *C. picta* laid significantly more eggs on leaves of non-infected plants when compared to "*Ca.* P. mali" infected plants (Mayer *et al.*, 2011; Görg *et al.*, 2021). Moreover, infection of apple by "*Ca.* P. mali" has been showed to decreased offspring body size and increase the mortality of *C. picta* (Mayer *et al.*, 2011). "*Ca.* P. mali" direct impacts on insect fitness have also been demonstrated. Transcriptome comparative analyses of *Cacopsylla melanoneura* infected and non-infected with "*Ca.* P. mali" revealed that phytoplasma infection was correlated with an upregulation of genes involved in signalling and neurogenesis, light response, molecular clock and circadian rhythm (Weil *et al.*, 2020). In particular, the phytoplasma infection may have an impact on the NF-kB mediated insect defence resulting in a down regulation of the immune response and stress signalling that could result in the increased survival of the vector. Moreover, phytoplasma infection could have major effects on the insect flight behaviour. The results suggested an increase in movement of infected insects, as already observed in *E. variegatus* infected with CYp (Galetto *et al.*, 2018).

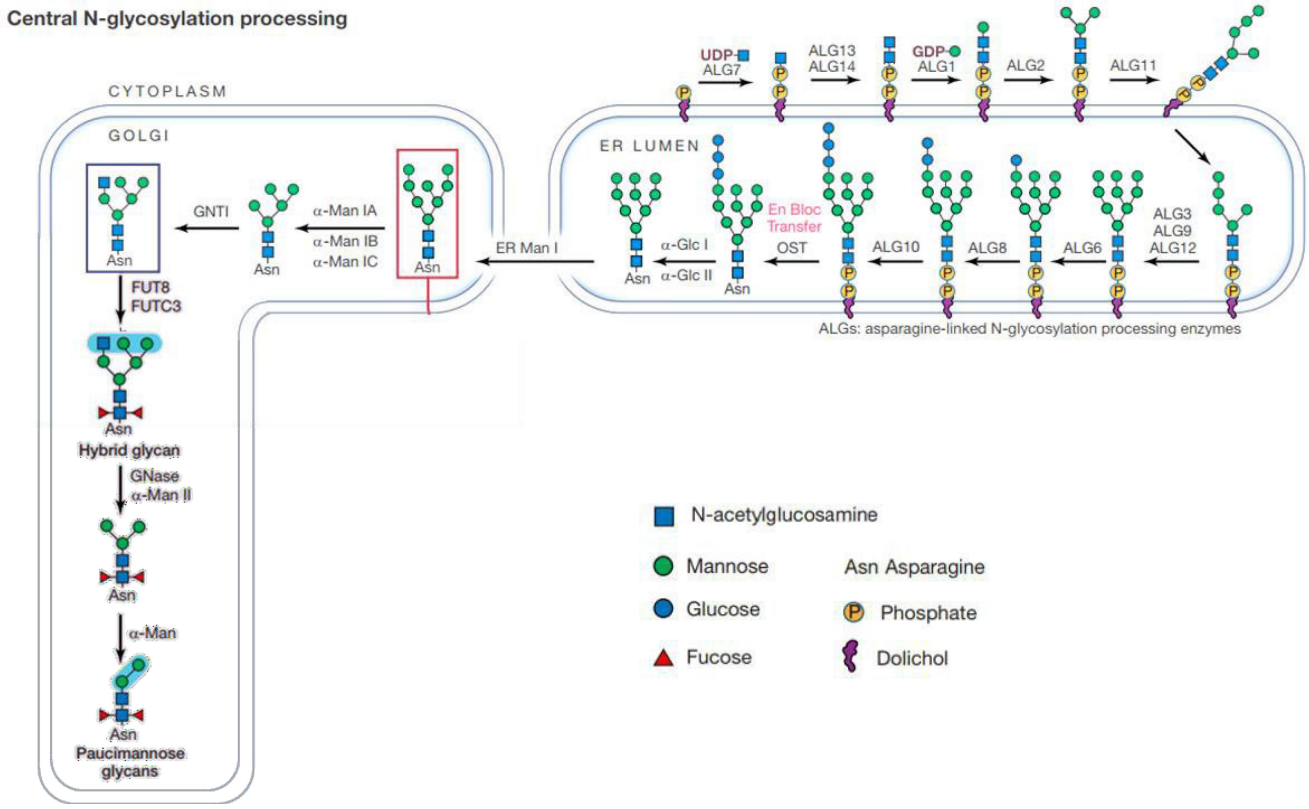

Figure 9. Schematic representation of N-linked glycosylation pathways in insects *(adapted from Chung* et al.*, 2017)*

3.2.2. Structure of the insect midgut

Hemipterans digestive tube is characterised by possessing a perimicrovillar membrane (PMMs), a membrane covering the microvillar membrane in the gut lumen. This structure is considered a specialisation typical of insect having a very diluted diet, such as xylem and phloem feeders (reviewed in Gutiérrez-Cabrera *et al.*, 2016). In fact, in terms of nutrients absorption, especially when present at very low concentration, PMMs is more efficient in terms of exchanges than the classic chitin-containing peritrophic membrane (PM) characterising the majority of insect orders. PMM actively transports potassium ions from the perimicrovillar space to the midgut cells, generating a gradient which enable the absorption of nutrients like amino acids and sugars from the sap in the gut lumen into the perimicrovillar space through the carriers present at PMM level and then at microvillar membrane (MM) level. This specialisation, coupled with the presence of filter chamber linked to PMM at midgut level, is important to cope with diluted diets and to avoid the extreme dilution of haemolymph. PMM composition is similar to that of MM as both are rich in sterols, Mg^{2+} and $Na^{+}K^{+}$ ATPases, carbohydrate-binding molecules and glycoconjugates, especially rich in mannose residues (Gutiérrez-Cabrera *et al.*, 2016).

Glycosylation is a post translational modification consisting in the attachment of an oligosaccharide chain to the peptide backbone and it consists of two categories depending on the amino acids on which the oligosaccharide chain is linked. The N-glycosylation is linked to asparagin residues and the O-glycosylation to serine or threonine residues. N-glycosylation is the most abundant glycosylation in insects and paucimannose N-glycan type, characterized by a reduced number of mannose residues, has been shown to be the most abundant protein glycosylation in *Drosophila melanogaster* (Schachter, 2009). N-glycosylation occurs at the level of endoplasmic reticulum and Golgi apparatus during protein maturation. The initial processing pathway of N-linked glycosylations takes place in the endoplasmic reticulum and it is quite similar for all eukaryotes (**Figure 9**). Several asparagine-linked N-glycosylation processing enzymes (ALGs) generates a lipid-linked oligosaccharide which is then transferred onto the polypeptide backbone by an oligosacharyl transferase (OST). The polypeptide modification occurs at the level of an asparagine (N) residue followed in the protein amino acidic sequence by any amino acid but proline (P) and then by a serine (S) or threonine (T) (NxS/T sequence). The process continues in the Golgi apparatus, where modifications diverge

significantly among distant species. In insects, mannosidase and N-acetylglucosaminidase trim the mannose and N-acetylglucosamine residues (GlcNAc), resulting in the formation of paucimannosidic glycans ($Man_{1-3}GlcNAc_2$) or oligomannosidic glycans ($Man_{5-9}GlcNAc_2$). Another feature of N-glycosylation typical of insects is the presence of up to two fucose residues on the innermost GlcNAc.

A comparative survey led to the description of the glycoproteome of five insect species belonging to five different orders and revealed a huge diversity in glycosylation profiles (Vandenborre *et al.*, 2011). In this study, insect glycoproteins were purified using a Galanthus Nivalis Lectin (GNA)-coupled affinity column, which specifically bind to mannose, and the retained proteins were identified through mass spectrometry analysis. The five species shares only 1.5% of common glycosylated proteins. The percentage of glycosylated proteins categorised according to their biological role varies depending on the orders. Among the glycoproteins identified in the global set, the authors found typical membrane proteins such as laminin, cadherin, contactin, chaoptin, C-type lectins, transport proteins, metabolic processes-related proteins and many transmembrane proteins containing leucine-rich repeat (LRR). The number of identified LRR proteins in the different orders reflect the diversity in glycoproteome profiles. For instance, 14 glycosylated LRR proteins have been found in *Acyrthosiphon pisum* (Hemiptera) meanwhile only 4 LRR have been identified in *Tribolium castaneum* (Coleoptera) and only one in *Drosophila melanogaster* (Diptera). Glycosylated LRR proteins were neither found in *Bombyx mori* (Lepidoptera) nor in *Apis mellifera* (Hymenoptera). Glycosylation profiles can change even within the same species according to reproductive and developmental stages (Vandenborre *et al.*, 2011).

4. Adhesion of bacteria to eukaryotic cells and entry

Bacteria have evolved a plethora of mechanisms to interact with their host cells, but we can resume the early stages of this interaction in two main strategies, the “zipper” and the “trigger” mechanism (Swanson and Baer, 1995). Both mechanisms innescate the reorganisation of the cytoskeleton of the host cells, culminating in the internalisation of the bacteria. The “zipper” mechanism begins with the binding of the bacteria to the receptors present at the surface of their host cell through adhesins. For example, *Listeria*

monocytogenes InlA and InlB surface proteins interact respectively with E-cadherin and the hepatocyte growth factor receptor, two proteins exposed at the surface of epithelial cells. This interaction triggers a signal cascade which also involves the chlatrin mediated endocytosis machinery (reviewed in Ribet and Cossart, 2015). The "trigger" mechanism implicates the secretion of bacterial effectors which, once injected in the cytosol of the host cell, allow the extensive rearrangement of cytoskeleton forming membrane protrusions, called "ruffles", which ultimately inglobe the bacterial cell. This process involves the bacterial type III secretion system (T3SS), a needle-like complex of proteins called the injectisome, which allows the injection of secreted soluble effectors into the host cells. *Salmonella typhimurium* exploits it to deliver in the cytosol of the host cells a mix of effectors activating Rho GTPases stimulating actin rearrangements and allowing membrane ruffling (Hardt *et al.*, 1998).

A very peculiar "trigger" strategy involving adhesins has been described in enteropathogenic and enterotoxigenic *E. coli*. These *E. coli* strains are characterised by a genomic region called *locus* of enterocyte effacement (LEE) which codes for a T3SS, chaperons and effectors that will be translocated through the bacterial cell wall and the host cell membrane into the host cytosol via the T3SS injectisome. One of these effectors named "translocated intimin receptor" (Tir), will be integrated into the host cell membrane and serve as a receptor for a LEE encoded adhesin, the intimin (Kenny *et al.*, 1997). In other words, the pathogen not only codes for its adhesin but also for its receptor which is delivered through the injectisome and integrated into the host cell surface. The Tir-intimin interaction triggers a signal cascade leading to cytoskeletal rearrangements allowing the formation of a pedestal-like structure for the attachment of bacteria to host intestinal epithelial cells (reviewed in Pizarro-Cerdá and Cossart, 2006).

Regarding phytoplasmas, only the Sec-dependent protein secretion system was found to be encoded in their genomes (Kube *et al.*, 2012). As this system was not reported to support injection of bacterial proteins in the host-cell from extracellular bacteria, we will therefore illustrate examples of "zipper" mechanisms of interaction between pathogens and their hosts. Even though the strategies and structures used to achieve adhesion can be very different, we will see with examples how they share common features such as the bacterial adhesin binding to glycosylated proteins of the eukaryotic host.

Streptococcus suis is a worldwide zoonotic agents causing meningitis in both pigs and humans and a model in the study of streptococcal infections. It has been shown that *S. suis* adhesion to the pig pharyngeal epithelium involves the binding of its adhesin SadP to Galα1-4Gal- (galabiose) containing glyconcojugates. SadP is anchored in the cell wall and presents in its C-terminal part seven tandem repeats of 57 amino acids rich in glutamate and proline (Kouki *et al.*, 2011). *Streptococcus pyogenes,* responsible for cutaneo-mucosal infection in humans is characterised by a variety of adhesins. The process of its adhesion to cells begins with the adhesion to host extracellular matrix proteins, in particular fibronectins and collagen, with more than a dozen different adhesins. The binding with extracellular matrix fibronectin creates a sort of bridge allowing the integrin-mediated internalisation of bacteria into host cell (Kreikemeyer *et al.*, 2004). Interestingly, the same adhesion and internalisation strategy has evolved in the phylogenetically distant *Staphylococcus aureus* (Massey *et al.*, 2001).

Particular bacterial structures, the fimbrias, are bacterial pili with a role in adhesion to a surface. They are anchored to the bacterial outer membrane and are characterised by the presence of an adhesin conferring binding specificity at the tip of their scaffold. Uropathogenic *E. coli* strains present pyelonephritis-associated pili (P-pili) and type I pili. The first type mediates the binding to Galα-(1-4)-Gal moieties of different glycolipids presents on urinary tract cells through the adhesin PapG. Differential expression of PapG variants has been shown to drive tissue and host specificity (Hultgren *et al.*, 1991). The type I pili characteristic adhesin is called FimH. It recognizes mannose residues on glycoprotein of host cells with different affinity depending on the virulence of the strain. In fact, FimH of commensal bacteria shows an higher affinity for trimannose residues meanwhile uropathogenic strains FimH are characterised by an higher affinity to monomannose residues that are particularly enriched on urinary tract cells. The binding of FimH to the manomannose residues of the uroplakin 1a present on bladder cells triggers a signaling cascades leading to the uptake of bacteria (reviewed in Pizarro-Cerdá and Cossart, 2006).

The role of adhesins in the early stages of host infection is also important for vector-borne plant pathogens. For example, *Xylella fastidiosa* is capable of infecting a variety of host plant species. *X. fastidiosa* cycle in the vector is multiplicative but not circulative and after molting, the vector loses its infectivity due to the shed of the foregut which is the part of the exoskeleton colonised by this bacterium, at the precibarium and the cibarium (Purcell and

Finlay, 1979; Almeida and Purcell, 2006). In the plant, *X. fastidiosa* colonizes the xylem vessels and can only be acquired by its insect vectors sharpshooters, leafhoppers and spittlebugs, once its cell population achieves a critical density within the plant vessels, switching from a plant to an insect-colonising phenotype (Newman *et al.*, 2004; Almeida *et al.*, 2005). Plant pectin degradation by *X. fastidiosa* during xylem vessel colonisation induces an important shift in its phenotype and gene expression, allowing the bacteria acquisition by the vector. In fact, a building block of pectin, the Na-galuctoronate, freed by its degradation, is responsible for the up regulation of several *X. fastidiosa* genes involved in its pathogenicity and ability to adhere to surfaces. This includes the afimbrial adhesins HxfA and HxfB which are involved in the initial colonisation of the vector mouthparts (Killiny and Almeida, 2009b; Killiny and Almeida, 2014). Adhesion competition assays performed on foregut extracts of leafhopper vector revealed that HxfA and HxfB have an affinity for mannose and a stronger one for N-acetylglucosamine, the monomeric moiety of chitin. The presence of N-acetylglucosamine completely disrupts bacterial adhesion to foregut protein extracts (Killiny and Almeida, 2009a). Transmission assays indicated that HxfA and HxfB were primarily important for early adhesion to vectors, while the fimbrial adhesin FimA was necessary for both adhesion and retention to the insect vector foregut. (Killiny and Almeida, 2014).

The mollicute *Spiroplasma citri* is a cell wall-less helicoidal and motile bacteria which is cultivable *in vitro*. *S. citri*, like phytoplasmas, is transmitted to plant by leafhoppers such as *Circulifer haematoceps* in a persistent and propagative manner. Two spiroplasma adhesins have demonstrated to be central for its adhesion to vector cells and insect infection. *In vitro* interaction assays demonstrated that spiralin, the *S. citri* most abundant membrane lipoprotein, binds to glycoproteins of the insect vector (Killiny *et al.*, 2005). Laser scanning microscopy observations allowed to demonstrate that spiralin relocalizes in the portion of the *S. citri* membrane surface in contact with vector cells, that the ability of spiralin-lacking mutants to adhere to the insect cells was impaired and that latex beads coated with recombinant spiralin were able to adhere to vector cells. Moreover, competition assays with lectins indicated that spiralin had lectin type properties similar to that of the *Vicia villosa* agglutinin (VVA) lectin (Duret *et al.*, 2014). Plasmids pSci1 to pSci5 present in insect-transmissible strains of *S. citri* contain eight genes coding for *S. citri* adhesion related proteins (ScARPs) (Yu *et al.*, 2000; Berg *et al.*, 2001; Saillard *et al.*, 2008). ScARPs share a common

structure consisting in a N-terminal signal peptide, a domain consisting in 6-8 repeated sequences of 39-42 amino acids, a C-terminal transmembrane helix followed by a conserved stretch of charged amino acids. It has been demonstrated that the ScARP domain (Rep3d) of ScARP3d is implicated in the binding of *S. citri* to *C. haematoceps* cells in culture but also in the internalisation of Rep3d coated latex beads triggering a mechanism involving actin polymerisation of insect cells (Béven *et al.*, 2012).

4.1. Membrane proteins of phytoplasmas and interaction with insect vectors

Phytoplasmas are cell-wall less bacteria and therefore their membrane proteins have an important role in the interaction with host cells, being at the interface between the two organisms. The most studied phytoplasma membrane proteins are the so called immunodominant membrane proteins (IDPs), namely immunodominant membrane protein (Imp), immunodominant membrane protein A (IdpA) and antigenic membrane protein (Amp) (Kakizawa *et al.*, 2006b). IDPs are characterised by a high amino acid sequence variability among closely related phytoplasma strains. The high proportion of non-synonymous mutations found in *amp* and *imp* genes of phytoplasma strains indicated that these genes were submitted to a strong diversifying positive selection pressure and hence suggesting their role in adaptation (Kakizawa *et al.*, 2006a; Fabre *et al.*, 2011; Siampour *et al.*, 2013).

The Amp of the "*Ca.* P. asteris" strain OY (OYp) colocalises with microfilaments of the visceral smooth muscle surrounding the intestine of its insect vector *Macrosteles striifrons*. *In vitro* interaction assays confirmed that Amp binds to actin, myosin light and heavy chains (Suzuki *et al.*, 2006). Moreover, it has been shown that the Amp-microfilament complexes (AM complex) have a role in vector specificity. Indeed, affinity columns exposing the OYp Amp was able to retain the actin of three vectoring leafhoppers species but not the actin of two non-vectoring leafhopper species. In another study, Amp of the "*Ca.* P. asteris" strain chrysantemum yellow phytoplasma (CYp) has been shown to interact with actin and subunits α and β of ATP synthase of the vector *E. variegatus* (Galetto *et al.*, 2011). Even though ATP synthase is known to be a mitochondrial protein, confocal microscopy observation and *in vitro* interaction assays also revealed its ectopic localisation at the outer surface of midgut and salivary gland cells of the insect, suggesting its role as receptors for Amp protein. The role of

CYp Amp protein in the competence of the insect vectors *Macrosteles quadripunctulatus* and *E. variegatus* has been confirmed *in vivo* by demonstrating that pre-feeding of insect with anti-Amp antibody decreased both the acquisition efficiency of phytoplasma and its inoculation to plants (Galetto *et al.*, 2011; Rashidi *et al.*, 2015).

The Imp protein of FD phytoplasma has been shown to bind to membrane protein extract of vector species such as *E. variegatus* and *S. titanus* but not to extract of non-vector species, suggesting its role in vector specificity (Trivellone *et al.*, 2019). Imp protein of Wheat Blue Dwarf (WBD) phytoplasma interacts with α-tubulin of its vector leafhopper *Psammotettix striatus* (Ding *et al.*, 2022). The inhibition of α-tubulin expression in living insects achieved upon RNAi technology resulted in a significant decrease of the phytoplasma transmission efficiency to wheat seedlings when compared to control insects.

Variable membrane proteins (Vmps) are exposed to the outer side of phytoplasma cell and are characterised by a common organisation. They possess a signal peptide at their N-terminus, a variable number of large repeated domains of 78-82 amino acids and a C-terminal hydrophobic transmembrane domain anchoring the protein into the cell membrane. Variability of *vmp*1 among twelve different isolates of "*Ca.* P. solani" (formerly known as Stolbur phytoplasma) revealed differences in protein size due to variations in the number of repeated domains as well punctual, essentially non-synonymous mutations. Vmp1 appeared much more variable than house-keeping genes taken as reference (Cimerman *et al.*, 2009).

Two genes, *vmpA* and *vmpB*, encoding proteins with no homology with each other or with Vmp1 but displaying a similar organisation with repeated domains of 78 amino acids were found in the chromosome of the FDp strain FD92. As we detailed above, *vmpA* and *vmpB* turned out to be variable in size and sequence. Both VmpA and VmpB of the FDp strain FD92 (map genotype M54, map-FD2 cluster) possesses three repeated domains while VmpA and VmpB of strain FD-CAM05 (*map* genotype M50, cluster map-FD1) possess four and two repeated domains respectively. Variation of VmpA and VmpB in a set of European isolates revealed that their sequences grouped into three phylogenetic clusters that corresponded to transmission specificity by different leafhopper species: only cluster II and III could be transmitted by Deltocephalinae leafhoppers including *S. titanus* (Malembic-Maher *et al.*, 2020). According to their structure, VmpA and VmpB are anchored by their C-terminal transmembrane hydrophobic domain to the FDp membrane. The large central hydrophilic part

of the proteins containing the repeated domains are therefore exposed to the FDp surface. Antibodies raised against their repetitive central hydrophilic parts allowed to detect VmpA and VmpB in FDp infected *Vicia faba* and in infected *E. variegatus* indicating that both genes are expressed during plant and insect vector colonisation (Malembic-Maher *et al.*, 2020).

VmpA has been demonstrated to mediate the binding to the midgut epithelium cells of the insect vector *E. variegatus* (Arricau-Bouvery *et al.*, 2018). Beads coated with recombinant VmpA-His_6, showed an increased adhesion to *E. variegatus* cells in culture when compared to control beads coated with GFP. Moreover, competition assays revealed a strong decrease in VmpA-coated beads adhesion to cells after incubation of the beads with anti-His_6-VmpA antibodies. The important role of VmpA in adhesion to insect cells have been demonstrated by using a recombinant *S. citri* deficient for adhesion and expressing VmpA at its surface (Renaudin *et al.*, 2015): spiroplasmas expressing VmpA showed a statistically significant increase in adhesion to *E. variegatus* cells when compared to control spiroplasmas. Ingestion of fluorescent VmpA-coated beads by *E. variegatus* insects allowed to observe the presence of such beads in dissected midguts and filter chambers at 1-, 2- and 4-days post acquisition feeding. Observation by transmission electron microscopy on dissected digestive tubes confirmed the observation made by fluorescence microscopy and revealed the presence of beads embedded in the perimicrovillar membranes covering the apical surface of epithelial cells in the midgut (Arricau-Bouvery *et al.*, 2018).

Digestive tubes and salivary glands of infected *E. variegatus* and *S. titanus* have been stained with different fluorescent lectins and observed by laser scanning microscopy, revealing patches of phytoplasma localised nearby aggregates of GNA, Lens Culinaris lectin (LCA) and Lycopersicon Esculentum lectin (LEL) (Arricau-Bouvery *et al.*, 2021). Such structures could not be seen in control uninfected insect organs, suggesting that phytoplasmas induce the gathering of glycoproteins that can be bound by these lectin types. Recombinant VmpA-His_6 was then incubated with the different sugars recognised by GNA (mannose), LCA (glucose and mannose), and LEL (N-acetylglucosamine) at different concentration. Then, the adhesion ratio of recombinant VmpA to cells have been estimated. When pre-incubated with mannose, VmpA showed an increased adhesion to cells in a dose-dependent manner meanwhile pre-incubation with N-acetylglucosamine results in the decreased VmpA adhesion to cells. In competition assays, a statistically significant decrease in VmpA-His_6 coated fluorescent beads

adhesion to Euva cells has been observed when cells were pre-incubated with LCA, GNA and LEL lectins, suggesting VmpA shares the same substrates, *i. e.* glycoproteins exposing mannose and N-acetylglucosamine residues (Arricau-Bouvery *et al.*, 2021). Far-western blot analysis revealed two interesting features of VmpA interaction with Euva cells proteins: i) pre-incubation of VmpA with N-acetylglucosamine totally inhibited the VmpA interaction with Euva proteins larger than 40 kDa and ii) pre-incubation of VmpA with mannose resulted in a stronger interaction with high molecular weight proteins, in agreement with the enhanced adhesion of recombinant VmpA-His_6 to Euva cells in the presence of mannose. Moreover, VmpA-coated beads pre-incubated with mannose and observed at fluorescent microscopy tends to form aggregates when compared to untreated VmpA-coated beads. Taken together these results suggest that VmpA binds to mannose and the binding results in the formation of VmpA multimers that can increase the affinity of this adhesin for proteins glycosylated with N-acetylglucosamine residues.

Pull down assays using VmpA-His_6 coated beads and proteins extracted from *E. variegatus* salivary glands shows that VmpA interacts, at least in vitro with AP-2, an adaptor protein involved in clathrin-dependent endocytosis (Arricau-Bouvery *et al.*, 2023). The internalisation of FDp by *Drosophila* S2 cells in the presence of drugs inhibiting the clathrin-dependent endocytosis such as chlorpromazine was decreased when compared to FDp entry into non treated cells. RNAi mediated gene silencing targeting clathrin heavy chain of the S2 cells showed a similar inhibition of FDp internalisation. However, phytoplasma entry has not completely been impaired, suggesting either a residual internalisation due to a residual expression of clathrin or another entry pathway into the cells. This latter hypothesis is supported by the strongest inhibition of phytoplasma entry into S2 cells treated with cytochalasin D, an inhibitor of actin polymerisation implicated in other endocytosis processes. Laser scanning microscopy observations on FDp infected S2 cells expressing recombinant clathrin heavy chain coupled with GFP revealed a colocalization of phytoplasmas stained with an anti-VmpA antibody and clathrin heavy chain at the surface of the cells. *In vivo* RNAi experiments performed on *E. variegatus* through ingestion of dsRNA targeting clathrin heavy chain revealed a significant lower quantity of phytoplasma elongation factor (*Tuf*) transcripts in both heads and abdomens when compared to control uninfected insects (Arricau-Bouvery *et al.*, 2023).

In summary, VmpA is involved in the interaction between FDp and insect cells since the early stages of insect infection, in particular in the adhesion to insect cells and the subsequent internalisation of the bacteria.

4.2. The pathogen-host interface as target to cope with vector-borne diseases

FAO pesticide definition is “substance or mixture of substances attended for controlling, preventing, destroying any pest, animal, or human disease-causing vectors, undesirable plants, or animal species affecting food production, managing, selling, storage, and transportation”. In 2019, the global amount of pesticide applied was approximately 4.19 million metric tons, and insecticides account for 29.5% of the total (reviewed in Pathak *et al.*, 2022). Nowadays, the deleterious off-target impact of insecticides on the environment and on human health has been widely reported by researchers. The threat concerning the environment includes pesticides persistence, their degradation and migration outside their area of application by transfer processes such as adsorption, leaching, volatilization, spray drift, and runoff (reviewed in Tudi *et al.*, 2021) as well as their bioaccumulation in off-target species leading to detrimental effects on biodiversity. The impact on human health can virtually impact all consumers, although the most concerned categories are farmworkers directly applying the products in their field and the inhabitants of rural areas surrounding cultivated fields, especially in countries that still employs persistent organic pollutants such as dichlorodiphenyltrichloroethane (DDT) (Pathak *et al.*, 2022).

Main measures for limiting the spread of vector-borne diseases include the application of insecticide treatments but promising preliminary results suggest that alternative approaches, aiming at reducing the transmission instead of the vector population could be possible. The disruption of the interaction between a pathogen and its vector could use two different approaches, targeting the pathogen protein or the insect receptor binding site. In the field of human health, bacterial adhesins are promising targets for new antimicrobial drugs to overcome the problematics associated with the use of antibiotics. Various strategies acting at the level of the adhesion of bacterial cells have been undertaken for disease treatments (Asadi *et al.*, 2019). The use of compounds mimicking the natural ligand of the adhesin made it less likely that the bacteria develop resistance to the drugs than with bactericidal

compounds (Ofek *et al.*, 2003). Similarly, new strategies of vector-borne diseases management could be developed targeting proteins involved in early stages of insect vectors infection due to their central role in pathogen transmission. Approaches giving promising preliminary results are the use of molecules, proteins or recombinant peptides to outcompete bacterial adhesin binding to the vector proteins. In the case of *X. fastidiosa* HxfsA and HxfsB, the administration of particular sugars or lectins to insect has been demonstrating to lower the transmission efficiency of the pathogen to plants (Killiny *et al.*, 2012). Indeed, the addition of lectins binding N-acetylglucosamine residues in the artificial diet of the vector leafhopper *Graphocephala atropunctata*, partially impaired the transmission of *X. fastidiosa* to plants due to the saturation of receptor binding sites. Similarly, addition of carbohydrates containing N-acetylglucosamine binding to the bacteria cell surface lectins, resulted in a reduced rate of successful transmission (Killiny *et al.*, 2012). However, transmission was not completely blocked, suggesting the complexity of biofilm formation allowing vector colonisation. Promising results have been obtained through the synthesis of recombinant peptides designed on *X. fastidiosa* chitin binding proteins. Recombinant peptides delivered *via* an artificial diet system outcompeted bacterial adhesion to insect mouthparts cells, lowering or completely blocking vector transmission efficiency to plants up to 10 days post acquisition in controlled conditions (Labroussaa *et al.*, 2016).

Similarly, a peptide (GBP 3.1) binding to the midgut and hindgut of the aphid *Acyrthosiphon pisum* has been identified and tested for its role in relation to Pea enation mosaic virus (PEMV) infection. Aphids fed on artificial diet containing GBP 3.1 prior to acquisition of PEMV from infected plants showed a reduced uptake of virions from the gut to the haemocoel of the vector, impairing the viral persistent transmission requiring virion accumulation in the haemocoel in the insect (Liu *et al.*, 2010). Another study demonstrated how transgenic rice expressing the spike protein of Rice ragged stunt oryzavirus (RRSV) showed a good resistance to viral infection. Furthermore, the planthopper vector of RRSV *Nilaparvata lugens* fed on transgenic plants was well protected against RRSV infection once transferred onto RRSV infected plants (Chaogang *et al.*, 2003).

Preliminary works focusing on plantibody-mediated resistance approach have proven, at least conceptually, to be worth of further investigation as a way to cope with phytoplasma infection. Again, in this strategy, phytoplasma adhesins could be interesting targets for the

production of antibodies by transgenic plant hosts. This could decrease the infection ratio of the insect vector thanks to the masking of the adhesin as demonstrated *in vitro/ex vivo* for Amp of CY aster yellow phytoplasma (Rossi *et al.*, 2019b).

Silencing mediated by dsRNA gave promising results on both the experimental and natural vector of FDp in laboratory conditions. The administration of dsRNA targeting actin filaments and ATP synthase β by microinjection leads to an almost complete silencing of both genes which lasts up to 14 days, resulting in a significant decrease of insects survival (Abbà *et al.*, 2019). Furthermore, the microinjection of *E. variegatus* with dsRNA targeting ATP synthase β induces nearly complete female sterility (Galetto *et al.*, 2021b) as well as significant decrease in phytoplasma multiplication within the vectors (Galetto *et al.*, 2021a). The impact has been evaluated on *S. titanus* females as well, revealing an alteration of developing eggs morphology in ovaries (Ripamonti *et al.*, 2022b). dsRNA targeting clathrin heavy chain and delivered *via* artificial feeding to *E. variegatus* efficiently decreased the expression of the gene in both insects heads and abdomens and resulted in a decreased phytoplasma colonization of midgut and salivary glands (Arricau-Bouvery *et al.*, 2023).

Efforts are made to better understand the potential and the limits of dsRNA delivery in field conditions. Host Induced Gene Silencing (HIGS) rely on the expression of dsRNA or siRNA by the plant host. Once the insect, in our case, feeds on the plant, it acquires the RNA molecules which will trigger its RNAi response. The first transgenic commercial corn plant expressing an hairpin dsRNA targeting an essential gene of the western corn rootworm has recently received the authorisation for commercialisation in China and USA (SmartStax® Pro, Bayer CropScience). Virus induced Gene Silencing (VIGS) exploits recombinant viruses for specific delivery of dsRNAs (reviewed in Kolliopoulou *et al.*, 2017). One of the main advantages of this techniques is that virus can be very host-specific, thus not impacting off-target organisms. Furthermore, dsRNAs production would take place directly in the insect cells, overcoming the difficulty in dsRNAs uptake from the environment that could explain the low response to RNAi characterising certain insect species. Other VIGS-like technologies exploits various engineered micro-organisms such as bacteria, yeast as well as insects symbionts (Whitten *et al.*, 2016; Zhang *et al.*, 2019; Mysore *et al.*, 2021). However, the release of recombinant viruses and engineered organisms in the environment arises serious questions about the ecological implications of such treatments *i.e.* effects on off-target species and

possible widening of the host range. Furthermore, the possibility of using GMOs for agricultural application is still controversial in Europe. Nevertheless, other methods not involving transgenic organisms can be exploited to trigger RNAi response in insect in the field. Spray Induced Gene Silencing (SIGS) consists in the application of solutions containing dsRNAs on the host plant surfaces and delivered to the insect upon its feeding on plant tissues. Efforts to adapt RNA molecules delivery to field conditions have recently been made aiming at overcoming the limits of SIGS, such as the short persistence of "naked" dsRNA in the environment. Chemical modification of naked dsRNAs, using of nanocarriers such as lyposomes, polymers (Jain *et al.*, 2022) and peptides (Numata *et al.*, 2014) as well as delivery in the plant by trunk injections or petiole absorption (Dalakouras *et al.*, 2018) have been showed to increase the stability of dsRNAs in the environment, resulting in a boost in the efficiency of RNAi strategies to cope with pests in the field (reviewed in Christiaens *et al.*, 2020).

5. Aim of the work and experimental outline

The management of FD spreading preconizes the control of the vector population size through insecticide treatments. In a context of reduction of pesticides, other approaches and tools need to be developed to control crop related vector-borne diseases. To achieve this goal, we need to gain as much information as possible on the interactions occurring between the pathogen and its vectors, in order to identify the main factors involved in vector infection, competence and transmission to the host plant.

As we mentioned in the previous section, sequences of VmpA and B of FD phytoplasma are correlated with *Scaphoideus titanus* capability to transmit the pathogen and therefore, to the epidemic potential of the phytoplasma strain (Malembic-Maher *et al.*, 2020). VmpA is a phytoplasma adhesin implicated in the binding to the midgut of the insect vectors *S. titanus* and *E. variegatus* (Arricau-Bouvery *et al.*, 2018; Malembic-Maher *et al.*, 2020). VmpA shows lectin properties, with a specific binding to N-acetylglucosamine and mannose residues on insect cells (Arricau-Bouvery *et al.*, 2021). Identifying the proteins interacting with VmpA in insect cells could not only allow to better understand the early stages of insect infection and

cell colonisation but could also help in the development of new strategies to control FD spread, disrupting the insect infection and, therefore, the transmission of the pathogen within the vineyard. Moreover, deciphering the factors responsible for vector competence in epidemic strains of FD phytoplasma could allow the prediction of new potential insect vectors among the emergent allochthonous species that could spread within new areal distribution in the climate change context.

We started to look for insect vector proteins potentially interacting with FDp VmpA using two different approaches. On one side we employed a targeted approach, with special emphasis on insect vector transmembrane proteins with potential for glycosylation. To do so, we performed two different *in vitro* interaction assays, to enrich and identify through mass spectrometry analysis the *E. variegatus* proteins experimentally interacting with VmpA. Among the identified proteins, the more interesting candidates were screened for their role as receptor in a simplified model system consisting in *E. variegatus* cultured cells (the interface of the vector) and latex fluorescent beads coated with a recombinant VmpA of the FDp strain FD92 ("mimicking" the phytoplasma). This gave us the opportunity to assess the efficiency of dsRNA mediated RNAi response of *E. variegatus* cultured cells, up to this day demonstrated only in *E. variegatus* insects through feeding or microinjection (Abbà *et al.*, 2019; Galetto *et al.*, 2021a; Galetto *et al.*, 2021b; Ripamonti *et al.*, 2022b; Arricau-Bouvery *et al.*, 2023). In order to assess the role of protein interaction with VmpA in the vector competence, we attempted to compare in our assays VmpA from both a *S. titanus* transmissible and non-transmissible strain of phytoplasmas belonging to 16Sr group V, strains FD92 and PGYA, respectively. This approach and the obtained results are described in chapter 1.

On the other side, we tried to investigate the protein-protein interactions possibly occurring between VmpA and the insect vector proteins at a wide transcriptome level. In chapter 2, we will present the setting up of a classic Yeast Two-Hybrid assay to assess if *E. variegatus* proteins interact with VmpA of the *S. titanus* transmissible strain FD92 in an heterologous expression system consisting in *Saccharomyces cerevisiae* cells.

Materials and Methods

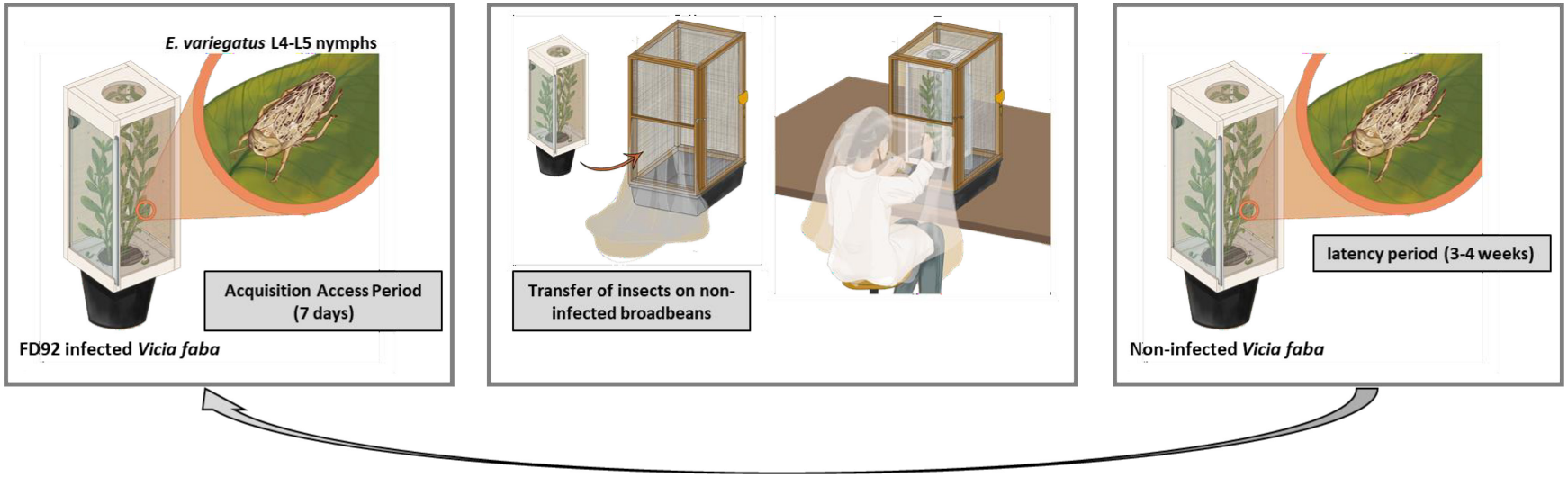

Figure 10. Acquisition transmission assays to propagate FD phytoplasma isolate FD92 in controlled conditions. Custom illustrations by Gaëlle Duflot (https://www.gaelleduflot-illustrations.net/).

1. Insect rearing, cell lines and bacteria

E. variegatus leafhoppers were originally collected in Villenave d'Ornon, France. They were reared in cages on broad beans *Vicia faba* var. aquadulce and oats *Avena sativa* from seeds purchased from Castros Gerand and Jardiland, respectively, at 25 °C in green house under 16 h light/8 h dark photoperiod.

The *E. variegatus* Euva-11 cell line was established from embryos of *E. variegatus* (Arricau-Bouvery *et al.*, 2018). In brief, the eggs were sterilized with bleach solution and then with 70% ethanol. After rinsing, the eggs were ground in culture medium made of 350 mL Schneider's Drosophila medium (Invitrogen), 100 mL Grace's insect cell culture medium (Invitrogen), 50 mL heat-inactivated foetal bovine serum (Eurobio) and 2 mL G-5 supplement (Invitrogen). The Euva-11 cells were cultivated at 25 °C in culture flasks (Falcon) in a refrigerated oven. After the first colonies developed and the cell line was established, the cells were passed using trypsinization every week with an appropriate dilution to keep the cells at 70% of confluence with an additional change in modified culture medium made of 350 mL Schneider's Drosophila medium, 100 mL Grace's insect cell culture medium and 50 mL heat-inactivated foetal bovine serum during the week.

The phytoplasma strain FD92 was originally transmitted to broad bean by infected *Scaphoideus titanus* sampled in FD-diseased vineyards in southwest France (Caudwell *et al.*, 1970; Angelini *et al.*, 2001). FDP was then continuously maintained in broad beans by *E. variegatus* transmission according to a published protocol (Caudwell *et al.*, 1972). Briefly, to obtain infected *E. variegatus*, L4–L5 nymphs were transferred by groups of 100 on FDP-infected broad bean for phytoplasma acquisition. Seven days later, *E. variegatus* were placed in cages on healthy broad bean for a latency period of 3–4 weeks (**Figure 10**). This study complies with relevant institutional, national, and international guidelines and legislation.

Escherichia coli strains DH10β, BL21, and chemically competent HST08 (Stellar cells, TakaraBio) were cultured in LB media at 37°C.

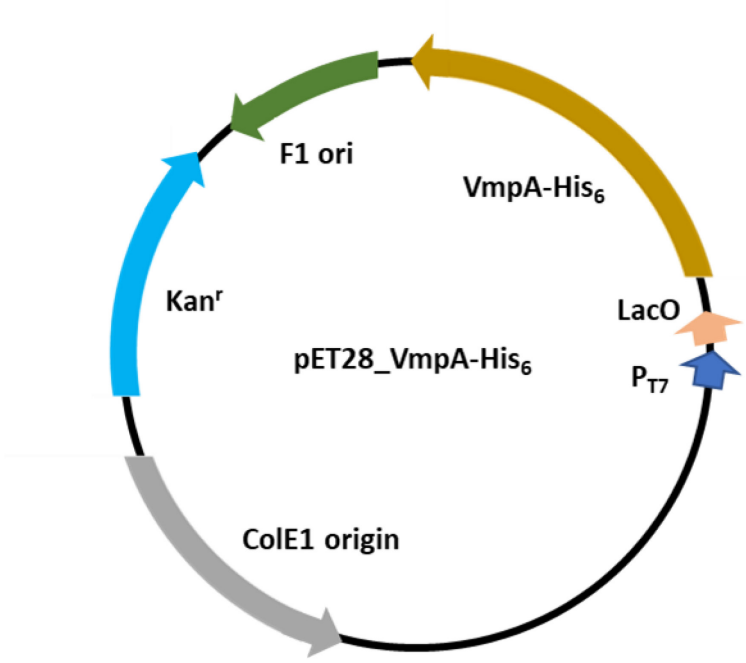

Figure 11. Schematic representation of pET28_VmpA-His$_6$. The size of the plasmid is 6166 bp for VmpA-His$_6$_FD92 and 6403 bp for VmpA-His$_6$_PGYA. It consists in the 322 amino acid long central hydrophilic part between the N-terminal signal peptide (amino acid 34) and the C-terminal transmembrane segment (amino acid 355) of vmpA of strain FD92 that contains the three repeated domains. The PGYA VmpA contains one additional repeated domain.

Yeast cells were cultured using different liquid media and incubated at 30°C. Yeast strains Y2H Gold and Y187 (Matchmaker® Gold Yeast Two-Hybrid System, Clontech) were used to perform double yeast hybrid assays. Strain Y2H Gold was used to transform the bait plasmid and to perform yeast retrotransformation meanwhile strain Y187 has been used to host cDNA *E. variegatus* bank.

2. Identification of *E. variegatus* proteins interacting with VmpA

2.1. Purification of VmpA-*E. variegatus* proteins complexes on affinity column

The recombinant VmpA-His_6 proteins were obtained as previously described (Arricau-Bouvery *et al.*, 2018). In brief, the proteins were expressed in *E. coli* BL21 Star (DE3) cells containing the plasmid pET28-VmpA-His_6 (**Figure 11**) and, in the case of VmpA_His_6_PGYA, purified on a His-select nickel affinity gel packed column (Sigma) according to the manufacturer's protocol. VmpA_His_6_FD92 proteins were purified on a 1 mL Protino® Ni-NTA column (Macherey Nagel) using the ÄKTA start protein purification system (cytiva) according to the manufacturer's instructions. Briefly, columns were equilibrated with 10 mL of lysis buffer before loading the sample onto the column. Washing steps includes a first step of 10 mL of a solution containing phosphate buffer 1x (20 mM trisodium phosphate pH 7.4, 500 mM NaCl) + 0.1 % Triton X-100. Then 10 mL of phosphate buffer 1x only were loaded to the column. A step gradient of imidazole was performed to elute retained proteins: 2 mL of 50 mM, 2 mL 100 mM, 2mL 250 mM, 2mL 500 mM and a final step at 1 M of imidazole to remove any residual protein bound to the column. Fractions collected during the elution steps (1 mL each) were automatically dispensed by the system in 1.5 mL Eppendorf. After purification all fractions containing VmpAHis_6_FD92 were tested for the presence of the purified protein by SDS-PAGE (**Figure 12.B**). Once the presence of the protein was confirmed, fractions containing only VmpA (15, 16 and 17) were pooled and desalted on PD10 desalting column (cytiva) according to manufacturer instructions and eluted in MES buffer 50mM pH 6.1. An SDS-PAGE on desalted proteins was performed as a control (**Figure 12.C**) and their concentrations were assessed using Biorad Protein Assay (BioRad) according to the manufacturer's instructions.

Three 75 cm^2 flasks of *E. variegatus* Euva cells were trypsinized. The cellular pellet obtained from 54 mL of culture were washed once with PBS 1x and then resuspended in 100

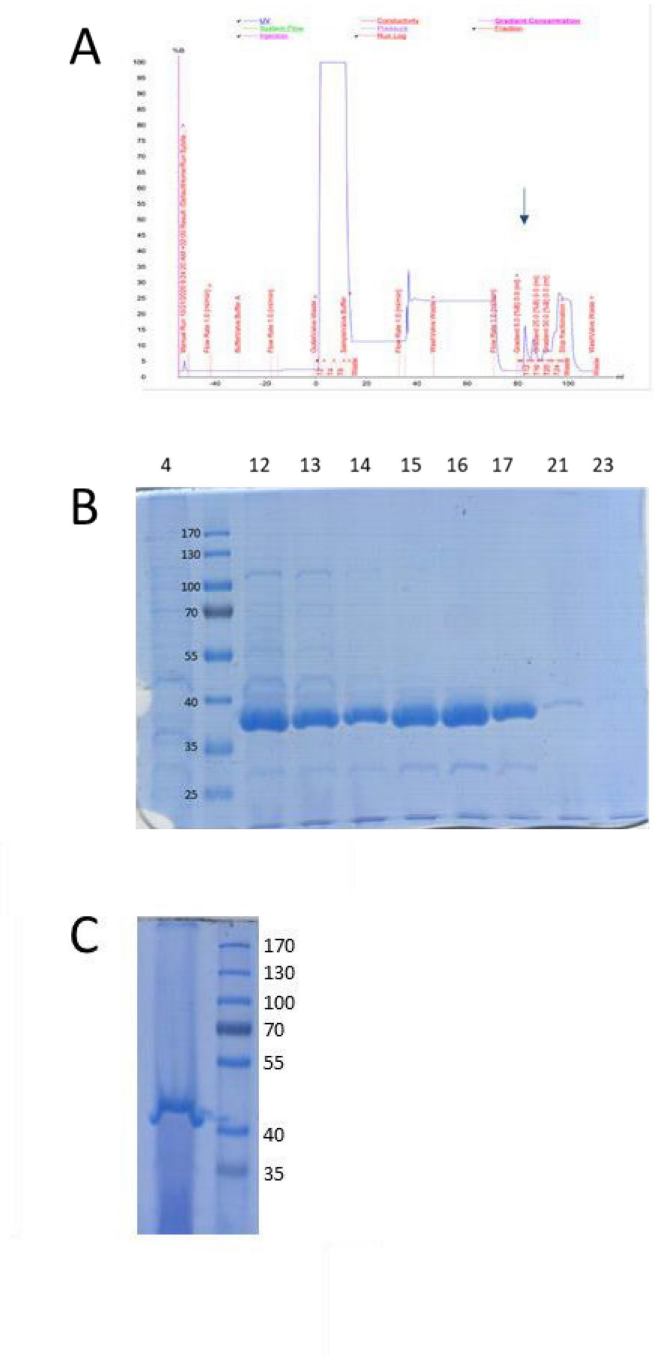

Figure 12. Purification of VmpAHis$_6$_FD92. (A) spectrum of VmpA-His$_6$_FD92 purification performed with ÄKTA start protein purification system. The blue arrow indicates the beginning of the injection of step gradient of imidazole allowing the elution of the proteins bound to the Ni column. (B) Coomassie blue gel of the fractions obtained during VmpAHis$_6$_FD92 purification with the Akta system. Lane 4: fraction collected before the beginning of elution steps, representing sample protein who have not fixed onto the column. Lanes 12-17 fractions containing VmpAHis$_6$_FD92 eluted with 50 mM (12) 100mM (13-16) and 250 mM (17) of imidazole. Lanes 21-23 fractions collected upon injection of 500 mM of imidazole (serve as a control of absence of residual VmpAHis$_6$_FD92).
(C) Coomassie blue gel of purified and desalted VmpAHis$_6$_FD92 from fraction 15, 16 and 17.

µL in Rx buffer (0.1% Triton X-100, 100 mM KCl, 3 mM NaCl, 3.5 mM $MgCl_2$, 1.25 mM EGTA, 10 mM Hepes, pH 7.3, Suzuki *et al.*, 2006; Galetto *et al.*, 2011). The sample was vortexed, incubated at room temperature for 5 min and centrifuged for 3 min at 14 000 g. The supernatant of Euva proteins was then recovered and the concentration of proteins was measured using the Biorad Protein Assay (BioRad). Resuspended Euva proteins (1.3 mg) were incubated overnight at 4°C with 1 mg of the recombinant protein VmpA-His_6 of the FD92 phytoplasma and protease inhibitor cocktail (Sigma-Aldrich). Then, the mixture was purified on an affinity nickel column using the ÄKTA start protein purification system as previously described. As a negative control, a purification on affinity nickel column was performed using 1.3 mg of Euva cell supernatant proteins alone.

2.2. Far-western blot analysis

The pellet resulting from the extraction with Rx buffer described previously was resuspended in Rx-T-DOC buffer (1% Triton X100, 0.5 % DOC, 100 mM KCl, 3 mM NaCl, 3.5 mM $MgCl_2$, 1.25 mM EGTA, 10 mM Hepes, pH 7.3), vortexed and then incubated at 4°C on an orbital shaker for 1 h. A centrifugation of three minutes was performed at a speed of 14000 g at a temperature of 4°C. The supernatant was then recovered and the pellet directly mixed with 26 µL of Laemmli buffer. An amount of 30 µg of proteins present in the Rx supernatant fraction and the equivalent in volume of supernatant recovered with Rx-T-DOC, were suspended in Laemmli buffer to a final volume of 26 µL. It was not possible to assess concentration of proteins extracted with the Rx-T-DOC due to the increased presence of detergent in the extract, so we choose an approach of V-V to charge the same amount of sample in the gel for the different fractions. Samples were boiled just before being separated by SDS-PAGE electrophoresis on two equivalent 10% acrylamide gels. Proteins from the first gel were then electrotransferred on a nitrocellulose membrane for 1.25 h in at 70V and then stained with Ponceau S staining solution (0.1% Ponceau red dye, 1% acetic acid) to assess the quality of proteins transfer. The membrane was washed with purified water and then saturated with a blocking buffer consisting in a solution of PBS containing 5% of skimmed milk for 4 h at room temperature. After saturation, the membrane was incubated overnight at 4°C on an orbital shaker with the protease inhibitor cocktail (1/1000) (Sigma-Aldrich) and the recombinant protein VmpA-His_6 at a concentration of 45 $\mu g.mL^{-1}$. The membrane was then

washed in PBS then in PBS Tween 20 0.2% prior to incubation with a primary anti-VmpA monospecific polyclonal antibody diluted 1:7000 (Covalab). After incubation, the membrane was washed with PBS, then with PBS Tween 20 0.2% and incubated with the secondary antibody anti-IgG rabbit-HRP (Sigma-Aldrich). After washing with PBS, the membrane was incubated with HRP substrate and visualized through ChemiDoc Imaging System (BioRad).

The second gel, carefully treated to avoid cross contamination such as keratin, was stained with Coomassie blue. It was conserved at 4°C in a solution containing 1% of acetic acid. The bands corresponding to the signals observed on the far-western blot anti-VmpA were excised and sent to Bordeaux proteomic platform (to Stéphane Claverol, https://proteome.u-bordeaux.fr/) to perform a mass spectrometry analysis. Gel pieces were faded in 25 mM ammonium bicarbonate 50% acetonitrile (ACN), rinsed twice in ultrapure water and shrunk in ACN for 10 min. After ACN removal, gel pieces were dried at room temperature, covered with the trypsin solution (10 $ng.\mu l^{-1}$ in 50 mM NH_4HCO_3), rehydrated at 4°C for 10 min, and finally incubated overnight at 37°C. Gel slices were then incubated for 15 min in 50 mM NH_4HCO_3 at room temperature with rotary shaking. The supernatant was collected, and an H_2O/ACN/HCOOH (47.5:47.5:5) extraction solution was added onto gel slices for 15 min. The extraction step was repeated twice. Supernatants were pooled and dried in a vacuum centrifuge. Digests were finally solubilized in 0.1% HCOOH.

A far-western blot analysis comparing Euva proteins interacting with VmpA of a *S. titanus* transmissible phytoplasma isolate (FD92) and a non-transmissible isolate (PGYA) was performed. 90 µg of Euva cell proteins resulting from extraction with Rx buffer, 30 µg of proteins extracted with Rx-T-DOC buffer, and proteins in the pellet directly resuspended in Laemllii buffer were separated onto two 10% acrylamide gels. Separated proteins were electrotransferred onto two nitrocellulose membranes. The same protocol used is described above with minor differences. One membrane was incubated with VmpA-His_6_FD92 and the other with VmpA-His_6_PGYA. The primary antibody anti-VmpA to recognise the VmpA-His_6_PGYA was diluted 1/3000, in reason of the different affinity of the antibody towards the two VmpA.

2.3. Mass spectrometry analysis (nLC-MS/MS)

Peptide mixture was analyzed on a Vanquish Neo nanoLC system (Thermo Fisher Scientific) coupled to an Electrospray Eclipse™ Tribrid™ Mass Spectrometer (Thermo Fisher Scientific). Ten microliters of peptide digests were loaded onto a 300-µm-inner diameter x 5-mm C_{18} PepMap™ trap column (LC Packings) and peptides were eluted from the trap column onto an analytical 75-mm id x 50-cm C18 Pep-Map column (LC Packings) with a 4–40% linear gradient of solvent B in 96 min (solvent A was 0.1% formic acid and solvent B was 0.1% formic acid in 80% ACN) followed by a 25 min gradient from 40% to 90% solvent B. The separation flow rate was set at 300 $nL.min^{-1}$. The mass spectrometer operated in positive ion mode at a 1.9-kV needle voltage. Data were acquired using Xcalibur 4.4 software in a data-dependent mode. MS scans (*m/z* 375-1500) were recorded in the Orbitrap at a resolution of R = 120 000 (@ m/z 200) and an AGC target of 4 x 10^5 ions collected within 50 ms. Dynamic exclusion was set to 30 s and top speed fragmentation in Higher Energy Collision Dissociation (HCD) mode was performed over a 3 s cycle. MS/MS scans were collected in the orbitrap with a resolution of R = 30 000 (@ m/z 200) and a with a maximum injection time of 54 ms. Only +2 to +7 charged ions were selected for fragmentation. Other settings were as follows: no sheath nor auxiliary gas flow, heated capillary temperature, 275 °C; normalized HCD collision energy of 28%, isolation width of 1.6 m/z, AGC target of 5 x 10^4 and normalized AGC target of 100%. Monoisotopic precursor selection (MIPS) was set to Peptide and an intensity threshold was set to 2.5 x 10^4.

2.4. Database search and results processing

Data were searched by SEQUEST through Proteome Discoverer 2.5 (Thermo Fisher Scientific Inc.) against a Swissprot protein database (version 2022-01; 478,954 entries) and a collection of peptide sequences originating from the conceptual translation of RNAseq data from *E. variegatus*. The dataset analyzed during the current study are available in the Transcriptome Shotgun Assembly database on NCBI: *E. variegatus*, transcriptome shotgun assembly repository, GenBank accession: GFTU00000000.1. Spectra from peptides higher than 5000 Da or lower than 350 Da were rejected. Precursor Detector node was included. Search parameters were as follows: mass accuracy of the monoisotopic peptide precursor and peptide fragments was set to 10 ppm and 0.02 Da respectively. Only b- and y-ions were

considered for mass calculation. Oxidation of methionines (+16 Da), methionine loss (-131 Da), methionine loss with acetylation (-89 Da) and protein N-terminal acetylation (+42 Da) were considered as variable modifications while carbamidomethylation of cysteines (+57 Da) was considered as fixed modification. Two missed trypsin cleavages were allowed. Peptide validation was performed using Percolator algorithm (Käll *et al.*, 2007) and only "high confidence" peptides were retained corresponding to a 1% False Positive Rate at peptide level.

For the proteins selected after chromatography affinity and identified through mass spectrometry analysis, a first selection step consisted in the determination of VmpA specific retention ratio using the following equation:

$$100 * \frac{(\text{«VmpA column » abundance} - \text{« control column » abundance})}{\text{«VmpA column » abundance}}$$

The proteins were classified based on this value. A threshold of 90% of VmpA specific retention was set in order to eliminate the proteins showing an affinity for the column itself. A gene ontology search was then performed in order to categorise the proteins based on their biological role.

Proteins identified by mass spectrometry analysis performed on excised bands were first selected restraining the results to peptides specifically matching sequences of the *E. variegatus in silico* predicted proteome. A second selection based on the molecular weight of the proteins followed, according to the signal observed in the far-western blot comparing the positions of bands to the ladder. As the signal observed on the far-western blot was common to the soluble and insoluble fractions, the analysis of bands G and H was restricted to proteins identified in both bands.

The parameters considered to further select the VmpA putative targets were the presence of potential N-glycosylation sites predicted by the prediction tool Glycomine (glycomine.erc.monash.edu.) and the prediction of NxS/T pattern, and the presence of predicted transmembrane domains using TMHMM v2.0 software (Krogh *et al.*, 2001) in the amino acidic sequence.

Table 2. List of primers and plasmids used in this study. T7 promoter sequence is in bold.

Target gene	Primer names	Organism/Plasmid	5'-3' sequence	Product size (n)	Application	qPCR efficiency (%)	Plasmid resulting
endoplasmin	c_endoplasmine_F	*E. variegatus*	cccATGGGGAGAAAACATTCTCACC	2358	cloning	-	pGEMT-Easy_endoplasmine
	c_endoplasmine_R		CGGTTACAGTTCGTCGTGTTCC				
	db_endoEv_T7p_F		**TAATACGACTCACTATAGGGG**GAGGACAGCGAGTACCATGA	495	dsRNA synthesis	-	-
	db_endoEv_T7p_R		**TAATACGACTCACTATAGGGG**TACCTTGGACGACTGGAACC				-
	q_endo_F1		CATTACGGACACAGGCATCG	224	RT-PCR	2.033	-
	q_endo_R1		AGACCAGCTGTTTGTCCTCA				-
EGFR	c_EGFR_F3	*E. variegatus*	GACTGCACCGTTATCGAG	1137	cloning	-	pMINIT_2.0_EGFR
	c_EGFR_R4		ACCGTAGCAGCCTCTGCAC				
	db_EGFR_T7p_F		**TAATACGACTCACTATAGGGG**TGCTCAGGGAGTGGACTGGAAG	417	dsRNA synthesis	-	-
	db_EGFR_T7p_R		**TAATACGACTCACTATAGGGG**CCCTGGCAGCCGTACACACAG				-
	c_EGFR_F3		GACTGCACCGTTATCGAG	246	RT-PCR	2.01	-
	q_EGFR_R3		GTATTCCGTCAATGTTCTTCCT				-
HERC4	c_HERC4_Ev_F	*E. variegatus*	CAACGCCAAGAACTGTGACAAG	916	cloning	-	pMINIT_2.0_HERC4
	c_HERC4_Ev_R		TCCGAGCAGCTTCTTGTACAG				
	db_HERC4_T7p_F		**TAATACGACTCACTATAGGGG**AGATCAAGCCCTACAGATGC	431	dsRNA synthesis	-	-
	db_HERC4_T7p_R		**TAATACGACTCACTATAGGGG**GGAATGGCAGCGCGATGATG				-
	c_HERC4_Ev_F		CAACGCCAAGAACTGTGACAAG	221	RT-PCR	2.04	-
	q_HERC4_R		CCGTTAGCATCCCCTCGTAC				-
wengen	c_wng_F	*E. variegatus*	ATGGGGATAAATACAAAGAAGG	1516	cloning	-	pMINIT_2.0_TNFwng
	c_wng_R		CTTAGCTAAGCGGTCTTTTCTG				
	db_wng_T7p_F		**TAATACGACTCACTATAGGGG**AGGATTAGCACCACCTGTTG	404	dsRNA synthesis	-	-
	db_wng_T7p_R		**TAATACGACTCACTATAGGGG**CGGGGTTCAATAGATGCGAC				-
	q_wng_F		CGGTCTGCAGTACTGGAGC	223	RT-PCR	1.903	-
	q_wng_R		CTTCTCGGCTGACACGTCGC				-
uk1_LRR	LRR_15247_cF	*E. variegatus*	ATGGGCAGTGCGAGTGCAG	2350	cloning	-	pMINIT_2.0_LRR
	LRR_15247_cR		GCTGTCATTTACGATGTTTCACC				
	db_LRR_15247_T7p_F		**TAATACGACTCACTATAGGGG**GACGACTGCGACTGCCACTAC	483	dsRNA synthesis	-	-
	db_LRR_15247_T7p_R		**TAATACGACTCACTATAGGGG**CGGGTTGCCTGACAGATCTAG				-
	LRR_15247_qF		CTTAGCAGCCCAGAGAACG	265	RT-PCR	1.936	-
	LRR_15247_cR		GCTGTCATTTACGATGTTTCACC				-
uk2_TLR	TLR_14488_cF	*E. variegatus*	ATGAAGGTCGCTGTAATACTCTC	2170	cloning	-	pMINIT_2.0_TLR
	TLR_14488_cR		GGAATGTTTACACGACATCATCA				
	TLR_144888_T7p_F		**TAATACGACTCACTATAGGGG**GCAGATATCCATGAGTAGTTCG	610	dsRNA synthesis	-	-
	TLR_144888_T7p_R		**TAATACGACTCACTATAGGGG**CTGTGGCCTGTCTAACATTTCC				-
	TLR_14488_cF		ATGAAGGTCGCTGTAATACTCTC	239	RT-PCR	1.942	-
	TLR_14488_qR		GCTTTCTCCAATCCGATGG				-
CD36-like	CD36_cF	*E. variegatus*	ATGCAGAACAAACGGGGG	1623	cloning	-	pMINIT_2.0_CD36
	CD36_cR		TTACGTTGTGTGTTCGTCG				
	db_CD36_T7pF		**TAATACGACTCACTATAGGGG**GAGTTCGGACTGATGTATGG	549	dsRNA synthesis	-	-
	db_CD36_T7pR		**TAATACGACTCACTATAGGGG**CATTTCCGGTTGGACATCGATG				-
	CD36_cF		ATGCAGAACAAACGGGGG	259	RT-PCR	1.982	-
	CD36_qR		ACTCCTCCGCGTTGGTGAC				-
draper	c_draper_F	*E. variegatus*	ATGCTGCAGGTCTCAGCAATG	3003	cloning	-	pMINIT_2.0_draper
	c_draper_R		CTACTCCGGTAGGTTAGGGT				
	T7_draper_F		**TAATACGACTCACTATAGGGG**GTTGAGATCAGCTTCCCTG	566	dsRNA synthesis	-	-
	T7_draper_R		**TAATACGACTCACTATAGGGG**GTGAAATATGCCCAGAAGG				-
	c_draper_F		ATGCTGCAGGTCTCAGCAATG	207	RT-PCR	1.952	-
	q_draper_R		GACTTTGTACCTGGAGCAC				-
uk3	c_UK1_f2	*E. variegatus*	CAGCTCATTGACACTACCATG	1370	cloning	-	pMINIT_2.0_uk1
	c_UK1_r2		GTTTTTGGTTTAGGAGGTCATAC				
	T7_F_UK1		**TAATACGACTCACTATAGGGG**GCGAATCTTGCGACCAACAC	750	dsRNA synthesis	-	-
	T7_R_UK1		**TAATACGACTCACTATAGGGG**GGACACCTCGGCGATCACC				-
	q_F_UK1		GGCTGGCCTGCGACCATTTC	232	RT-PCR	1.832	-
	c_UK1_r2		GTTTTTGGTTTAGGAGGTCATAC				-
integrin β	c_IntegrinB_F	*E. variegatus*	ATGAAGATGGAGGTGAGACT	2470	cloning	-	pMINIT_2.0_integrinB
	c_IntegrinB_R		ATCATTTCCCAGCGTATGTG				
	T7_intB_F		**TAATACGACTCACTATAGGGG**GCGAATCGGCAGTCATCTTC	460	dsRNA synthesis	-	-
	T7_intB_R		**TAATACGACTCACTATAGGGG**AGTTCTGCGAGTGTGACAAC				-
	q_intB_F9		GCGACGTGTACTCGTTGTC	256	RT-PCR	1.854	-
	c_IntegrinB_F		ATGAAGATGGAGGTGAGACT				-
fasciclin	c_fasciclin_F	*E. variegatus*	CTCCGCAGCAGACAAAG	1886	cloning	-	pMINIT_2.0_fasciclin
	c_fasciclin_R2		CAGCATTATCCTTCTGTCAG				
	T7_fasciclin_Ev_F		**TAATACGACTCACTATAGGGG**AGAGTCAACATCTACCCG	578	dsRNA synthesis	-	-
	T7_fasciclin_Ev_R		**TAATACGACTCACTATAGGGG**GTGGTGTGGTTAGACGA				-
	c_fasciclin_F		CTCCGCAGCAGACAAAG	220	RT-PCR	1.922	-
	q_fasciclin_R		CTTCATGGCCTCGTCTAC				-
cueball	c_cueball_ Ev_F	*E. variegatus*	CATGAAAGCCGAAAATTC	1818	cloning	-	pMINIT_2.0_cueball
	c_cueball_Ev_R		CAAGGTCAGTAAAGGTC				
	T7_cueball_Ev_F		**TAATACGACTCACTATAGGGG**GGCGAGAGGTGTGAGATC	508	dsRNA synthesis	-	-
	T7_cueball_Ev_R		**TAATACGACTCACTATAGGGG**CCATATTTCCTAAAAGCCCTC				-
	qF cueball		GCACCTCTCACTATTCCAG	298	RT-PCR	1.953	-
	c_cueball_ Ev_F		CGACCAGAAGACAGACCGA				-
Na/Ca exchanger	c_NaCaex_F	*E. variegatus*	GATGTGATGAGCCACGGTC	2582	cloning	-	pMINIT_2.0_Na/Caexch
	c_NaCaex_R		TCAGAAGTTGAATGGCAGTAC				
	T7_Na/Ca_exchanger_Ev_F		**TAATACGACTCACTATAGGGG**CGGTTCAAGGTTTTCATCG	524	dsRNA synthesis	-	-
	T7_Na/Ca_exchanger_Ev_R		**TAATACGACTCACTATAGGGG**GCTGTTGTCTCTTTGTGCTC				-
	q_NaCaex_F		GCCGTGTACCACTTTAGC	264	RT-PCR	1.87	-
	c_NaCaex_R		TCAGAAGTTGAATGGCAGTAC				-
Glutathione-S-transferase	GST1_F257c[a]	*E. variegatus*	CCAAGGACCCCAAGAAGCGA	113	RT-PCR	1.96	-
	GST1_R369c[a]		TGGCGCTCCTCCAAACATCA				-
Tubulin β	Tub_β_F1	*E. variegatus*	CGCCCAGAGGTCTCAAGATG	148	RT-PCR	1.94	-
	Tub_β_R2		ATCTCGTCCATGCCCTCGC				-
Elongation Factor 1	EF1_F215α	*E. variegatus*	CCATCGACATTGCCCTGTGG	111	RT-PCR	2.05	-
	EF1_R325α		CCTGTGAGGTTCCAGTGATCATG				-
Elongation factor Tu (EFTu)	3Fbl[b]	FDp strain FD92	TGAAGATCCAGTACGTGATTTAGAC	158	RT-PCR	1.95	-
	3R1[b]		TTTTAGTTTCTTTAATACCTATGATTTC				-
VmpA	VMPA-FY2H	FDp strain FD92	CATGGAGGCCGAATTCAAAGCTATTACAGATTTGAGTGG	936	cloning	-	pGBKT7_VmpA
	VMPA-RY2H		GCAGGTCGACGGATCCTTAACTTTTTTTCTTAACAGTAAAC				
YZH prey library preparation	CDS oligo-dT primer		ATTCTAGAGGCCGAGGCGGCCGACATG-d(T)30VN	-	first strand cDNA synthesis	-	-
	SMART III Oligo		AAGCAGTGGTATCAACGCAGAGTGGCCATTATGGCCGGG				
	5' PCR Primer		TTCCACCCAAGCAGTGGTATCAACGCAGAGTGG		cDNA LD-PCR		
	3' PCR Primer		GTATCGATGCCCACCCTCTAGAGGCCGAGGCGGCCGACA				
pGADT7_insert	pGAD_F1	pGADT7	GATGATGAAGATACCCCACC	-	screening by PCR	-	-
	pGAD_R1		AGATGGTGCACGATGCACAG				
GFP	eGFP-ds-T7F1	peGFP(Clontech)	**TAATACGACTCACTATAGGGG**CAAGGAGGACGGCAACATCC	323	dsRNA synthesis	-	-
	eGFP-ds-T7R1		**TAATACGACTCACTATAGGGG**CGAACTCCAGCAGGACCATG				

3. Setting up of a simplified system *ex vivo*

3.1. Cloning of *E. variegatus* CDS

RNAs were extracted using Trizol reagent (Thermo Fisher Scientific) under manufacturer instructions. Reverse transcription was performed on 1 µg of *E. variegatus* RNA as template using SuperScript IV (Thermo Fisher) and random hexamers primers (Thermo Fisher) according to the manufacturer's instruction. The inserts were amplified by PCR and cloned into pGEM®-T Easy vector (Promega) or pMINI-T2 (NEB) using primers listed in **Table 2** and according to manufacturers instructions. Plasmids were propagated in competent *E. coli* DH10β cells.

The DH10β bacteria conserved in 15% glycerol stock at -80°C were plated on LB solid media and incubated at 37°C overnight. The obtained colonies were inoculated in liquid LB media and incubate at 37°C overnight on an orbital shaker set at 200 rpm. Optical density at 600 nm was regularly checked until the culture reached a value of 0.6. Liquid cultures were kept on ice and a centrifugation of 15 minutes at 4°C and 4500 rpm was performed in order to pellet the cells. Bacteria cells were washed twice with cold sterile water and once in glycerol 10%, repeating the centrifugation after each washing step. Optical density at 600 nm of the pellet was assessed. The cells were suspended in a proper volume of glycerol 10% solution to reach an equivalent of final OD_{600} of 200. Suspended cells were aliquoted in 1.5 mL tubes rapidly chilled in a dry-ice and ethanol bath and conserved at -80°C.

Competent *E. coli* strain DH10β cells were kept on ice to defrost for 10 min prior the addition of 10-1000 ng of the plasmid of interest. The tubes were then gently flicked 4-5 times and incubated on ice for 20 min. Heat shock was performed in a bath at 42°C for 30 s and the tubes were then incubated for 5 min on ice. Transformed cells were suspended in 950 µL of NEB-10β/Stable Outgrowth Media (NEB) and then incubated for 1 h at 30°C on an orbital shaker set at 200 rpm for phenotypic expression. Volumes of 50 µL and 5 µL of the culture were plated onto selective media (LB + Ampicillin [100 $\mu g.mL^{-1}$]) and incubated overnight at 37°C. The presence of the insert was checked through sequencing by Sanger technology (GENEWIZ, Azenta) using primers matching flanking region on the plasmid. The sequence analysis and alignment onto reference sequences (TSA *Euscelidius variegatus* taxid:13064*)* were performed using ApE v3.1.3 (Davis and Jorgensen, 2022).

3.2. RNA interference on Euva-11 cells, RNA extraction and mRNA analysis

The putative VmpA targets and GFP sequences were amplified by PCR from *E. variegatus* cDNA and a pEGFP plasmid (Clontech) as templates using sequence-specific primers 5' extended with 20 bp of T7 RNA polymerase promotor (**Table 2**). The HiScribeTM T7 High Yield RNA synthesis Kit (New England Biolabs) was used on the PCR products to obtain the dsRNAs. dsRNAs were ethanol precipitated in the presence of sodium acetate 0.3 M and were resuspended in 20 µL of RNAse free water. The purity and integrity of dsRNAs were determined through migration on agarose gel electrophoresis of 1/10 and 1/100 dilutions of the transcription products.

Euva cells were cultivated in 24-well plates (Falcon) to nearly 80% confluence and transfected with 1 µg dsRNA using FuGENE HD Transfection Reagent (Promega) under manufacturer instructions. At the end of incubation time of three or seven days, the transfected Euva cells were collected using TRIzol Reagent (Thermo Fisher Scientific) and then stored at -20°C until extraction which was performed according to the manufacturer's instructions. cDNAs of the samples were obtained using SuperScript^{TM} III Reverse Transcripase (Thermo Fisher Scientific) and 2.5 µM Random hexamer primers (Invitrogen). Real time PCR was performed on the LightCycler 480 Real-Time PCR system (Roche Diagnostics Corp) using sequence-specific primers (**Table 2**) and N',N'-dimethyl-N-[4-[(E)-(3-methyl-1,3-benzothiazol-2-ylidene)methyl]-1-phenylquinolin-1-ium-2-yl]-N-propylpropane-1,3-diamine (SYBR Green, Roche). The cycling programs for all amplifications was 95°C for 15 min, followed by 40 cycles of 95°C for 30 s, 60°C for 30 s and 72°C for 30 s. The two housekeeping genes glutathione S-transferase (GST) and tubulin β (tubβ) served as reference genes for mRNA quantification. The relative fold change in gene expression was calculated using the $2^{-\Delta\Delta Ct}$ method (Livak and Schmittgen, 2001).

3.3. Adhesion assays of VmpA-His_6-coated beads to Euva cells

Red fluorescent latex beads exposing amine at their surface (4 x 10^9 beads at 1 µm, Sigma-Aldrich) were coated with the recombinant VmpA-His_6. The beads were washed with MES buffer 50 mM pH 6.1 and then incubated with recombinant proteins at a final concentration of 9 µM of VmpA-His_6 + 1 µM BSA. EDAC 16 mM was added to activate the reaction. The beads were then incubated for two hours in the dark on an orbital shaker. After

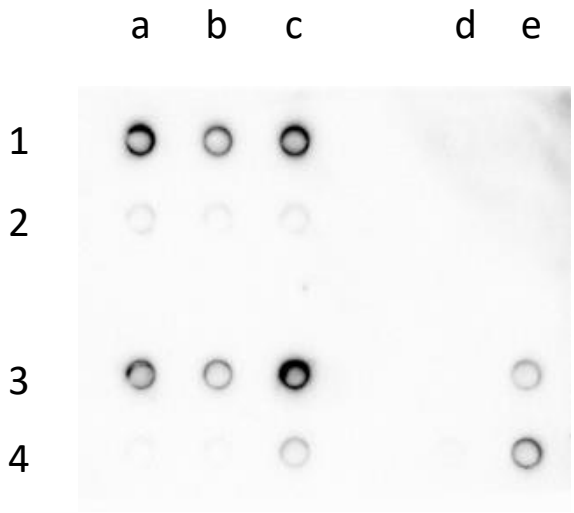

Figure 13. Example of dot blot anti-VmpA on coated beads. For each experiment of beads adhesion assay an aliquot of the beads employed have been stocked at -20°C. in the left part the VmpA coated beads used in the adhesion assay (1 a,b,c, 3 a,b,c) and the 1/0 dilution of the same beads (2 a,b,c, 4 a,b,c), on the right the negative control consisting in non coated beads (2d), and the positive control consisting in different concentrations of VmpA-His_6 (3d: 0,001 ng; 4d: 0,01 ng; 3e: 0,1 ng; 4e:0,5 ng).

a 3 min centrifugation, the coated beads were washed once with MES buffer 50 mM pH 6.1 and then resuspended in 200 µL of the same buffer. The coated beads were stored in the dark at 4°C up to 7 days. Coating of the beads was verified for each experiment performing a dot blot using a rabbit antibody anti-VmpA (**Figure 13**).

Three days post transfection with dsRNA, to allow the turnover of the target proteins (Clemens et al., 2000), Euva cells on coverslip in 24-well plates were washed twice with Schneider's medium (Gibco) and 400 µL of Schneider medium were added to the cells. Beads were diluted in Schneider's medium (1/100) and 100 µL were dispensed on the cells. The cells were then incubated at 25°C for 1 h.

3.4. Immunofluorescent staining and microscopic observations

After incubation of Euva cells with fluorescent beads, the cells were washed twice with 0.5 mL Schneider medium and then twice with PBS 1X (Eurobio Scientific). The cells were then fixed using paraformaldehyde at a final concentration of 4% (Electron Microscopy Science) during 15 min. The fixed cells were washed for three times with PBS 1X, then in distilled water and stained with DAPI 1 $mg.mL^{-1}$ during 5 min. The cells were then washed in water and mounted in ProLong Gold antifade reagent (Invitrogen). Then, the cells were imaged using a Zeiss AxioImager epifluorescent microscope with an objective with a numerical aperture of 1.4. The filters used for excitations and emissions were BP 377/50 and BP 447/60 for DAPI and BP 562/40 and LP 593 for red fluorescent beads. For Z-stack acquisition, images were acquired every 0.3 µm from the bottom to the top of Euva cells and Z-projections were performed before counting of adherent beads with the free software ImageJ (v. 1.53f) (Schindelin *et al.*, 2012). Twenty random positions were captured for each treatment.

After transfection of Euva cells with dsRNA, the cells were observed with the inverted microscope Eclipse TS100 (Nikon) at three days post transfection, prior to RNA extraction. Images were taken in random positions of the well at magnifications of 4, 10 and 20.

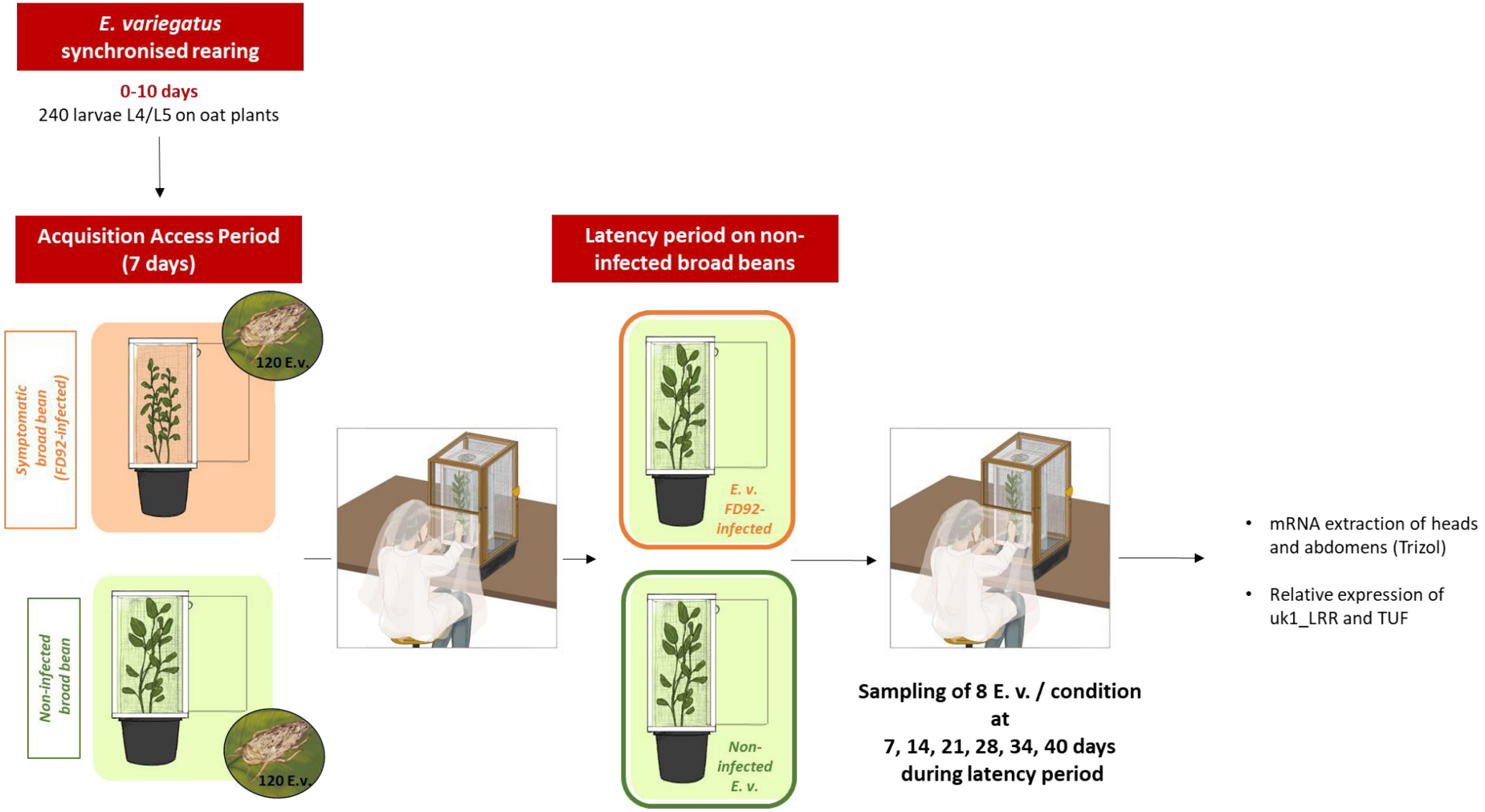

Figure 14. Protocol for the assessment of uk1_LRR expression in FD92-infected and non-infected E. variegatus. Custom illustrations by Gaëlle Duflot (https://www.gaelleduflot-illustrations.net/).

4. Assessment of uk1_LRR expression on *E. variegatus*

Twenty-four non-infected *E. variegatus* young adults sampled from a synchronised rearing were dissected at the stereomicroscope. Male and female tissues were analysed separately. Seven salivary glands from females and 7 from males, 7 midgut organs from females and 11 from males, and 6 ovaries with eggs were recovered, pooled to have a sufficient amount of biological material to analyse and kept in Trizol. Total RNA extraction was performed as previously described and relative quantification of *uk1_LRR* transcripts was assessed through real time RT-PCR. Glutathione S-transferase (GST), Tubulin β (tub β) and elongation factor 1 (EF1) were used as reference genes to normalise expression values.

A total of 240 nymphs of stage 4 and 5 were put on broad beans to obtain a synchronised rearing. After 10 days, half of young insects was transferred onto healthy broad beans meanwhile the other half was transferred onto broad beans infected with FDP for acquisition. After 7 days, eight insects were sampled for each condition and the remaining insects were transferred onto healthy broad beans for latency. Eight insects were sampled every 7 days up to 40 days after beginning of acquisition (**Figure 14**). The head and the abdomen of each insect were analysed separately. Total RNA was extracted as described previously. Relative quantification of *uk1_LRR* transcripts was assessed through real time RT-PCR as well as the expression of FDp *tuf* gene hereby used as a proxy of FDp titre and transcriptional activity. *E. variegatus* glutathione S-transferase (GST) was used as reference gene to normalise expression values.

5. Yeast Two-Hybrid

5.1. Bait clone preparation for yeast two-hybrid

The gene of interest (VmpA) sequence was cloned into the bait plasmid pGBKT7, in fusion with the *GAL4* DNA-binding domain using Clontech's In-Fusion® HD Cloning Kit and specific primers (**Table 2**). Differences with the native VmpA of FD92 strain consists in lack of signal peptide (at the N-term portion of the protein) and of transmembrane domain (at C-term). Modified VmpA

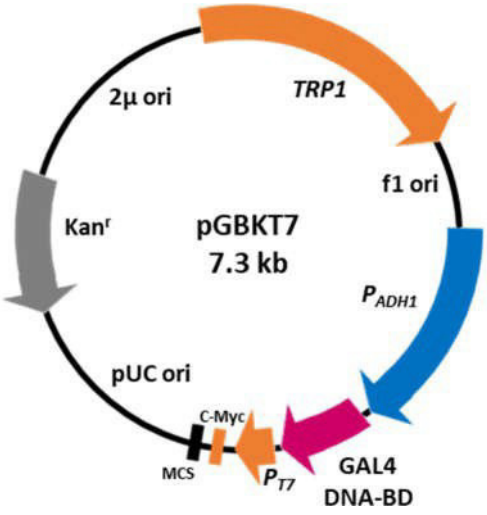

Figure 15. Schematic representation of bait plasmid pGBKT7. The main features consist in the presence of a gene for the biosynthesis of tryptophan (TRP1) which constitutes the auxotrophic marker for the selection of the yeast strain transformed with the plasmid, a c-Myc tag which will results cloned in frame between the bait protein and the Gal4 DNA- binding domain. VmpA sequence is inserted in correspondence of the multi cloning site (MCS).

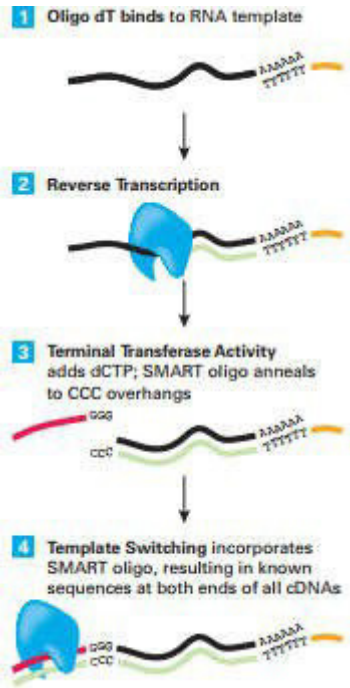

Figure 16. Schematic representation of SMART cDNA synthesis. This technology generates cDNA ends with homology to pGADT7. From "Make your Own "Mate and Plate™" Library System User Manual".

was cloned downstream the Gal4 DNA binding domain and a c-Myc tag (**Figure 15**). Once produced in Stellar competent *Escherichia coli* cells and purified, the plasmid has

been sent to a platform to assess the quality of cloning through Sanger sequencing. The bait plasmid pGBKT7_VmpA was then transformed in the *Saccharomyces cerevisiae* strain Y2H Gold. The bait plasmid was tested for protein expression, cell toxicity and for autoactivation of the yeast two-hybrid reporter system.

5.2. Prey library preparation for yeast two-hybrid

All kits were used according to manufacturer instructions. Salivary glands and midguts from 500 adults of *E. variegatus* were dissected on ice, stocked temporarily in RNA later (Invitrogen), freezed in liquid nitrogen and grinded with metal beads and a grinder machine. A total RNA extraction was performed on the lysate using the kit NucleoSpin RNA Plus (Machery Nagel) and was followed by a DNAse treatment using the kit rDNase Set (Machery Nagel). Total RNAs were purified using the RNA clean-up Kit (Machery Nagel) and their concentration assessed using a spectrophotometer. The mRNA fraction was isolated using the NucleoTrap mRNA kit (Machery Nagel). The cDNA synthesis was obtained using the the kit "Make your own «Mate & Plate™» library system" (Clontech). Briefly, denaturation of RNA with CDS III oligodT primers (**Table 2**) was performed during 2 min at 72°C. Then, a 1 h incubation with a modified SMART III Oligo (**Table 2**) was performed, in order to obtain known sequences at both ends of all synthetized cDNAs. This primer exploits SMART (Switching Mechanism At 5' end of RNA Template) technology (Zhu *et al.*, 2001) (**Figure 16**): when the retrotransciptase used in this cDNA synthesis (SMART Moloney Murine Leukemia Virus RT) encounters a 5' end on RNA template, its terminal transferase activity adds few additional nucleotides (deoxycytidines) to the 3' of cDNA. The SMART primer binds to these overhangs on first strand of cDNA and consent template switching, so that RT continues replicating to the end of the primer. This step is crucial for the subsequent long distance PCR step (LD PCR) which will be performed with primers presenting a complementary sequence to the one included by the use of SMART primer at 5' of end of sscDNA (**Table 2**). The quality of the double strands of cDNA obtained with the procedure was assessed through electrophoresis on 1.2 %

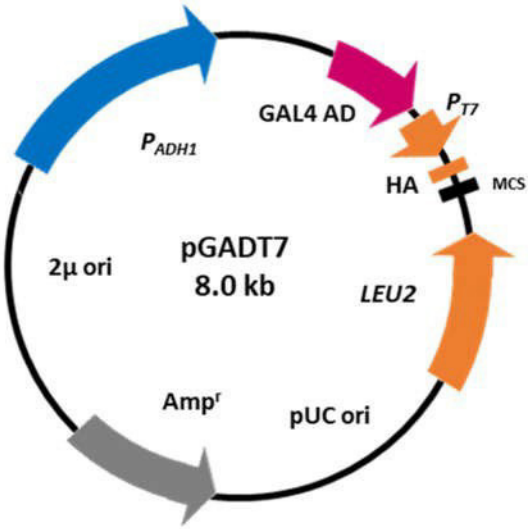

Figure 17. Schematic representation of prey plasmid. The main features consists in the presence of a gene for the biosynthesis of leucine (LEU2) which constitutes the auxotrophic marker for the selection of the yeast strain transformed with the plasmid, a HA epitope tag which will results cloned in frame between the N–term of the bait protein and the Gal4 activation domain. The insert of *E. variegatus* cDNA bank is inserted in the correspondence of the multi cloning site (MCS).

agarose gel. ds-cDNA were purified on a CHROMA SPIN TE-400 column (provided with the kit used) and their concentration quantified at the spectrophotometer.

The yeast library of *E. variegatus* cDNA was obtained using Kit Yeastmaker Yeast transformation system 2 (Clontech). An overnight culture of yeast strain Y187 was used as a starter to obtain a 100 mL culture in liquid medium YPDA. Once the culture attended a DO_{600} between 0.4 and 0.6, cells were pelleted through a 5 min centrifugation at 700 rcf and resuspended in 30 ml of sterile purified water. After another 5 min centrifugation at 700 rcf, supernatant was discard and pellet was resuspended in 3 mL of a solution of 1.1x lithium acetate-TE (1.1x TE/LiAc). Cells were pelleted and resuspended in 1 mL of 1.1x TE/LiAc. 600 µL of resuspended cells were mixed with 20 µL of ds-cDNA fragments and 6 µL of SmaI linearized pGADT7-Rec plasmid (**Figure 17**) were mixed with 20 µL denaturated Yeastmaker carrier DNA. After the addition of 2.5 mL of lithium acetate and polyethylene glycol solution (PEG/LiAc), cells were incubated for 45 min at 30°C with gently mixing every 15 min. 16 µL of DMSO was added to the tubes that were then incubated during 20 min in a bath at 42°C with gently and carefully vortexing every 5 min. Cells were pelleted through a 5 min centrifugation at 700 rcf, resuspended in 3 mL of YPD Plus media (supplied with the kit) and incubating for 90 min at 30°C on an orbital shaker (200 rpm). Cells were then pelleted and resuspended in 15 mL of 0.9% NaCl solution. Transformed yeasts were then plated on SD/-Leu medium to assess the efficiency of transformation and to calculate the number of independent clones in the library. Colonies were then removed from petri dishes using beads and freezing medium. The suspensions concentration was assessed and cells were then aliquoted and stocked at -80°C.

5.3. Two-hybrid library screening using yeast mating

The bait strain (Y2H Gold/pGBKT7_VmpA) was maintained in SD/-Trp liquid culture until it reached the OD_{600} of 0.8 (16-20h). The yeast cells were then pelleted and resuspended in 4 mL of SD/-Trp media, then incubated with 1 mL of the previously prepared library in a final volume of 47 mL of YPDA 2x medium in a 2 L flask. The co-culture was then incubated at 30°C for 16-24 h and slowly shaking at 27-30 rpm. A drop of the co-culture was observed at the phase contrast microscope to check the presence of try lobate structures corresponding

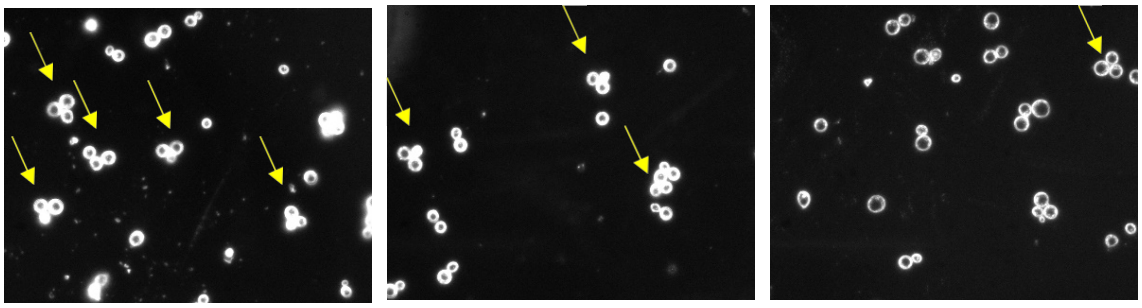

Figure 18. A drop of culture after 16 hours of incubation observed at phase contrast microscope(magnification x40). The three lobes structures are the zygotes and are indicated by yellow arrows. The lobes represent the two haploid parental cells and the budding diploid cell.

to the zygotes (**Figure 18**). The mated culture was then pelleted, resuspended in YPDA 0.5x and plated on depleted medium plates subsequently incubated for 3 days at 30°C.
A quality control of the mating was performed in order to determine the number of screened clones and the mating efficiency. The number of screened cloned was calculated multiplying the obtained number of colonies who grew on control plates by the volume in which yeast cells have been resuspended prior to plating. A good mating experience must achieve a minimum of 1 000 000 screened clones, since using less than this will result in less chance of detecting genuine interaction on selective media. The mating efficiency, which consists in the percentage of diploids obtained during the mating, was calculated using the following formula:

$$100 * \frac{\text{n° of colony-forming unit (cfu)/ml of diploids (colonies who grew on control plates)}}{\text{n° of cfu/ml of limiting partner}}$$

where the limiting partner is the strain, bait or prey, with the lowest viability.
A good mating efficiency range from 2% and 5% of diploids.
The colonies grown on selective plates were then isolated and propagated using another selection marker (plates with media depleted in histidine) to operate a further selection step.

5.4. Rescue of the prey plasmid

We tested different extraction methods to rescue prey plasmids from yeast colonies obtained after mating.

5.4.1. Quick and Dirty protocol

Colonies were picked and struck to form patch on a petri dish containing the selective media SD/-Leu to help keeping the selective pressure on the prey plasmid. The plates were incubated at 30°C for 2-3 days to allow the growth of yeast. The patches were then collected with a tip and soaked into an Eppendorf containing 90 µL of Zymoliase/ME buffer. The samples were then incubated at 37°C for 1h. 10 µL of SDS 2% were added in the tubes that were then vortexed and incubated for 15 min at 70°C. 11 µL of potassium acetate 5M were added in the tubes that were then vortexed and incubated for 15 min on ice. The tubes are then centrifuged

for 10 min at 22 000 g at 4°C. 90 µL of the supernatant were transferred into a new Eppendorf tube containing 90 µL of isopropanol. The tubes were mixed by inversion and centrifuged for 10 min at 4°C at 22 000 g. The supernatant was then discarded and the pellet was allowed to dry overnight. Once dried the pellet was rehydrated with 20 µL of purified water. Samples were stocked at -20°C until analysis.

5.4.2. Kit Easy Yeast Plasmid Isolation (Clontech)

Starting material for this protocol consisted in yeast patches as described in the previous protocol. The patches were then collected with a tip and soaked into an Eppendorf containing 500 µL of 10 mM EDTA. The tubes were centrifuged for 1 min at 11 000 g. The supernatants were discarded and the pellets were resuspended with 200 µL of ZYM Buffer and 20 µL of Zymolyase suspension (both provided with the kit). The tubes were then vortexed and incubated at 30°C under agitation during 1 h. The tubes were centrifuged at 2 000 g during 10 min then the supernatants were discarded. The spheroplasts were then suspended in 250 µL of Y1 Buffer/RNAse A solution and 250 µL Y2 Lysis Buffer (both provided with the kit). Tubes were mixed by inversion and incubated during 5 min at room temperature. 300 µL of Y3 Neutralization Buffer (provided with the kit) was added and tubes were mixed by inversion and centrifuged at 11 000 g during 5 min. The supernatant was then transferred into a column inserted in a collection tube (provided with the kit). The samples were centrifuged at 11 000 g for 1 min. The columns were washed with 450 µL of Y4 Wash Buffer (provided with the kit). The samples were centrifuged at 11 000 g for 3 min. The elution step was performed adding 50 µL of YE Elution Buffer to the column inserted into an Eppendorf tube and incubating for 1 min prior centrifugation during 1 min at 11 000 g.

*5.4.3. Manual extraction adapted from **Hoffman and Winston (1987)***

Yeast colonies were cultivated in liquid depleted medium for two days in order to rescue the prey plasmid through DNA extraction using a specific lysis tampon (2% Triton X-100, 1% SDS, 0.1 M NaCl, 10 mM TrisHCl pH 8, 1 mM EDTA in sterilised purified water). The phase separation was performed through the addition of glass beads (425-600 µm in diameter) and 200 µL of phenol-chloroforme/isoamyl alcohol 24:1 solution. The tubes were vortexed for 2 min and after a centrifugation at 18 500 g for 5 min, the supernatant was

precipitated using 1/10 volumes of sodium acetate 3M and 2.5 volumes of absolute ethanol and mixed by inverting the tubes. After an incubation of 1 h at -20°C the cells were pelleted centrifugating the tubes for 10 min at 18 500 g. Supernatant was discarder and the resulting pellet was washed with a solution containing 70% of ethanol. Tubes were centrifuged for 10 min at 18 500 g. Ethanol solution was discarder and, once dried, the pellet was resuspended in 30 µL of DNAse/RNAse free water.

The rescued plasmids were propagated in *Escherichia coli* strain DH10β competent cells through electroporation. Overnight culture of transformed *E. coli* were then treated with a plasmid purification kit (MN) in order to recover the purified plasmid. The plasmid was then prepared and sent to perform Sanger sequencing (GENEWIZ/Awenta). In order to characterize the prey sequence, the resulting sequencing underwent a homology search using BLAST (NCBI) nucleotide collection and, more specifically, to the database consisting of the transcriptome shotgun assembly of *E. variegatus* (taxid: 13064).

5.5. Yeast colony PCR

In order to screen easily our prey transformants when needed, we operated PCR on yeast colony (Robertson *et al.*, 2021). Each colony was picked with a 200 µL tip and resuspended in 30 µL of purified and sterile water. The same tip, after resuspension, was used to patch the remaining cells onto a petri dish containing a selective media to help keeping the selective pressure on the plasmid. 6 µL of this solution were then mix with 14µ L of 0.02 M NaOH and the heated at 95°C for 45 min. The tubes were pulse spinned to pellet the cell debris and 1 µL of the surnatant was used as a template to perform a PCR using specific primers designed on the prey plasmid (**Table 2**) at 10 µM concentration and the polymerase OneTaq (NEB). Samples were heated in a thermocycler at 94°C for 4 min prior to undergo a 30 cycle program consisting of a denaturation step of 30 sec at 94°C, 30 sec at 60°C to allow the annealing of primer on the target sequence and 30 sec of elongation step et 68°C. A final step of 5 min at 68°C complete the program. PCR products were then analysed through electrophoresis on 1% agarose TAE 1X gel.

5.6. Yeast transformation

Yeast transformations were performed in order to exclude the autoactivation of yeast two-hybrid reporter system by the plasmid containing the prey only and to confirm the interaction(s) observed during the mating experiments. The purified plasmids containing the prey were transformed in the strain Y2H Gold containing the bait pGBKT7_VmpA and plated onto selective media. The yeast transformation was performed using the lithium acetate (LiAc) – mediated method described in the user manual of the kit Matchmaker® Gold Yeast Two-Hybrid System (Clontech) with some modifications to adapt it to our experimental conditions: an overnight pre-culture of wild type yeast strain Y2H Gold (for autoactivation test) or transformed Y2H Gold_pGBKT7_VmpA (for validation test) was diluted and then incubated et 30°C on an orbital shaker at 200 rpm until reaching the OD_{600} of 1. The culture was then centrifuged, washed and resuspended in 0.1 M LiAc/TE-1X. After being incubated at 30°C during 1 h the cells were pelleted, resuspended in a mix of 0.1 M LiAc/TE-1X, 50 µg of denatured salmon sperm DNA carrier and 1 µg of plasmid of interest. Then, 40% PEG4000/0.1M LiAc/TE-1X and 1/10 volume of DMSO were added prior to incubation of the samples at 30°C during 30 min. A heat shock at 42°C during 25 min was then performed. The transformed cells were then pelleted, resuspended in 100 µl of sterile water and then plated onto an SD media depleted of leucine and tryptophan (SD/-Leu-Trp) in order to verify the presence of both bait and prey plasmids in yeast cells.

To exclude the autoactivation of the gene reporter system by the prey protein alone, Y2H Gold has been transformed with the prey plasmid alone and then the transformed cells were spread onto an SD media depleted of leucine (SD/-Leu). Plates were incubated at 30°C for three days for yeast colonies to grow.

Three colonies for each plate were then used to start a culture in the appropriate SD media (SD/-Leu for prey plasmid alone and SD/-Leu-Trp for cotransformation) to maintain the plasmids and incubated overnight at 30°C at 200 rpm on an orbital shaker. Serial dilutions of the culture were plated onto appropriate selective SD media: for autoactivation assessment SD/-Leu and SD/-Leu + AbA and for interaction verification SD/-Leu-Trp and SD/-Leu-Trp + AbA. The plates were then incubated for three days at 30°C. Colonies grown on SD/-Leu and SD/-Leu-Trp were then streaked onto an SD media depleted of histidine (SD/-His) as a

confirmation of results. We included two positive controls in our yeast retro transformation experiences. In addition to the bait plasmid pGBKT7-53 and its interacting prey pGADT7-T provided with the kit used, we recovered two plasmids coding for two interacting *Arabidopsis thaliana* RTM proteins pGBKT7_RTM3 and pGADT7_RTM1 from Luc Sofer (Virology Team, UMR 1332 BFP, Cosson *et al.*, 2010).

5.7. Yeast proteins extraction

Glycerol stocks of the yeast colonies obtained after plating the mating solution were conserved at -80°C. 500 µL of the stock was used to start a culture in 20 mL of liquid media depleted of leucine in order to maintain the prey plasmid contained in the cells. Condition of growth were set at 30°C on orbital shaker at 200 rpm until the culture reach an OD_{600} ranging from 0.4 to 0.6. The number of cfu/mL was calculated multiplying the culture volume by the OD_{600} value. The cultures were then cooled by placing them on ice and then centrifuged at 4°C for 5 min at 1000 g. The pellet was then resuspended in 20 mL of cold purified and sterile water prior to a further centrifugation at the same condition as the previous one. The pellet was frozen in liquid nitrogen and stocked at – 80°C. The pellet was then resuspended with an appropriate volume of freshly prepared cracking buffer [1 mL cracking buffer stock solution (8 M urea, 5% SDS, 40 mM TrisHCl ph 6.8, 0.1 mM EDTA, 0.4 mg/ml blue bromophenol, H_2O), 10 µL β-mercaptoethanol, 70 µL protease inhibitor cocktail P8340, 50 µL PMSF 0.1 M] according to the cfu/ml calculated before. The solution obtained was transferred in a microcentrifuge tube containing an appropriate amount of glass beads (425-600 µm of diameter) depending on the concentration of the culture. The tubes were then incubated for 10 min at 70°C, mixed using a vortex for 1 min and then centrifuged for 5 min at 14000 g and at 4°C. The supernatant was then transferred to a new Eppendorf tube and stocked on ice. The resultant pellet was incubated at 100°C for 5 min vortexed for 1 min, centrifuged for 5 min and the supernatant was added to the supernatant recovered previously and stocked on ice. Samples were stock at -20°C and boiled just before being separated on acrylamide gel for SDS-PAGE.

5.8. Western Blot analysis

Samples were separated by SDS-PAGE on 10% acrylamide gel. Proteins were then transferred on a nitrocellulose membrane by electrophoretic transfer for 1 h and 15 min at 70 V. The membrane was then stained with Ponceau S staining solution in order to assess the quality of proteins transfer. The membrane was washed with purified water to remove Ponceau S staining solution and saturated with a blocking buffer consisting in a solution of PBS and 5% skimmed milk for 4 h at room temperature. Then, the membrane was incubated in PBS and protease inhibitor cocktail P8340 (1/1 000) (Sigma-Aldrich) overnight at 4°C on an orbital shaker. The membrane was then washed in PBS and PBS Tween 20 0.2% prior to incubation with an antibody anti-HA (1/2 000) (Sigma-Aldrich) to verify the expression of our tagged protein in yeast. After incubation, and washing with PBS and PBS Tween 20 0.2% the membrane has been incubated with the secondary antibody anti-IgG mouse coupled with HRP (Sigma-Aldrich). After washing, membrane was incubated with HRP substrate (SuperSignal™ West Pico PLUS Chemiluminescent Substrate, Thermo Fisher) for 5 min in the dark and then visualized through ChemiDoc Imaging System (BioRad). The images have been analyzed using ImageLab (BioRad).

We compared the mass of the proteins visualized on the western blots with the theorical molecular weight of the proteins coded in the prey plasmids of the tested clones. This theorical molecular weight was based on the length of the insert obtained by PCR amplification with primers flanking insert region (pGAD_F1/R1, **Table 2**). We estimated the length of the sequences by agarose gel electrophoresis and we divided the base pair observed by 3 to get the number of amino acids of the insert. The number of amino-acids were multiplied by the mean molecular weight of an amino-acid (110 Da, Promega). Then, we add the 12.4 kDa of the Gal4 activation domain normally fused to the prey protein.

5.9. Prey proteins sequences analysis

After purification of prey plasmids from transformed yeast, the nucleotidic sequence of the insert was obtained through sequencing by Sanger technology (GENEWIZ, Azenta) using primers matching region flanking the insertion site on the plasmid. The sequence analysis and

alignment onto reference sequences (TSA *Euscelidius variegatus* taxid:13064) and onto prey plasmid pGADT7 backbone map were performed using ClustalW (https://www.ebi.ac.uk/Tools/msa/clustalo/).

6. Statistical analysis

All statistical analysis were performed using R 4.0.3 through the R commander (Rcmdr) package performing the Kruskal-Wallis rank sum test.

Chapter 1 - Looking for VmpA receptors in *Euscelidius variegatus*

Looking for VmpA receptors in *Euscelidius variegatus*

1. Justification of the experimental strategy

Phytoplasmas are not cultivable *in vitro* up to this day. They are maintained in their living hosts in greenhouses and they are continuously propagated through cycles of infection of vectors from infected plants and transmission to non-infected ones. Because of its ecology (*i.e.* univoltine, ampelophagous, laying of eggs in grapevine woods), it is not possible to rear the natural vector of FDp, *S. titanus*. An alternative experimental pathosystem has been set up to study flavescence dorée in controlled condition (Caudwell *et al.*, 1973): grapevine was replaced by the alternative plant host, the broad bean (*Vicia faba*), meanwhile the experimental vector employed was *Euscelidius variegatus*, a leafhopper belonging to the same subfamily than *S. titanus* (Deltocephalinae). *E. variegatus* can be reared in greenhouses on oat plants (*Avena sativa*), provides new generations almost throughout the year and lays its eggs in the thin oat leaves. The possibility to easily recover the eggs has allowed the set-up of *E. variegatus* cell culture, the Euva cells (Arricau-Bouvery et al., 2018). This cellular system, even though it represents only an approximation of the whole organism, allows to perform assays in which we can virtually control all experimental conditions, a factor which contributes to a more stable reproducibility of results among different technical replicates.

The objective of this study was to design a strategy to identify VmpA receptors. To look for VmpA receptors in insect vectors we performed *in vitro* interaction assays as this approach has already been successful for the identification of molecular mechanisms underlying the interaction between phytoplasma and their insect vectors. Soluble proteins extracted from *Macrosteles striifrons*, the vector of aster yellow OY phytoplasma, have been loaded onto an affinity column exposing Amp protein. Insect proteins binding Amp have been eluted and separated by SDS PAGE and 2D electrophoresis (Suzuki *et al.*, 2006). The bands on the gel have been then excised and sent to mass spectrometry analysis. This allowed to demonstrate that Amp interacts with actin and light and heavy chain of myosin of the insect vector. A similar approach consisting in affinity chromatography coupled with mass spectrometry has been followed to identify the interaction between Amp of another strain of *Candidatus*

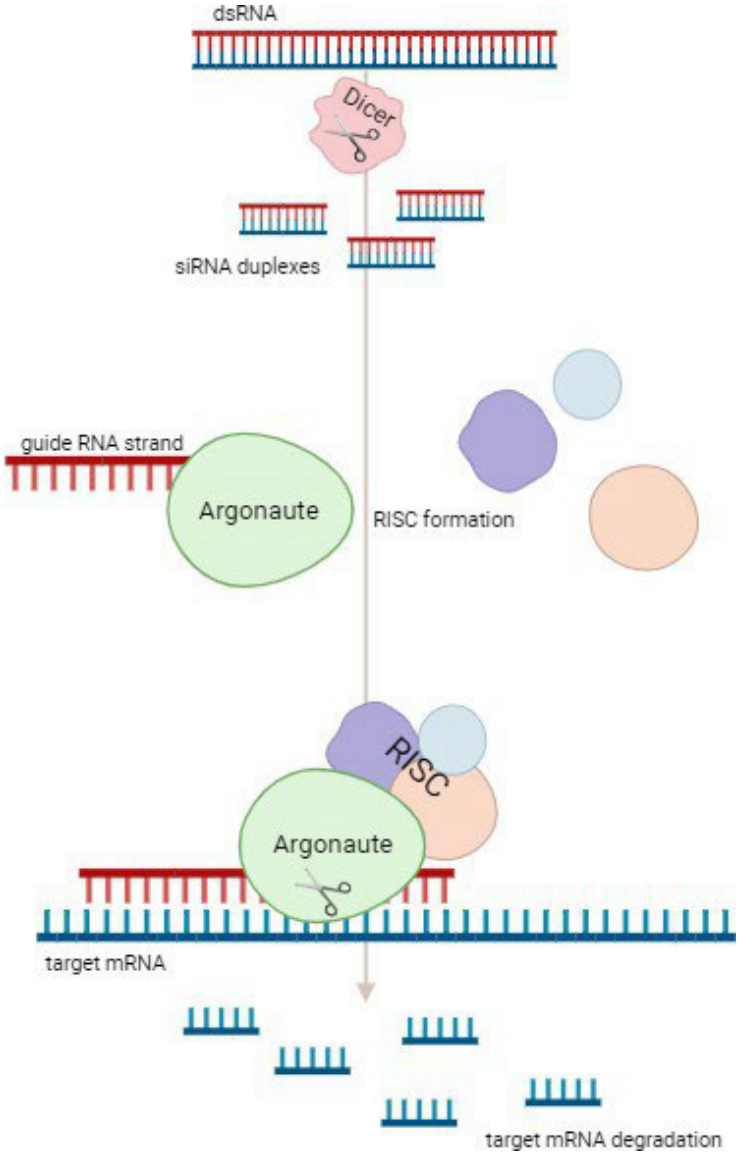

Figure 19. Schematic representation of RNAi machinery. dsRNAs are uptaken from the environment and are cleaved by the protein Dicer in siRNA duplexes. One siRNA strand (guide RNA strand) is loaded onto the protein Argonaute and, upon recruitment of other proteins, the RNA induced silencing complex (RISC) is formed. The guide RNA strand mediates the recognition of the complementary mRNA which is then cleaved by the endonuclease activity of Argonaute. Thus translation of the corresponding protein is impaired (post-transcriptional silencing). The figure has been realised using BioRender.

Phytoplasma asteris, the Chrysantemum Yellow Phytoplasma, and actin and ATP synthase of their leafhopper vectors (Galetto *et al.*, 2011).

We first identified by mass spectrometry proteins present at the surface of the cell line Euva-11, which potentially interact with the adhesin VmpA by purification on affinity column and far-western blot assays. Once the candidate proteins interacting with VmpA were identified and selected, their role as receptors had to be validated.

Knockdown gene expression is a powerful tool to elucidate gene function and can be achieved by long double-stranded RNA (dsRNA) introduced into the organism or the cells (Baum *et al.*, 2007; Mondal *et al.*, 2020). In RNA interference (RNAi) the long dsRNAs are processed in small interfering RNAs (siRNAs) that trigger degradation of the complementary target mRNA. This technique consists in exploiting the cells endogenous RNAi machinery, common to almost all eukaryotic organisms. The biological role of RNAi mechanism is involved in the regulation of gene expression, antiviral immunity and genome protection against transposable elements (Ketting, 2011). The first step consists in the cell uptake of dsRNA from the environment that can be achieved by i) transmembrane channels for dsRNA ii) endocytotic processes. Once in the cell, dsRNAs are cut into 20-22 bp siRNA duplexes by the protein Dicer, a ribonuclease III-like protein. One of the two strands of the siRNA constitutes the guide RNA strand which is loaded onto the Argonaute protein, one of the components of the RNA-induced silencing complex (RISC) (**Figure 19**). RISC recognises mRNAs having a complementary sequence to its guide RNA strand. The RISC binds to the target mRNA forming a duplex which is cleaved thanks to the endonucleolytic activity of the Argonaute protein. The RISC components are then recycled meanwhile the degradated fragments of the target mRNA can be used as template by RNA-dependent RNA Polymerase (RdRP) to produce new siRNA resulting in an amplification loop effect. RdRPs have been reported to be unnecessary in RNAi machinery in Drosophila (Schwarz *et al.*, 2002) and their sequences were only sporadically found in insect genomes (Pinzón *et al.*, 2019). *E. variegatus* transcriptome has been surveyed to look for core components of RNAi machinery revealing the presence of Argonaute2, Dicer2, and R2D2, three of the main components of the siRNA pathway, as well as genes involved in micro RNA (miRNA) and PIWI-interacting RNAs (piRNA) pathways (Abbà *et al.*, 2019).

RNAi in mammal cells is performed using siRNA while in insects it is generally performed using long double-stranded RNA (Jackson *et al.*, 2003). This approach had been

used for instance to inactivate genes in several *Drosophila* cells in culture (Clemens *et al.*, 2000; Echeverri and Perrimon, 2006). The long dsRNAs are processed in short ssRNA targeting different regions of the same mRNA, increasing the specificity of action and reducing the possible silencing effect on other transcripts, as demonstrated for post-transcriptional silencing induced by the delivery of multiple siRNAs in mammalian cells (Kittler *et al.*, 2007; Hannus *et al.*, 2014).

DsRNA mediated RNAi effectiveness vary greatly among insect orders. Experiments comparing the cultured cells RNAi response confirm the previously reported highly responsiveness of coleopterans and the lower efficiency of lepidopteran response to RNAi treatment (Shukla *et al.*, 2016). The first step of dsRNA uptake from the media was efficiently achieved by both the coleopteran *Leptinotarsa decemlineata* and the lepidopteran *Heliothis virescens* cell lines. However, the dsRNA derived siRNA could only be detected in the total RNA extract from *L. decemlineata*, suggesting that an impaired processing of long dsRNA is responsible for the poor RNAi response observed in lepidopteran insects. Concerning leafhoppers, previous works shows an efficient response to dsRNAs treatments in *E. variegatus*, upon both feeding and microinjection delivery (Abbà *et al.*, 2019; Galetto *et al.*, 2021a; Galetto *et al.*, 2021b; Arricau-Bouvery *et al.*, 2023) but the response of Euva cells in culture was not evaluated yet.

We tried then to set up a simplified experimental model to screen for the insect proteins interacting with VmpA previously identified by mass spectrometry. We started from the assumption that reducing the expression of VmpA receptors in the leafhopper cells in culture should be correlated to a decrease in the ability of cells to bind VmpA. We measured the effect of a decrease of the candidates expression by Euva cells on their ability to bind VmpA-coated latex beads. In the context of this project, we optimized RNAi to simultaneously knockdown up to 13 genes coding these candidates in the cell line Euva-11, in order to test the potential additive effect of multiple insect VmpA receptors.

To assess the vector specificity underlying interaction between VmpA and its putative receptors in the insect, we used a recombinant VmpA belonging to a *S. titanus* non-transmissible phytoplasma isolate of Palatinate Grapevine Yellow (PGYA) to perform both *in vitro* interaction assays with Euva cells extracted proteins and latex beads adhesion assays on dsRNA treated cells.

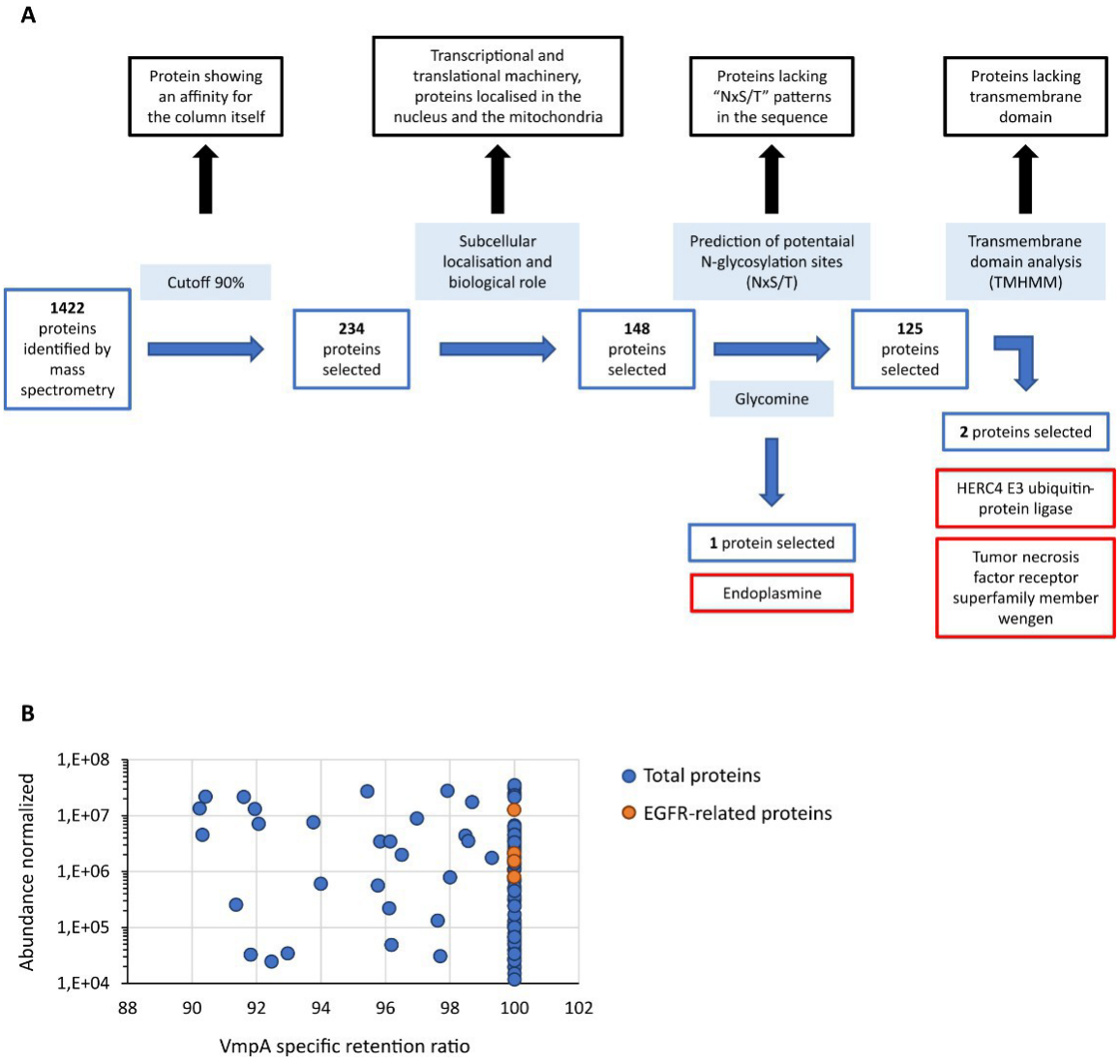

Figure 20. Proteins of Euva cells that interact with VmpA-His$_6$. (A) Process of selection of candidates that interact with VmpA-His$_6$. The different steps of the process are indicated inside light blue boxes. The proteins without interest are indicated in boxes lined with black. The proteins selected at each step are indicated in boxes lined with blue and the name of the three proteins finally selected are in boxes lined with red. (B) Abundance of the proteins interacting with VmpA-His$_6$ selected with a retention ratio superior to 90%. The five proteins interacting with EGFR and implicated in its recycling process are indicated in orange.

2. Results

2.1. Selection of Euva proteins interacting with VmpA collected through affinity column

Euva proteins solubilised in Rx buffer were incubated overnight with recombinant VmpA-His_6 of strain FD92 to allow interaction complexes to form. The protein mixture was then loaded onto an affinity Nickel resin column and eluted proteins were identified by mass spectrometry (nLC-MS/MS). The control consisted on purification of the Euva proteins on Ni-NTA column. Mass spectrometry analysis identified 1422 proteins among proteins binding VmpA-His_6 retained by the column and 1604 for the control condition (Euva proteins only). A cut-off of 90% was applied to the specific VmpA retention ratio and allowed the selection of 239 proteins (**Figure 20.A**). They were classified based on the KEGG classification (**Table 3**). Proteins belonging to the transcriptional and translational machinery, and proteins localized in the nucleus and mitochondria were removed from the pool of protein candidates that could interact with VmpA. The 148 remaining proteins were analysed based on the presence of predicted glycosylation sites using Glycomine software that selected only the endoplasmin (endo) protein (1 site with p=0.958 and 4 sites with p>0.8). We additionally searched the 'NxS/T' glycosylation site patterns in the amino acidic sequence of the identified proteins and selected 125 candidates. Among them, the transmembrane segments were identified using TMHMM 2.0 software and only two membrane proteins were identified, the HERC4 E3 ubiquitin-protein ligase (HERC4) and the Tumor necrosis factor receptor super family member wengen (wengen). Interestingly, five proteins that are known to be implicated in the turnover of the epidermal growth factor receptor (EGFR) were found among the pool of 148 proteins (**Figure 20.B**). Despite the absence of the EGFR in this pool and because it is a 92 kDa glycosylated protein present at the surface of almost all cells, we decided to additionally test EGFR as a fourth candidate. Indeed, it has been shown previously that VmpA-His_6 interacted essentially with Euva proteins with apparent masses of 90-95 kDa (Arricau-Bouvery *et al.,* 2021).

Table 3. Repartition of Euva proteins that interacted with VmpA-His$_6$ in relation to their KEEG classification.

KEEG classification	Number of proteins
Global cellular processes	142
Cytoskeleton	18
Vesicular trafficking	17
Binding to membrane / to membrane receptor	9
Other	53

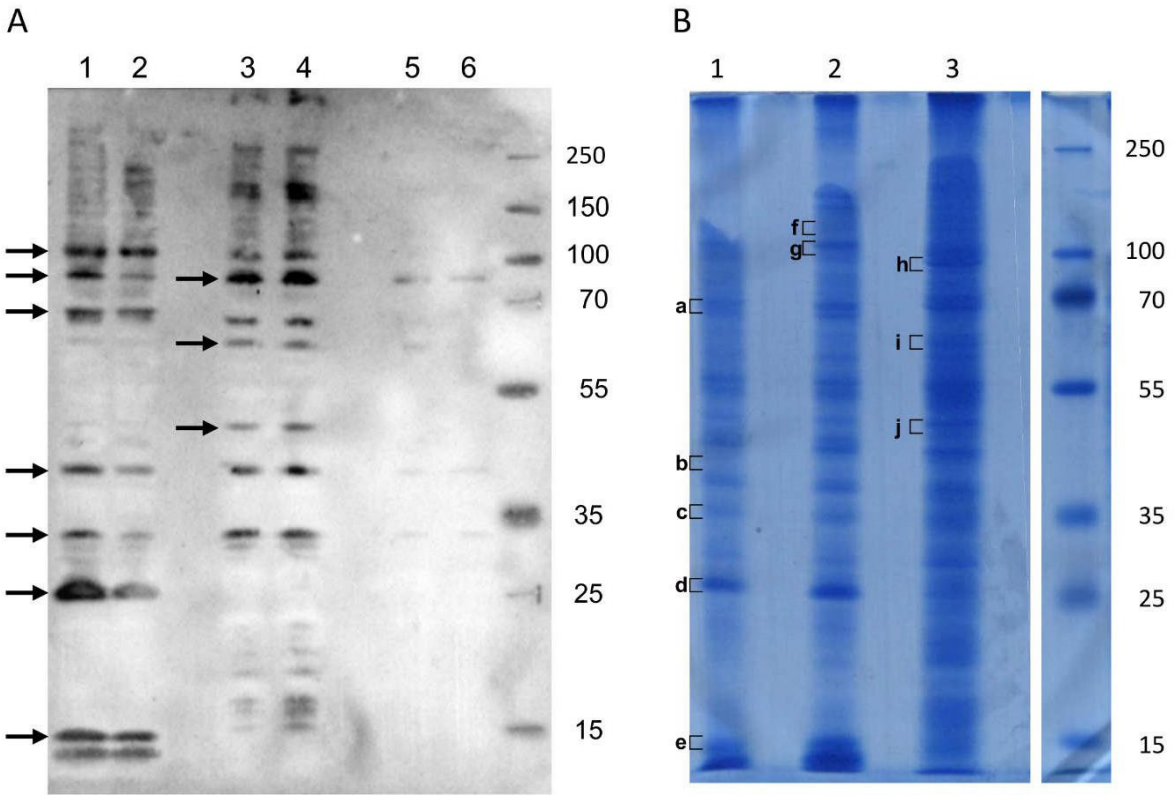

***Figure 21. Interaction of VmpA-His$_6$ with Euva cell proteins* in vitro.** (A) Euva proteins transferred to nitrocellulose membrane were incubated with recombinant VmpA-His$_6$. Arrows indicated the insect proteins selected to be extracted from SDS PAGE gel indicated with square bracket in B. (B) Euva proteins coloured with Coomassie blue. Euva-12 (1) and Euva-11 (2) proteins present in the pellet (insoluble fraction). Euva-12 (3) and Euva-11 (4) proteins soluble in Rx-T-DOC buffer. Euva-12 (5) and Euva-11 (6) proteins soluble in the Rx buffer. a to j, bands of proteins that were analysed with LC-MS-MS.

2.2. Selection of transmembrane Euva proteins interacting with VmpA using far-western blot interaction assay

To better enrich protein fractions in transmembrane proteins, we increased the concentration of Triton-X-100, from 0.1% to 1%, and added 0.5% sodium deoxycholate (DOC) to the Rx buffer (Rx-T-DOC). The proteins were separated into three fractions, the proteins soluble in Rx fraction, the Rx-T-DOC soluble fraction and the insoluble fraction, i.e. pellet suspended directly in Laemmli buffer. The two cell lines Euva-11 and Euva-12 that showed different cell morphologies were used for the protein extraction process. The Euva-11 cell line was more homogenous and mostly contained cells that looked like epithelial cells. The Euva-12 cell line was more heterogenous but also contained epithelial-like cells. The different fractions of proteins extracted from Euva cells were submitted to far-western blot using VmpA-His_6 for interaction (**Figure 21.A**). Even though the two cell lines did not fully look the same, no difference was observed between the VmpA-His_6 interaction patterns of Euva-11 proteins and Euva-12 proteins. The profile of proteins that interacted with VmpA-His_6 had bands in common between the different extracted fractions but for some bands the intensity of the signal observed was increased (**Figure 21.A**). Seven main bands were visible in the fraction submitted to Rx-T-DOC extraction and eight in the insoluble fraction. Four bands were in common between insoluble and soluble fractions, in detail bands of 32, 45, 90 and 110 kDa. In parallel of far-western blot, Euva proteins with masses corresponding to that observed on far-western blot were excised from a Coomassie blue-stained gel and send to nLC-MS/MS mass-spectrometry analysis. The bands of proteins removed from the gel are indicated by square brackets from “a” to “j” on the **Figure 21.B**. A total of 205 proteins were selected because they both have TMHMM-predicted transmembrane segments and ‘NxS/T’ potential N-glycosylation sites (**Table 4**, details in **Table S1**). Among these proteins we selected 9 proteins that were predicted to be mostly localized at the surface of the cell according to TMHMM prediction (**Table 4** and **5**).

2.3. RNAi knock-down gene expression on Euva cells

RNA interference (RNAi) was used in the Euva cells to inhibit the production of the candidate proteins interacting with VmpA-His_6. Quantification of the mRNA of the 4 first

Table 4. Repartition of Euva proteins extracted with the buffer Rx Triton 1% + DOC 0.1% and that interacted with VmpA-His$_6$. The proteins were selected sequentially by their weight, the presence of predicted transmembrane domain using TMHMM and the presence of 'NxS/T' indicated potential site of glycosylation. The proteins selected for adhesion assays were indicated with their abbreviation

Band	Property	Number of proteins	Number of proteins selected by					protein selected for adhesion assays	candidates abbreviation
			weight (range of selection)		transmembrane segment (TMHMM)		NxS/T pattern		
a	insoluble	1295	340	(60 - 80 kDa)	21	(6%)	21	lysosome membrane protein 2 [Homalodisca vitripennis] protein cueball isoform X1 [Homalodisca vitripennis]	CD36-like cueball
b	insoluble	1446	333	(40 - 50 kDa)	23	(7%)	17		
c	insoluble	950	280	(30 - 40 kDa)	17	(6%)	14		
d	insoluble	886	240	(20 - 30 kDa)	17	(7%)	16		
e	insoluble	322	19	(13 - 15 kDa)	1	(5%)	1		
f	insoluble	1077	153	(100 - 120 kDa)	13	(8%)	13	transforming growth factor-beta-induced protein ig-h3-like [Homalodisca vitripennis] protein draper isoform X1 [Zootermopsis nevadensis]	fasciclin draper
g+h	insoluble + soluble	684	133	(85 - 110 kDa)	14	(11%)	14	Protein containing LRR domains (identification via interpro) integrin β sodium/calcium exchanger 3-like isoform X1 [Homalodisca vitripennis] transforming growth factor-beta-induced protein ig-h3-like [Homalodisca vitripennis] leucine-rich repeat-containing protein 15-like [Homalodisca vitripennis]	uk1_LRR integrin β Na/Ca exchanger fasciclin uk2_TLR
i	soluble	1441	421	(55 - 68 kDa)	58	(14%)	54	protein cueball isoform X1 [Homalodisca vitripennis] lysosome membrane protein 2 [Homalodisca vitripennis]	cueball CD36-like
j	soluble	1222	462	(40 - 55 kDa)	63	(14%)	55	uncharacterized protein LOC124356975 [Homalodisca vitripennis]	uk3

Table 5. Characteristics of the Euva proteins selected for adhesion assays.

Band	TSA Euscelidius variegatus (NCBI)	Séquence (BLASTP)	abbreviation	Predicted transmembrane segments (TMHMM)	NxS/T	MW (kDa) protein
a	ORF01214079_GFTU01004399.1_00136_01779_f1	lysosome membrane protein 2 [Homalodisca vitripennis]	CD36-like	2	6	61
	ORF03010044_GFTU01011408.1_00185_01996_f2	protein cueball isoform X1 [Homalodisca vitripennis]	cueball	1	6	67
f	ORF02093016_GFTU01007852.1_00001_02736_f1	transforming growth factor-beta-induced protein ig-h3-like [Homalodisca vitripennis]	fasciclin	1	5	94
	ORF03898939_GFTU01016123.1_00223_03282_f1	protein draper isoform X1 [Zootermopsis nevadensis]	draper	1	11	109
g+h	ORF03757228_GFTU01015247.1_00222_02681_f3	Protein containing LRR domains (identification via interpro)	uk1_LRR	1	14	87
	ORF03985247_GFTU01016611.1_00180_02645_f3	integrin beta	integrin β	1	7	91
	ORF03874906_GFTU01015965.1_00117_02747_f3	sodium/calcium exchanger 3-like isoform X1 [Homalodisca vitripennis]	Na/Ca exchanger	12	6	95
	ORF02093016_GFTU01007852.1_00001_02736_f1	transforming growth factor-beta-induced protein ig-h3-like [Homalodisca vitripennis]	fasciclin	1	5	94
	ORF03639633_GFTU01014488.1_00117_02468_f3	leucine-rich repeat-containing protein 15-like [Homalodisca vitripennis]	uk2_TLR	1	7	82
i	ORF03010044_GFTU01011408.1_00185_01996_f2	protein cueball isoform X1 [Homalodisca vitripennis]	cueball	1	6	67
	ORF01214079_GFTU01004399.1_00136_01779_f1	lysosome membrane protein 2 [Homalodisca vitripennis]	CD36-like	2	6	61
j	ORF00560024_GFTU01001746.1_00401_01750_f2	uncharacterized protein LOC124356975 [Homalodisca vitripennis]	uk3	1	2	48

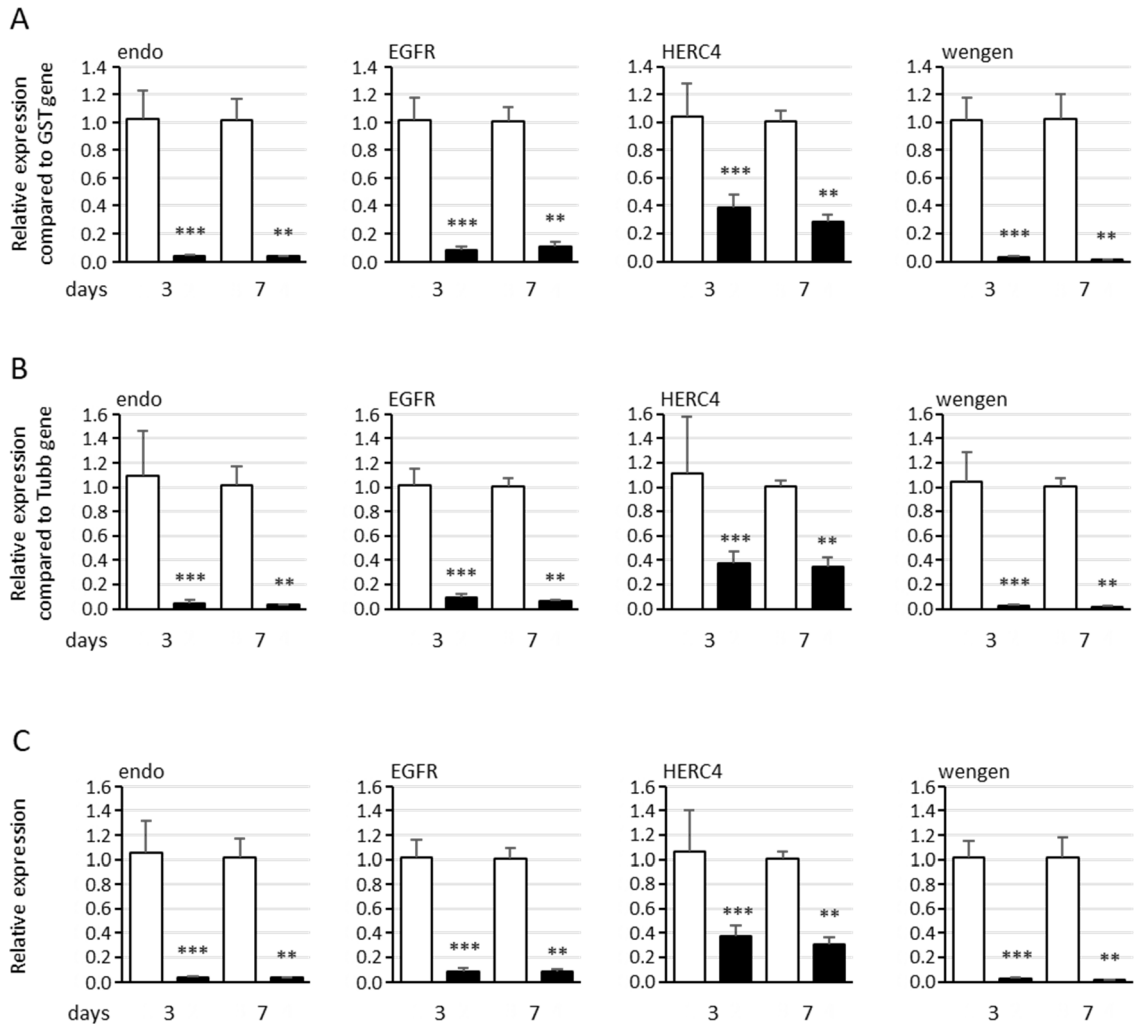

Figure 22. Relative expression of the 4 genes endoplasmin (endo), epidermal growth factor receptor (EGFR), HERC4 E3 ubiquitin-protein ligase (HERC4) and tumor necrosis factor receptor super family member wengen (wengen) in Euva cells regards to the reference gene glutathione S-transferase (A), tubulin β (B) and both genes (C). White boxes correspond to Euva cells transfected with GFP dsRNA and black boxes correspond to Euva cells transfected with dsRNA targeting the gene indicated above the graphs. ** indicates a significant difference with $p<0.01$ and *** with $p<0.001$ under the Kruskal- Wallis rank sum test of the R commander package of R software version 4.0.3.

candidates, *i.e.* endo, EGFR, HERC4 and wengen, was performed 3 and 7 days after insect cell transfection with dsRNA. The dsRNA negative control corresponded to the GFP gene. Total RNAs were extracted and real time RT-PCR was used to quantify the effect of dsRNAs on the expression of these 4 genes. Two relative expression levels were calculated using the glutathione S-transferase (GST) and tubulin β (tubβ) genes as references. Whatever the gene considered a significant inhibition of expression was observed 3- and 7-days post-transfection with dsRNA (**Figure 22**). The inhibition factors varied between 3 and 68 depending on the gene and the time post transfection. No difference in inhibition rates were observed when we referred to the two reference genes, so only the GST reference gene was kept for the further experiments. No difference was observed between 3 and 7 days whatever the gene considered except for the wengen gene expression for which a slight decrease was observed at 7 days (p=0.03 under the Kruskal-Wallis rank sum test of the R commander package of R software version 4.0.3). Therefore, extraction of mRNAs and further experiments were performed three days post-transfection that should be adequate for turnover of the target protein as reported by Clemens and colleagues (Clemens *et al.*, 2000).

When we tested the 9 other genes, we found that the expression rate of the gene uk3 was too low to performed RNAi assay (Ct values of 34-35). For the remaining eight genes, namely integrin β, uk1_LRR, CD36-like, fasciclin, Na/Ca exchanger, cueball, uk2_TLR and draper, a statistically significant inhibition of gene expression was achieved (**Figure 23**, black bars) with fold change values ranging from 2.03 for the fasciclin gene to 51.4 for the uk1_LRR gene.

2.4. Simultaneous multiplexing RNAi on Euva cells

The adhesin VmpA potentially interacts with several insect receptors, as multiple bands were observed after far-western blot with VmpA-$His_{6.}$ (**Figure 21.A**). To maximize the chances to inhibit different VmpA receptor(s) at once, we performed assays in which several genes were inhibited simultaneously with dsRNA targeting the different genes selected. For all the twelve genes, significant differences were observed with the control condition, *i.e.* GFP dsRNA, whatever the number of genes inhibited simultaneously including the targeted gene (**Figure 23**, grey bars). For the genes endo, wengen, integrin β, uk1_LRR, CD36-like, fasciclin,

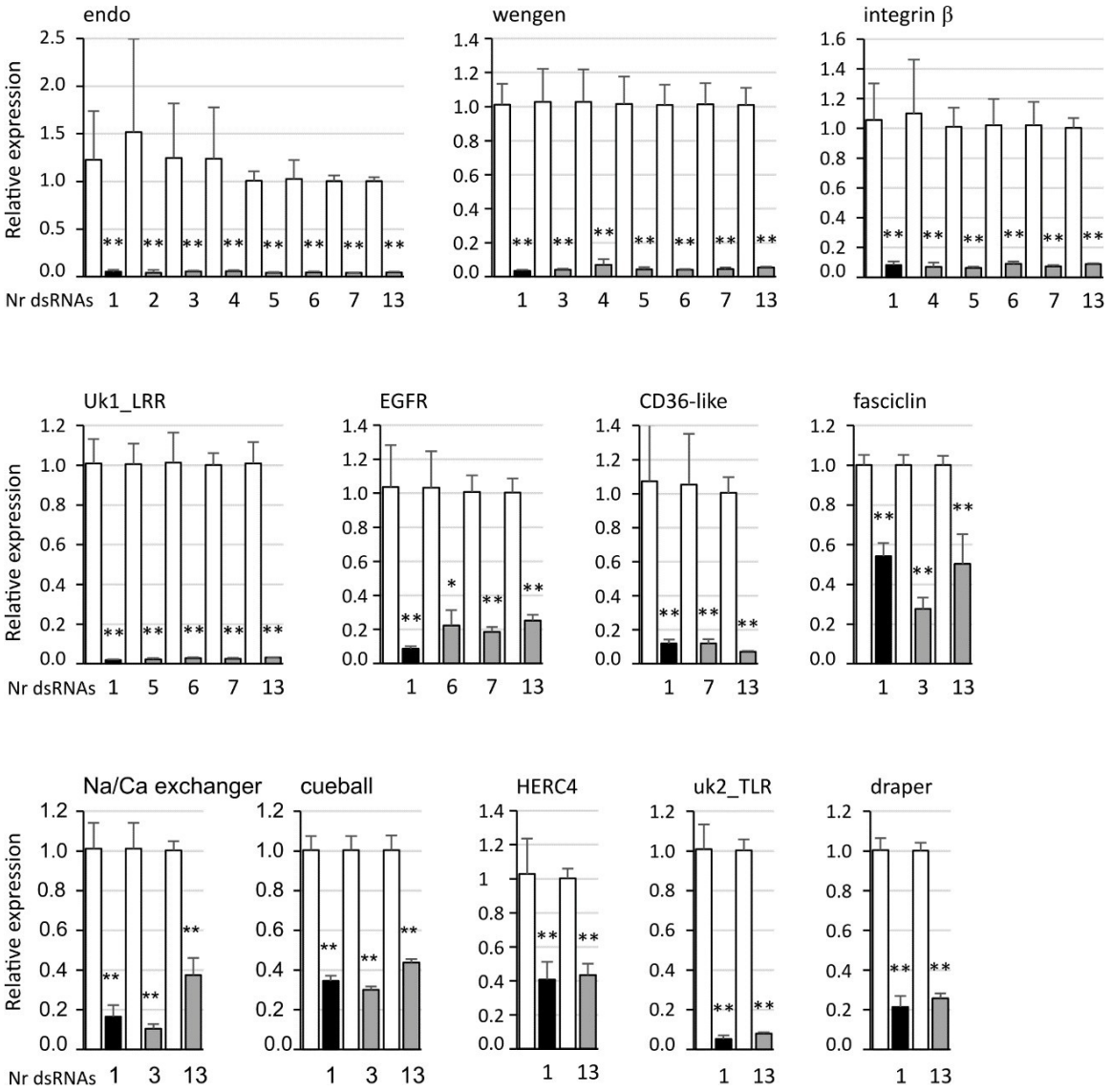

Figure 23. Relative expression of the candidate genes endoplasmin (endo), tumor necrosis factor receptor super family member wengen (wengen), integrin β, protein containing LRR domains (uk1_LRR), epidermal growth factor receptor (EGFR), lysosome membrane protein 2 (CD36-like), transforming growth factor-beta-induced protein ig-h3-like (fasciclin), sodium/calcium exchanger 3-like isoform X1 (Na/Ca exchanger), protein cueball isoform X1 (cueball), HERC4 E3 ubiquitin-protein ligase (HERC4), leucine-rich repeat-containing protein 15-like (uk2_TLR) and protein draper isoform X1 (draper) in Euva cells. Glutathione S-transferase was the reference gene of this study. White boxes correspond to Euva cells transfected with GFP dsRNA, black boxes with dsRNA targeting the gene indicated above the graphs, and grey boxes with several dsRNA including the gene studied, the number of which is indicated under the graph. * indicates a significant difference with $p<0.05$ and ** with $p<0.01$ under the Kruskal-Wallis rank sum test of the R commander package of R software version 4.0.3 regards to the GFP dsRNA control.

cueball, HERC4, uk2_TLR and draper no difference was observed between the inhibition with dsRNA targeting the gene studied alone and the inhibition induced with up to 13 several different dsRNA, including the targeted gene studied. The dsRNAs designed on uk3 sequences was also included in the multiplex silencing although its inhibition in transfected cells was not assessed. For the genes EGFR and Na/Ca exchanger, a lower gene expression inhibition efficiency of was observed when 12 other genes were simultaneously inhibited with the gene studied compared to the single inhibition of the EGFR and Na/Ca exchanger genes.

We tested the effect of off target on the expression of 4 genes when 2 to 6 other genes were simultaneously inhibited. The results show that no significant difference was observed when dsRNA targeted genes other than the studied one compared to GFP dsRNA (**Figure 24**).

It must be noticed that the phenotype of transfected cells observed with light microscope and their ability to achieve confluence was not impacted by the silencing of any of the candidate genes nor when the thirteen candidate genes were inhibited simultaneously (**Figures 25** and **26**).

2.5. Adhesion assays to Euva cells of VmpA-coated beads

The VmpA-His_6-beads adhesion assays were first performed three days after transfection using Euva-11 cells transfected with dsRNA targeting one gene. On average, 51 (±5) Euva-11 cells and 200 (±50) beads were observed per field. Twenty fields were photographed per condition and three independent experiments were performed and pooled. The results show that, whatever the gene inhibited, no difference of bead adhesion was observed between the cells transfected with the dsRNA targeting candidate genes and GFP dsRNA (**Figure 27.A**) except for the gene uk1_LRR (**Figure 28.A**). For the gene uk1_LRR, the three repetitions were very homogeneous, i.e. 0.89± 0.21, 0.87±0.25 and 0.87±0.28 of relative adhesion of beads with medians of 0.90, 0.82 and 0.75, respectively. At the same time as adhesion assays, the inhibition of the targeted genes was checked. Results show that for each gene a significant decrease of the mRNA was measured (**Figures 27.B** and **28.B**). The strongest inhibitions were observed for the genes uk1_LRR and wengen with 38.5-fold and 33-fold change of mRNA quantities respectively, and the weakest inhibition was observed for the gene fasciclin with 2-fold change.

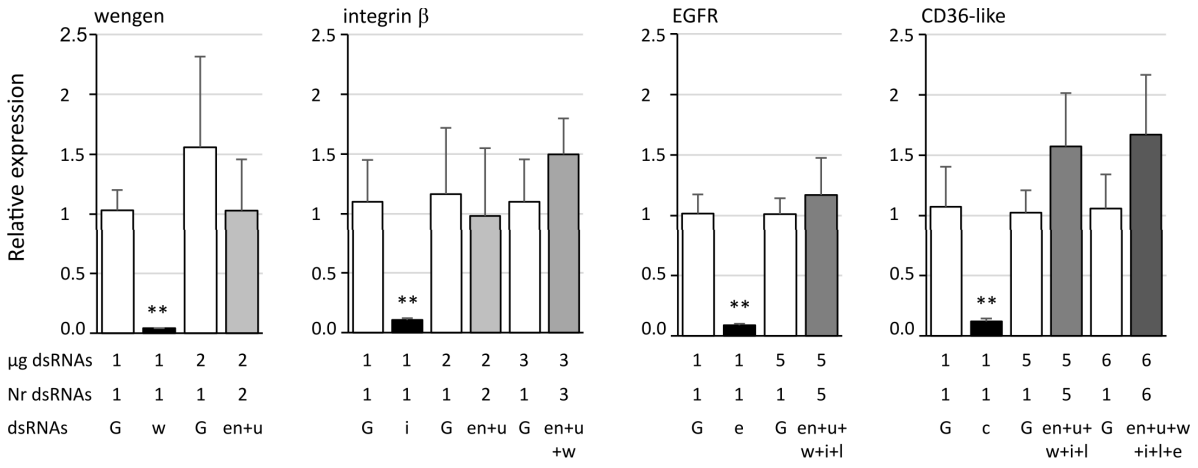

Figure 24. Expression of the candidate genes tumor necrosis factor receptor super family member wengen (wengen), integrin β, epidermal growth factor receptor (EGFR) and lysosome membrane protein 2 (CD36-like) in Euva cells regards to the reference gene glutathione S-transferase. White boxes correspond to Euva cells transfected with GFP dsRNA (G) at the quantities indicated under the graph (µg dsRNA), black boxes with dsRNA targeting the gene studied and indicated above the graphs, and grey boxes with several dsRNA without dsRNA targeting the gene studied, the number of which is indicated under the graph (Nr dsRNA). dsRNAs indicates the targeted genes endoplasmin (en), uk3 (u), wengen (w), integrin β (i), unk1_LRR (l), CD36-like (c) and EGFR (e). ** indicates a significant difference with $p<0.01$ under the Kruskal-Wallis rank sum test of the R commander package of R software version 4.0.3 regards to the GFP dsRNA control.

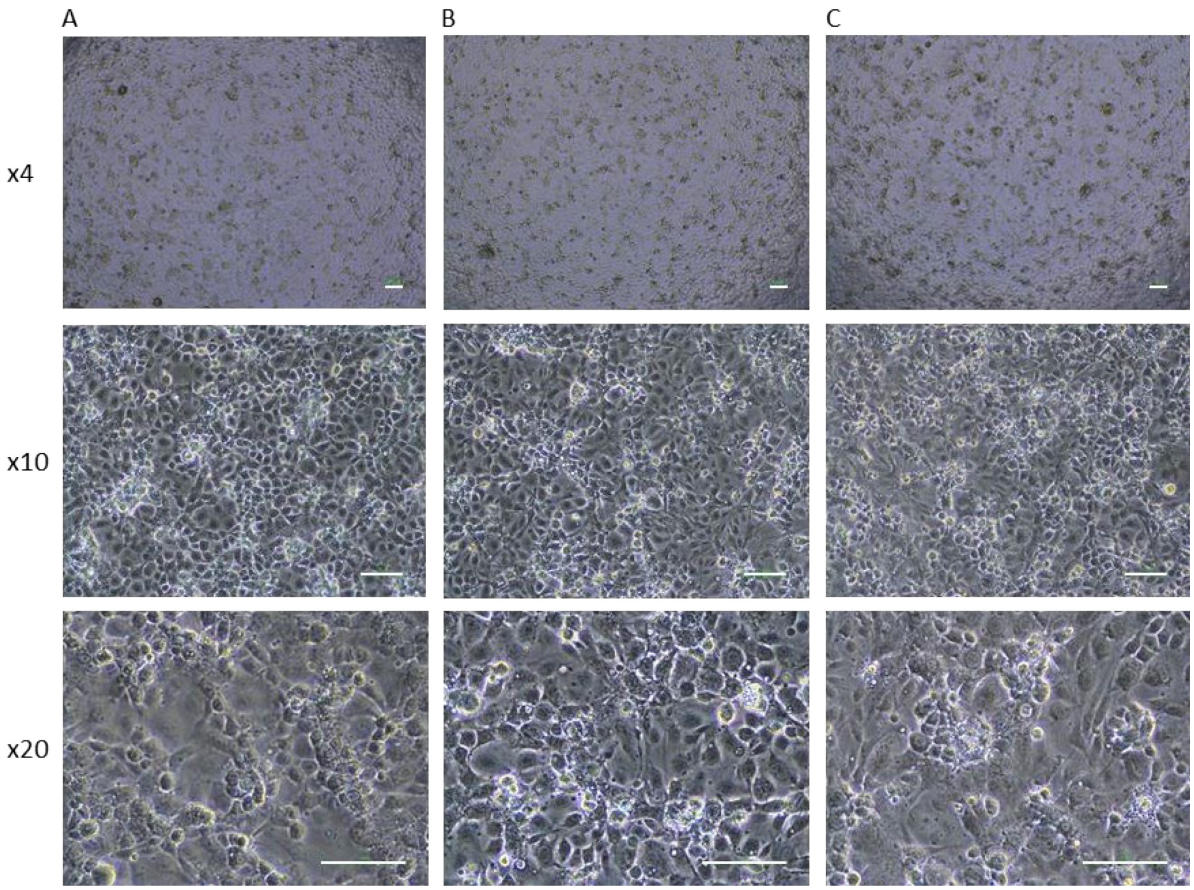

Figure 25. Euva11 cells observed at the inversed microscope 3 days post transfection. (A) Control condition in which the Euva-11 cells were cultivated in culture medium without transfection for 3 days, (B) after transfection with GFP dsRNA and (C) after transfection with uk1-LRR dsRNA. The magnification of observations is shown to the left of the panels. Scale bar 100 µm.

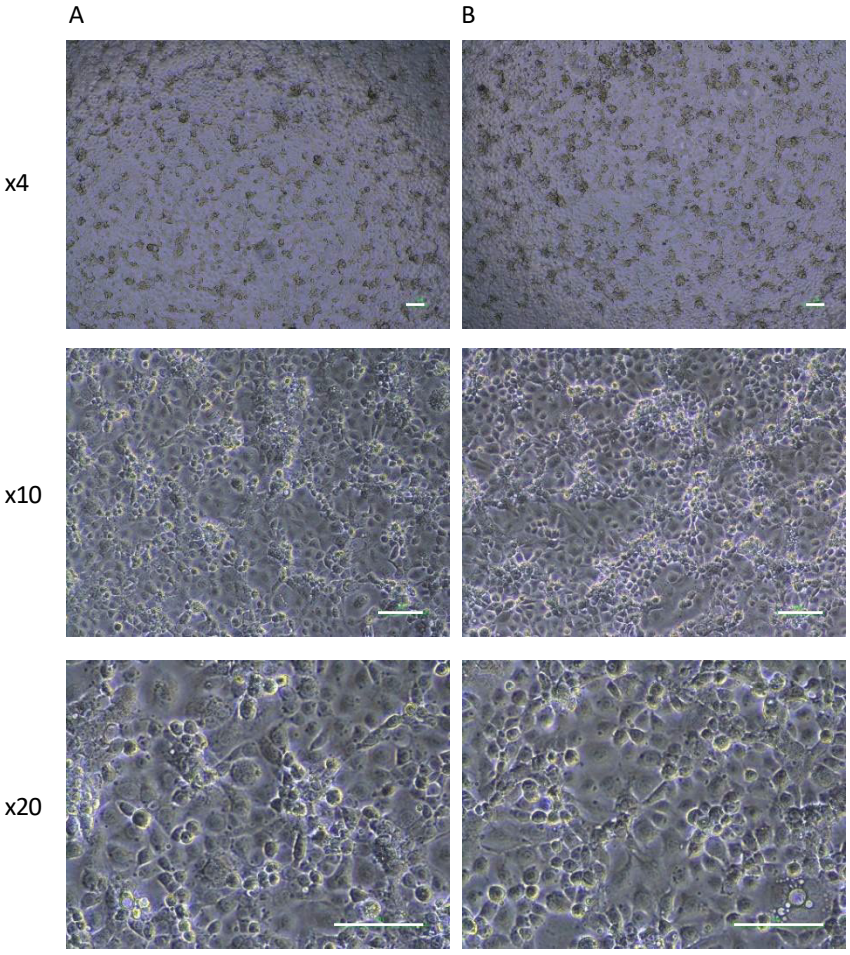

Figure 26. Euva11 cells observed at the inversed microscope at 3 days post transfection. Euva11 cells transfected with 13 µg of dsRNAGFP (A) and 1µg of each of the 13 candidates selected for screening (B). The magnification of observations is shown to the left of the panels. Scale bar 100 µm.

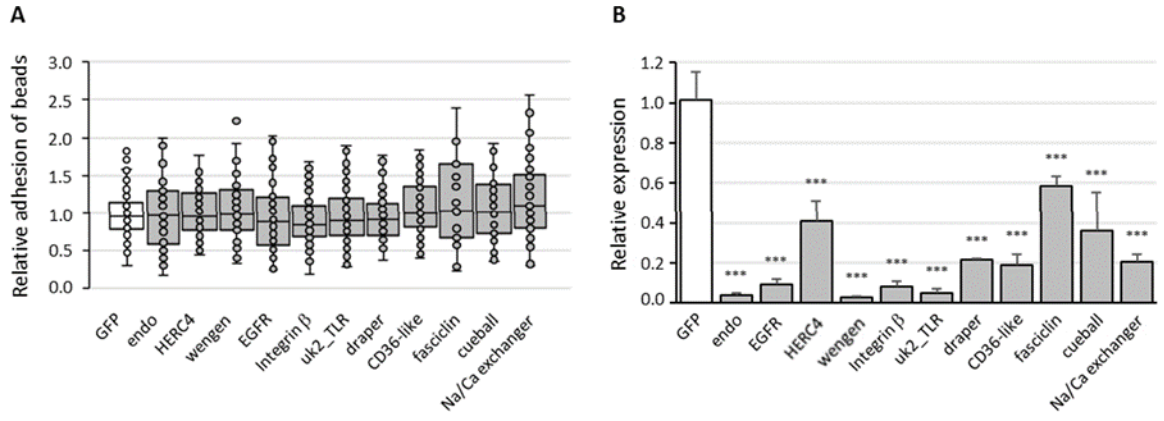

Figure 27. Adhesion of the VmpA-His$_6$-coated beads to the Euva-11 cells in presence of dsRNA of candidate genes and GFP as control. (A**)** adhesion of VmpA-His$_6$-coated beads to Euva-11 cells three days after the cells were transfected with GFP dsRNA (white) or dsRNA of candidate genes (grey) the name of which is indicated under the graph. (B) control of RNAi efficiency into Euva-11 cells transfected at the same time as cells incubated with beads in A. The expression of the candidate genes in Euva-11 cells was measured regards to the reference gene glutathione S-transferase. White box corresponds to Euva-11 cells transfected with GFP dsRNA and grey boxes with dsRNA targeting the gene indicated below the graphs. *** indicates a significant difference with p<0.001, under the Kruskal-Wallis rank sum test of the R commander package of R software version 4.0.3 regards to the GFP dsRNA control.

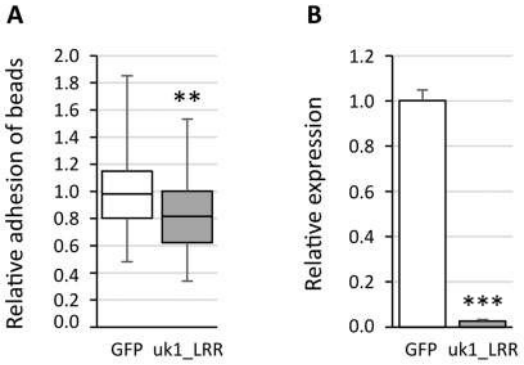

Figure 28. Adhesion of the VmpA-His$_6$-coated beads to the Euva-11 cells in presence of dsRNA of uk1_LRR gene and GFP as control. (A) Adhesion of VmpA-His$_6$-coated beads to Euva-11 cells three days after the cells were transfected with GFP dsRNA (white) or uk1_LRR dsRNA (grey). ** indicates a significant difference with p=0.003671 for uk1_LRR under the Kruskal-Wallis rank sum test. (B) Control of RNAi efficiency into Euva-11 cells transfected at the same time as cells incubated with beads in A. The expression of the uk1_LRR gene was measured in Euva-11 cells regards to the reference gene glutathione S-transferase. White box corresponds to Euva-11 cells transfected with GFP dsRNA and grey box with uk1_LRR dsRNA. *** indicates a significant difference with p=0.0004912 under the Kruskal-Wallis rank sum test of the R commander package of R software version 4.0.3 regards to the GFP dsRNA control.

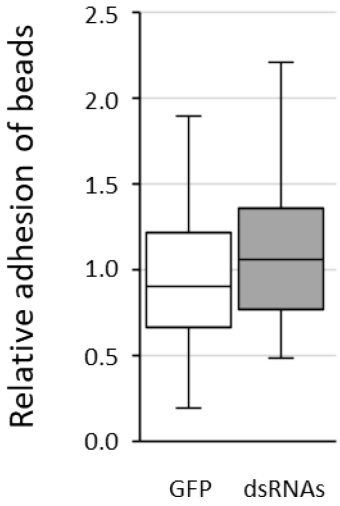

Figure 29. Adhesion of the VmpA-His$_6$-coated beads to the Euva-11 cells in presence of dsRNAs targeting 13 genes simultaneously (grey) and GFP as control (white).

As inhibition of the 13 genes simultaneously by RNAi did not show difference with the inhibition of a single gene, we thus inhibited the 13 genes simultaneously before to incubate the transfected cells with VmpA-His_6-coated beads. Statistical analysis revealed no differences in adhesion of VmpA-His_6-coated beads on cells where the expression of the thirteen candidates was inhibited at once (**Figure 29**).

2.6. Characterization of the uk1_LRR gene

The uk1_LRR amino acidic and nucleotide sequences were investigated through a BLAST search, revealing several homologs in other organisms present in the databases (**Table 6**). Uk1_LRR was predicted by TMHMM v2.0 to be a transmembrane protein anchored in the plasma membrane by a single 22-23 amino acids-long transmembrane segment located in the C-terminal part (**Figure 30.A** and **D**). Most of the protein was predicted to be exposed to the cell surface. The uk1_LRR protein contains four leucine-rich-repeat (LRR) domains of 219, 163, 80 and 146 aa (from N-ter to C-ter sequence) classified in the ribonuclease inhibitor-like group (RI). Furthermore, consistent with sequence prediction indicating LRR domains, structural prediction (Robetta, BakerLab) revealed a horseshoe-shaped molecule consisting of parallel β-strands on the inner concave side and helical elements on the outer convex sites (**Figure 30.B**). Fourteen potential N-glycosylation sites (NxS/T motif) were found in uk1_LRR amino acid sequence and are localized on the protein predicted structure in **Figure 30.C**.

No paralogous gene was found in *E. variegatus* transcriptome. However, it has been possible to identify an ortholog gene in *S. titanus* (Transcriptome Shotgun Assembly ref. "Scaphoideus titanus taxid:376741"), the natural vector of flavescence dorée phytoplasmas, with an amino acid identity of 90.6 % (Clustal 2.1). *E. variegatus* uk1_LRR consists of 781 amino acids meanwhile *S. titanus* sequence is 779 amino acids long. Potential N-glycosylation sites were conserved between the two proteins, both in number (14) and position, with a shift that reflects the difference in protein sequence length. uk1_LRR ortholog in the FDp non-competent vector *Macrosteles quadrilineatus* (XP_054266502.1) showed a 91.6 % identity with *E. variegatus* uk1_LRR amino acidic sequence. The sequence is 778 amino acids long and presents an additional N-glycosylation site at the C-terminal part of the protein, predicted to

Table 6. Homologs of uk1_LRR in NCBI databases using Blast and domains found with InterPro.

description	Blast output						interpro prediction	
	Blast	organism	query cover (%)	E value	identity %	accession number	number of LRR domains	type of LRR domains
carboxypeptidase N subnit 2-like	blastn	*Macrosteles quadrilineautus*	84	0.0	81.23	XM_054410529.1 XM_054410528.1 XM_054410527.1	no prediction no prediction no prediction	no prediction no prediction no prediction
carboxypeptidase N subnit 2-like	blastp	*Macrosteles quadrilineautus*	99	0.0	91.63	XP_054266502.1	no prediction	no prediction
protein artichoke-like	blastp	*Homalodisca vitripennis*	96	0.0	72.33	XP_046674361.1	4	RI
hypothetical protein J6590_064756	blastp	*Homalodisca vitripennis*	88	0.0	73.03	KAG8256621.1	3	RI
Toll pathway protein	blastp	*Laodelphax striatellus*	86	0.0	62.70	AMQ10343.1	5	RI
hypotethical protein LSTR_LSTR014165	blastp	*Laodelphax striatellus*	86	0.0	62.85	RZF39866.1	5	RI
chaoptin	blastp	*Nilaparvata lugens*	86	0.0	62.76	XP_022200047.1	5	RI
PREDICTED: insulin-like growth factor binding protein complex acid labile subunit	blastp	*Bemisia tabaci*	93	0.0	57.44	XP_018904807.1	5	RI
unnamed protein product	blastp	*Bemisia tabaci*	93	0.0	57.30	CAH0754027.1	5	RI
insulin-like growth factor binding protein complex acid labile subunit	blastp	*Halyomorpha halys*	95	0.0	56.13	XP_014293272.1	5	RI
unnamed protein product	blastp	*Nezara viridula*	95	0.0	55.98	CAH1406343.1	5	RI
toll-like receptor Tollo	blastp	*Daktulosphaira vitifoliae*	94	0.0	56.64	XP_050535112.1	5	RI
carboxypeptidase N subunit 2-like	blastp	*Sipha flava*	94	0.0	56.56	XP_025425654.1	5	RI
uncharacterised protein LOC126845587	blastp	*Adelges cooleyi*	86	0.0	59.41	XP_050440269.1	5	RI
hypothetical protein AGLY_013745	blastp	*Aphis glycines*	93	0.0	56.27	KAE9526114.1	5	RI
carboxypeptidase N subunit 2-like	blastp	*Melanaphis sacchari*	94	0.0	56.02	XP_025196330.1	5	RI

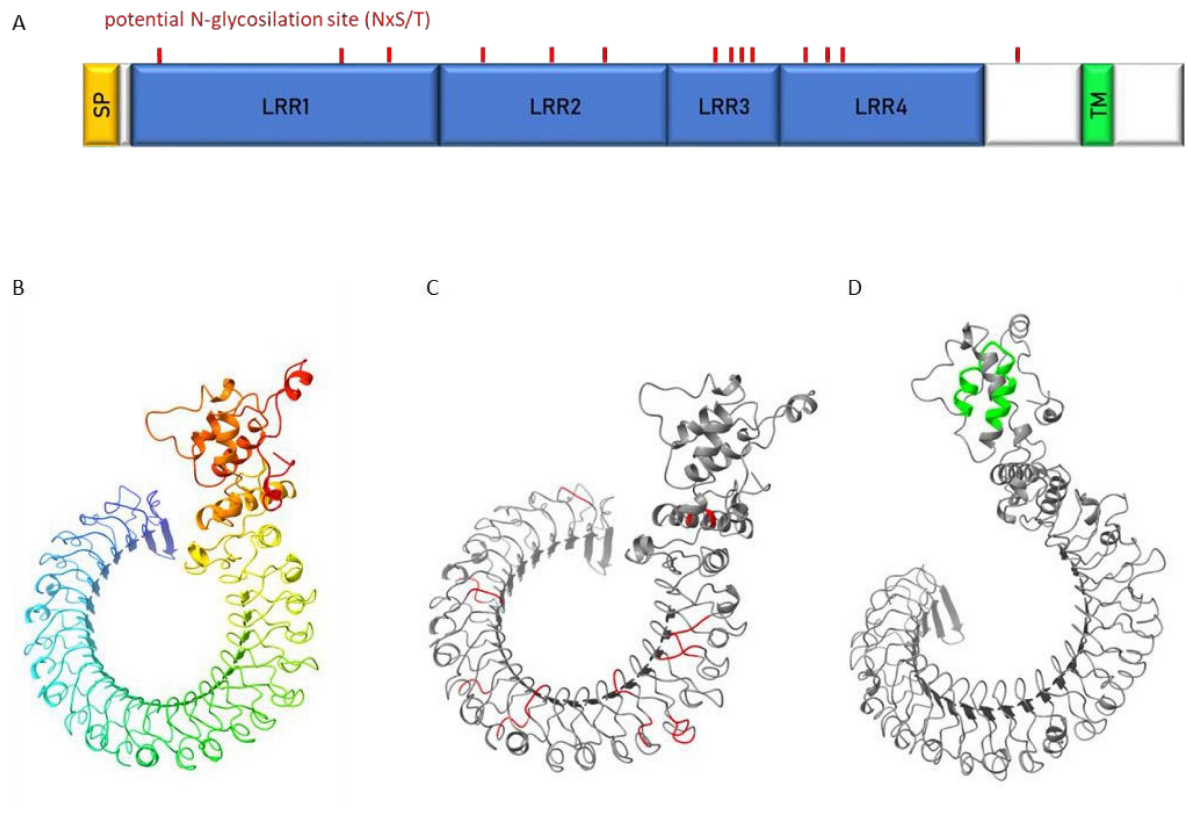

Figure 30. Characterisation of uk1_LRR protein. (A) Schematic representation of uk1_LRR protein where the signal peptide (SP) predicted by InterPro and TMHMM is coloured in yellow, the LRR domains predicted by InterPro in blue and the transmembrane domain predicted by TMHMM (TM) in green. Predicted protein structures by Robetta (BakerLab) were visualised with the software Chimera X (v.1.5) without signal peptide (B), with the potential N-glycosylation sites (aminoacidic motif «NxS/T») highlighted in red (C) and the transmembrane domain highlighted in green (D).

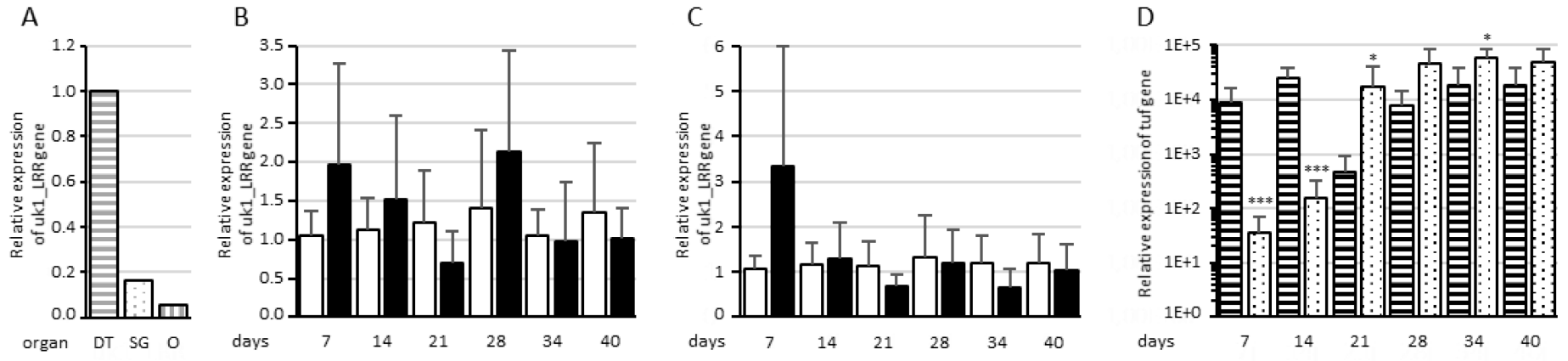

Figure 31. Assessment of uk1 LRR expression in E. variegatus. (A) Relative expression of uk1_LRR in *E*. *variegatus* digestive tube (grey horizontal stripes) and salivary glands (grey dots) of male and female insects, and ovary and eggs (grey vertical stripes). (B) Relative expression of uk1_LRR of *E*. *variegatus* regards to the reference gene glutathione S-transferase in abdomens or (C) in heads at different time points on non-infected plants (white bars) or on FD92 phytoplasma infected plants (black bars). (D) Relative expression of phytoplasma tuf gene at different time points in abdomens (horizontal stripes) and heads (dots) of *E*. *variegatus*. * indicates a significant difference with $p<0.05$ and *** $p<0.001$ (under the Kruskal-Wallis rank sum test of the R commander package of R software version 4.0.3) in tuf expression between abdomens and heads at each time point.

be in the cytoplasmatic portion of the protein, but it shares with *E. variegatus* and *S. titanus* the presence and the position of all fourteen other "NxS/T" sites.

2.7. Assessment of uk1_LRR expression in *E. variegatus*

To assess uk1_LRR expression in the different organs of the insect vector, real time RT-PCR was performed on salivary glands, digestive tubes and ovaries with eggs dissected from healthy *E. variegatus*. Uk1_LRR relative expression was normalised on three *E. variegatus* housekeeping genes, namely GST, Tub β and EF1. The organ showing the highest uk1_LRR expression values was the digestive tube (**Figure 31.A**). Salivary glands and ovaries expressed 6 and 18-time less the gene, respectively, when compared to digestive tubes.

Uk1_LRR expression was then measured on synchronised *E. variegatus* adults up to 40 days after feeding onto FD92 phytoplasma infected broad beans or onto healthy plants as control, both in abdomens (**Figure 31.B**) and heads containing the salivary glands (**Figure 31.C**). Even though no statistically significant differences were found in expression of uk1_LRR between healthy and FD92 infected insects, a trend is clearly visible. At 7 days post acquisition, uk1_LRR gene was more expressed in FD92 infected insects, both in the heads and in the abdomens, than in non-infected insects. While the uk1_LRR gene expression remained stable in the insects that fed on non-infected plants, the uk1_LRR mRNA decreased over time in the insects fed on phytoplasma infected plants. An increase in abdomens and heads was observed 28 days post acquisition, before uk1_LRR mRNA expression decreased.

As far as phytoplasma tuf mRNA relative quantities are concerned, both heads and abdomens were found to be positive to phytoplasma detection since the first sampling date, 7 days after the beginning of acquisition (**Figure 31.D**). At 7 and 14 days, quantities of tuf mRNA in the abdomens were significantly higher than in the heads, then titres were significantly higher in the heads than in the abdomens. The quantities of tuf mRNA were nearly stable in the abdomen over the latency while they increased over time in the heads.

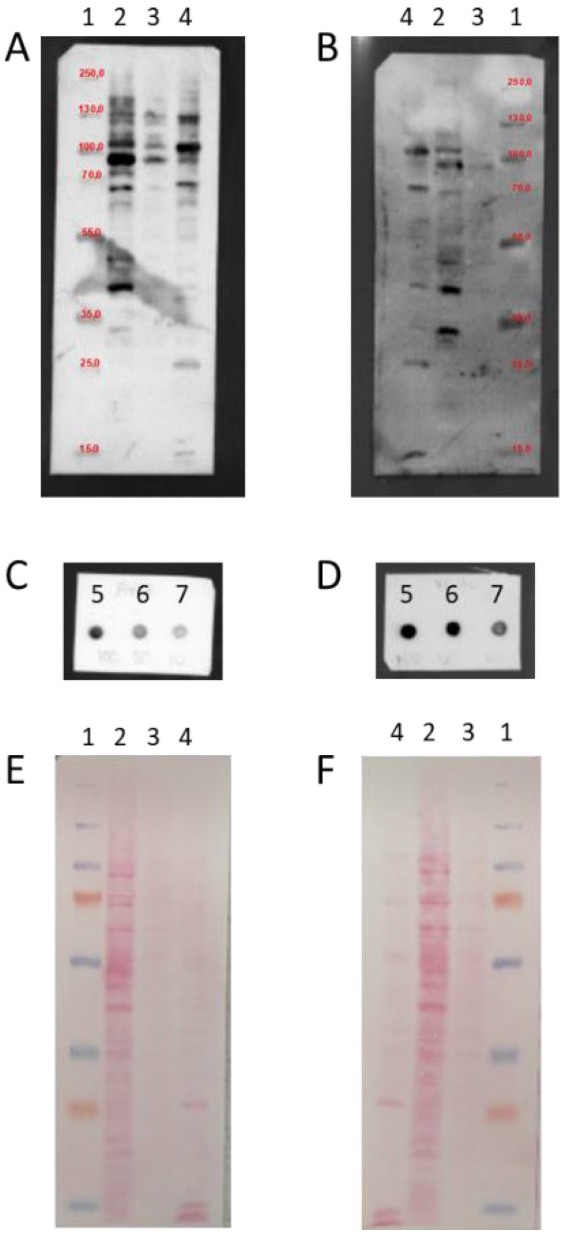

Figure 32. ***Far western blot on Euva proteins incubated with VmpA-His$_6$ PGYA (A) and VmpA-His$_6$ FD92 (B).*** Lanes represent ladder (PageRuler™ Plus Prestained protein ladder) (1), Euva11 proteins extracted with Rx buffer (2), with Rx-T-DOC buffer (3), and Euva11 insoluble fraction (4). Positive control consists in 100 ng (5), 50 ng (6) and 10 ng (7) of VmpA-His$_6$_PGYA (C) and VmpA-His$_6$_FD92 (D). Exposition time: 1s. E and F, Ponceau S staining of Euva proteins electrotransferred onto nitrocellulose membranes A and B, respectively.

2.8. Far-western blot VmpA FD92 vs PGYA

To assess if there were differences in the Euva cell proteins interacting with VmpA-His_6-FD92 and VmpA-His_6-PGYA, we performed a far-western blot in the same condition as previously described both VmpA proteins. Bands indicating interactions between Euva cells extracted proteins and both VmpA-His_6_FD92 and VmpA-His_6_PGYA were present in the Rx-buffer extracted fraction, the Rx-T-DOC fraction and the insoluble fraction (**Figure 32**). All the bands indicating Euva cell proteins interaction with VmpA-His_6_FD92 are also visible in the blot treated with VmpA-His_6_PGYA.

2.9. Adhesion assays on Euva cells using VmpA_PGYA coated beads

To assess if the interaction of VmpA with uk1_LRR protein could be implicated in the specificity of vection, we performed adhesion assays with VmpA of the *S*. *titanus* transmissible isolate FD92 and with VmpA of the *S. titanus* non-compatible phytoplasma isolate PGYA on Euva cells in which the uk1_LRR gene was knocked down using RNAi.

The VmpA-His_6-beads adhesion assays were performed three days after transfection of Euva-11 cells with dsRNA targeting the gene uk1_LRR and GFP as a control. Twenty fields were photographed per condition and three independent experiments were performed and pooled. No differences in adhesion to cells was observed between treatments and controls for VmpA-His_6_PGYA-coated beads (**Figure 33.A, Table 7**). In contrast with previous results, no difference in beads adhesion was observed when VmpA-His_6_FD92 coated beads were incubated with cell transfected with dsRNA of uk1_LRR when compared to the control condition. It must be indicated that for the first time we used a different type of fluorescent latex beads (COOH-) meanwhile in previous experiments -NH_2 fluorescent latex beads were used.

At the same time as adhesion assays, the inhibition of uk1_LRR was checked by real time PCR, confirming a significant decrease of the transcripts in dsRNA uk1_LRR treated cells when compared to control cells, from a minimum of 32-fold to 58-fold change (**Figure 33.B**).

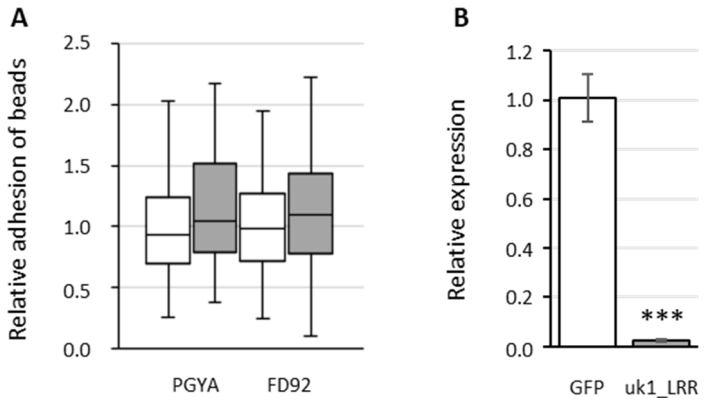

Figure 33. Adhesion of the VmpA-His$_6$_PGYA and VmpA-His$_6$_FD92 coated beads to the Euva-11 cells in presence of dsRNA of uk1_LRR gene and GFP as control. (A) Adhesion of VmpA-His$_6$_PGYA and VmpA-His$_6$_FD92 coated beads to Euva-11 cells three days after the cells were transfected with GFP dsRNA (white) or uk1_LRR dsRNA (grey). (B) Control of RNAi efficiency into Euva-11 cells transfected at the same time as cells incubated with beads in A. The expression of the uk1_LRR gene was measured in Euva-11 cells regards to the reference gene glutathione S-transferase. White box corresponds to Euva-11 cells transfected with GFP dsRNA and grey box with uk1_LRR dsRNA. *** indicates a significant difference with *p*=0.0003486 under the Kruskal-Wallis rank sum test of the R commander package of R software version 4.0.3 regards to the GFP dsRNA control.

Table 7. Adhesion of the VmpA-His$_6$_PGYA and VmpA-His$_6$_FD92 coated beads to the Euva-11 cells in presence of dsRNA of uk1_LRR gene and GFP as control (raw values). The first column indicates the phytoplasma strain to which belongs the VmpA-His$_6$ employed; the second one identifies the experiment; the third column indicates the type of fluorescent latex beads employed; the fourth column indicates the mean number of Euva cells counted per observed field; the fifth column indicates the number of beads counted per observed field; the sixth column indicates the mean number of counted beads per cell.

	VmpA-His$_6$	exp.	type of beads used	n cell	n beads	n beads per cell
dsRNA GFP	**PGYA**	**1**	red COOH	93.8 (± 7.2)	170.1 (± 53.7)	1.8 (± 0.56)
		2	red COOH	36.2 (± 8.0)	148.4 (± 28.8)	4.1 (± 1.2)
		3	green NH_2	52.4 (± 8.9)	45.2 (± 19.5)	0.9 (± 0.31)
	FD92	**1**	red COOH	86.6 (± 9.1)	126.0 (± 22.7)	1.5 (± 0.3)
		2	red COOH	31.0 (± 4.7)	77.1 (± 21.4)	2.6 (± 0.9)
		3	green NH_2	48.7 (± 9.5)	21.3 (± 7.3)	0.5 (± 0.2)
dsRNA uk1_LRR	**PGYA**	**1**	red COOH	85.8 (± 6.8)	147.7 (± 25.3)	1.7 (± 0.3)
		2	red COOH	25.5 (± 4.3)	128.3 (± 39.6)	4.8 (± 1.9)
		3	green NH_2	51.0 (± 10.7)	66.9 (± 31.5)	1.5 (± 0.7)
	FD92	**1**	red COOH	89.8 (± 8.0)	145.0 (± 24.0)	1.7 (± 0.3)
		2	red COOH	28.5 (± 7.2)	73.2 (± 24.9)	2.7 (± 1.0)
		3	green NH_2	47.7 (± 9.3)	29.3 (± 11.2)	0.6 (± 0.2)

Chapter 2 - Yeast Two-Hybrid

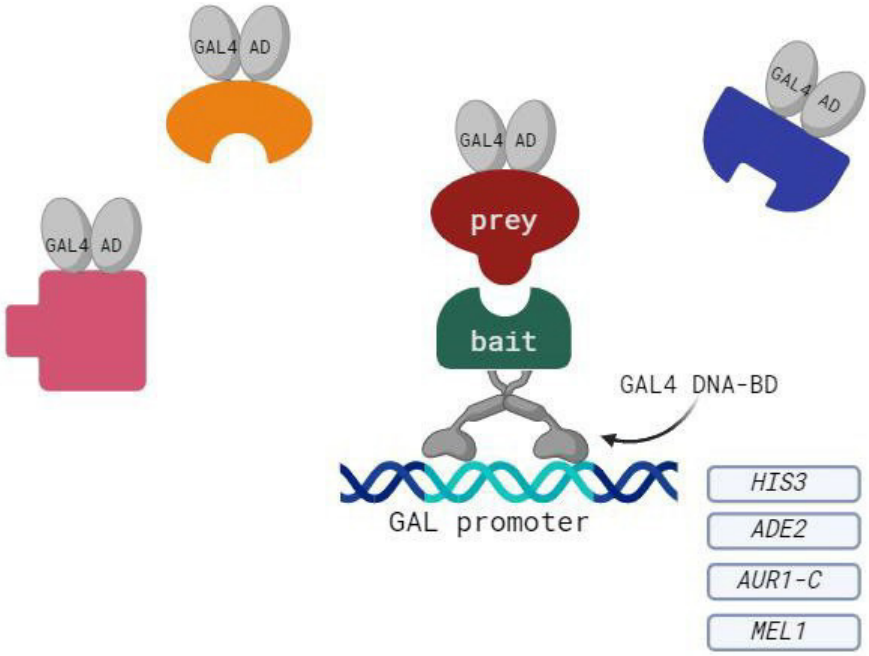

Figure 34. Double yeast hybrid principle. The bait protein is expressed in fusion to the DNA binding domain yeast transcription factor Gal4 meanwhile the prey protein(s) are fused with the activation domain of Gal4. If an interaction between the bait protein and a prey protein occurs, the Gal4 transcription factor in reconstituted and it activates the transcription of the reporter genes downstream the activating sequences (UAS) region to which Gal4 binds. The expression of the reporter genes allows the selection of yeast colonies in which such protein-protein interaction occurred. The figure has been realised using BioRender.

Yeast Two-Hybrid

1. Justification of the experimental strategy

Yeast two-hybrid (Y2H) is a widely used technique to test protein-protein interaction *in vivo* and to explore the interactions between a protein of interest and its unknown target(s). This technique has been firstly described in 1989 by Fields and Song (Fields and Song, 1989) and it consists in expressing both the protein of interest (bait) and their potential targets (preys) in suitably modified yeast strains. The bait protein is fused to the N-terminal part of the transcription factor Gal4, which contains the nuclear localization domain (NLS) and DNA binding domain, meanwhile the prey will be fused to the activation domain of Gal4 and a NLS. Bait and prey proteins are translated in the yeast cytosol and then translocated in the nucleus. If the proteins interact with one another, the transcription factor will be reconstituted becoming functional and activating the expression of reporter genes (**Figure 34**).

Promoters regulating the reporter genes are different from each other, except for the short protein binding sites in the upstream activating sequences (UAS) region, which is specifically bound by Gal4 DNA-binding domain. The UAS are *cis*-acting elements, able to enhance transcription from adjacent downstream TATA-box. The promoters of reporter genes in yeast two-hybrid commercial systems are often artificial constructs of TATA and UAS sequences derived from different genes. Reporter genes allow the selection of yeast cells in which the interaction between the bait and the prey occurred and consist in auxotrophy-complementing genes, antibiotic resistance genes and enzymes *i.e*. β-galactosidase, allowing the survival of cells when yeast culture is plated onto appropriate selective media.

A classical Y2H assay begins with the preparation of the plasmids containing the bait and the prey(s) sequences (**Figure 35**). Then, two different yeast strains compatible for mating are transformed with such plasmids. The transformed cells are selected exploiting the presence of auxotrophic markers on the plasmid backbones of both bait and prey plasmids. The two strains are then put in suitable condition to mate. The product of mating is then plated onto petri dishes containing selective media, in order to allow the growth of the yeast hybrids containing a prey protein interacting with the bait protein. The colonies are then picked and streaked for further selection to limit the presence of false positive. The following step consists in the recovery of the prey plasmid in order to transform yeast with both the bait and the prey

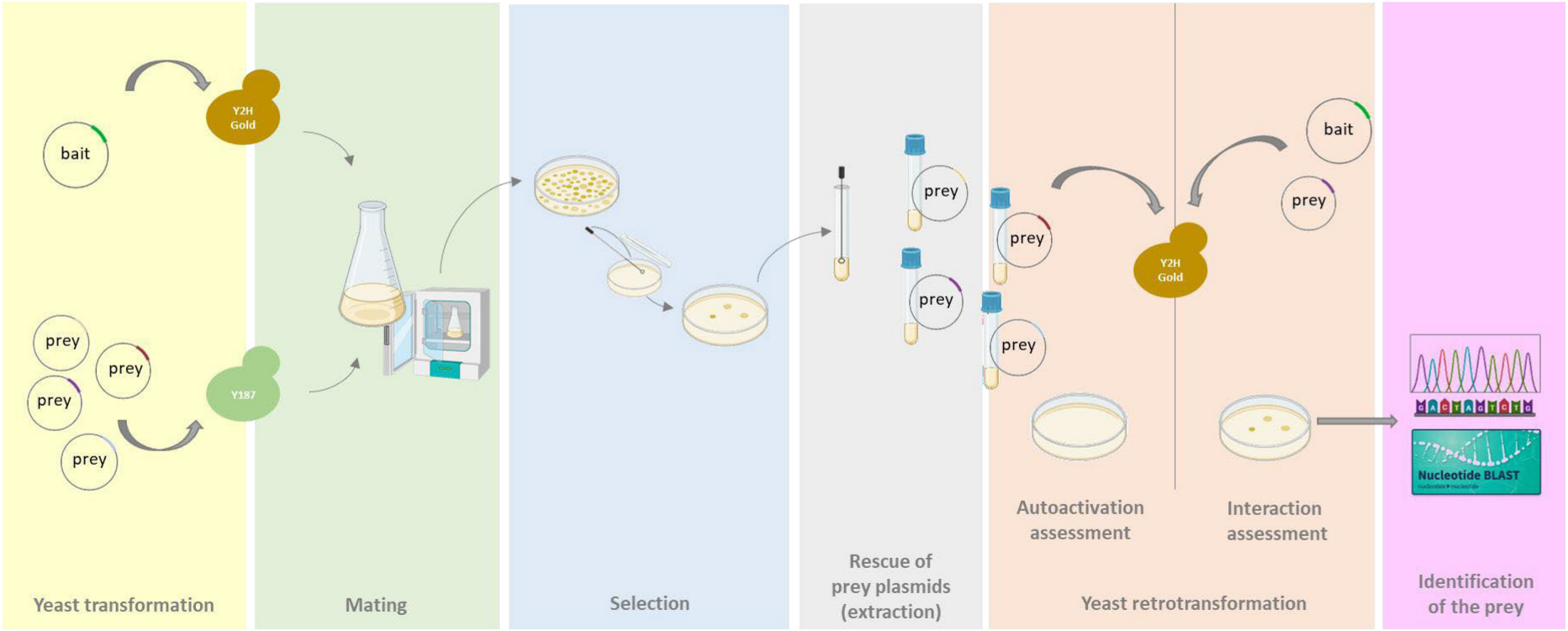

Figure 35. Workflow of a classic double yeast hybrid assay. Two yeast strains compatible for mating are transformed with the plasmids containing the bait and the prey proteins. The two strains are then cultured in a rich media in conditions promoting mating. The co-culture is then plated onto selective media to allow the growth of yeast colonies in which the expression of reporter genes occurred. The colonies are then picked and inoculated in liquid selective media and the prey plasmids are purified from yeast cultures with suitable extraction protocols. To confirm the interaction between bait and prey, the plasmids are used to perform yeast retrotransformation. To exclude the autoactivation of the reporter gene expression by the prey plasmid alone, a simple transformation of yeast is then plated onto selective media. If no colonie growths onto selective plates, a co-transformation is performed to assess the reproducibility of the interaction between bait and prey observed after mating. If the interaction is confirmed the insert contained in the prey plasmid is sequenced and identified through a homology search. The figure has been realised using BioRender.

plasmids simultaneously, to validate the interaction that occurred during yeast mating. Last step consists in the identification of the prey protein involved in the interaction with the bait *i.e*. through sequencing of the prey plasmid.

Then, other techniques of validation of the interaction such as co immunoprecipitation, FRET, western and far-western blot must be applied to confirm the preliminary results obtained with Y2H assay.

VmpA proteins are able to stick together when they are coated to beads in presence of mannose (Arricau-Bouvery *et al.*, 2021). This implies that protein/protein interactions occurred in addition to protein/glycoside interactions. Moreover, the multiple VmpA interaction signals revealed by our far-western blot analysis performed on Euva cells proteins suggest that VmpA interacts with several insect proteins (**Figure 21**). Thus, we check if VmpA could interact with insect proteins through protein-protein interactions using a classical yeast two-hybrid assay.

2. Results

2.1. Yeast Two-Hybrid

A yeast two-hybrid library was constructed with *E. variegatus* cDNA fused to the Gal4-activation domain for prey. The cDNA library represents 1.7 million of independent clones and has been successfully used to identify interactants of flavescence dorée phytoplasma effectors in other experiments performed in the laboratory (personal communication, Sybille Duret). A truncate version of VmpA was produced by deleting the two transmembrane domains (amino acids 1 to 35 and 347 to 381) and fused to Gal4-DNA binding domain resulting in the plasmid pGBKT7_VmpA, which has been used as a bait in the Y2H assays. When the control of autoactivation was performed with the empty vector containing the Gal4-activation domain (AD) and the vector containing the protein fusion VmpA-Gal4-DNA binding domain (BD), no clone developed on selected medium showing that VmpA alone could not induce transcription of the reporter genes in yeast. We performed five mating experiments characterised by a variable number of screened clones and mating efficiency (**Table 8**). For all mating experiences the mating efficiency was lower than the 2-5% threshold defining a good mating efficiency

Table 8. Summary of the five mating experiences performed using Y2H Gold transformed with pGBKT7_VmpA as bait and Y187 transformed with pGADT7_cDNA_E.variegatus as preys. The number of screened clones represents an estimation of the different clones present in the bank aliquot used during the mating. The mating efficiency defines the percentage of diploids obtained during yeast mating. In the fourth column is represented the number of colonies grew on the selective media on which the yeast co-culture was plated after mating. In the fifth column are represented the number of colonies who survived upon striking onto the second selection media.

mating	n° of screened clones	mating efficiency	first selection step (SD/-Leu -Trp + AbA)	second selection step (SD/-His)
1	149500	0,50%	49	41
2	67500	0,29%	24	16
3	9450	0,01%	3	0
4	495000	0,04%	27	11
5	2160000	0,30%	58	18
total			161	86

according to the kit manufacturer's guidelines. The number of screened clones calculated after each mating experience revealed that only in mating n° 5 a satisfactory number of screened cloned was achieved. Taken all the results together, during the first selection using Synthetic Defined (SD) medium containing the antibiotic aureobasidin A and lacking the amino-acids leucine and tryptophan (SD/-Leu-Trp+AbA), 161 clones were found to activate the reporter genes and were selected for the next step. The second selection, aiming at reducing the number of false positive, was performed on SD medium without histidine (SD/-His) and only 86 clones grew on this selective media.

After plasmid purification and subcloning in *E. coli*, sequencing of the 68 plasmid inserts with a length superior of 350 bp was performed. Indeed, a random survey led on 5/18 sequences shorter than 350 bp revealed that these inserts represented only yeast elements. Sequencing revealed that 11/68 clones contained only yeast sequences or very short sequences matching nucleotide homologies databases. We decided not to test these 29 clones further in the validation of interaction. On the remaining 57 clones (**Table 9**), 12 clones could not be sequenced with a sufficient quality or due to the presence of multiple inserts when amplified by PCR. Only 45 inserts had significant homologies with the transcriptome shotgun assembly (TSA) of *E. variegatus* or other sequences in the NCBI database (clone 48, **Table 9**). Among the 45 sequenced inserts 19 clones represented redundant sequences of ferritin, pyruvate kinase PKM-like, proteins of unknown function GFTU01005228.1 and GFTU01013998.1.

2.2. Rescue of the prey plasmids

We tested three different methods to recover the prey plasmids from the yeast plated after mating step. The method named "Quick and Dirty" was characterised by satisfying yield of total plasmid DNA (ranging from 60 to 1200 ng/µL). However, PCR amplification and propagation in *E. coli* were negatively affected by this extraction protocol. In fact, seven inserts over the sixteen tested could not be amplified by PCR using "Quick and Dirty" extract DNA as a matrix and we did not achieve to obtained *E. coli* colonies upon transformation with the same plasmids. DNA extraction performed with the Kit "Easy Yeast Plasmid Isolation" (Clontech) results in a cleaner product which allows PCR amplification and *E. coli* competent

Table 9. Prey sequences identified in the different clones obtained during mating experiments. The first two columns summarise the results of the homology search carried out on the sequences obtained by Sanger sequencing of the rescued pGADT7 plasmids (redundant sequences represented by multiple clones are in bold). The third column indicates the number identifying the clone. The fourth and fifth columns contain the results of yeast strain Y2H Gold retro transformation with pGADT7_E.variegatus alone (to assess autoactivation of reporter genes system) and with pGADT7_E.variegatus and pGBKT7_VmpA (to assess interaction), respectively.

insert BLASTn	insert BLAST TSA *Euscelidius variegatus*	ciEvVmpa	autoactivation	interaction with VmpA
Protein from *Nigrivalveus* mitochondrion	GFTU01008494.1	**1**	+	
multiple bands		**2**	-	-
Epinephelus lanceolatus cathepsin L.1	GFTU01000453.1 and GFTU01000454.1	**6**	-	-
Protéine S15 ribosomale 40S	GFTU01003897.1	**7**	-	-
Aedes albopictus ADP,ATP carrier protein 1	GFTU01009830.1	**8**	-	-
Pecten maximus pyruvate kinase PKM-like	**GFTU01000371.1 and GFTU01004496.1**	**9**	-	-
Anopheles vigilin	GFTU01005891.1	**10**	-	-
ATP synthase subunit alpha	GFTU01011708.1	**11**	-	-
Myzus persicae merlin (LOC111038193), mRNA	GFTU01006879.1 and GFTU01006880.1	**14**	-	-
bad quality sequencing		**19**	-	-
bad quality sequencing		**21**	-	-
26S proteasome non-ATPase regulatory subunit 14	GFTU01003474.1	**23**	-	-
	GFTU01015051.1	**24**	-	-
multiple bands		**26**	-	-
Tubuline beta 1	GFTU01006818.1	**28**	-	-
(*Galleria mellonella* uncharacterized m ARN)	GFTU01007970.1 and GFTU01007969.1	**29**	-	-
		31	-	-
multiple bands		**34**	-	-
insect'transcription initiation factor TFIID subunit 1	GFTU01011507.1	**35**	-	-
	GFTU01005228.1	**36**	-	-
Drosophila erecta 40S ribosomal protein S9	GFTU01016432.1	**42**	**not possible to transform *E. coli***	
	GFTU01011370.1 and GFTU01011367.1	**44**	-	-
	GFTU01003938.1	**45**	-	-
bad quality sequencing		**47**	-	-
Euscelis spp. 16S		**48**	-	-
Pecten maximus pyruvate kinase PKM-like	GFTU01000371.1 and GFTU01004496.1	**49**	-	-
	GFTU01005660-64.1	**50**	+	
NADH deydrogenase subunit 4	GFTU01008494.1	**53**	-	-
bad quality sequencing		**54**	-	-
Anopheles cytochrome oxidase subunite	GFTU01003141.1	**55**	-	-
Pecten maximus pyruvate kinase PKM-like	**GFTU01000371.1 and GFTU01004496.1**	**56**	redundant insert	
Pecten maximus pyruvate kinase PKM-like	**GFTU01000371.1 and GFTU01004496.1**	**58**	redundant insert	
Green rice leafhopper EF-hand calcium binding protein	**GFTU01005228.1**	**67**	-	-
bad quality sequencing		**68**	-	-
bad quality sequencing		**69**	-	-
Euscelidius variegatus isolate 1292 cytochrome c oxidase subunit I (COX1) gene, partial cds; mitochondrial	GFTU01004811.1	**72**	-	-
	GFTU01008907.1	**85**	-	-
PREDICTED: *Nilaparvata lugens* V-type proton ATPase 116 kDa subunit a (LOC111058708), transcript variant X3, mRNA	GFTU01008481.1	**86**	+	
	GFTU01002488.1	**87**	-	-
	GFTU01005228.1	**89**	redundant insert	
	GFTU01013998.1	**90**	+	
	GFTU01013998.1	**91**	+	
Lethocerus distinctifemur clone v86 venom 5' nucleotidase 2 mRNA	GFTU01016199.1	**92**	+	
ferritin	**GFTU01013547.1**	**97**	+	
	GFTU01013998.1	**98**	redundant insert	
	GFTU01013998.1	**99**	redundant insert	
Pecten maximus pyruvate kinase PKM-like	**GFTU01000371.1**	**106**	-	-
ferritin	**GFTU01013547.1**	**108**	redundant insert	
ferritin	**GFTU01013547.1**	**112**	redundant insert	
	GFTU01015301.1	**129**	+	
	GFTU01013998.1	**130**	redundant insert	
Kryptolebias marmoratus flavin-containing monooxygenase FMO GS-OX-like 2	GFTU01011918.1 and GFTU01001541.1	**144**	-	-
bad quality sequencing		**147**	-	-
bad quality sequencing		**148**	-	-
Pecten maximus pyruvate kinase PKM-like	**GFTU01000371.1 and GFTU01004496.1**	**149**	redundant insert	
Pecten maximus pyruvate kinase PKM-like	**GFTU01000371.1 and GFTU01004496.1**	**150**	redundant insert	
ferritin	**GFTU01013547.1**	**154**	+	

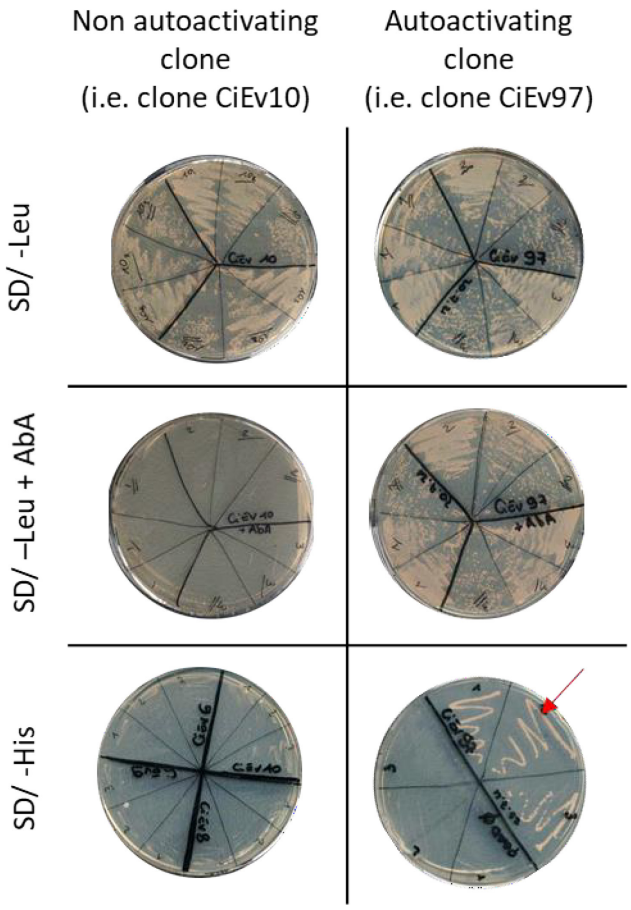

Figure 36. Y2H Gold yeast strain transformed with prey plasmid alone. Transformed yeast were plated on SD/-Leu medium and after a 3 days incubation at 30°C three colonies for each transformed yeast were plated onto SD/-Leu medium (as a control) and onto SD/-Leu + AbA medium to check for autoactivation of reporter genes system. In case of yeast growing onto selective media containing the antibiotic, three colonies were picked and streaked onto SD/-His selective media to confirm the result. On the right an example of an autoactivating clone. The red arrows indicate the side of the petri dish containing SD/-His on which the colonies were streaked.

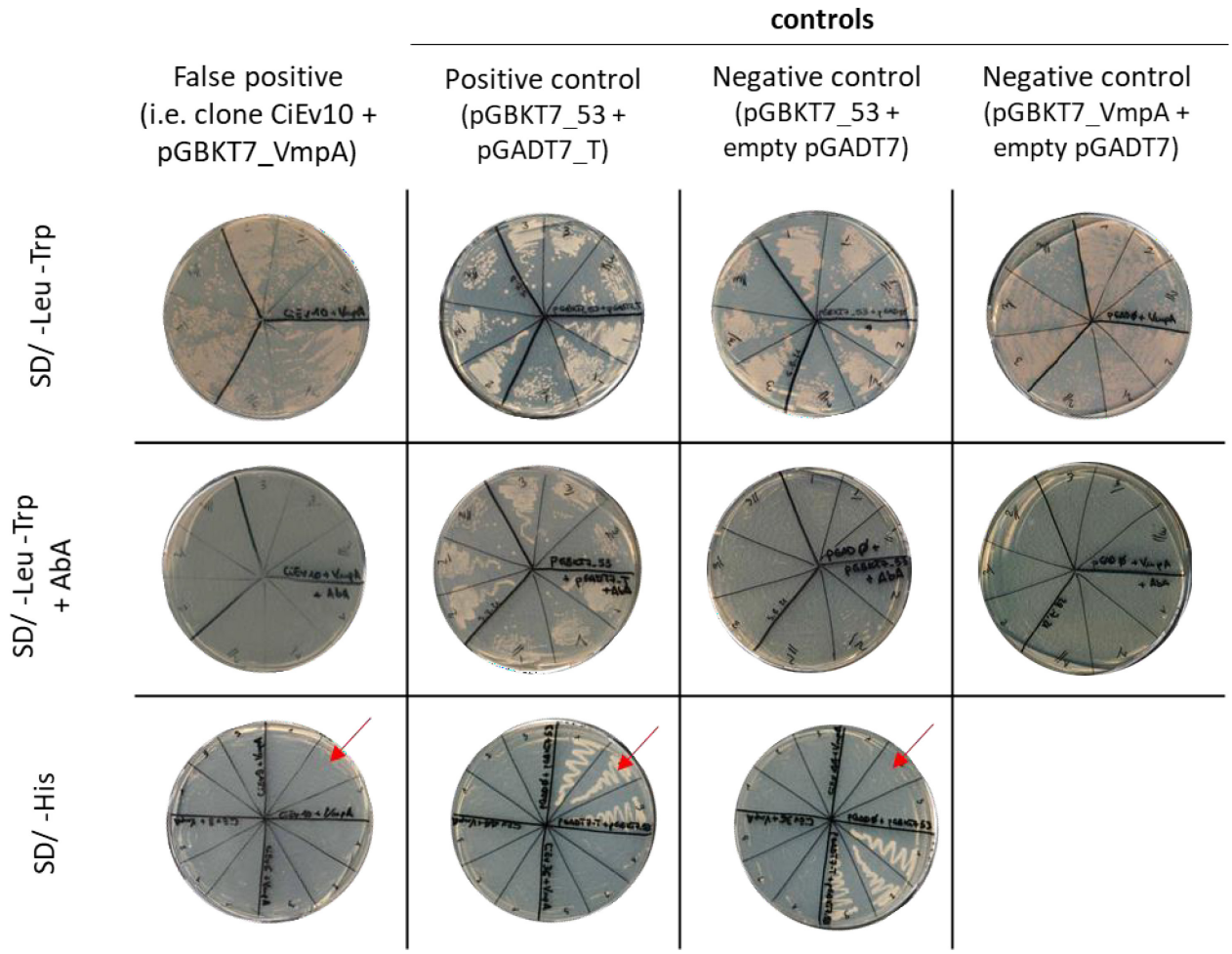

Figure 37**. **Y2H Gold yeast strain transformed with prey plasmid and pGBKT7_VmpA. The growth of co-transformed yeast was assessed in SD/-Leu-Trp medium, and after 3 d at 30°C, three colonies for each co-transformation experiment were plated on SD/-Leu-Trp (as a control), SD/Leu-Trp + AbA and SD/-His media and were left 3 days at 30 °C. The red arrows indicate the side of the petri dish containing SD/-His on which the colonies were streaked. pGAD-T7_T and pGBKT7_53 are the clones supplied in the Clontech kit to be used as positive controls of interaction.

cell transformation for all eight clones tested. However, the extraction yield was very poor (3-9 ng/µL). The method adapted from (Hoffman and Winston, 1987) was considered the best one for yield of the plasmid (200-700 ng/µL) and for its suitability for the downstream applications *i.e.* cloning in *E. coli* cells, that could be achieved for all clones but one (clone 42).

2.3. Yeast retro transformation

To confirm the interactions, we performed retro transformations in yeast with the 45 prey plasmids containing confirmed *E. variegatus* sequences and with the 12 clones who could not be sequenced. Unfortunately, we failed multiple times to clone insert n°42 into *E. coli*, thus it was impossible to recover the plasmid and to assess its possible interaction through yeast retro transformation. We chose to test only two or three different clones representing redundant sequences (details in **Table 9**). In summary, we tested 35 prey plasmids by yeast retro transformation represented, in total, by 46 different clones.

We first transformed yeast strain Y2H Gold with the prey plasmids only, to assess the possible autoactivation of the reporter genes system by the prey protein alone (**Figure 36**). Nine out of thirty-five inserts allowed the yeast to growth on selective media (**Table 9**). They coded for different proteins, and for four of them their sequence had no homology in databases using BLAST. Then, we transformed Y2H Gold_pGBKT7_VmpA with the prey plasmids of the remaining 26 clones to confirm the interaction occurring in the mating experience (**Figure 37**). None of the interactions was confirmed. Thus, this system did not allow us to identify insect proteins that interact with VmpA through the yeast two-hybrid system.

2.4. Western blot and insert sequences analysis

The lack of confirmed interactions in Y2H experiment made us questioning about the possible reasons. We decided to perform a western blot on a pool of six yeast cultures representing different clones obtained during mating, to assess the expression of proteins coded by the prey plasmids in Y187 yeast cells. To detect the proteins, we exploited the HA tag cloned upstream the prey protein coding sequence, using a primary antibody anti-HA. We

Table 10. Theorical molecular weight of the prey proteins contained in the clones tested in western blot for protein expression (first column). We first assessed the size of the prey insert analysing the PCR product separated on an agarose gel (second column). Then we calculated the number of amino-acids constituting the protein (third column). We then obtained an approximation of the molecular weight of the insert (fourth column). Then, we added the molecular weight of the activation domain to the mass of our insert (fifth column). In the sixth column is reported the –HA tagged prey protein molecular weight observed on the blot.

clone number	insert lenght (bp)	approximate mw of fusion protein if not stop and in frame (kDa)	band observed on blot (kDa)
1	900	45,4	~ 32
2	2000	85,66	-
	850	43,53	-
7	800	41,66	~ 32
8	1500	67,4	~ 25
10	1500	67,4	~ 80

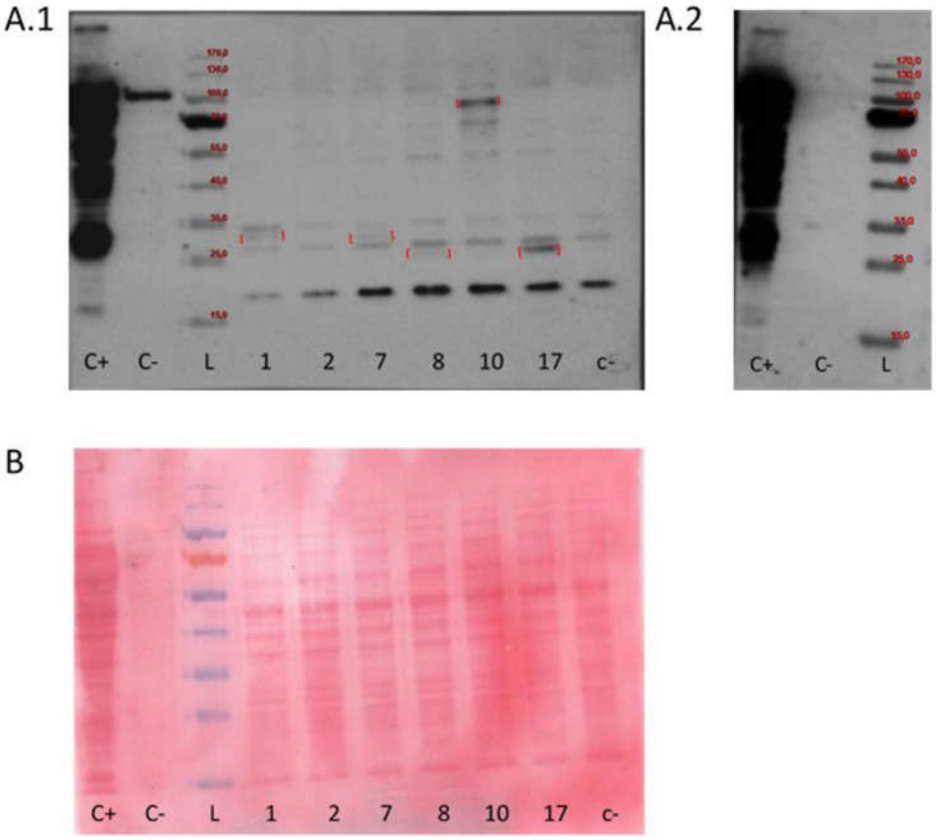

Figure 38. Western blot anti-HA on yeast expressing prey proteins (A.1). C+ is positive control for HA tag consisting in a whole cell extract of *Mycoplasma mycoides* subsp. *capri* (MMCAP2_0582-HA) (Nottelet *et al.*, 2021); C- is negative control consisting in Euva cell soluble proteins; L indicates the ladder (PageRuler prestained, ThermoFisher); c- is negative control consisting in yeast strain 2YH Gold not transformed. Interaction signal of prey proteins tagged with HA are highlighted by red brackets. A.2) The blot was repeated to assess the presence of a contamination of the negative control occured during sample loading on acrylammide gel before SDS-PAGE electrophoresis.B) Red Ponceau staining of the membrane after electrotransfer of yeast proteins separated by SDS-PAGE electrophoresis.

chose to include in this analysis a yeast clone that did not survive to the second step of selection after mating (striking onto SD/-His media) and therefore, considered a false positive (clone 17) as well as a clone containing putative multiple prey inserts (multiple bands visible in PCR product electrophoresis, clone 2). The theorical molecular weight of each insert (**Table 10**) has then been compared to the signal observed on the western blot. We observed a supplementary signal on five out of six clones expressing prey plasmids when compared to the proteins expressed by the 2YH Gold strain not transformed, but none of them was characterised by a kDa estimation matching with the theorical molecular weight previously calculated (**Figure 38**, **Table 10**). We investigated the results of the Sanger sequencing performed on 33 plasmids prey extracted from transformed yeast. Alignment with reference sequences (TSA *Euscelidius variegatus* taxid:13064) and with the prey plasmid backbone map revealed that 20 % of the sequenced inserts were not in frame and 80 % of the in frame clones were truncated early (around 10-40 amino acids after cloning site) in the putative translation of the protein coded in our plasmids.

To summarise, all clones that were selected upon Y2H either autoactivated the reporter system or their interaction with VmpA was not reproducible through yeast retro-transformation and were therefore considered as false positives.

Discussion

Discussion

Phytoplasmas ingested with the infected sap arrive in the gut lumen of the leafhopper and adhere to its epithelium. Once internalised, phytoplasmas have to cross the basal membrane of midgut epithelium, circulate in the haemolymph to systemically colonise the insect and reach the salivary glands (Gouranton and Maillet, 1973; Lefol *et al.*, 1994), in order to be successfully transmitted to plants by their vectors through the emission of infected saliva during feeding. This cycle implies the occurrence of several interactions between phytoplasmas and insect proteins, which require a certain degree of specialisation. In fact, not all insects are competent to transmit phytoplasma, in reason of the specificity of such interactions. We have briefly introduced the variability of insect vector range for different phytoplasmas, suggesting the existence of different mechanisms of interactions underlying the different vector-pathogen associations. The specificity of interaction can act at the level of the midgut barrier as it is the case for FD phytoplasma of vectotype I that cannot be acquired by *E. variegatus* and *S. titanus* (Malembic-Maher *et al.*, 2020), but it can also take place lateron in the propagative cycle in the vector. For instance, FD phytoplasma was efficiently acquired by *Circulifer haematoceps and Fieberiella florii* leafhoppers after feeding on FD phytoplasma infected *V. faba*, efficiently multiplied but could not be transmitted by these two leafhoppers, demonstrating that specificity could take place at the crossing of the salivary glands (Bressan *et al.*, 2006).

Mechanisms driving the colonization of insect vector cells by phytoplasmas are poorly deciphered. The first phytoplasma protein reported to be able to interact with protein of insect vector was the Antigenic Membrane Protein (Amp). It was demonstrated that Amp of "C*andidatus* Phytoplasma asteris" was able to interact with the cellular microfilament and more specifically with the actin of vectoring leafhopper species but not with actin of non-vectoring insects (Suzuki *et al.*, 2006). In addition, the *amp* gene and its ortholog *stamp* in *"Ca*. P. solani" were shown to be submitted to heavy positive selection indicating a possible adaptation process acting on this gene (Kakizawa *et al.*, 2006a; Fabre *et al.*, 2011). However, the interaction of Amp with actin is certainly involved in the intracellular trafficking of phytoplasmas once they are internalized into the insect vector cells.

Genes encoding membrane proteins VmpA and VmpB of group 16SrV-C and V-D phytoplasmas are highly variable and their variability correlates with the specific transmission of Vmp variants of cluster II and III by leafhoppers of the subfamily *Deltocephalinae* (Malembic-Maher *et al.*, 2020). Vmps seem to directly define the epidemic potential of 16SrV-C and V-D phytoplasma strains. This suggests the importance of investigating the molecular mechanisms underlying the interaction between such proteins and the insect vector proteins in the context of flavescence dorée management. Indeed, identifying these mechanisms might help to define innovative strategies to block FD phytoplasma transmission by *S. titanus.*

It was previously demonstrated that VmpA acts as an adhesin able to bind cells of its insect vector in a lectin-like manner (Arricau-Bouvery *et al.*, 2018; Arricau-Bouvery *et al.*, 2021). After this initial step of adhesion, flavescence dorée phytoplasma enters insect cells by a clathrin-mediated endocytosis allowing infection of its insect vector (Arricau-Bouvery *et al.*, 2023). However, the insect vector proteins interacting with VmpA still remain unknown. The aim of my doctoral thesis was to identify the insect vector proteins interacting with VmpA at very early stages, by looking for a surface receptor of vector cells in culture involved in the VmpA-mediated phytoplasma adhesion. In addition to identifying by mass spectrometry insect vector glycoproteins able to form complexes with VmpA due to its lectin-like activity, I also looked for insect vector proteins able to interact with VmpA through protein-protein interactions.

1. Looking for VmpA glycoprotein receptors in *Euscelidius variegatus*

The very first step of insect vector infection relies on phytoplasma interaction with the surface proteins of the insect cells. Due to the demonstrated lectin activity of VmpA, we currently hypothesize that leafhopper species able to acquire FD phytoplasma have a glycoprotein set different to that of leafhopper species unable to achieve acquisition. Variations in the cortege of glycoproteins can lead to variations in the binding of lectins at the surface of hemipteran insect cells. For instance, an enhanced binding of the mannose-specific *Galanthus nivalis* lectin GNA to the gut glycoproteins of the rice planthopper *Nilaparvata lugens* by comparison to that of the rice leafhopper *Nephottetix cincticeps* is associated to a higher toxicity of GNA to *N. lugens* (Foissac *et al.*, 2000). To identify the glycoprotein receptors

for VmpA, we first enrich Euva cells membrane protein fractions into proteins able to interact with VmpA. Then the VmpA-His_6/Euva proteins complex were submitted to a purification on a Nickel column. However, the number of proteins identified through mass spectrometry was large and very few of them were predicted to contain transmembrane hydrophobic domains characteristic of membrane proteins. We therefore undertake to selectively extract membrane proteins of Euva cells with different detergents and submitted the different fractions to far-western blot interaction assays with strain FD92 VmpA-His_6. The far-western blot analysis revealed several interaction signals between VmpA-His_6_FD92 and Euva cells protein extracts. The bands excised from the gel and corresponding to the signal observed on the blot revealed a high number of proteins identified by mass spectrometry analysis. To reduce this complexity, we could perform the VmpA far-western blot after separating Euva cells proteins on a 2D electrophoresis. This would allow us not only to have a better resolution on proteins separation but, also, to have parameter other than their molecular weight such as the isoelectric point to screen for the potential candidates. Other works aiming at the identification of insect proteins interacting with phytoplasma membrane proteins included an affinity chromatography step before SDS-PAGE (Suzuki *et al.*, 2006; Galetto *et al.,* 2011). The extraction buffer we used during this study contained detergents in order to enrich the extracted fraction in membrane proteins. Both the concentration and the nature of the detergents was not compatible with the system we used during our first assay to purify VmpA-His_6-Euva proteins complexes on a Nickel affinity column. Furthermore, the proteins contained in the insoluble fraction resulting from detergent extraction once separated by SDS-PAGE revealed the presence of additional VmpA interacting proteins which could not be visible in the soluble fractions. To overcome these technical limits, we could work on the improvement of the buffer used, trying to test different detergents at different concentrations that could both be compatible with affinity column purification and allow us to recover proteins contained in the insoluble fraction. To look for other potential VmpA interacting proteins, and to confirm the results we already obtained on Euva cells we should perform a similar *in vitro* interaction assays followed by a new mass spectrometry analysis on proteins extracted from another matrix, consisting in whole insect vectors of FD phytoplasma or their dissected midgut/salivary glands.

In order to validate their interaction with VmpA, we measured the binding of VmpA-coated beads to Euva cells in which the expression of the corresponding genes were silenced by RNAi.

RNAi is an efficient selective silencer of target genes but it is not absolutely specific. Three main off-target effects due to siRNA delivery in an organism can be described and are reviewed by Jackson and Linsley (Jackson and Linsley, 2010). The first one, which is expected to not have influence in our study, is an inflammatory response against the siRNAs and/or the transfectant used to deliver dsRNAs in mammals. The second off-target effect is linked to the siRNA-induced sequence-dependent regulation of unintentional transcripts through partial sequence complementary to their 3'UTRs. Checking the effect on the other target genes showed that no off-target effect was observed in our case. However, even though no partial sequence homology was found in the *E. variegatus* transcriptome for the genes we tested, we cannot exclude that the expression of other non-considered genes could have been affected. A study showed that pooling 10 synthetic siRNAs targeting the same mRNA reduced the number and magnitude of off-target silencing compared to the use of a single siRNA (Kittler *et al.*, 2007) and that the use of low concentrations of complex pool formed by up to 60 different siRNAs targeting the same gene completely eliminates off-target effects in HeLa cells (Hannus *et al.*, 2014). In our case, we used long dsRNA instead of siRNA. The dsRNAs are taken by the RNAi machinery to produce several siRNAs targeting the same mRNA and could then induce a reduction of off-target effects. The third off-target effect is due to a saturation of the endogenous RNAi machinery by exogenous siRNAs. In our case, when we compared the efficiency of the RNAi using one dsRNA (1 µg of dsRNAs) or up to thirteen different dsRNA (13 µg of dsRNAs), we did not find any differences for 10 over 12 genes tested, suggesting that the quantity of dsRNAs used did not saturate the RNAi machinery. Usually, one gene at a time is knocked down by RNAi using either long dsRNA or multiple siRNAs targeting one gene and introduced by transfection into insect cells or vertebrate cells, respectively. We did not found example of cultured cells transfected with multiple long dsRNA targeting several genes. However, an example of three gene silenced using Y-shape siRNAs was described in a bone metastatic prostate cancer cell line (Kozuch *et al.*, 2018). RNAi targeting several genes has been described in insects that were injected with or ingested dsRNA. For example, when two genes were targeted with two dsRNAs injected into the planthopper *N. lugens*, or with two

dsRNAs or a concatemer ingested by the whitefly *Bemisia tabaci*, knockdown of genes were similar to that observed with injection or ingestion of individual dsRNA. Use of concatemer showed an increase of gene knockdown efficacy when compared to mixed dsRNAs. (Mao *et al.*, 2021; Jain *et al.*, 2022).

Another off-target effect that should be taken into account, especially when using dsRNAs mediated RNAi as a strategy to cope with pests in field conditions, is the impact of dsRNAs uptake by off-target species. A perfect match of at least sixteen nucleotides in the central part of the siRNA is required to efficient target mRNA recognition and cleavage in *Drosophila*, even though G:U wobble base pair and A:C mismatches are generally well tolerated (Du *et al.*, 2005). A study led on off target species belonging to 10 different families of 4 different orders aiming to characterise the insecticidal spectrum activity of dsRNA mediated RNAi targeting western corn rootworm (*Diabrotica virgifera virgifera*) revealed that the 270 bp dsRNAs activity discriminate between species characterised by an homology up to 90% (Bachman *et al.*, 2013). In this study, the authors demonstrated that the presence of at least three contiguous 21 nt homology sequences in the region chosen to design dsRNA is required to observe a significant lethal or sublethal effect following diet bioassays. However, if we consider to apply a strategy based on dsRNAs delivery to disrupt *S. titanus* transmission in the field, RNAi effects on off-target insect species present at the vineyard level should carefully be evaluated exploiting *in silico* as well as *in vivo* methods *i.e.* target sequences analyses and evaluation of the RNAi treatment impact on the fitness of off-target species in controlled conditions.

Our results revealed that 1 µg of dsRNA was sufficient to achieve a satisfactory level of inhibition in Euva cells ranging from 2 folds reduction for fasciclin to 58 reduction for uk1-LRR gene. A lack of efficient silencing was measured for the target fasciclin. By comparison with the other dsRNAs produced, fasciclin dsRNA appeared faint on gel with an additional band above the dsRNA. Our hypothesis is that T7 RNA polymerase faced difficulty to transcribe the fasciclin dsRNA and transcripted one brand of RNA more efficiently than the other strand. Then, the additional strand in excess formed secondary structures that migrate differently in the agarose gel than the dsRNA. RNA fold prediction revealed an elevated minimum free energy of the fasciclin single strand RNA, suggesting that the probability of secondary structure formation by the strand in excess is elevated. An attempt to improve the dsRNA

synthesis and lateron the RNAi efficiency should target another region of the fasciclin gene, using different primers for dsRNA synthesis. Indeed, fasciclin is a relevant candidate for interaction with VmpA as its molecular weight of 94 kDa, without taking into consideration post-translational glycosylations, is corresponding to the molecular weight of 90-95 kDa of the major signal observed in VmpA far-western blot on Euva cells (**Figure 21**). This signal was totally abolished by addition of N-acetyl glucosamine (Arricau-Bouvery *et al.,* 2021). It is interesting to notice that Fasciclin 1, its *Drosophila* ortholog, is a glycophosphatidylinositol (GPI) anchored membrane protein modified by N-acetylglucosamine residues (Walsh and Doherty, 1991; Clout *et al.*, 2003).

In our experiments we exploited an *ex vivo* model consisting in cultured cells of the insect vector *E. variegatus* and fluorescent latex beads coated with VmpA to "mimick" the phytoplasma. Of course, this system is a simplification of the much more complicated natural conditions in which phytoplasma infection of the insect vector occurs. Therefore, results must be interpreted with the opportune precautions. However, this system allowed us to rapidly screen for putative VmpA interacting proteins. Using VmpA-coated beads instead of a living phytoplasma allowed us to avoid problems due to the concentration and the viability of FD phytoplasmas recovered from infected insects or infected plants. In fact, as phytoplasmas cannot be cultivated in cell free media up to this day, the obtention of infectious material and the bacteria recovery is space and time-consuming. Moreover, this simplified system allows us to study the role of the sole VmpA in the interaction with the insect cells without the masking effect of other Vmps or membrane factors. This strategy, applied to 12 candidates, revealed the possible implication of *E. variegatus* uk1_LRR protein in the adhesion to the vector cell mediated by VmpA of strain FD92. However, the inhibition of the adhesion of VmpA coated beads to Euva cells in culture was only partially achieved. The amount of uk1_LRR transcripts, as all of the gene candidates tested, was successfully decreased through RNAi but not completely knockout.

We have only few indications about the uk1_LRR function. Proteins with such LRR structures are frequently implicated in cell adhesion and protein-protein interactions and have a variety of functions including immune response, apoptosis, autophagy and neuronal development (Kobe and Kajava, 2001; Matsushima *et al.*, 2019). The uk1_LRR protein of *E. variegatus* contains LRR domains classified in the ribonuclease inhibitor (RI)-like group.

However, uk1_LRR does not show sequence homology with RI, and is predicted to be exposed to the surface cell whereas the RI protein is cytosolic (Dickson *et al.*, 2005). It is therefore likely that uk1_LRR protein has a different function from RI. The other proteins sharing homologies with uk1_LRR protein also contain LRR domain classified in the RI-like group. However, the diversity of the proteins found, *i.e.* artichoke-like protein, Toll pathway protein or Toll-like receptor Tollo, as examples, only share their extracellular position and LRR domains. Several proteins matching amino acidic sequence of uk1_LRR were annotated as carboxypeptidase N subunit-like, but the short stretch of homology before and after the LRR domains were not carrying the Interpro domains for carboxypeptidase N activity. Therefore, the function of uk1_LRR remains to be deciphered.

We identified an ortholog gene in the natural vector of FD phytoplasma *S. titanus* sharing 90.6% of identity in the amino acidic sequence with *E. variegatus* uk1_LRR. The two proteins possess the same number and positions of potential N-glycosylation sites and their length sequence differs for two amino acids. To compare, we looked for an ortholog in an insect non-competent for the transmission of flavescence dorée phytoplasmas. A sequence matching with a 91.6% identity at the amino acid level with *E. variegatus* uk1_LRR amino acid sequence has been deposited in NCBI databases and annotate as N-carboxypeptidase of *Macrosteles quadrilineatus*. The sequence is 3 amino acids shorter than *E. variegatus* uk1_LRR and 1 amino acid shorter than *S. titanus* uk1_LRR, but the potential N-glycosylation sites found in *E. variegatus* and *S. titanus* uk1-LRR were conserved. In the future, it will be interesting to determine and compare the uk1_LRR orthologs sequences of non-vectoring insect for vectotype II and III such as *Oncopsis alni* as well as to that of alternative vectors for these vectotypes *such as Orientus ishidae*, *Allygus mixtus* and *A. modestus*.

We found that uk1_LRR was expressed in both phytoplasma-infected and non-infected insect vectors and was somehow stable over the time of insect colonisation by the phytoplasma. However, in the early stages of vector infection, right after ingestion of phytoplasmas, the expression of uk1_LRR was higher in infected insects when compared to that of adults of the same age fed on healthy plants, although the difference was not statistically significant. Interestingly, a similar increase in expression was found in infected insect abdomens at 28 days latency, when insects acquire again phytoplasmas from the faba beans that became systemically infected upon the feeding of infected insects. Indeed, at this

time-point, the phytoplasma titre measured in insect abdomens increased, suggesting that the expression level of uk1_LRR follows the *de novo* ingestion of phytoplasmas. Furthermore, the evaluation of uk1_LRR expression in different non-infected insect tissues revealed that the digestive tubes were characterised by the highest level of transcripts when compared to salivary glands and ovaries and eggs. Taken these considerations together, uk1_LRR could be implicated in the binding with VmpA in the early stages of insect infection following phytoplasmas ingestion, *i.e.* at the surface of intestine epithelial cells.

The far-western blot analysis performed on Euva cells proteins incubated with VmpA-His_6_PGYA revealed unexpected results. Due to the pivotal role of VmpA in vector competence, we would expect that the VmpA of PGYA, a non *S. titanus*-transmissible strain, would interact with less proteins when compared to VmpA-His_6 of the *S. titanus* transmissible strain-FD92. On the contrary, interaction signals visible on the blot incubated with VmpA-His_6_FD92 were also present on the membrane treated with VmpA-His_6 of strain-PGYA. Even though both VmpAs were simultaneously tested, the differences in anti-VmpA antibody concentration applied to reveal VmpA interactions on the two membranes cannot allow us to discuss about the higher signal intensity of the bands detected for PGYA VmpA. Moreover, the strong interaction signals on the blots could mask the interaction between VmpA and other less-represented proteins of the same molecular weight. Again, this possible bias could be overcome by far-western blot analysis on insect proteins separated by two-dimensional electrophoresis. In addition, even though the insect protein(s) conferring specificity to vector is recognised by VmpA of both the *S. titanus* transmissible and non-transmissible strains, the compatibility for transmission could result from the higher affinity of VmpA_FD92 for the receptor protein. Indeed, during far-western blot assays, VmpA is incubated overnight and such a long incubation may not be optimal to distinguish differences in affinity of VmpA to the targets.

To assess the role of uk1_LRR in conferring vector competence we performed adhesion assays using fluorescent beads coated with VmpA-His_6 from PGYA and FD92 strains on uk1_LRR inhibited Euva cells. Observations deriving from adhesion assays performed on dsRNA treated Euva cells using beads coated with VmpA-His_6_PGYA revealed no difference in the adhesion of coated beads to cells inhibited for uk1_LRR when compared to control cells transfected with dsRNA targeting GFP. However, a higher absolute number of beads were

observed to bind to Euva cells, no matter the dsRNA treatment, in the case of beads coated with PGYA when compared to FD92. It must be noticed that the hydrophilic region of VmpA of FD92 strain consists in 3 repeats of 78 amino acids exposed to the surface of phytoplasma cells meanwhile VmpA corresponding to PGYA strain is characterised by 4 repeats (Malembic-Maher *et al.*, 2020). These repeated domains are expected to contain the carbohydrates binding sites and therefore, these differences in VmpA structure could explain an increased interaction to the vector cells. Thus, the VmpA-His_6_PGYA increased interaction with Euva cells proteins could derive from the higher number of repeats characterising VmpA sequence in PGYA strain.

However, in contrast to the previous results described in chapter 1 (**section 2.5**), we did not find significant differences between the adhesion of VmpA-His_6_FD92 to Euva cells when transfected with dsRNA targeting uk1_LRR when compared to the control condition. One possible explanation is a change occurred in the protocol applied to coat the beads. In fact, for the last experiments of the project, we shift from NH_2 beads to COOH beads. This could explain the non-repeatability of our results when compared to previous experiments that were characterised by a high reproducibility and a constant level of decrease in beads adhesion to cells in which uk1_LRR transcripts level was significantly decreased. Even though the charges are distributed evenly on the VmpA structure, and so, virtually, there is no reason to prefer one beads type over the other the experiments should be repeated using NH_2- beads in order to exclude the presence of any bias in this experimental setting and results.

2. Search for insect vector protein-VmpA interaction by yeast two-hybrid screening

To investigate interactions between plant pathogen and their vectors, yeast two-hybrid assays have been helpful to better understand the biochemical processes underlying transmission and infection. As an example, the coat protein of Tomato leaf curl Bangalore virus (ToLCBV) has been used as a bait to screen for protein-protein interactions against a prey library consisting in the cDNA of *Bemisia tabaci*, the main vector of the virus in tomato cultivations (Prasannakumar and Maruthi, 2021). This first screening has allowed the

identification of 102 putative insect proteins interacting with ToLCBV coat protein, which will be further tested by RNA interference to validate their role and interaction.

Rhopalosiphum padi is the aphid involved in the vection of barley yellow dwarf virus-GPV (BYDV-GPV). A Y2H assays has led to the identification of twenty-five proteins potentially interacting with the readthrough protein of BYDV-GPV and eight who interact with its coat protein (Wang *et al.*, 2015). The interactions have been then tested by retro-transformation of yeast, where their strength has been assessed too. The confirmed positive interactions have been then validated through co-immunoprecipitation assays in mammalian cells. These results have been coupled with an analysis based on differential expressed proteins (iTRAQ and LC-MS/MS) in viruliferous and non-viruliferous aphids, making it possible to enrich the protein interaction network characterizing BYDV-GPV infection in *R. padi*. Similarly, the cDNA of *Sogatella furcifera*, the white backed planthopper vector of the southern rice black-streaked dwarf virus (SRBSDV) has been used as a prey library in a yeast two-hybrid assay in which the bait consists in the membrane protein P7-1 of the virus (Mar *et al.*, 2014). The results of the screening have been confirmed through chemiluminescence Co-IP assays in mammalian cells and have revealed that several different vector proteins are implicated in the successful transmission of the virus.

Yeast two-hybrid assays have been useful to explore the functions and roles of phytoplasma effectors in the interaction with their hosts. Several Y2H screens have been performed using *Arabidopsis thaliana* cDNA as prey library to characterize the Aster Yellow phytoplasma strain Witches Broom (AY-WB) effectors. To resume the most remarkable results, researchers found that SAP05 interacts with both SPLs and GATAs transcription factors of the plant host, mediating their degradation by proteasome 26S (Huang *et al.*, 2021). Transcription factors belonging to these two subfamilies are indeed involved in regulation of developmental transition in plant thus, their degradation results in a proliferation of vegetative tissues and shoots of the plant host as well as in its delayed aging. Type II MADS-domain transcription factors (MTFs) AGL12, SEP3 and MAF1 have been found to interact with the effector SAP54 which mediates their degradation binding both to MTFs and to ubiquitin binding proteins RAD23C and RAD23D (MacLean *et al.*, 2014). The degradation of this MTFs lead to the production of sterile leaf-like flowers which interestingly result in conferring to the

plant more attractive phenotype for visit and oviposition of the phytoplasma vector *Macrosteles quadrilineatus.*

It has been demonstrated that VmpA acts as a lectin in its interaction with *E. variegatus* cells in culture with a specificity for N-Acetylglucosamine and mannose (Arricau-Bouvery *et al.*, 2021). However, lectins can contain a second type of binding site that interacts with non-carbohydrate ligand (Barondes, 1988). They can participate in heterophilic (binding to a counter protein) or homophilic (binding to another subunit of the same lectin) protein-protein interactions (reviewed in Nagae and Yamaguchi, 2015). For example, human galectin-8, a galactose-specific human lectin, is able to recruit Nuclear Dot Protein 52 kDa (NPD52) to achieve anti-bacterial autophagy of *Salmonella* (Thurston *et al.*, 2012). NPD52 binds to the C-terminal convex side of galectin-8 whereas the galactose-binding domain is present on the concave side, suggesting that galectin-8 can bind simultaneously to the glycosylated moieties and to NPD52. Similarly, galectin-3 binds in a carbohydrate independent manner with the protein Alix, which mediates the interaction with apoptosis-linked-gene-2 (ALG-2), in processes involved in protein transportation and in the regulation of cell surface expression of T-cell receptors (Chen *et al.*, 2009).

Furthermore, phytoplasmas are bacteria characterised by a reduced genome and their proteins could show more than one function or role at a time. In fact, it has been shown how several proteins of bacteria, in particular pathogens, are characterised by the ability to have more than one biological action, with alternative roles that can be involved in pathogen virulence or in interaction with the host (reviewed in Henderson and Martin, 2011). These proteins, called moonlighting proteins, typically belong to glycolytic pathway, metabolic and enzymatic pathways, or are folding catalysts and molecular chaperones. The most commonly identified moonlighting virulence functions of these bacterial proteins are modulation of leucocyte activity and adhesion. Comparative studies on protein-protein interaction networks among reduced genome bacteria has showed how the average number of interaction partners per protein is inversely proportional to genome size (Kelkar and Ochman, 2013). This means that proteins in smaller genomes are characterised by functional innovation and are more prone to “moonlighting” comparing to their orthologs in larger genomes. The hypothesis is that this increase in diversification aims to compensate for gene loss, especially in the case of

endosymbionts or pathogens, which experience genetic drift upon invasion of their host specific niche.

Previous results revealed that FD phytoplasma VmpA is implicated in the adhesion of the phytoplasma to insect cells of *E. variegatus* (Arricau-Bouvery *et al.*, 2018), probably through an interaction involving membrane proteins exposed at the surface of the insect cells that could potentially involve other type of interactions than the binding to the glycosylated moieties. VmpA could then serve as multiple scopes, interacting with several proteins of different organs of the vector, which allow phytoplasma to perform and complete its multiplicative-circulative cycle in the insect. This hypothesis is supported by the results of the far-western blot analysis presented in chapter 1 (**section 2.2**), which highlighted the presence of several signals of interaction between phytoplasma VmpA and insect's proteins.

To assess the occurrence of protein-protein interaction with proteins of the insect vector we performed a classic yeast two-hybrid assay using a library of *E. variegatus* cDNA as a prey. Results did not evidenced any protein-protein interactions.

Yeast two-hybrid technique has allowed to boost the available knowledge in protein interaction network in a lot of organisms and specific biological processes. It is a relatively cheap technique, and it can be performed without the necessities of specific and high technical specialisation demanding material, especially when compared to classical protein identification through mass spectrometry analysis (Brückner *et al.*, 2009). Nevertheless, results of the assays need to be interpreted being conscious that this technique is characterised by intrinsic problems of false positive and false negative results, which led to issues in the reproducibility of such assays. False negative results are defined as real protein-protein interactions which cannot be detected through Y2H assays. This could be due to several reasons which include non-symmetric interaction between proteins, steric hindrance, transient interactions, proteins interactions physically involving membranes, and post translational modification of the proteins, which are generally very specific to the organism concerned. We cannot exclude that the lack of confirmed interaction in our system is due to one of these reasons. We observed that colonies obtained on selective media after mating were characterised by truncated and non-in-frame prey proteins, and therefore consisted in false positive results that cannot be confirmed by yeast retro transformation. However, the library used in our study was successfully employed to perform other Y2H assays in the

laboratory, leading to the identification of interacting proteins with the bait of choice (Sybille Duret, personal communication). Thus, we can exclude that the lack of confirmed interactions derived by bias in the building of the *E. variegatus* cDNA library itself.

Taken these considerations together, our results suggest that VmpA does not interact with *E. variegatus* proteins when these are expressed in yeast cells.

VmpA has been cloned in the bait vector deprived of its signal peptide and transmembrane domain. In fact, bait and prey fusion proteins are translated and processed in the yeast cytosol but then are translocated in the nucleus due to the NLS present on AD and BD of Gal4 portions cloned in fusion with the bait and prey proteins. This allows the activation of the reporter genes transcription upon reconstitution of Gal4 transcription factor. We cannot exclude that the ectopic expression of VmpA does not allow the interaction with its targets. Declinations of the classic Y2H techniques have been developed to adapt to different needs in the study of protein-protein interactions. To investigate interactions with and between membrane proteins a split-ubiquitin assay has been developed (Stagljar *et al.*, 1998). In this case, the bait is an integral membrane protein fused with the C-terminal of *Saccharomyces cerevisiae* ubiquitin and with an artificial transcription factor, meanwhile the preys are fused to the N-terminal of the ubiquitin. If bait and prey interact, the pseudo-ubiquitin is reassembled: it will be then recognized by cytosolic ubiquitin specific proteases (UBP) which will cleave the molecule leading to the release of the transcription factor which will activate the transcription of reporter genes in the nucleus. This technique could be helpful to overcome the limit of ectotopic VmpA expression in the cell but still, even with this method, we cannot exclude that the different post translational modifications operated by yeast on prey proteins could prevent the real interactions occurring between VmpA and its vector partner(s). Indeed, difference in glycosylation pathways between insect and yeasts is striking. Insects are characterised by paucimannosidic and oligomannosidic glycans meanwhile hyper-mannosylation is typical of the yeast *Saccharomyces cerevisiae*, resulting in the formation of glycans with up to 200 mannose residues (Chung *et al.*, 2017).

Conclusions and perspectives

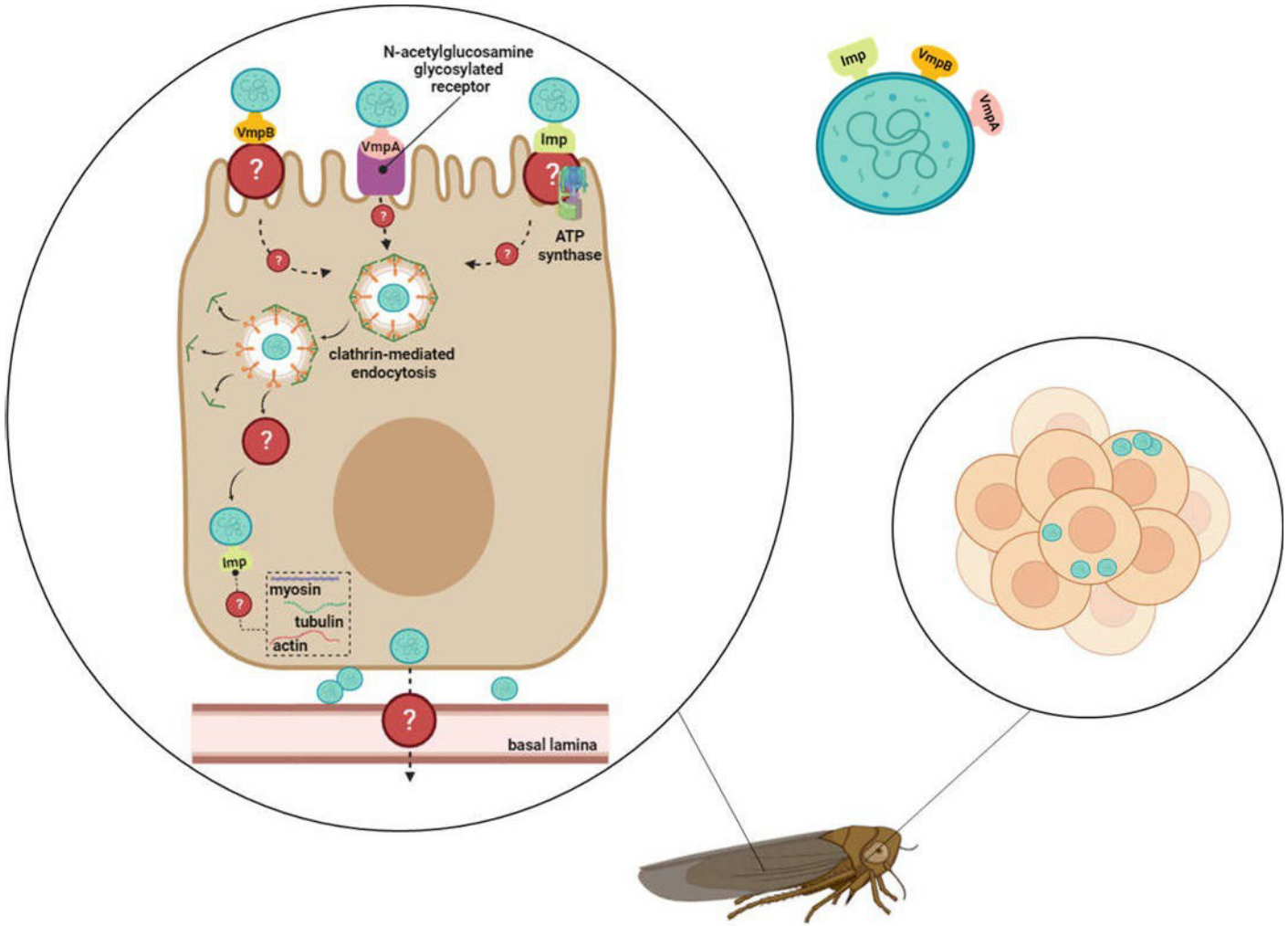

Figure 39. Flavescence dorée phytoplasma membrane proteins and their interaction with host cells. VmpA acts as a lectin and mediates the phytoplasma binding to the gut epithelium of the insect vector. Its receptor is likely an N-acetylglucosamine glycosylated transmembrane protein. VmpB is another less studied FDp adhesion but its binding properties are not determined yet. Imp of lime witches' broom phytoplasma interacts with *S. titanus* actin, myosin and ATP synthase, meanwhile Imp of wheat blue dwarf phytoplasma has been demonstrated to interact with α tubulin of its insect vector. Phytoplasmas have been observed by TEM between the basal lamina and the midgut epithelium but the way phytoplasma cross from basal lamina to access the haemocoel is still unknown. Phytoplasmas then reach the salivary glands where they infect only certain cells. The mechanisms of infection of salivary gland cells still need to be identified. The figure has been realized using BioRender.

Conclusions and perspectives

FDp membrane proteins are the first contact point with insect vector cells and, therefore, play a crucial role in early stages of the vector infection. However, the mechanisms underlying FDp adhesion to cells, internalisation and intracellular trafficking still need to be clarified. In **Figure 39**, we summarised the state of the knowledge about the interactions occurring between FDp membrane proteins and insect vector cells, as well as the questions that still lay unanswered.

VmpA acts as a lectin and mediates the phytoplasma binding to the gut epithelium of the insect vector. Its receptor is a N-acetylglucosamine glycosylated transmembrane protein (Arricau-Bouvery *et al.*, 2021). VmpB has a similar organization with repeated domains reminiscent of bacterial surface proteins involved in the colonisation of eukaryotic cells, and is therefore supposed to be a lectin-like adhesin similar to VmpA. According to FDp genome FDp does not possess an Amp ortholog but has an Imp protein. FDp Imp has been demonstrated to selectively interact *in vitro* with insect vector species (Trivellone *et al.*, 2019), but its insect targets still needs to be identified. Imp of wheat blue dwarf phytoplasma has been demonstrated to interact with α tubulin of its insect vector and silencing of α tubulin by RNAi decreased the transmission efficiency of the phytoplasma (Ding *et al.*, 2022). Imp of lime witches broom phytoplasma was found to bind *in vitro* to three unknown proteins of its leafhopper vector *Hishimonus phycitis* and to ATP synthase, actin and myosin of *S. titanus* (Siampour *et al.*, 2011). RNAi silencing of ATP synthase in *E. variegatus* negatively impact FDp multiplication in the insect (Galetto *et al.*, 2021b). Moreover, the ectotopic expression of ATP synthase in plasma membrane of midgut and salivary gland of *E. variegatus* has been demonstrated (Galetto *et al.*, 2011). Do FDp-Imp and vector ATP synthase interacts, and if so, is their interaction important for insect cells colonisation?

After their initial adhesion to host cells, FD phytoplasmas are internalised by clathrin-mediated endocytosis (Arricau-Bouvery *et al.*, 2023) but their intracellular trafficking still need to be investigated. Do FDp escape out of the endosomal vesicle or not? Do FDp block the fusion of endosomal and lysosomal vesicles to escape degradation as *Shigella flexneri* do (Sun *et al.*, 2021)? Electronic microscopy observations suggest that FDp multiplication occurs in the

cytosol of midgut epithelial cells and salivary gland cells (Gouranton and Maillet, 1973), supporting the fact that FDp escape endocytosis vescicles.

When phytoplasmas exit from epithelial cells, they have to cross the basal lamina to access the haemocoel. Is FDp able to disrupt basal lamina or does it take advantage of its renewal to go through? When entering the haemocoel FDp colonises all insect vector organs but Malpighian tubes, ovaries and testis (Lefol *et al.*, 1994). FDp binds the salivary glands through where they infect only certain cells (Arricau-Bouvery *et al.*, 2018) and particularly acini III, IV and V (Lefol *et al.*, 1993). The mechanisms of infection of these cells still need to be identified. Do Vmp adhesins play a role in the invasion of salivary gland cells or are other membrane proteins involved? Adhesion assays of latex beads coated with Vmps on dissected salivary glands should be performed to test this hypothesis.

The experimental set up used to carry on our experiments demonstrated to be adapted to the study of interactions between pathogen proteins and their vector cells, allowing us to gain some preliminary insights on the role of a putative VmpA receptor in FDp adhesion to its vector cells. Therefore, it could be exploited to investigate at least some of the critical points mentioned before about FDp interaction with host cells. Moreover, it could be, with the opportune adaptations, applied to other pathosystems of interest to help in better understanding the mechanisms underlying this kind of interactions.

We successfully achieved to implement our RNAi protocol in order to inhibit the expression of up to 12 genes in Euva cells, without negatively impacting their ability to grow and multiply. This could open new possibilities in the inhibition of gene networks in the cells and provide a useful tool to clarify the molecular interactions between phytoplasmas and their insect vectors. The inhibition of multiple targets through dsRNAs should also be assessed *in vivo*, as well the impact of the treatment on off-targets genes and on insect survival and development through injection and ingestion delivery on *E. variegatus* and *S. titanus*.

According to far-western blot analyses, VmpA interacts with more than one protein of *E. variegatus* (Arricau-Bouvery *et al.*, 2021, chapter 1 **section 2.2**). The multiplex RNAi protocol will be useful to test other proteins found upon VmpA affinity column or far-western blot followed by mass spectrometry analysis. Once other protein candidates for which a decrease expression correlates with a decrease of adhesion of VmpA-coated beads to *E. variegatus* cells

in culture will be selected, it will be possible to deliver combinations of dsRNA to evaluate the additive effect of the decrease of their expression on the adhesion of VmpA-coated beads to the insect cells.

The experiments carried out during this project revealed the implication of an insect vector LRR protein in the adhesion of VmpA to the vector cells. However, the involvement of this protein in transmission to plants and in vector specificity still need to be demonstrated. In order to assess the impact of the protein in the insect survival and in the transmissibility of phytoplasma to plants, *in vivo* RNAi targeting uk1_LRR in *E. variegatus* and *S. titanus* should be performed prior to acquisition and transmission assays. Several works have shown how efficiently dsRNA mediated RNAi achieves to decrease target mRNA expression on both *E. variegatus* and *S. titanus* (Abbà *et al.*, 2019; Ripamonti *et al.*, 2022b; Arricau-Bouvery *et al.*, 2023). We demonstrated that the level of uk1_LRR transcript in Euva cells decrease up to 58 time when compared to control condition. We cannot take for granted that such effectiveness will be the same when RNAi treatment will be imposed to living insects, but this strategy is worth to be explored.

In order to further validate the uk1_LRR-VmpA interaction, the expression of *E. variegatus* uk1_LRR in a heterologous expression system like *Drosophila* S2 cells would be necessary in order to produce a protein with a glycosylation profile similar to that of leafhopper cells that can then be used to perform *in vitro* interaction assays. In case our results are confirmed, this would be the first report of a VmpA receptor in the insect vector of FD phytoplasma. On the other hand, the interaction of uk1_LRR with VmpA of non-transmissible phytoplasma genotypes such as PGYA with both *E. variegatus* and *S. titanus* will have to be measured with optimised assays, in order to evaluate the impact of uk1_LRR-VmpA interaction in the transmission specificity. Conversely, the uk1_LRR orthologs of non-vectoring leafhopper species such as *Oncopsis alni* will have to be expressed and check for its ability to interact or not with FD92 VmpA.

If transmission and vector specificity assays will reveal an important role of uk1_LRR in the disruption of FD phytoplasma transmission to plants, we could imagine the development of new strategies to manage the epidemics. If the receptor silencing mediated by dsRNAs results to be efficient in insect, Spray Induced Gene Silencing technology could be exploited and adapted to application in vineyards. The uk1_LRR receptor will need to be better

structurally and functionally characterised. This could help in the development of approaches to disrupt insect mediated transmission by competition as it was developed for *Xylella fastidiosa* (Killiny et al., 2011, Labroussaa et al., 2016). These tools could help in setting up new strategies for the management of FD epidemics in vineyards, with the aim of reducing the insecticide input for the control of vector populations.

References

Abbà, S., Galetto, L., Ripamonti, M., Rossi, M., and Marzachì, C. (2019) RNA interference of muscle actin and ATP synthase beta increases mortality of the phytoplasma vector Euscelidius variegatus. *Pest Manag Sci* **75**: 1425–1434.

Adrakey, H.K., Malembic-Maher, S., Rusch, A., Ay, J.-S., Riley, L., Ramalanjaona, L., and Fabre, F. (2022) Field and Landscape Risk Factors Impacting Flavescence Dorée Infection: Insights from Spatial Bayesian Modeling in the Bordeaux Vineyards. *Phytopathology®* **112**: 1686–1697.

Alma, A., Lessio, F., Gonella, E., Picciau, L., Mandrioli, M., and Tota, F. (2018) New insights in phytoplasma-vector interaction: acquisition and inoculation of flavescence dorée phytoplasma by Scaphoideus titanus adults in a short window of time. *Ann Appl Biol* **173**: 55–62.

Almeida, R.P.P., Blua, M.J., Lopes, J.R.S., and Purcell, A.H. (2005) Vector Transmission of Xylella fastidiosa: Applying Fundamental Knowledge to Generate Disease Management Strategies. *Ann Entomol Soc Am* **98**: 775–786.

Almeida, R.P.P., and Purcell, A.H. (2006) Patterns of Xylella fastidiosa Colonization on the Precibarium of Sharpshooter Vectors Relative to Transmission to Plants. *Ann Entomol Soc Am* **99**: 884–890.

Andersen, M.T., Liefting, L.W., Havukkala, I., and Beever, R.E. (2013) Comparison of the complete genome sequence of two closely related isolates of 'Candidatus Phytoplasma australiense' reveals genome plasticity. *BMC Genomics* **14**: 529.

Angelini, E., Clair, D., Borgo, M., Bertaccini, A., and Boudon-Padieu, E. (2001) Flavescence doree in France and Italy - Occurrence of closely related phytoplasma isolates and their near relationships to Palatinate grapevine yellows and an alder yellows phytoplasma. *VITIS - J Grapevine Res* **40**: 79–79.

Angelini, E., Luca Bianchi, G., Filippin, L., Morassutti, C., and Borgo, M. (2007) A new TaqMan method for the identification of phytoplasmas associated with grapevine yellows by real-time PCR assay. *J Microbiol Methods* **68**: 613–622.

Arnaud, G., Malembic-Maher, S., Salar, P., Bonnet, P., Maixner, M., Marcone, C., *et al.* (2007) Multilocus Sequence Typing Confirms the Close Genetic Interrelatedness of Three Distinct Flavescence Dorée Phytoplasma Strain Clusters and Group 16SrV Phytoplasmas Infecting Grapevine and Alder in Europe. *Appl Environ Microbiol* **73**: 4001–4010.

Arricau-Bouvery, N., Dubrana, M.-P., Canuto, F., Duret, S., Brocard, L., Claverol, S., *et al.* (2023) Flavescence dorée phytoplasma enters insect cells by a clathrin-mediated endocytosis allowing infection of its insect vector. *Sci Rep* **13**: 2211.

Arricau-Bouvery, N., Duret, S., Dubrana, M.-P., Batailler, B., Desqué, D., Béven, L., *et al.* (2018) Variable Membrane Protein A of Flavescence Dorée Phytoplasma Binds the Midgut Perimicrovillar Membrane of Euscelidius variegatus and Promotes Adhesion to Its Epithelial Cells. *Appl Environ Microbiol* **84**: e02487-17.

Arricau-Bouvery, N., Duret, S., Dubrana, M.-P., Desqué, D., Eveillard, S., Brocard, L., *et al.* (2021) Interactions between the flavescence dorée phytoplasma and its insect vector indicate lectin-type adhesion mediated by the adhesin VmpA. *Sci Rep* **11**: 11222.

Asadi, A., Razavi, S., Talebi, M., and Gholami, M. (2019) A review on anti-adhesion therapies of bacterial diseases. *Infection* **47**: 13–23.

Bachman, P.M., Bolognesi, R., Moar, W.J., Mueller, G.M., Paradise, M.S., Ramaseshadri, P., *et al.* (2013) Characterization of the spectrum of insecticidal activity of a double-stranded RNA with targeted activity against Western Corn Rootworm (Diabrotica virgifera virgifera LeConte). *Transgenic Res* **22**: 1207–1222.

Bai, X., Correa, V.R., Toruño, T.Y., Ammar, E.-D., Kamoun, S., and Hogenhout, S.A. (2009) AY-WB phytoplasma secretes a protein that targets plant cell nuclei. *Mol Plant-Microbe Interact MPMI* **22**: 18–30.

Bai, X., Zhang, J., Ewing, A., Miller, S.A., Jancso Radek, A., Shevchenko, D.V., *et al.* (2006) Living with Genome Instability: the Adaptation of Phytoplasmas to Diverse Environments of Their Insect and Plant Hosts. *J Bacteriol* **188**: 3682–3696.

Barondes, S.H. (1988) Bifunctional properties of lectins: lectins redefined. *Trends Biochem Sci* **13**: 480–482.

Baum, J.A., Bogaert, T., Clinton, W., Heck, G.R., Feldmann, P., Ilagan, O., *et al.* (2007) Control of coleopteran insect pests through RNA interference. *Nat Biotechnol* **25**: 1322–1326.

Beanland, L., Hoy, C.W., Miller, S.A., and Nault, L.R. (2000) Influence of Aster Yellows Phytoplasma on the Fitness of Aster Leafhopper (Homoptera: Cicadellidae). *Ann Entomol Soc Am* **93**: 271–276.

Berg, M., Melcher, U., and Fletcher, J. (2001) Characterization of Spiroplasma citri adhesion related protein SARP1, which contains a domain of a novel family designated sarpin. *Gene* **275**: 57–64.

Bertaccini, A., Arocha-Rosete, Y., Contaldo, N., Duduk, B., Fiore, N., Montano, H.G., *et al.* (2022) Revision of the 'Candidatus Phytoplasma' species description guidelines. *Int J Syst Evol Microbiol* **72**: 005353.

Bertazzon, N., Bagnaresi, P., Forte, V., Mazzucotelli, E., Filippin, L., Guerra, D., *et al.* (2019) Grapevine comparative early transcriptomic profiling suggests that Flavescence dorée phytoplasma represses plant responses induced by vector feeding in susceptible varieties. *BMC Genomics* **20**: 526.

Béven, L., Duret, S., Batailler, B., Dubrana, M.-P., Saillard, C., Renaudin, J., and Arricau-Bouvery, N. (2012) The Repetitive Domain of ScARP3d Triggers Entry of Spiroplasma citri into Cultured Cells of the Vector Circulifer haematoceps. *PLoS ONE* **7**: e48606.

Bonfils, J., and Schvester, D. (1960) Les cicadelles (Homoptera Auchenorhyncha) dans leurs rapports avec la vigne dans le SudOuest de la France. *Ann Epiphyt* **3**: 325–336.

Boudon-Padieu, E. (2005) Phytoplasmes de la vigne et vecteurs potentiels/Grapevine phytoplasmas and potential vectors. *Bulletin OIV* **78**: (891-892), 299-320.

Bressan, A., Clair, D., Sémétey, O., and Boudon-Padieu, E. (2006) Insect Injection and Artificial Feeding Bioassays to Test the Vector Specificity of Flavescence Dorée Phytoplasma. *Phytopathology®* **96**: 790–796.

Bressan, A., Girolami, V., and Boudon-Padieu, E. (2005) Reduced fitness of the leafhopper vector Scaphoideus titanus exposed to Flavescence dorée phytoplasma. *Entomol Exp Appl* **115**: 283–290.

Brückner, A., Polge, C., Lentze, N., Auerbach, D., and Schlattner, U. (2009) Yeast Two-Hybrid, a Powerful Tool for Systems Biology. *Int J Mol Sci* **10**: 2763–2788.

Carle, P., Malembic-Maher, S., Arricau-Bouvery, N., Desque, D., Eveillard, S., Carrere, S., and Foissac, X. (2011) “Flavescence doree” phytoplasma genome: a metabolism oriented towards glycolysis and protein degradation. *Bull Insectology* **64**: S13.

Caudwell, A. (1957) Deux années d’étude sur la flavescence dorée, nouvelle maladie grave de la vigne. *Ann Amélioration Plantes* **4**: 359–363.

Caudwell, A. (1961) Les phénomènes de rétablissement chez la Flavescence dorée de la vigne. *Ann Epiphyt* **12**: 347–354.

Caudwell, A., Gianotti, J., Kuszala, C., and Larrue, J. (1971) Etude du rôle de particules de type “Mycoplasme” dans l’étiologie de la Flavescence dorée de la vigne. Examen cytologique des plantes malades et des cicadelles infectieuses. *Ann Phytopathol* **3**: 107–123.

Caudwell, A., Kuszala, C., Bachelier, J.C., and Larrue, J. (1970) Transmission de la Flavescence doree de la vigne aux plantes herbacees par l’allongement du temps d’utilisation de la cicadelle Scaphoideus littoralis Ball et l’etude de sa survie sur en grand nombre d’especes vegetales. *Ann Phytopathol* **1572**: 415–428.

Caudwell, A., Kuszala, C., and Larrue, J. (1973) Techniques Utilisables Pour L’etude De La Flavescence Doree De La Vigne. *Riv Patol Veg* **9**: 269–276.

Caudwell, A., Kuszala, C., Larrue, J., and Bachelier, J.C. (1972) Transmission de la Flavescence dorée de la fève à la fève par des cicadelles des genres Euscelis et Euscelidius. *Ann Phytopathol* **1572**: 181–189.

Caudwell, A., Larrue, J., Boudon-Padieu, E., and McLean, G.D. (1997) Flavescence doree elimination from dormant wood of grapevines by hot-water treatment. *Aust J Grape Wine Res* **3**: 21–25.

Caudwell, A., Larrue, J., Tassart, V., Boidron, R., Grenan, S., Leguay, M., and Bernard, P. (1994) Ability of grapevine rootstocks varieties to transmit Flavescence dorée - study case of 3309-C and Fercal. *Agronomie* **14**: 83–94.

Chang, S.H., Tan, C.M., Wu, C.-T., Lin, T.-H., Jiang, S.-Y., Liu, R.-C., *et al.* (2018) Alterations of plant architecture and phase transition by the phytoplasma virulence factor SAP11. *J Exp Bot* **69**: 5389–5401.

Chaogang, S., Jianhua, W., Guoying, Z., Gang, S., Baozhen, P., Juanli, L., *et al.* (2003) Ectopic expression of the spike protein of Rice Ragged Stunt Oryzavirus in transgenic rice plants inhibits transmission of the virus to insects. *Mol Breed* **11**: 295–301.

Chen, H.-Y., Fermin, A., Vardhana, S., Weng, I.-C., Lo, K.F.R., Chang, E.-Y., *et al.* (2009) Galectin-3 negatively regulates TCR-mediated CD4+ T-cell activation at the immunological synapse. *Proc Natl Acad Sci U S A* **106**: 14496–14501.

Christensen, N.M., Nicolaisen, M., Hansen, M., and Schulz, A. (2004) Distribution of Phytoplasmas in Infected Plants as Revealed by Real-Time PCR and Bioimaging. *Mol Plant-Microbe Interactions®* **17**: 1175–1184.

Christiaens, O., Whyard, S., Vélez, A.M., and Smagghe, G. (2020) Double-Stranded RNA Technology to Control Insect Pests: Current Status and Challenges. *Front Plant Sci* **11**.

Chuche, J., and Thiéry, D. (2014) Biology and ecology of the Flavescence dorée vector Scaphoideus titanus: a review. *Agron Sustain Dev* **34**: 381–403.

Chung, C.-Y., Majewska, N.I., Wang, Q., Paul, J.T., and Betenbaugh, M.J. (2017) SnapShot: N-Glycosylation Processing Pathways across Kingdoms. *Cell* **171**: 258-258.e1.

Chung, W.-C., Chen, L.-L., Lo, W.-S., Lin, C.-P., and Kuo, C.-H. (2013) Comparative Analysis of the Peanut Witches'-Broom Phytoplasma Genome Reveals Horizontal Transfer of Potential Mobile Units and Effectors. *PLOS ONE* **8**: e62770.

Cimerman, A., Pacifico, D., Salar, P., Marzachì, C., and Foissac, X. (2009) Striking Diversity of *vmp1* , a Variable Gene Encoding a Putative Membrane Protein of the Stolbur Phytoplasma. *Appl Environ Microbiol* **75**: 2951–2957.

Clemens, J.C., Worby, C.A., Simonson-Leff, N., Muda, M., Maehama, T., Hemmings, B.A., and Dixon, J.E. (2000) Use of double-stranded RNA interference in Drosophila cell lines to dissect signal transduction pathways. *Proc Natl Acad Sci* **97**: 6499–6503.

Clout, N.J., Tisi, D., and Hohenester, E. (2003) Novel fold revealed by the structure of a FAS1 domain pair from the insect cell adhesion molecule fasciclin I. *Struct Lond Engl 1993* **11**: 197–203.

Constable, F.E. (2009) Phytoplasma epidemiology: grapevines as a model. *Phytoplasmas Genomes Plant Hosts Vectors* 188–212.

Cosson, P., Sofer, L., Le, Q.H., Léger, V., Schurdi-Levraud, V., Whitham, S.A., *et al.* (2010) RTM3, which controls long-distance movement of potyviruses, is a member of a new plant gene family encoding a meprin and TRAF homology domain-containing protein. *Plant Physiol* **154**: 222–232.

Dalakouras, A., Jarausch, W., Buchholz, G., Bassler, A., Braun, M., Manthey, T., *et al.* (2018) Delivery of Hairpin RNAs and Small RNAs Into Woody and Herbaceous Plants by Trunk Injection and Petiole Absorption. *Front Plant Sci* **9**

Davis, M.W., and Jorgensen, E.M. (2022) ApE, A Plasmid Editor: A Freely Available DNA Manipulation and Visualization Program. *Front Bioinforma* **2**

Davis, R.E., and Dally, E.L. (2001) Revised Subgroup Classification of Group 16SrV Phytoplasmas and Placement of Flavescence Dorée-Associated Phytoplasmas in Two Distinct Subgroups. *Plant Dis* **85**: 790–797.

Debonneville, C., Mandelli, L., Brodard, J., Groux, R., Roquis, D., and Schumpp, O. (2022) The Complete Genome of the "Flavescence Dorée" Phytoplasma Reveals Characteristics of Low Genome Plasticity. *Biology* **11**: 953.

Dickson, K.A., Haigis, M.C., and Raines, R.T. (2005) Ribonuclease Inhibitor: Structure and Function. In *Progress in Nucleic Acid Research and Molecular Biology*. Academic Press, pp. 349–374

Ding, L., Lu, W., Yang, Y., Zhong, Q., Zhou, T., Wang, G., *et al.* (2022) Immunodominant membrane protein (Imp) promotes the transmission of wheat blue dwarf (WBD) phytoplasma by directly interacting with α-tubulin in leafhoppers. *Eur J Plant Pathol* **162**: 357–367.

Doi, Y., Teranaka, M., Yora, K., and Asuyama, H. (1967) Mycoplasma- or PLT Group-like Microorganisms Found in the Phloem Elements of Plants Infected with Mulberry Dwarf, Potato Witches' Broom, Aster Yellows, or Paulownia Witches' Broom. *Jpn J Phytopathol* **33**: 259–266.

Droulia, F., and Charalampopoulos, I. (2021) Future Climate Change Impacts on European Viticulture: A Review on Recent Scientific Advances. *Atmosphere* **12**: 495.

Du, Q., Thonberg, H., Wang, J., Wahlestedt, C., and Liang, Z. (2005) A systematic analysis of the silencing effects of an active siRNA at all single-nucleotide mismatched target sites. *Nucleic Acids Res* **33**: 1671–1677.

Duret, S., Batailler, B., Dubrana, M.-P., Saillard, C., Renaudin, J., Béven, L., and Arricau-Bouvery, N. (2014) Invasion of insect cells by *S piroplasma citri* involves spiralin relocalization and lectin/glycoconjugate-type interactions: Spiralin relocalization and insect cell adhesion. *Cell Microbiol* **16**: 1119–1132.

Ebbert, M., and Nault, L. (2001) Survival in Dalbulus leafhopper vectors improves after exposure to maize stunting pathogens. *Entomol Exp Appl* **100**: 311–324.

Echeverri, C.J., and Perrimon, N. (2006) High-throughput RNAi screening in cultured cells: a user's guide. *Nat Rev Genet* **7**: 373–384.

Eveillard, S., Jollard, C., Labroussaa, F., Khalil, D., Perrin, M., Desqué, D., *et al.* (2016) Contrasting Susceptibilities to Flavescence Dorée in Vitis vinifera, Rootstocks and Wild Vitis Species. *Front Plant Sci* **7**: 1762.

Fabre, A., Danet, J.-L., and Foissac, X. (2011) The stolbur phytoplasma antigenic membrane protein gene stamp is submitted to diversifying positive selection. *Gene* **472**: 37–41.

Fields, S., and Song, O. (1989) A novel genetic system to detect protein–protein interactions. *Nature* **340**: 245–246.

Filippin, L., Jović, J., Cvrković, T., Forte, V., Clair, D., Toševski, I., *et al.* (2009) Molecular characteristics of phytoplasmas associated with Flavescence dorée in clematis and grapevine and preliminary results on the role of Dictyophara europaea as a vector. *Plant Pathol* **58**: 826–837.

Foissac, X., Thi Loc, N., Christou, P., Gatehouse, A.M.R., and Gatehouse, J.A. (2000) Resistance to green leafhopper (Nephotettix virescens) and brown planthopper (Nilaparvata lugens) in transgenic rice expressing snowdrop lectin (Galanthus nivalis agglutinin; GNA). *J Insect Physiol* **46**: 573–583.

Galetto, L., Abbà, S., Rossi, M., Ripamonti, M., Palmano, S., Bosco, D., and Marzachì, C. (2021a) Silencing of ATP synthase β reduces phytoplasma multiplication in a leafhopper vector. *J Insect Physiol* **128**: 104176.

Galetto, L., Abbà, S., Rossi, M., Vallino, M., Pesando, M., Arricau-Bouvery, N., *et al.* (2018) Two Phytoplasmas Elicit Different Responses in the Insect Vector Euscelidius variegatus Kirschbaum. *Infect Immun* **86**: 10.1128/iai.00042-18.

Galetto, L., Bosco, D., Balestrini, R., Genre, A., Fletcher, J., and Marzachì, C. (2011) The Major Antigenic Membrane Protein of "Candidatus Phytoplasma asteris" Selectively Interacts with ATP Synthase and Actin of Leafhopper Vectors. *PLoS ONE* **6**: e22571.

Galetto, L., Miliordos, D.E., Pegoraro, M., Sacco, D., Veratti, F., Marzachì, C., and Bosco, D. (2016) Acquisition of Flavescence Dorée Phytoplasma by Scaphoideus titanus Ball from Different Grapevine Varieties. *Int J Mol Sci* **17**: 1563.

Galetto, L., Ripamonti, M., Abbà, S., Rossi, M., Manfredi, M., Bosco, D., and Marzachì, C. (2021b) Silencing of ATP synthase β induces female sterility in a leafhopper phytoplasma vector. *Entomol Gen* 497–510.

Gal-Mor, O., and Finlay, B.B. (2006) Pathogenicity islands: a molecular toolbox for bacterial virulence. *Cell Microbiol* **8**: 1707–1719.

Gasparich, G.E., Bertaccini, A., and Zhao, Y. (2020) 'Candidatus Phytoplasma.' In *Bergey's Manual of Systematics of Archaea and Bacteria*. John Wiley & Sons, Ltd, pp. 1–39

Görg, L.M., Gallinger, J., and Gross, J. (2021) The phytopathogen 'Candidatus Phytoplasma mali' alters apple tree phloem composition and affects oviposition behavior of its vector Cacopsylla picta. *Chemoecology* **31**: 31–45.

Gouranton, J., and Maillet, P.L. (1973) High resolution autoradiography of mycoplasmalike organisms multiplying in some tissues of an insect vector for clover-phyllody. *J Invertebr Pathol* **21**: 158–163.

Gutiérrez-Cabrera, A.E., Córdoba-Aguilar, A., Zenteno, E., Lowenberger, C., and Espinoza, B. (2016) Origin, evolution and function of the hemipteran perimicrovillar membrane with emphasis on Reduviidae that transmit Chagas disease. *Bull Entomol Res* **106**: 279–291.

Hannus, M., Beitzinger, M., Engelmann, J.C., Weickert, M.-T., Spang, R., Hannus, S., and Meister, G. (2014) siPools: highly complex but accurately defined siRNA pools eliminate off-target effects. *Nucleic Acids Res* **42**: 8049–8061.

Hardt, W.D., Chen, L.M., Schuebel, K.E., Bustelo, X.R., and Galán, J.E. (1998) S. typhimurium encodes an activator of Rho GTPases that induces membrane ruffling and nuclear responses in host cells. *Cell* **93**: 815–826.

Henderson, B., and Martin, A. (2011) Bacterial virulence in the moonlight: multitasking bacterial moonlighting proteins are virulence determinants in infectious disease. *Infect Immun* **79**: 3476–3491.

Hirumi, H., and Maramorosch, K. (1969) Mycoplasma-like bodies in the salivary glands of insect vectors carrying the aster yellows agent. *J Virol* **3**: 82–84.

Hoffman, C.S., and Winston, F. (1987) A ten-minute DNA preparation from yeast efficiently releases autonomous plasmids for transformaion of Escherichia coli. *Gene* **57**: 267–272.

Hogenhout, S.A., Oshima, K., Ammar, E.-D., Kakizawa, S., Kingdom, H.N., and Namba, S. (2008) Phytoplasmas: bacteria that manipulate plants and insects. *Mol Plant Pathol* **9**: 403–423.

Hoshi, A., Oshima, K., Kakizawa, S., Ishii, Y., Ozeki, J., Hashimoto, M., *et al.* (2009) A unique virulence factor for proliferation and dwarfism in plants identified from a phytopathogenic bacterium. *Proc Natl Acad Sci* **106**: 6416–6421.

Hren, M., Boben, J., Rotter, A., Kralj, P., Gruden, K., and Ravnikar, M. (2007) Real-time PCR detection systems for Flavescence dorée and Bois noir phytoplasmas in grapevine: comparison with conventional PCR detection and application in diagnostics. *Plant Pathol* **56**: 785–796.

Huang, C.-T., Cho, S.-T., Lin, Y.-C., Tan, C.-M., Chiu, Y.-C., Yang, J.-Y., and Kuo, C.-H. (2022) Comparative Genome Analysis of 'Candidatus Phytoplasma luffae' Reveals the Influential Roles of Potential Mobile Units in Phytoplasma Evolution. *Front Microbiol* **13**

Huang, W., MacLean, A.M., Sugio, A., Maqbool, A., Busscher, M., Cho, S.-T., *et al.* (2021) Parasitic modulation of host development by ubiquitin-independent protein degradation. *Cell* **184**: 5201-5214.e12.

Hultgren, S.J., Normark, S., and Abraham, S.N. (1991) Chaperone-assisted assembly and molecular architecture of adhesive pili. *Annu Rev Microbiol* **45**: 383–415.

Jackson, A.L., Bartz, S.R., Schelter, J., Kobayashi, S.V., Burchard, J., Mao, M., *et al.* (2003) Expression profiling reveals off-target gene regulation by RNAi. *Nat Biotechnol* **21**: 635–637.

Jackson, A.L., and Linsley, P.S. (2010) Recognizing and avoiding siRNA off-target effects for target identification and therapeutic application. *Nat Rev Drug Discov* **9**: 57–67.

Jain, R.G., Fletcher, S.J., Manzie, N., Robinson, K.E., Li, P., Lu, E., *et al.* (2022) Foliar application of clay-delivered RNA interference for whitefly control. *Nat Plants* **8**: 535–548.

Janik, K., Mithöfer, A., Raffeiner, M., Stellmach, H., Hause, B., and Schlink, K. (2017) An effector of apple proliferation phytoplasma targets TCP transcription factors—a generalized virulence strategy of phytoplasma? *Mol Plant Pathol* **18**: 435–442.

Jeger, M., Bragard, C., Caffier, D., Candresse, T., Chatzivassiliou, E., Dehnen-Schmutz, K., *et al.* (2016) Risk to plant health of Flavescence dorée for the EU territory. *EFSA J* **14**: e04603.

Jollard, C., Foissac, X., Desqué, D., Razan, F., Garcion, C., Beven, L., and Eveillard, S. (2020) Flavescence Dorée Phytoplasma Has Multiple ftsH Genes that Are Differentially Expressed in Plants and Insects. *Int J Mol Sci* **21**: 150.

Jomantiene, R., Zhao, Y., and Davis, R.E. (2007) Sequence-variable mosaics: composites of recurrent transposition characterizing the genomes of phylogenetically diverse phytoplasmas. *DNA Cell Biol* **26**: 557–564.

Kakizawa, S., Oshima, K., Jung, H.-Y., Suzuki, S., Nishigawa, H., Arashida, R., *et al.* (2006a) Positive selection acting on a surface membrane protein of the plant-pathogenic phytoplasmas. *J Bacteriol* **188**: 3424–3428.

Kakizawa, S., Oshima, K., and Namba, S. (2006b) Diversity and functional importance of phytoplasma membrane proteins. *Trends Microbiol* **14**: 254–256.

Käll, L., Canterbury, J.D., Weston, J., Noble, W.S., and MacCoss, M.J. (2007) Semi-supervised learning for peptide identification from shotgun proteomics datasets. *Nat Methods* **4**: 923–925.

Kelkar, Y.D., and Ochman, H. (2013) Genome reduction promotes increase in protein functional complexity in bacteria. *Genetics* **193**: 303–307.

Kenny, B., DeVinney, R., Stein, M., Reinscheid, D.J., Frey, E.A., and Finlay, B.B. (1997) Enteropathogenic E. coli (EPEC) transfers its receptor for intimate adherence into mammalian cells. *Cell* **91**: 511–520.

Ketting, R.F. (2011) The many faces of RNAi. *Dev Cell* **20**: 148–161.

Killiny, N., and Almeida, R.P.P. (2009a) Xylella fastidiosa Afimbrial Adhesins Mediate Cell Transmission to Plants by Leafhopper Vectors. *Appl Environ Microbiol* **75**: 521–528.

Killiny, N., and Almeida, R.P.P. (2009b) Host structural carbohydrate induces vector transmission of a bacterial plant pathogen. *Proc Natl Acad Sci U S A* **106**: 22416–22420.

Killiny, N., and Almeida, R.P.P. (2014) Factors Affecting the Initial Adhesion and Retention of the Plant Pathogen Xylella fastidiosa in the Foregut of an Insect Vector. *Appl Environ Microbiol* **80**: 420–426.

Killiny, N., Castroviejo, M., and Saillard, C. (2005) Spiroplasma citri Spiralin Acts In Vitro as a Lectin Binding to Glycoproteins from Its Insect Vector Circulifer haematoceps. *Phytopathology* **95**: 541–548.

Killiny, N., Rashed, A., and Almeida, R.P.P. (2012) Disrupting the Transmission of a Vector-Borne Plant Pathogen. *Appl Environ Microbiol* **78**: 638–643.

Kitazawa, Y., Iwabuchi, N., Himeno, M., Sasano, M., Koinuma, H., Nijo, T., *et al.* (2017) Phytoplasma-conserved phyllogen proteins induce phyllody across the Plantae by degrading floral MADS domain proteins. *J Exp Bot* **68**: 2799–2811.

Kittler, R., Surendranath, V., Heninger, A.-K., Slabicki, M., Theis, M., Putz, G., *et al.* (2007) Genome-wide resources of endoribonuclease-prepared short interfering RNAs for specific loss-of-function studies. *Nat Methods* **4**: 337–344.

Kobe, B., and Kajava, A.V. (2001) The leucine-rich repeat as a protein recognition motif. *Curr Opin Struct Biol* **11**: 725–732.

Koinuma, H., Maejima, K., Tokuda, R., Kitazawa, Y., Nijo, T., Wei, W., *et al.* (2020) Spatiotemporal dynamics and quantitative analysis of phytoplasmas in insect vectors. *Sci Rep* **10**: 4291.

Kolliopoulou, A., Taning, C.N.T., Smagghe, G., and Swevers, L. (2017) Viral Delivery of dsRNA for Control of Insect Agricultural Pests and Vectors of Human Disease: Prospects and Challenges. *Front Physiol* **8**.

Kouki, A., Haataja, S., Loimaranta, V., Pulliainen, A.T., Nilsson, U.J., and Finne, J. (2011) Identification of a novel streptococcal adhesin P (SadP) protein recognizing galactosyl-α1-4-galactose-containing glycoconjugates: convergent evolution of bacterial pathogens to binding of the same host receptor. *J Biol Chem* **286**: 38854–38864.

Kozuch, S.D., Cultrara, C.N., Beck, A.E., Heller, C.J., Shah, S., Patel, M.R., *et al.* (2018) Enhanced Cancer Theranostics with Self-Assembled, Multilabeled siRNAs. *ACS Omega* **3**: 12975–12984.

Kreikemeyer, B., Klenk, M., and Podbielski, A. (2004) The intracellular status of Streptococcus pyogenes: role of extracellular matrix-binding proteins and their regulation. *Int J Med Microbiol IJMM* **294**: 177–188.

Krogh, A., Larsson, B., Heijne, G. von, and Sonnhammer, E.L. (2001) Predicting transmembrane protein topology with a hidden Markov model: application to complete genomes. *J Mol Biol* **305**: 567–580.

Krstić, O., Cvrković, T., Marinković, S., Jakovljević, M., Mitrović, M., Toševski, I., and Jović, J. (2022) Genetic Diversity of Flavescence Dorée Phytoplasmas in Vineyards of Serbia: From the Widespread Occurrence of Autochthonous Map-M51 to the Emergence of Endemic Map-FD2 (Vectotype II) and New Map-FD3 (Vectotype III) Epidemic Genotypes. *Agronomy* **12**: 448.

Kube, M., Mitrovic, J., Duduk, B., Rabus, R., and Seemüller, E. (2012) Current View on Phytoplasma Genomes and Encoded Metabolism. *Sci World J* **2012**: e185942.

Kube, M., Schneider, B., Kuhl, H., Dandekar, T., Heitmann, K., Migdoll, A.M., *et al.* (2008) The linear chromosome of the plant-pathogenic mycoplasma "Candidatus Phytoplasma mali." *BMC Genomics* **9**: 306.

Labroussaa, F., Zeilinger, A.R., and Almeida, R.P.P. (2016) Blocking the Transmission of a Noncirculative Vector-Borne Plant Pathogenic Bacterium. *Mol Plant-Microbe Interact MPMI* **29**: 535–544.

Lee, I.-M. (1993) Universal Amplification and Analysis of Pathogen 16S rDNA for Classification and Identification of Mycoplasmalike Organisms. *Phytopathology* **83**: 834.

Lee, I.-M., Davis, R.E., and Gundersen-Rindal, D.E. (2000) Phytoplasma: Phytopathogenic Mollicutes. *Annu Rev Microbiol* **54**: 221–255.

Lefol, C., Caudwell, A., Lherminier, J., and Larrue, J. (1993) Attachment of the Flavescence doree pathogen (MLO) to leafhopper vectors and other insects. *Ann Appl Biol* **123**: 611–622.

Lefol, C., Lherminier, J., Boudon-Padieu, E., Larrue, J., Louis, C., and Caudwell, A. (1994) Propagation of Flavescence dorée MLO (Mycoplasma-like Organism) in the Leafhopper Vector Euscelidius variegatus Kbm. *J Invertebr Pathol* **63**: 285–293.

Lepka, P., Stitt, M., Moll, E., and Seemüller, E. (1999) Effect of phytoplasmal infection on concentration and translocation of carbohydrates and amino acids in periwinkle and tobacco. *Physiol Mol Plant Pathol* **55**: 59–68.

Lessio, F., and Alma, A. (2004) Dispersal patterns and chromatic response of Scaphoideus titanus Ball (Homoptera Cicadellidae), vector of the phytoplasma agent of grapevine flavescence dorée. *Agric For Entomol* **6**: 121–128.

Lessio, F., Tota, F., and Alma, A. (2014) Tracking the dispersion of Scaphoideus titanus Ball (Hemiptera: Cicadellidae) from wild to cultivated grapevine: use of a novel mark-capture technique. *Bull Entomol Res* **104**: 432–443.

Lim, P.O., and Sears, B.B. (1989) 16S rRNA sequence indicates that plant-pathogenic mycoplasmalike organisms are evolutionarily distinct from animal mycoplasmas. *J Bacteriol* **171**: 5901–5906.

Lim, P.-O., and Sears, B.B. (1991) DNA sequence of the ribosomal protein genes rp12 and rps19 from a plant-pathogenic mycoplasma-like organism. *FEMS Microbiol Lett* **84**: 71–74.

Lim, P.O., and Sears, B.B. (1992) Evolutionary relationships of a plant-pathogenic mycoplasmalike organism and Acholeplasma laidlawii deduced from two ribosomal protein gene sequences. *J Bacteriol* **174**: 2606–2611.

Lim, P.O., Sears, B.B., and Klomparens, K.L. (1992) Membrane properties of a plant-pathogenic mycoplasmalike organism. *J Bacteriol* **174**: 682–686.

Liu, S., Sivakumar, S., Sparks, W.O., Miller, W.A., and Bonning, B.C. (2010) A peptide that binds the pea aphid gut impedes entry of Pea enation mosaic virus into the aphid hemocoel. *Virology* **401**: 107–116.

Livak, K.J., and Schmittgen, T.D. (2001) Analysis of Relative Gene Expression Data Using Real-Time Quantitative PCR and the 2−ΔΔCT Method. *Methods* **25**: 402–408.

Lu, Y.-T., Li, M.-Y., Cheng, K.-T., Tan, C.M., Su, L.-W., Lin, W.-Y., *et al.* (2014) Transgenic Plants That Express the Phytoplasma Effector SAP11 Show Altered Phosphate Starvation and Defense Responses. *Plant Physiol* **164**: 1456–1469.

MacLean, A.M., Orlovskis, Z., Kowitwanich, K., Zdziarska, A.M., Angenent, G.C., Immink, R.G.H., and Hogenhout, S.A. (2014) Phytoplasma Effector SAP54 Hijacks Plant Reproduction by Degrading MADS-box Proteins and Promotes Insect Colonization in a RAD23-Dependent Manner. *PLOS Biol* **12**: e1001835.

MacLean, A.M., Sugio, A., Makarova, O.V., Findlay, K.C., Grieve, V.M., Tóth, R., *et al.* (2011) Phytoplasma effector SAP54 induces indeterminate leaf-like flower development in Arabidopsis plants. *Plant Physiol* **157**: 831–841.

Maejima, K., Iwai, R., Himeno, M., Komatsu, K., Kitazawa, Y., Fujita, N., *et al.* (2014) Recognition of floral homeotic MADS domain transcription factors by a phytoplasmal effector, phyllogen, induces phyllody. *Plant J Cell Mol Biol* **78**: 541–554.

Maejima, K., Kitazawa, Y., Tomomitsu, T., Yusa, A., Neriya, Y., Himeno, M., *et al.* (2015) Degradation of class E MADS-domain transcription factors in Arabidopsis by a phytoplasmal effector, phyllogen. *Plant Signal Behav* **10**: e1042635.

Maillet, P.L., and Gouranton, J. (1971) Etude du cycle biologique du mycoplasme de la phyllodie du trèfle dans l'insecte vecteur, Euscelis lineolatus Brullé Homoptera, Jassidae. *Journal de Microscopie* **11**: 143–165.

Maixner, M., Reinert, W., and Darimont, H. (2000) Transmission of grapevine yellows by *Oncopsis alni* (Schrank) (Auchenorrhyncha: Macropsinae). *VITIS - J Grapevine Res* **39**: 83–83.

Malembic-Maher, S., Constable, F., Cimerman, A., Arnaud, G., Carle, P., Foissac, X., and Boudon-Padieu, E. (2008) A chromosome map of the Flavescence doree phytoplasma. *Microbiol Read Engl* **154**: 1454–1463.

Malembic-Maher, S., Desqué, D., Khalil, D., Salar, P., Bergey, B., Danet, J.-L., *et al.* (2020) When a Palearctic bacterium meets a Nearctic insect vector: Genetic and ecological insights into the emergence of the grapevine Flavescence dorée epidemics in Europe. *PLOS Pathog* **16**: e1007967.

Mao, K., Ren, Z., Li, W., Cai, T., Qin, X., Wan, H., *et al.* (2021) Carboxylesterase genes in nitenpyram-resistant brown planthoppers, Nilaparvata lugens. *Insect Sci* **28**: 1049–1060.

Mar, T., Liu, W., and Wang, X. (2014) Proteomic analysis of interaction between P7-1 of Southern rice black-streaked dwarf virus and the insect vector reveals diverse insect proteins involved in successful transmission. *J Proteomics* **102**: 83–97.

Marcone, C. (2014) Molecular biology and pathogenicity of phytoplasmas. *Ann Appl Biol* **165**: 199–221.

Marcone, C., Neimark, H., Ragozzino, A., Lauer, U., and Seemüller, E. (1999) Chromosome sizes of phytoplasmas composing major phylogenetic groups and subgroups. *Phytopathology* **89**: 805–810.

Martini, M., Murari, E., Mori, N., and Bertaccini, A. (1999) Identification and Epidemic Distribution of Two Flavescence Dorée—Related Phytoplasmas in Veneto (Italy). *Plant Dis* **83**: 925–930.

Massey, R.C., Kantzanou, M.N., Fowler, T., Day, N.P., Schofield, K., Wann, E.R., *et al.* (2001) Fibronectin-binding protein A of Staphylococcus aureus has multiple, substituting, binding regions that mediate adherence to fibronectin and invasion of endothelial cells. *Cell Microbiol* **3**: 839–851.

Matsushima, N., Takatsuka, S., Miyashita, H., and Kretsinger, R.H. (2019) Leucine Rich Repeat Proteins: Sequences, Mutations, Structures and Diseases. *Protein Pept Lett* **26**: 108–131.

Mayer, C.J., Vilcinskas, A., and Gross, J. (2008a) Phytopathogen Lures Its Insect Vector by Altering Host Plant Odor. *J Chem Ecol* **34**: 1045–1049.

Mayer, C.J., Vilcinskas, A., and Gross, J. (2008b) Pathogen-induced Release of Plant Allomone Manipulates Vector Insect Behavior. *J Chem Ecol* **34**: 1518–1522.

Mayer, C.J., Vilcinskas, A., and Gross, J. (2011) Chemically mediated multitrophic interactions in a plant–insect vector-phytoplasma system compared with a partially nonvector species. *Agric For Entomol* **13**: 25–35.

Minato, N., Himeno, M., Hoshi, A., Maejima, K., Komatsu, K., Takebayashi, Y., *et al.* (2014) The phytoplasmal virulence factor TENGU causes plant sterility by downregulating of the jasmonic acid and auxin pathways. *Sci Rep* **4**: 7399.

Mondal, M., Brown, J.K., and Flynt, A. (2020) Exploiting somatic piRNAs in Bemisia tabaci enables novel gene silencing through RNA feeding. *Life Sci Alliance* **3**.

Mori, N., Bressan, A., Martin, M., Guadagnini, M., Girolami, V., and Bertaccini, A. (2002) Experimental transmission by *Scaphoideus titanus* Ball of two Flavescence doree-type phytoplasmas. *VITIS - J Grapevine Res* **41**: 99–99.

Mysore, K., Sun, L., Hapairai, L.K., Wang, C.-W., Igiede, J., Roethele, J.B., *et al.* (2021) A Yeast RNA-Interference Pesticide Targeting the Irx Gene Functions as a Broad-Based Mosquito Larvicide and Adulticide. *Insects* **12**: 986.

Nagae, M., and Yamaguchi, Y. (2015) Sugar recognition and protein-protein interaction of mammalian lectins conferring diverse functions. *Curr Opin Struct Biol* **34**: 108–115.

Newman, K.L., Almeida, R.P.P., Purcell, A.H., and Lindow, S.E. (2004) Cell-cell signaling controls Xylella fastidiosa interactions with both insects and plants. *Proc Natl Acad Sci U S A* **101**: 1737–1742.

Nishigawa, H., Miyata, S.-I., Oshima, K., Sawayanagi, T., Komoto, A., Kuboyama, T., *et al.* (2001) In planta expression of a protein encoded by the extrachromosomal DNA of a phytoplasma and related to geminivirus replication proteins. *Microbiol Read Engl* **147**: 507–513.

Nottelet, P., Bataille, L., Gourgues, G., Anger, R., Lartigue, C., Sirand-Pugnet, P., *et al.* (2021) The mycoplasma surface proteins MIB and MIP promote the dissociation of the antibody-antigen interaction. *Science Advances* **7**: eabf2403.

Numata, K., Ohtani, M., Yoshizumi, T., Demura, T., and Kodama, Y. (2014) Local gene silencing in plants via synthetic dsRNA and carrier peptide. *Plant Biotechnol J* **12**: 1027–1034.

Ofek, I., Hasty, D.L., and Sharon, N. (2003) Anti-adhesion therapy of bacterial diseases: prospects and problems. *FEMS Immunol Med Microbiol* **38**: 181–191.

Orlovskis, Z., and Hogenhout, S.A. (2016) A Bacterial Parasite Effector Mediates Insect Vector Attraction in Host Plants Independently of Developmental Changes. *Front Plant Sci* **7**.

Oshima, K., Ishii, Y., Kakizawa, S., Sugawara, K., Neriya, Y., Himeno, M., *et al.* (2011) Dramatic transcriptional changes in an intracellular parasite enable host switching between plant and insect. *PloS One* **6**: e23242.

Oshima, K., Kakizawa, S., Nishigawa, H., Jung, H.-Y., Wei, W., Suzuki, S., *et al.* (2004) Reductive evolution suggested from the complete genome sequence of a plant-pathogenic phytoplasma. *Nat Genet* **36**: 27–29.

Oshima, K., Kakizawa, S., Nishigawa, H., Kuboyama, T., Miyata, S., Ugaki, M., and Namba, S. (2001) A Plasmid of Phytoplasma Encodes a Unique Replication Protein Having Both Plasmid- and Virus-like Domains: Clue to Viral Ancestry or Result of Virus/Plasmid Recombination? *Virology* **285**: 270–277.

Osler, R., Loi, N., Carraro, L., Musetti, R., Loschi, A., and Ermacora, P. (2004) Spontaneous recovery in grapevines affected by flavescence doree phytoplasma. *Acta Physiol Plant* **26**.

Papura, D., Burban, C., Helden, M. van, Giresse, X., Nusillard, B., Guillemaud, T., and Kerdelhué, C. (2012) Microsatellite and Mitochondrial Data Provide Evidence for a Single Major Introduction for the Neartic Leafhopper Scaphoideus titanus in Europe. *PLOS ONE* **7**: e36882.

Pathak, V.M., Verma, V.K., Rawat, B.S., Kaur, B., Babu, N., Sharma, A., *et al.* (2022) Current status of pesticide effects on environment, human health and it's eco-friendly management as bioremediation: A comprehensive review. *Front Microbiol* **13**: 962619.

Pecher, P., Moro, G., Canale, M.C., Capdevielle, S., Singh, A., MacLean, A., *et al.* (2019) Phytoplasma SAP11 effector destabilization of TCP transcription factors differentially impact development and defence of Arabidopsis versus maize. *PLOS Pathog* **15**: e1008035.

Pelletier, C., Salar, P., Gillet, J., Cloquemin, G., Very, P., Foissac, X., and Malembic-Maher, S. (2009) Triplex real-time PCR assay for sensitive and simultaneous detection of grapevine phytoplasmas of the 16SrV and 16SrXII-A groups with an endogenous analytical control. *VITIS - J Grapevine Res* **48**: 87–87.

Pinzón, N., Bertrand, S., Subirana, L., Busseau, I., Escrivá, H., and Seitz, H. (2019) Functional lability of RNA-dependent RNA polymerases in animals. *PLoS Genet* **15**: e1007915.

Pizarro-Cerdá, J., and Cossart, P. (2006) Bacterial Adhesion and Entry into Host Cells. *Cell* **124**: 715–727.

Plavec, J., Budinšćak, Ž., Križanac, I., Škorić, D., Foissac, X., and Šeruga Musić, M. (2019) Multilocus sequence typing reveals the presence of three distinct flavescence dorée phytoplasma genetic clusters in Croatian vineyards. *Plant Pathol* **68**: 18–30.

Prasannakumar, N.R., and Maruthi, M.N. (2021) Identification of whitefly (Bemisia tabaci) proteins interacting with Tomato leaf curl Bangalore virus coat protein gene using Y2H system. *Int J Trop Insect Sci* **42**: 445–455.

Purcell, A.H., and Finlay, A. (1979) Evidence for Noncirculative Transmission of Pierce's Disease Bacterium by Sharpshooter Leafhoppers. *Phytopathology* **69**: 393.

Rahola, J., Reyes, J., and Giralt, L. (1997) La flavescencia dorada en los viñedos del Alt Empordá (Girona) Bol. San. Veg. Plagas, **23**: 403-416.

Rao, D.P., Bertaccini, A., Fiore, N., and Liefting, L. (2018) Characterisation and epidemiology of phytoplasma-associated diseases. In *Plant pathogenic bacteria,* Springer.

Rashidi, M., Galetto, L., Bosco, D., Bulgarelli, A., Vallino, M., Veratti, F., and Marzachì, C. (2015) Role of the major antigenic membrane protein in phytoplasma transmission by two insect vector species. *BMC Microbiol* **15**: 193.

Rekab, D., Carraro, L., Schneider, B., Seemüller, E., Chen, J., Chang, C.-J., *et al.* (1999) Geminivirus-related extrachromosomal DNAs of the X-clade phytoplasmas share high sequence similarity. *Microbiol Read Engl* **145 (Pt 6)**: 1453–1459.

Renaudin, J., Béven, L., Batailler, B., Duret, S., Desqué, D., Arricau-Bouvery, N., *et al.* (2015) Heterologous expression and processing of the flavescence dorée phytoplasma variable membrane protein VmpA in Spiroplasma citri. *BMC Microbiol* **15**: 82.

Ribet, D., and Cossart, P. (2015) How bacterial pathogens colonize their hosts and invade deeper tissues. *Microbes Infect* **17**: 173–183.

Rigamonti, I.E., Salvetti, M., Girgenti, P., Bianco, P.A., and Quaglino, F. (2023) Investigation on Flavescence Dorée in North-Western Italy Identifies Map-M54 (16SrV-D/Map-FD2) as the Only Phytoplasma Genotype in Vitis vinifera L. and Reveals the Presence of New Putative Reservoir Plants. *Biology* **12**: 1216.

Ripamonti, M., Galetto, L., Maron, F., Marzachì, C., and Bosco, D. (2022a) Scaphoideus titanus fitness on grapevine varieties with different susceptibility to Flavescence dorée phytoplasma. Journal of Applied Entomology **146**: 1260–1271.

Ripamonti, M., Cerone, L., Abbà, S., Rossi, M., Ottati, S., Palmano, S., *et al.* (2022b) Silencing of ATP Synthase β Impairs Egg Development in the Leafhopper Scaphoideus titanus, Vector of the Phytoplasma Associated with Grapevine Flavescence Dorée. *Int J Mol Sci* **23**: 765.

Ripamonti, M., Pegoraro, M., Morabito, C., Gribaudo, I., Schubert, A., Bosco, D., and Marzachì, C. (2021) Susceptibility to flavescence dorée of different Vitis vinifera genotypes from north-western Italy. *Plant Pathol* **70**: 511–520.

Robertson, W.E., Funke, L.F.H., Torre, D. de la, Fredens, J., Wang, K., and Chin, J.W. (2021) Creating custom synthetic genomes in Escherichia coli with REXER and GENESIS. *Nat Protoc* **16**: 2345–2380.

Rodrigues Jardim, B., Tran-Nguyen, L.T.T., Gambley, C., Al-Sadi, A.M., Al-Subhi, A.M., Foissac, X., *et al.* (2023) The observation of taxonomic boundaries for the 16SrII and 16SrXXV phytoplasmas using genome-based delimitation. *Int J Syst Evol Microbiol* **73**.

Roggia, C., Caciagli, P., Galetto, L., Pacifico, D., Veratti, F., Bosco, D., and Marzachì, C. (2014) Flavescence dorée phytoplasma titre in field-infected Barbera and Nebbiolo grapevines. *Plant Pathol* **63**: 31–41.

Rossi, M., Galetto, L., Bodino, N., Beltramo, J., Gamalero, S., Pegoraro, M., *et al.* (2023) Competition among Flavescence Dorée Phytoplasma Strains in the Experimental Insect Vector Euscelidius variegatus. *Insects* **14**: 575

Rossi, M., Pegoraro, M., Ripamonti, M., Abbà, S., Beal, D., Giraudo, A.,et al.(2019a) Genetic Diversity of Flavescence Dorée Phytoplasmas at the Vineyard Scale.Appl Environ Microbiol85: e03123-18.

Rossi, M., Samarzija, I., Šeruga-Musić, M., and Galetto, L. (2019b) Diversity and FunctionalImportance of Phytoplasma Membrane Proteins. In *Phytoplasmas: Plant Pathogenic Bacteria - III:Genomics, Host Pathogen Interactions and Diagnosis*. Bertaccini, A., Oshima, K., Kube, M., and Rao,G.P. (eds). Springer, Singapore. pp. 69–88.

Rossi, M., Vallino, M., Galetto, L., and Marzachì, C. (2020) Competitive Exclusion of Flavescence dorée Phytoplasma Strains in Catharanthus roseus Plants. *Plants* **9**: 1594.

Saillard, C., Carle, P., Duret-Nurbel, S., Henri, R., Killiny, N., Carrère, S., *et al.* (2008) The abundant extrachromosomal DNA content of the Spiroplasma citri GII3-3X genome. *BMC Genomics* **9**: 195.

Schachter, H. (2009) Paucimannose N-glycans in Caenorhabditis elegans and Drosophila melanogaster. *Carbohydr Res* **344**: 1391–1396.

Schindelin, J., Arganda-Carreras, I., Frise, E., Kaynig, V., Longair, M., Pietzsch, T., *et al.* (2012) Fiji - an Open Source platform for biological image analysis. *Nat Methods* **9**: 10.1038/nmeth.2019.

Schneider, B., Ahrens, U., Kirkpatrick, B.C., and Seemüller, E. (1993) Classification of plant-pathogenic mycoplasma-like organisms using restriction-site analysis of PCR-amplified 16S rDNA. *J Gen Microbiol* **139**: 519–527.

Schvester, D., Carle, P., and Moutous, G. (1961) Sur la transmission de la flavescence dorée des vignes par une cicadelle. *Comptes Rendus Acad Sci* **18**: 1021–1024.

Schwarz, D.S., Hutvágner, G., Haley, B., and Zamore, P.D. (2002) Evidence that siRNAs function as guides, not primers, in the Drosophila and human RNAi pathways. *Mol Cell* **10**: 537–548.

Seemüller, E., Sule, S., Kube, M., Jelkmann, W., and Schneider, B. (2013) The AAA+ ATPases and HflB/FtsH Proteases of 'Candidatus Phytoplasma mali': Phylogenetic Diversity, Membrane Topology, and Relationship to Strain Virulence. *Mol Plant-Microbe Interactions®* **26**: 367–376.

Shukla, J.N., Kalsi, M., Sethi, A., Narva, K.E., Fishilevich, E., Singh, S., *et al.* (2016) Reduced stability and intracellular transport of dsRNA contribute to poor RNAi response in lepidopteran insects. *RNA Biol* **13**: 656–669.

Siampour, M., Galetto, L., Bosco, D., Izadpanah, K., and Marzachì, C. (2011) In vitro interactions between immunodominant membrane protein of lime witches' broom phytoplasma and leafhopper vector proteins. *Bull Insectology* S149–S150.

Siampour, M., Izadpanah, K., Galetto, L., Salehi, M., and Marzachí, C. (2013) Molecular characterization, phylogenetic comparison and serological relationship of the Imp protein of several 'Candidatus Phytoplasma aurantifolia' strains. *Plant Pathol* **62**: 452–459.

Stagljar, I., Korostensky, C., Johnsson, N., and Heesen, S. te (1998) A genetic system based on split-ubiquitin for the analysis of interactions between membrane proteins in vivo. *Proc Natl Acad Sci U S A* **95**: 5187–5192.

Steffek, R., Reisenzein, H., and Zeisner, N. (2007) Analysis of the pest risk from Grapevine flavescence dorée phytoplasma to Austrian viticulture. *EPPO Bull* **37**: 191–203.

Strohmayer, A.,Moser, M., Si-Ammour, A., Krczal, G., and Boonrod, K. (2019) 'CandidatusPhytoplasma mali' Genome Encodes a Protein that Functions as an E3 Ubiquitin Ligase and CouldInhibit Plant Basal Defense.Mol Plant-Microbe Interactions®32: 1487–1495.

Sugawara, K., Honma, Y., Komatsu, K., Himeno, M., Oshima, K., and Namba, S. (2013) The Alteration of Plant Morphology by Small Peptides Released from the Proteolytic Processing of the Bacterial Peptide TENGU1[W]. *Plant Physiol* **162**: 2005–2014.

Sugio, A., Kingdom, H.N., MacLean, A.M., Grieve, V.M., and Hogenhout, S.A. (2011a) Phytoplasma protein effector SAP11 enhances insect vector reproduction by manipulating plant development and defense hormone biosynthesis. *Proc Natl Acad Sci U S A* **108**: E1254-1263.

Sugio, A., MacLean, A.M., Kingdom, H.N., Grieve, V.M., Manimekalai, R., and Hogenhout, S.A. (2011b) Diverse targets of phytoplasma effectors: from plant development to defense against insects. *Annu Rev Phytopathol* **49**: 175–195.

Sun, J., Wang, X., Lin, H., Wan, L., Chen, J., Yang, X., *et al.* (2021) Shigella escapes lysosomal degradation through inactivation of Rab31 by IpaH4.5. *J Med Microbiol* **70**: 001382.

Suzuki, S., Oshima, K., Kakizawa, S., Arashida, R., Jung, H.-Y., Yamaji, Y., *et al.* (2006) Interaction between the membrane protein of a pathogen and insect microfilament complex determines insect-vector specificity. *Proc Natl Acad Sci* **103**: 4252–4257.

Swanson, J.A., and Baer, S.C. (1995) Phagocytosis by zippers and triggers. *Trends Cell Biol* **5**: 89–93.

Tan, C.M., Li, C.-H., Tsao, N.-W., Su, L.-W., Lu, Y.-T., Chang, S.H., *et al.* (2016) Phytoplasma SAP11 alters 3-isobutyl-2-methoxypyrazine biosynthesis in Nicotiana benthamiana by suppressing NbOMT1. *J Exp Bot* **67**: 4415–4425.

The Irpcm Phytoplasma/Spiroplasma Working Team-Phytoplasma Taxonomy Group, null (2004) "Candidatus Phytoplasma", a taxon for the wall-less, non-helical prokaryotes that colonize plant phloem and insects. *Int J Syst Evol Microbiol* **54**: 1243–1255.

Thurston, T.L.M., Wandel, M.P., Muhlinen, N. von, Foeglein, A., and Randow, F. (2012) Galectin 8 targets damaged vesicles for autophagy to defend cells against bacterial invasion. *Nature* **482**: 414–418.

Toruño, T.Y., Musić, M.S., Simi, S., Nicolaisen, M., and Hogenhout, S.A. (2010) Phytoplasma PMU1 exists as linear chromosomal and circular extrachromosomal elements and has enhanced expression in insect vectors compared with plant hosts. *Mol Microbiol* **77**: 1406–1415.

Trivellone, V., Ripamonti, M., Angelini, E., Filippin, L., Rossi, M., Marzachí, C., and Galetto, L. (2019) Evidence suggesting interactions between immunodominant membrane protein Imp of Flavescence dorée phytoplasma and protein extracts from distantly related insect species. *J Appl Microbiol* **127**: 1801–1813.

Tudi, M., Daniel Ruan, H., Wang, L., Lyu, J., Sadler, R., Connell, D., *et al.* (2021) Agriculture Development, Pesticide Application and Its Impact on the Environment. *Int J Environ Res Public Health* **18**: 1112.

Vandenborre, G., Smagghe, G., Ghesquière, B., Menschaert, G., Rao, R.N., Gevaert, K., and Damme, E.J.M.V. (2011) Diversity in Protein Glycosylation among Insect Species. *PLOS ONE* **6**: e16682.

Walsh, F.S., and Doherty, P. (1991) Glycosylphosphatidylinositol anchored recognition molecules thatfunction in axonal fasciculation, growth and guidance in the nervous system.Cell Biol Int Rep15:1151–1166.

Wang, H., Wu, K., Liu, Y., Wu, Y., and Wang, X. (2015) Integrative proteomics to understand the transmission mechanism of Barley yellow dwarf virus-GPV by its insect vector Rhopalosiphum padi. *Sci Rep* **5**: 10971.

Wang, N., Li, Y., Chen, W., Yang, H.Z., Zhang, P.H., and Wu, Y.F. (2018a) Identification of wheat blue dwarf phytoplasma effectors targeting plant proliferation and defence responses. *Plant Pathol* **67**: 603–609.

Wang, N., Yang, H., Yin, Z., Liu, W., Sun, L., and Wu, Y. (2018b) Phytoplasma effector SWP1 induces witches' broom symptom by destabilizing the TCP transcription factor BRANCHED1. *Mol Plant Pathol* **19**: 2623–2634.

Wei, W., and Zhao, Y. (2022) Phytoplasma Taxonomy: Nomenclature, Classification, and Identification. *Biology (Basel)* **11**: 1119.

Wei, W., Davis, R.E., Jomantiene, R., and Zhao, Y. (2008) Ancient, recurrent phage attacks and recombination shaped dynamic sequence-variable mosaics at the root of phytoplasma genome evolution. *Proc Natl Acad Sci* **105**: 11827–11832.

Weil, T., Ometto, L., Esteve-Codina, A., Gómez-Garrido, J., Oppedisano, T., Lotti, C., *et al.* (2020) Linking omics and ecology to dissect interactions between the apple proliferation phytoplasma and its psyllid vector Cacopsylla melanoneura. *Insect Biochem Mol Biol* **127**: 103474.

Weintraub, P.G., and Beanland, L. (2006) Insect Vectors of Phytoplasmas. *Annu Rev Entomol* **51**: 91–111.

Weintraub, P.G., and Wilson, M.R. (2009) Control of phytoplasma diseases and vectors. *Phytoplasmas Genomes Plant Hosts Vectors* 233–249.

Whitten, M.M.A., Facey, P.D., Del Sol, R., Fernández-Martínez, L.T., Evans, M.C., Mitchell, J.J., *et al.* (2016) Symbiont-mediated RNA interference in insects. *Proc Biol Sci* **283**: 20160042.

Yu, J., Wayadande, A.C., and Fletcher, J. (2000) Spiroplasma citri Surface Protein P89 Implicated in Adhesion to Cells of the Vector Circulifer tenellus. *Phytopathology®* **90**: 716–722.

Zhang, Y., Xu, L., Li, S., and Zhang, J. (2019) Bacteria-Mediated RNA Interference for Management of Plagiodera versicolora (Coleoptera: Chrysomelidae). *Insects* **10**: 415.

Zhu, Y.Y., Machleder, E.M., Chenchik, A., Li, R., and Siebert, P.D. (2001) Reverse transcriptase template switching: a SMART approach for full-length cDNA library construction. *BioTechniques* **30**: 892–897.

Annexes

Supplementary Table 1. Euva proteins that interact with VmpA-His_6 having TMHMM-predicted transmembrane segments and 'NxS/T' patterns. The proteins selected in this study are in bold and underlined in grey.

Band	TSA *Euscelidius variegatus* (NCBI)	Séquence (BLASTP)	Predicted transmembrane segments (TMHMM)	NxS/T
A	ORF03088356_GFTU01011649.1_00277_02130_f1	PREDICTED: Homalodisca vitripennis ATPase family AAA domain-containing protein 3A homolog	1	1
	ORF03862500_GFTU01015892.1_00313_02331_f1	transmembrane protein 214-B isoform X1 [Homalodisca vitripennis]	1	2
	ORF03578890_GFTU01014139.1_00115_01908_f1	calnexin-like [Homalodisca vitripennis]	1	2
	ORF03010044_GFTU01011408.1_00185_01996_f2	**protein cueball isoform X1 [Homalodisca vitripennis]**	**1**	**6**
	ORF03468514_GFTU01013357.1_00081_01916_f3	dolichyl-diphosphooligosaccharide--protein glycosyltransferase subunit 1 [Homalodisca vitripennis]	1	2
	ORF01460866_GFTU01005403.1_00284_02236_f2	uncharacterized protein LOC106664528 isoform X3 [Cimex lectularius]	1	3
	ORF03397146_GFTU01012809.1_00455_02434_f2	T-cell immunomodulatory protein isoform X4 [Homalodisca vitripennis]	2	5
	ORF02280746_GFTU01008614.1_00587_02362_f2	hypothethical protein Homalodisca vitripennis LOC124363104 isoform X2 and J6590_050414	1	4
	ORF01214079_GFTU01004399.1_00136_01779_f1	**lysosome membrane protein 2 [Homalodisca vitripennis]**	**2**	**6**
	ORF00500949_GFTU01001590.1_00286_02226_f1	polypeptide N-acetylgalactosaminyltransferase 1-like isoform X1 [Homalodisca vitripennis]	1	2
	ORF01424621_GFTU01005272.1_00244_01983_f1	plexin domain-containing protein 2-like isoform X1 [Homalodisca vitripennis]	1	8
	ORF01046095_GFTU01003760.1_00286_02106_f1	polypeptide N-acetylgalactosaminyltransferase 5 isoform X1 [Homalodisca vitripennis]	1	2
	ORF03532966_GFTU01013866.1_00112_01845_f1	golgin (Homalodisca vitripennis)	1	3
	ORF01840417_GFTU01006919.1_00002_01687_f2	hypothetical protein H. viripennis	10	2
	ORF00137267_GFTU01000459.1_00003_01973_f3	uncharacterized protein LOC124354663 isoform X1 [Homalodisca vitripennis]	1	3
	ORF00766636_GFTU01002643.1_00132_01904_f3	D-glucuronyl C5-epimerase [Homalodisca vitripennis]	1	3
	ORF01956414_GFTU01007342.1_00121_02085_f1	dolichyl-diphosphooligosaccharide--protein glycosyltransferase subunit 2 [Homalodisca vitripennis]	3	2
	ORF01252837_GFTU01004577.1_00244_02139_f1	N-acetylgalactosaminyltransferase 6-like isoform X1 [Homalodisca vitripennis]	1	2
	ORF03537334_GFTU01013894.1_00064_02025_f1	hypothetical protein J6590_074417 [Homalodisca vitripennis]	2	4
	ORF03590659_GFTU01014209.1_00312_02150_f3	neutral and basic amino acid transport protein rBAT-like [Homalodisca vitripennis]	1	9
	ORF03587765_GFTU01014197.1_00076_02181_f1	nicastrin isoform X1 [Homalodisca vitripennis]	1	11
B	ORF03693862_GFTU01014848.1_00369_01463_f3	heparan sulfate 2-O-sulfotransferase 1-like [Homalodisca vitripennis]	1	2
	ORF03657744_GFTU01014605.1_00086_01171_f2	prohibitin-2-like [Homalodisca vitripennis]	1	1
	ORF00313454_GFTU01000993.1_00057_01349_f3	GDP-fucose protein O-fucosyltransferase 1-like [Homalodisca vitripennis]	1	1
	ORF00775440_GFTU01002668.1_00113_01303_f2	glutaminyl-peptide cyclotransferase-like [Homalodisca vitripennis]	1	1
	ORF00582827_GFTU01001844.1_00001_01110_f1	basigin isoform X2 [Homalodisca vitripennis]	1	6
	ORF00738628_GFTU01002531.1_00152_01321_f2	dnaJ homolog subfamily B member 14 [Homalodisca vitripennis]	1	2
	ORF03486590_GFTU01013538.1_00143_01228_f2	innexin inx2 [Homalodisca vitripennis]	4	1
	ORF02385866_GFTU01009016.1_00139_01251_f1	acyl-CoA Delta-9 desaturase-like [Homalodisca vitripennis]	4	3
	ORF04030053_GFTU01016892.1_00210_01373_f3	cysteine-rich with EGF-like domain protein 2 [Homalodisca vitripennis]	2	2
	ORF01207302_GFTU01004379.1_00053_01219_f2	SLIT and NTRK-like protein 4 [Homalodisca vitripennis]	1	2
	ORF03273504_GFTU01012324.1_00179_01489_f2	protein catecholamines up-like [Homalodisca vitripennis]	6	1
	ORF04005737_GFTU01016727.1_00069_01361_f3	V-type proton ATPase subunit S1 [Homalodisca vitripennis]	1	4
	ORF02908881_GFTU01010984.1_00080_01198_f2	solute carrier family 35 member F6 [Homalodisca vitripennis]	10	1
	ORF03617956_GFTU01014363.1_00184_01326_f1	ceramide synthase 6 [Homalodisca vitripennis]	7	2
	ORF01236041_GFTU01004522.1_00348_01424_f3	galactosylgalactosylxylosylprotein 3-beta-glucuronosyltransferase I-like isoform X1 [Homalodisca vitripennis]	1	2
	ORF03436733_GFTU01013123.1_00289_01524_f1	peptidyl-prolyl cis-trans isomerase FKBP8 [Homalodisca vitripennis]	1	4
	ORF02798948_GFTU01010594.1_00261_01460_f3	acid phosphatase like	1	2
C	ORF01780037_GFTU01006645.1_00109_01017_f1	integral membrane protein 2B-like [Homalodisca vitripennis]	1	2
	ORF03212397_GFTU01012093.1_00208_01215_f1	vesicular integral-membrane protein VIP36-like [Homalodisca vitripennis]	1	2
	ORF01363517_GFTU01005045.1_00122_01018_f2	syntaxin isoform X3 [Frankliniella occidentalis]	1	3
	ORF02444589_GFTU01009226.1_00223_01083_f1	voltage-dependent anion channel [Recilia dorsalis]/putative mitochondrial porin [Homalodisca vitripennis]	18	4
	ORF03099463_GFTU01011702.1_00153_01151_f3	apolipoprotein D-like [Homalodisca vitripennis]	1	1
	ORF03885779_GFTU01016029.1_00130_00987_f1	Syntaxin [Homalodisca vitripennis]	1	1
	ORF00932050_GFTU01003335.1_00105_01109_f3	renin receptor [Homalodisca vitripennis] /ATPase H(+)-transporting accessory protein 2 [Homalodisca vitripennis]	1	2
	ORF01417067_GFTU01005233.1_00001_00918_f1	prohibitin [Acyrthosiphon pisum]	1	1
	ORF02696019_GFTU01010220.1_00149_01096_f2	protein AGAP004871-like isoform X3 [Schistocerca americana]	2	6
	ORF01807241_GFTU01006798.1_00091_00969_f1	DDRGK domain-containing protein 1, variant 2 [Homalodisca vitripennis]	1	1
	ORF00675649_GFTU01002260.1_00154_01077_f1	SWI/SNF and RSC complex subunit Ssr1 [Homalodisca vitripennis]	1	3

	ORF03414034_GFTU01012926.1_00456_01385_f3	N-acetylglucosaminyl-phosphatidylinositol de-N-acetylase-like isoform X1 [Homalodisca vitripennis]	1	3
	ORF03229291_GFTU01012148.1_00149_01072_f2	ribonuclease Oy [Homalodisca vitripennis]	1	5
	ORF01846268_GFTU01006941.1_00102_01085_f3	decorin [Homalodisca vitripennis]	1	4
D	ORF01649733_GFTU01006110.1_00059_00856_f2	type 1 phosphatidylinositol 4,5-bisphosphate 4-phosphatase isoform X1 [Homalodisca vitripennis]	2	1
	ORF01650080_GFTU01006112.1_00156_00785_f3	transmembrane emp24 domain-containing protein-like [Homalodisca vitripennis]	1	1
	ORF00042812_GFTU01000143.1_00091_00750_f1	TMEM9/TMEM9B (identification *via* interpro)	1	3
	ORF04071547_GFTU01017136.1_00109_00867_f1	vesicle-associated membrane protein/synaptobrevin-binding protein [Homalodisca vitripennis]	1	1
	ORF02665838_GFTU01010090.1_00258_00932_f3	dnaJ homolog subfamily C member 5 isoform X3 [Homalodisca vitripennis]	2	1
	ORF02665501_GFTU01010089.1_00258_00992_f3	dnaJ homolog subfamily C member 5 isoform X2 [Homalodisca vitripennis]	2	1
	ORF00874963_GFTU01003092.1_00327_01094_f3	signal recognition particle receptor subunit beta-like [Homalodisca vitripennis]	1	1
	ORF01219637_GFTU01004432.1_00220_00822_f1	translocon-associated protein subunit beta [Homalodisca vitripennis]	1	2
	ORF01521166_GFTU01005634.1_00017_00550_f2	STI1-like protein [Homalodisca vitripennis]	2	2
	ORF00820901_GFTU01002861.1_00114_00920_f3	aquaporin AQPAe.a isoform X2 [Homalodisca vitripennis]	6	1
	ORF00821078_GFTU01002862.1_00114_00908_f3	aquaporin AQPAe.a isoform X4 [Homalodisca vitripennis]	6	1
	ORF03776752_GFTU01015372.1_00129_00854_f3	syntaxin-8 [Homalodisca vitripennis]	1	1
	ORF03420291_GFTU01012977.1_00417_01208_f3	CD63 antigen [Nephotettix cincticeps]	4	4
	ORF03441112_GFTU01013144.1_00157_00810_f1	vesicle-trafficking protein SEC22b [Homalodisca vitripennis]	1	2
	ORF01794428_GFTU01006722.1_00175_00837_f1	transmembrane emp24 domain-containing protein 7 [Homalodisca vitripennis]	1	1
	ORF02060243_GFTU01007701.1_00290_01039_f2	vesicle transport protein USE1 isoform X1 [Homalodisca vitripennis]	1	2
E	ORF03557296_GFTU01013999.1_00232_00624_f1	uncharacterised proteins	4	2
F	ORF03591272_GFTU01014213.1_00151_03195_f1	calcium-transporting ATPase sarcoplasmic/endoplasmic reticulum type isoform X3 [Cimex lectularius]	10	5
	ORF02774007_GFTU01010510.1_00279_03419_f3	sodium/potassium-transporting ATPase subunit alpha isoform X1 [Homalodisca vitripennis]	10	5
	ORF01543048_GFTU01005721.1_00407_03304_f2	lysosomal alpha-glucosidase-like [Homalodisca vitripennis]	1	13
	ORF04029061_GFTU01016887.1_00003_02834_f3	aminopeptidase-like protein [Homalodisca vitripennis]	1	5
	ORF00672315_GFTU01002249.1_00136_03036_f1	fasciclin-2-like [Homalodisca vitripennis]	2	7
	ORF00224802_GFTU01000703.1_01002_04178_r3	uncharacterized protein LOC124364686 [Homalodisca vitripennis]	1	13
	ORF02806491_GFTU01010616.1_00518_03514_f2	lysosomal alpha-glucosidase-like [Homalodisca vitripennis]	1	14
	ORF00577827_GFTU01001820.1_00276_03056_f3	uncharacterized protein LOC111864751 isoform X1 [Cryptotermes secundus]	1	4
	ORF01146851_GFTU01004135.1_00123_02915_f3	ER membrane protein complex subunit 1 [Homalodisca vitripennis]	1	4
	ORF03898939_GFTU01016123.1_00223_03282_f1	**protein draper isoform X1 [Zootermopsis nevadensis]**	**1**	**11**
	ORF02093016_GFTU01007852.1_00001_02736_f1	**transforming growth factor-beta-induced protein ig-h3-like [Homalodisca vitripennis]**	**1**	**5**
	ORF00406425_GFTU01001302.1_00108_03002_f3	calcium-transporting ATPase type 2C member 1-like [Homalodisca vitripennis]	10	4
	ORF01573661_GFTU01005820.1_00001_03258_f1	NAD(P) transhydrogenase, mitochondrial-like isoform X1 [Homalodisca vitripennis]	14	7
G+H	ORF01500200_GFTU01005554.1_00297_02693_f3	PREDICTED: Homalodisca vitripennis neurotactin-like (LOC124361907), mRNA	1	8
	ORF03757228_GFTU01015247.1_00222_02681_f3	**Protein containing LRR domains (identification via interpro)**	**1**	**14**
	ORF03985247_GFTU01016611.1_00180_02645_f3	**integrin beta**	**1**	**7**
	ORF01543048_GFTU01005721.1_00407_03304_f2	lysosomal alpha-glucosidase-like [Homalodisca vitripennis]	1	15
	ORF03874906_GFTU01015965.1_00117_02747_f3	**sodium/calcium exchanger 3-like isoform X1 [Homalodisca vitripennis]**	**12**	**6**
	ORF03008926_GFTU01011402.1_00250_02643_f1	Gelsolin, cytoplasmic [Cryptotermes secundus]	1	2
	ORF02638676_GFTU01009977.1_00162_02546_f3	AFG3-like protein 2 [Homalodisca vitripennis]	2	3
	ORF01921174_GFTU01007221.1_00361_02811_f1	mannosyl-oligosaccharide glucosidase-like [Homalodisca vitripennis]	1	4
	ORF02093016_GFTU01007852.1_00001_02736_f1	**transforming growth factor-beta-induced protein ig-h3-like [Homalodisca vitripennis]**	**1**	**5**
	ORF01868234_GFTU01007015.1_00149_02551_f2	extended synaptotagmin-2 isoform X3 [Homalodisca vitripennis]	2	5
	ORF01146851_GFTU01004135.1_00123_02915_f3	ER membrane protein complex subunit 1 [Homalodisca vitripennis]	1	4
	ORF03639633_GFTU01014488.1_00117_02468_f3	**leucine-rich repeat-containing protein 15-like [Homalodisca vitripennis]**	**1**	**7**
	ORF02805699_GFTU01010613.1_00159_02690_f3	mitochondrial proton/calcium exchanger protein [Homalodisca vitripennis]	2	3
	ORF00406425_GFTU01001302.1_00108_03002_f3	calcium-transporting ATPase type 2C member 1-like [Homalodisca vitripennis]	10	4
I	ORF03655252_GFTU01014587.1_00207_01721_f3	tumor necrosis factor receptor superfamily member wengen [Anoplophora glabripennis]	1	2
	ORF01196773_GFTU01004342.1_00189_01889_f3	stromal interaction molecule homolog isoform X2 [Homalodisca vitripennis]	2	2
	ORF04114081_GFTU01017546.1_00249_02021_f3	N-acetylgalactosaminyltransferase 7 [Homalodisca vitripennis]	1	2
	ORF03358881_GFTU01012628.1_00448_01920_f1	protein croquemort-like isoform X1 [Homalodisca vitripennis]	2	8
	ORF03008216_GFTU01011397.1_00217_01842_f1	probable cytochrome P450 6d5 [Homalodisca vitripennis]	1	1
	ORF03185639_GFTU01012013.1_00219_01796_f3	putative fatty acyl-CoA reductase CG8306 isoform X1 [Homalodisca vitripennis]	2	2

	ORF01900380_GFTU01007128.1_00486_02108_f3	KAG8267176.1 hypothetical protein J6590_057015 [Homalodisca vitripennis]	2	3
	ORF03737405_GFTU01015141.1_00137_01597_f2	cytochrome P450 2C31-like isoform X1 [Homalodisca vitripennis]	1	3
	ORF03903967_GFTU01016147.1_00084_01781_f3	proton-coupled amino acid transporter-like protein pathetic isoform X3 [Halyomorpha halys]	11	7
	ORF00673844_GFTU01002254.1_00165_01679_f3	X-linked interleukin-1 receptor accessory protein-like 2 [Homalodisca vitripennis]	1	8
	ORF01527703_GFTU01005654.1_00096_01697_f3	heme binding [Homalodisca vitripennis]	1	6
	ORF01668027_GFTU01006187.1_00257_01861_f2	UDP-glycosyltransferase UGT4-like [Homalodisca vitripennis]	1	2
	ORF03712827_GFTU01014988.1_00517_02010_f1	Golgi integral membrane protein 4-like isoform X1 [Homalodisca vitripennis]	1	1
	ORF03444976_GFTU01013184.1_00146_01954_f2	zinc transporter foi-like isoform X2 [Homalodisca vitripennis]	6	7
	ORF01840417_GFTU01006919.1_00002_01687_f2	delta(14)-sterol reductase TM7SF2 [Homalodisca vitripennis]	10	2
	ORF03010044_GFTU01011408.1_00185_01996_f2	**protein cueball isoform X1 [Homalodisca vitripennis]**	**1**	**6**
	ORF02440449_GFTU01009199.1_00119_01927_f2	GPI transamidase component PIG-T-like [Homalodisca vitripennis]	2	8
	ORF01967244_GFTU01007378.1_00019_01656_f1	amyloid precursor protein metabolic process [Homalodisca vitripennis]	3	3
	ORF01126207_GFTU01004066.1_00444_02081_f3	glutathione hydrolase 7-like isoform X1 [Homalodisca vitripennis]	1	5
	ORF04139556_GFTU01017799.1_00052_01656_f1	chondroadherin-like [Homalodisca vitripennis]	1	4
	ORF01424621_GFTU01005272.1_00244_01983_f1	plexin domain-containing protein 2-like isoform X1 [Homalodisca vitripennis]	1	8
	ORF03532966_GFTU01013866.1_00112_01845_f1	golgin-84-like [Homalodisca vitripennis]	1	3
	ORF03433846_GFTU01013097.1_00226_01893_f1	nicalin-1-like [Homalodisca vitripennis]	1	3
	ORF00064229_GFTU01000227.1_00351_01874_f3	activin receptor type-2A [Nilaparvata lugens]	1	4
	ORF01224055_GFTU01004452.1_00050_01720_f2	G-protein coupled receptor Mth2-like isoform X2 [Homalodisca vitripennis]	8	6
	ORF04034680_GFTU01016922.1_00055_01536_f1	probable cytochrome P450 6a13 [Homalodisca vitripennis]	1	1
	ORF03339069_GFTU01012554.1_00002_01780_f2	activin receptor type-1 isoform X1 [Zootermopsis nevadensis]	1	3
	ORF02142225_GFTU01008058.1_00314_01939_f2	protein wntless [Homalodisca vitripennis]	8	5
	ORF01126404_GFTU01004067.1_00066_01775_f3	Homalodisca vitripennis probable cytochrome P450 6d5 (LOC124365725), mRNA	1	1
	ORF03729559_GFTU01015089.1_00480_02093_f3	insulin-like growth factor-binding protein complex acid labile subunit [Homalodisca vitripennis]	1	3
	ORF01214079_GFTU01004399.1_00136_01779_f1	**lysosome membrane protein 2 [Homalodisca vitripennis]**	**2**	**6**
	ORF03944081_GFTU01016384.1_00181_01875_f1	PREDICTED: Cryptotermes secundus protein ST7 homolog (LOC111871312), transcript variant X1, mRNA	3	2
	ORF00487573_GFTU01001542.1_00181_01770_f1	UDP-glycosyltransferase UGT5-like isoform X1 [Homalodisca vitripennis]	1	2
	ORF03578890_GFTU01014139.1_00115_01908_f1	PREDICTED: Homalodisca vitripennis calnexin-like (LOC124358330), mRNA	1	2
	ORF02735221_GFTU01010376.1_00120_01757_f3	probable cytochrome P450 6a14 [Homalodisca vitripennis]	1	4
	ORF00707446_GFTU01002392.1_00094_01698_f1	UDP-glycosyltransferase UGT5 isoform X3 [Nilaparvata lugens]	1	4
	ORF00954693_GFTU01003435.1_00111_01808_f3	protein spinster isoform X2 [Homalodisca vitripennis]	12	4
	ORF00831169_GFTU01002905.1_00011_01504_f2	UDP-GalNAc:beta-1,3-N-acetylgalactosaminyltransferase 2-like isoform X1 [Homalodisca vitripennis]	1	5
	ORF00852307_GFTU01002995.1_00138_01805_f3	putative fatty acyl-CoA reductase CG5065 [Homalodisca vitripennis]	1	2
	ORF02295880_GFTU01008690.1_00240_02024_f3	melanocyte protein PMEL isoform X1 [Homalodisca vitripennis]	1	13
	ORF01632836_GFTU01006031.1_00129_01964_f3	PREDICTED: Homalodisca vitripennis facilitated trehalose transporter Tret1-2 homolog (LOC124354290), mRNA	12	1
	ORF02260132_GFTU01008545.1_00206_01705_f2	uncharacterized protein LOC124364991 isoform X1 [Homalodisca vitripennis]	1	7
	ORF00875556_GFTU01003096.1_00337_01950_f1	cleft lip and palate transmembrane protein 1-like protein [Nilaparvata lugens]	8	2
	ORF02363633_GFTU01008940.1_00356_01870_f2	major facilitator superfamily domain-containing protein 1-like [Homalodisca vitripennis]	12	6
	ORF02945676_GFTU01011139.1_00265_01836_f1	equilibrative nucleoside transporter 1 [Homalodisca vitripennis]	11	3
	ORF00772888_GFTU01002658.1_00178_01728_f1	PREDICTED: Bemisia tabaci protein halfway (LOC109035584), mRNA	1	8
	ORF03488356_GFTU01013548.1_00103_01815_f1	protein GPR107 [Homalodisca vitripennis]	7	3
	ORF00935122_GFTU01003349.1_00078_01886_f3	protein Malvolio-like isoform X5 [Homalodisca vitripennis]	12	3
	ORF03297927_GFTU01012417.1_00170_01831_f2	PREDICTED: Homalodisca vitripennis probable cytochrome P450 6a14 (LOC124355178), mRNA	1	1
	ORF02444245_GFTU01009225.1_00180_01838_f3	protein brambleberry-like [Homalodisca vitripennis]	3	3
	ORF01995855_GFTU01007457.1_00195_01676_f3	diacylglycerol O-acyltransferase 1 isoform X1 [Nilaparvata lugens]	9	1
	ORF03999079_GFTU01016699.1_00001_01743_f1	monocarboxylate transporter 13 isoform X1 [Homalodisca vitripennis]	12	8
	ORF00296300_GFTU01000932.1_00179_01981_f2	organic cation transporter protein isoform X1 [Homalodisca vitripennis]	12	5
	ORF03881511_GFTU01016002.1_00246_01973_f3	tyrosine-protein kinase Dnt [Homalodisca vitripennis]	1	6
J	ORF04005737_GFTU01016727.1_00069_01361_f3	V-type proton ATPase subunit S1 [Homalodisca vitripennis]	1	4
	ORF03540683_GFTU01013912.1_00212_01462_f2	endoplasmic reticulum junction formation protein lunapark-B isoform X5 [Homalodisca vitripennis]	2	1
	ORF02853024_GFTU01010796.1_00067_01248_f1	translocation protein SEC62 [Homalodisca vitripennis]	2	1
	ORF00057085_GFTU01000202.1_00329_01771_f2	calcium-binding mitochondrial carrier protein SCaMC-2 isoform X1 [Homalodisca vitripennis]	2	3
	ORF03087292_GFTU01011645.1_00253_01608_f1	uncharacterized protein LOC124354859 [Homalodisca vitripennis]	1	2

ORF03436733_GFTU01013123.1_00289_01524_f1	Homalodisca vitripennis peptidyl-prolyl cis-trans isomerase FKBP8	1	4
ORF02125708_GFTU01007996.1_00254_01681_f2	serine palmitoyltransferase 1 [Homalodisca vitripennis]	1	2
ORF03470760_GFTU01013384.1_00142_01362_f1	acyl-CoA-binding domain-containing protein 4 [Homalodisca vitripennis]	1	3
ORF00490218_GFTU01001550.1_00162_01538_f3	fasciclin-3 [Halyomorpha halys]	1	4
ORF03518135_GFTU01013773.1_00156_01433_f3	protein disulfide-isomerase TMX3 [Homalodisca vitripennis]	1	3
ORF02184618_GFTU01008239.1_00219_01595_f3	alpha-1,3-mannosyl-glycoprotein 2-beta-N-acetylglucosaminyltransferase-like [Homalodisca vitripennis]	1	2
ORF00202071_GFTU01000624.1_00003_01334_f3	heparan-sulfate 6-O-sulfotransferase 1 [Homalodisca vitripennis]	1	2
ORF03486590_GFTU01013538.1_00143_01228_f2	innexin inx2 [Homalodisca vitripennis]	4	1
ORF00582827_GFTU01001844.1_00001_01110_f1	basigin isoform X2 [Homalodisca vitripennis]	1	6
ORF01513979_GFTU01005613.1_00316_01674_f1	prostatic acid phosphatase-like isoform X3 [Homalodisca vitripennis]	1	5
ORF03657744_GFTU01014605.1_00086_01171_f2	prohibitin-2-like [Homalodisca vitripennis]	1	1
ORF01076354_GFTU01003873.1_00500_01660_f2	no identification even with interpro uncharacterized protein LOC124366327 [Homalodisca vitripennis]	1	4
ORF03384640_GFTU01012731.1_00475_01770_f1	beta-1,4-glucuronyltransferase 1-like [Homalodisca vitripennis]	1	1
ORF02660245_GFTU01010066.1_00198_01325_f3	glycoprotein-N-acetylgalactosamine 3-beta-galactosyltransferase 1-like [Homalodisca vitripennis]	1	2
ORF02385866_GFTU01009016.1_00139_01251_f1	acyl-CoA Delta-9 desaturase-like [Homalodisca vitripennis]	4	3
ORF03511067_GFTU01013724.1_00051_01310_f3	uncharacterized protein LOC124365941 [Homalodisca vitripennis]	1	5
ORF03871669_GFTU01015944.1_00414_01907_f3	facilitated trehalose transporter Tret1-like isoform X1 [Homalodisca vitripennis]	12	1
ORF00914527_GFTU01003269.1_00241_01365_f1	lactosylceramide 4-alpha-galactosyltransferase isoform X2 [Nilaparvata lugens]	1	3
ORF00748024_GFTU01002569.1_00005_01330_f2	minor histocompatibility antigen H13 isoform X2 [Homalodisca vitripennis]	9	3
ORF03178020_GFTU01011979.1_00333_01703_f3	transducin beta-like protein 2 [Homalodisca vitripennis]	1	1
ORF01842823_GFTU01006929.1_00321_01577_f3	soluble calcium-activated nucleotidase 1 [Homalodisca vitripennis]	1	2
ORF00936187_GFTU01003353.1_00246_01613_f3	sorting and assembly machinery component 50 homolog B [Homalodisca vitripennis]	16	3
ORF03666283_GFTU01014673.1_00036_01256_f3	cuticlin-4 [Homalodisca vitripennis]	1	2
ORF00120350_GFTU01000411.1_00625_02058_f1	zinc transporter 2 [Homalodisca vitripennis]	6	3
ORF03680891_GFTU01014752.1_00164_01375_f2	PREDICTED: Homalodisca vitripennis translocating chain-associated membrane protein 1	8	3
ORF03283506_GFTU01012354.1_00299_01654_f2	cystinosin homolog isoform X2 [Nilaparvata lugens]	7	3
ORF03510638_GFTU01013721.1_00044_01216_f2	growth hormone-inducible transmembrane protein-like [Homalodisca vitripennis]	9	1
ORF02861965_GFTU01010826.1_00151_01230_f1	cell cycle control protein 50A isoform X4 [Homalodisca vitripennis]	2	3
ORF02908881_GFTU01010984.1_00080_01198_f2	solute carrier family 35 member F6 [Homalodisca vitripennis]	10	1
ORF01227052_GFTU01004467.1_00235_01416_f1	PREDICTED: Homalodisca vitripennis lysophosphatidylserine lipase ABHD12-like (LOC124364729), transcript variant X2, mRNA	1	4
ORF01543686_GFTU01005723.1_00001_01446_f1	prolactin regulatory element-binding protein [Homalodisca vitripennis]	1	3
ORF00624853_GFTU01002044.1_00310_01548_f1	glycosylated lysosomal membrane protein-like [Homalodisca vitripennis]	1	11
ORF01384059_GFTU01005117.1_00356_01645_f2	zinc/cadmium resistance protein [Homalodisca vitripennis]	6	1
ORF00775000_GFTU01002666.1_00231_01415_f3	PREDICTED: innexin inx3 [Bemisia tabaci]	4	1
ORF01046563_GFTU01003761.1_00147_01544_f3	protein odr-4 homolog [Homalodisca vitripennis]	1	3
ORF03273504_GFTU01012324.1_00179_01489_f2	protein catecholamines up-like [Homalodisca vitripennis]	6	1
ORF01678053_GFTU01006215.1_00001_01314_f1	ER lumen protein-retaining receptor [Homalodisca vitripennis]	6	3
ORF01929554_GFTU01007246.1_00125_01513_f2	UNC93-like protein MFSD11 isoform X1 [Homalodisca vitripennis]	12	3
ORF03110745_GFTU01011746.1_00300_01667_f3	uncharacterized protein LOC124357838 [Homalodisca vitripennis]	1	6
ORF03791453_GFTU01015463.1_00172_01353_f1	endoplasmic reticulum-Golgi intermediate compartment protein 3-like isoform X1 [Homalodisca vitripennis]	2	4
ORF02798948_GFTU01010594.1_00261_01460_f3	PREDICTED: Homalodisca vitripennis prostatic acid phosphatase-like (LOC124371213), mRNA	1	2
ORF02848509_GFTU01010777.1_00460_01722_f1	PREDICTED: Homalodisca vitripennis endoplasmic reticulum-Golgi intermediate compartment protein 2 (LOC124364981), mRNA	2	1
ORF03748447_GFTU01015190.1_00026_01183_f2	fat storage-inducing transmembrane protein 2 [Homalodisca vitripennis]	6	1
ORF03509806_GFTU01013713.1_00318_01721_f3	UNC93-like protein MFSD11 [Homalodisca vitripennis]	12	1
ORF01844038_GFTU01006936.1_00254_01579_f2	PREDICTED: Homalodisca vitripennis transmembrane protein 268-like (LOC124364903), mRNA	2	3
ORF03617956_GFTU01014363.1_00184_01326_f1	ceramide synthase 6 [Homalodisca vitripennis]	7	2
ORF00560024_GFTU01001746.1_00401_01750_f2	**uncharacterized protein LOC124356975 [Homalodisca vitripennis]**	**1**	**2**
ORF03616652_GFTU01014357.1_00277_01377_f1	protein YIF1B [Nilaparvata lugens]	5	2
ORF00941208_GFTU01003375.1_00255_01664_f3	glycosaminoglycan xylosylkinase [Homalodisca vitripennis]	1	4
ORF00715920_GFTU01002430.1_00333_01784_f3	PREDICTED: Homalodisca vitripennis acidic mammalian chitinase-like (LOC124362433), transcript variant X1, mRNA	1	6

Abstract for the **XXIII Biennial Congress of the International Organisation for Mycoplasmology**

"First steps towards the identification of potential receptors to flavescence dorée phytoplasmas VmpA in the experimental leafhopper vector *Euscelidius variegatus*"

Francesca Canuto, Sybille Duret, Marie-Pierre Dubrana-Ourabah, Christophe Garcion, Nathalie Arricau-Bouvery and Xavier Foissac

Université de Bordeaux, INRAE, UMR 1332 de Biologie du Fruit et Pathologie, Villenave d'Ornon, France

Background – Phytoplasmas need to adhere to the surface of insect cells, penetrate the cells and go through in order to complete their compulsory multiplicative and circulative cycle into their vectoring insects. Current evidence indicates that the Variable Membrane Protein A (VmpA) of Flavescence dorée phytoplasma mediates the attachment to the surface of competent leafhopper cells. As insect cell surface are heavily glycosylated, we tested and showed that VmpA adhesin interacts with glycoproteins of *Euscelidius variegatus* like a lectin. Our aim was to identify VmpA targets. **Methods** – Recombinant VmpA-His_6 proteins were fixed to a Nickel affinity column. Proteins extracted from *E. variegatus* cultured cells (Euva cells) were then delivered to both the VmpA-Ni column and a protein-less Ni column as a control. Retained protein complexes were eluted and characterized by mass spectrometry. Peptide profiles were compared to the *in silico* proteome translated from *E. variegatus* transcriptome and to the Swiss-Prot database. **Results** – Peptides matching 239 putative *E. variegatus* proteins had a specific retention ratio above 90%. Among these, 26 proteins shared known cellular functions such as vesicular trafficking systems. **Conclusion** – Our results may lead to the identification of molecular interaction events promoted by VmpA.

Keywords – Flavescence dorée phytoplasma, variable membrane protein A, adhesion, insect vector, vesicular trafficking.

Phytopathogenic Mollicutes
Vol. 13 (1), June 2023,

doi:

Interaction

Identification of a "flavescence dorée" phytoplasma VmpA candidate receptor in the experimental insect vector *Euscelidius variegatus*

Francesca Canuto[1], Nathalie Arricau-Bouvery[1], Sybille Duret[1], Marie-Pierre Dubrana[1], Laure Beven[1], Christophe Garcion[1], Lysiane Brocard[2], Stéphane Claverol[3], Sylvie Malembic-Maher[1] and Xavier Foissac[1]

[1]University of Bordeaux, INRAE, Biologie du Fruit et Pathologie, UMR 1332, Villenave d'Ornon, France
[2]University of Bordeaux, CNRS, INSERM, Bordeaux Imaging Center, BIC, UAR 3420, US 4, Villenave d'Ornon, France
[3]Plateforme Protéome, University of Bordeaux, Bordeaux, France

Abstract

The "flavescence dorée" phytoplasma initiates the infection process using the adhesin VmpA to adhere to insect vector cells although the insect receptor for this protein still remains unknown. *In vitro* interaction assays were performed using recombinant VmpA-His_6 and cultured cells of the experimental vector *Euscelidius variegatus*. It was possible to identify thirteen interesting putative VmpA targets that have been tested for their role as VmpA receptors in cultured cells subjected to RNAi. These preliminary results show the implication of an unidentified protein containing several leucine-rich repeat domains in the adhesion of beads coated with recombinant VmpA to vector cells in culture.

Keywords: adhesion, insect cells, ''flavescence dorée'' phytoplasmas, *Euscelidius variegatus*

Introduction

"Flavescence dorée" (FD) phytoplasmas are transmitted from grapevine to grapevine in vineyards by the leafhopper *Scaphoideus titanus*, but the model system consisting of broad bean and the leafhopper *Euscelidius variegatus* results more convenient for studying this pathosystem in controlled conditions (Caudwell *et al.*, 1972). Phytoplasmas need to adhere to the surface of insect cells, penetrate the cells and go through in order to complete the multiplicative and circulative cycle into their vectoring insects. For the FD phytoplasma, variable membrane protein A (VmpA) was shown to be an adhesin that binds glycoconjugates at the surface of the insect cells (Arricau-Bouvery *et al.*, 2021). Furthermore, ecological and genetic insights into the emergence of the grapevine FD epidemics in Europe have shown that compatibility of FD phytoplasma strains with different subfamilies of insect vectors is correlated with *vmpA* gene sequence (Malembic-Maher *et al.*, 2020). Identifying the receptor for VmpA in the insect vector could not only improve the basic knowledge of the early stages of infection but can also help as a tool for the prediction of new potential emergent vector species. This study focus on the research and the screening for VmpA putative targets, using an *in cellula* model consisting in *E. variegatus* cultured cells.

Materials and Methods

Protein extracted from the *E. variegatus* cultured cells Euva11 using RX buffer (Suzuki *et al.*, 2006) have been incubated overnight with recombinant protein VmpA-His_6 of the FD phytoplasma strain FD92. The VmpA-Euva11 proteins complexes have been then purified on an affinity Nickel column and the fractions containing the retained proteins have been sent to proteomics platform of the University of Bordeaux (France) for mass spectrometry analysis. A database consisting in *in silico* translated transcriptome of *E. variegatus* has been used as reference for peptides identification. The matching putative proteins were screened basing on their VmpA specific retention ratio, the prediction of potential N-glycosylation sites in their sequence (NxS/T) as well as the presence of transmembrane domains (TMHMM 2.0). To increase the number of membrane proteins identified by MS analysis another experiment on protein extracts from Euva cells has been performed. It implemented the RX buffer with DOC and with an increased concentration of Triton X-100 (RX-T-DOC). A far western blot anti VmpA has been performed on these samples and the interesting bands have been excised on the corresponding Coomassie gel and sent to the proteomics platform for mass spectrometry analysis.

Corresponding author e-mail: Francesca Canuto (francesca.canuto@inrae.fr)

A selection of putative VmpA targets followed as described previously.

RNA interference experiments have been performed on Euva11 using double strand RNA (dsRNA) of about 500 bp for each putative target and a transfection reagent. dsRNA of the GFP sequence has been used as a control. Ratio of transcripts inhibition has been assessed using RT-qPCR and normalised using the insect reference gene glutathione S-transferase (GST). Adhesion assays on inhibited Euva11 cells have been performed incubating the cells three days post transfection with amine-modified fluorescent beads coated with recombinant VmpA-His_6 for one hour. Twenty fields were randomly observed per condition using a Zeiss AxioImager epifluorescent microscope. The ratio of retained beads per cell has been then calculated and compared to the control condition (Kruskal-Wallis test, p-value 0,05).

Results

The selection process of Euva11 proteins extracted with RX buffer and interacting with VmpA resulted in the identification of four candidates identified through BLASTn as endoplasmin, Epidermal Growth Factor Receptor, Tumor Necrosis Factor wengen and ubiquitin E3 ligase HERC4 –like. Nine putative candidates from Euva11 proteins extracted with RX-T-DOC buffer and interacting with VmpA were identified through BLASTn as unidentified protein 1 with LRR domains, unidentified protein 2 Toll-like receptor like, unidentified protein 3, integrin β, draper, scavenger receptor class B CD36, fasciclin, Na/Ca exchanger, and cueball LDL like protein. The inhibition of the target transcripts in *E. variegatus* cultured cells trough RNAi has been achieved, with variable efficacy depending on the target (fold change values in gene expression ranging from 2 to 80 times). Adhesion assays were performed using fluorescent VmpA-His_6-coated beads on dsRNA treated Euva11 cells targeting each of the 13 selected genes. Statistically significant differences have been observed between the number of beads adhering to Euva11 cells treated with dsRNA targeting the gene coding for the unidentified protein 1 with LRR domains when compared to control cells treated with dsRNA targeting green fluorescent protein (GFP).

Discussion

These results show that the unidentified protein 1 probably interacts with VmpA allowing adhesion of coated beads to *E. variegatus* cultured cells. This protein is predicted to be a transmembrane protein exposed to the surface of the cell and anchored in the plasma membrane by a transmembrane portion of 22 amino acids in its C-term part. An homology search (Interpro) has revealed the presence of four LRR domains of 219, 163, 80 and 146 aa (from N-ter to C-ter sequence). Furthermore, structural prediction (Robetta, BakerLab) revealed a horseshoe-shaped molecule consisting of parallel β-strands on the inner (concave) side and helical elements on the outer (convex) sites. Proteins with such a structure are frequently implicated in protein-protein interaction (Kobe and Kajava, 2001) and LRR domains are evolutionarily conserved in many pattern recognition receptors. Several studies have shown how LRR-only proteins are implicated in the binding with pathogen associated molecular patterns (PAMPs), which supports the obtained data suggesting that the unidentified protein 1 can act as a receptor for VmpA, and in the regulation of immune effectors (Zhang *et al.*, 2022; Wang *et al.*, 2016a, 2016; Sriphaijit *et al.*, 2007). Nevertheless, these results show only a partial inhibition of beads adhesion and a simultaneously inhibition of several *E. variegatus* LRR proteins could be interesting to investigate the possible redundancy of VmpA receptors in insect vector cells.

References

Arricau-Bouvery N, Duret S, Dubrana M-P, Desqué D, Eveillard S, Brocard L, Malembic-Maher S and Foissac X 2021. Interactions between the "flavescence dorée" phytoplasma and its insect vector indicate lectin-type adhesion mediated by the adhesin VmpA. *Scientific Reports*, 11: 11222.

Caudwell A, Kuszala C, Larrue J and Bachelier J, 1972. Transmission de la flavescence dorée de la fève à la fève par des cicadelles des genres *Euscelis* et *Euscelidius*. *Annales de Phytopathologie*, HS: 181–189.

Kobe B and Kajava AV, 2001. The leucine-rich repeat as a protein recognition motif. *Current Opinion in Structural Biology*, 11(6): 725-732.

Malembic-Maher S, Desqué D, Khalil D, Salar P, Bergey B, Danet J-L, Duret S, Dubrana-Ourabah M-P, Beven L, Ember I, Acs Z, Della Bartola M, Materazzi A, Filippin L, Krnjajic S, Krstic O, Tosevski I, Lang F, Jarausch B, Kölber M, Jovic J, Angelini E, Arricau-Bouvery N, Maixner M and Foissac X 2020. When a Palearctic bacterium meets a Nearctic insect vector: genetic and ecological insights into the emergence of the grapevine "flavescence dorée" epidemics in Europe. *Plos Pathogens*, 16: e1007967.

Sriphaijit T and Senapin S 2007. High expression of a novel leucine-rich repeat protein in hemocytes and the lymphoid organ of the black tiger shrimp *Penaeus monodon*. *Fish Shellfish Immunology*, 22(3): 264-271.

Suzuki, S, Oshima K, Kakizawa S, Arashida R, Jung H-Y, Yamaji Y, Nishigawa H, Ugaki M and Namba S 2006. Interaction between the membrane protein of a pathogen and insect microfilament complex determines insect-vector specificity. *Proceedings of National Academy of Sciences, USA*, 103: 4252–4257.

Wang M, Wang L, Guo Y, Yi Q, Song L 2016. An LRR-only protein representing a new type of pattern recognition receptor in *Chlamys farreri*. *Developmental and Comparative Immunology*, 54(1):145-55.

Wang M, Wang L, Xin L, Wang X, Wang L, Xu J, Jia Z, Yue F, Wang H and Song L 2016. Two novel LRR-only proteins in *Chlamys farreri:* similar in structure, yet different in expression profile and pattern recognition. *Developmental and Comparative Immunology*, 59: 99-109.

Zhang A, Liu Y, Guo N, Li S and Li F 2022. Two LRR-only proteins involved in antibacterial defense and prophenoloxidase system of swimming cram *Portunus trituberculatus*. *Frontiers in Marine Sciences*, 9: 946182.

frontiers | Frontiers in Cellular and Infection Microbiology

TYPE Original Research
PUBLISHED 06 November 2023
DOI 10.3389/fcimb.2023.1289100

OPEN ACCESS

EDITED BY
Luís Jaime Mota,
NOVA School of Science and Technology, Portugal

REVIEWED BY
Luciana Galetto,
Istituto per la Protezione Sostenibile delle Piante, Italy
Rita Musetti,
University of Padua, Italy

*CORRESPONDENCE
Francesca Canuto
francesca.canuto@inrae.fr

RECEIVED 05 September 2023
ACCEPTED 16 October 2023
PUBLISHED 06 November 2023

CITATION
Canuto F, Duret S, Dubrana M-P, Claverol S, Malembic-Maher S, Foissac X and Arricau-Bouvery N (2023) A knockdown gene approach identifies an insect vector membrane protein with leucin-rich repeats as one of the receptors for the VmpA adhesin of flavescence dore´ e phytoplasma. *Front. Cell. Infect. Microbiol.* 13:1289100. doi: 10.3389/fcimb.2023.1289100

A knockdown gene approach identifies an insect vector membrane protein with leucin-rich repeats as one of the receptors for the VmpA adhesin of flavescence dorée phytoplasma

Francesca Canuto[1]*, Sybille Duret[1], Marie-Pierre Dubrana[1], Ste´ phane Claverol[2], Sylvie Malembic-Maher[1], Xavier Foissac[1] and Nathalie Arricau-Bouvery[1]

[1]Univ. Bordeaux, INRAE, Biologie du Fruit et Pathologie, UMR 1332, Villenave d'Ornon, France, [2]Univ. Bordeaux, Bordeaux Proteome, Bordeaux, France

Introduction: The adhesion of flavescence dorée phytoplasma to the midgut epithelium cells of their insect vectors is partially mediated by the variable membrane protein A (VmpA), an adhesin which shows lectin properties. In order to identify the insect receptor for VmpA, we identified *Euscelidius variegatus* cell proteins interacting with recombinant VmpA-His_6.

Methods: The *E. variegatus* proteins were identified by mass spectrometry analysis of VmpA-*E. variegatus* protein complexes formed upon *in vitro* interaction assays. To assess their impact in VmpA binding, we reduced the expression of the candidate genes on *E. variegatus* cells in culture by dsRNA-mediated RNAi. The effect of candidate gene knockdown on VmpA binding was measured by the capacity of *E. variegatus* cells to bind VmpA-coated fluorescent beads.

Results and discussion: There were 13 candidate proteins possessing potential N-glycosylation sites and predicted transmembrane domains selected. The decrease of expression of an unknown transmembrane protein with leucine-rich repeat domains (uk1_LRR) was correlated with the decreased adhesion of VmpA beads to *E. variegatus* cells. The uk1_LRR was more expressed in digestive tubes than salivary glands of *E. variegatus*. The protein uk1_LRR could be implicated in the binding with VmpA in the early stages of insect infection following phytoplasmas ingestion

KEYWORDS

Euscelidius variegatus, phytoplasma, protein-protein interaction, LRR proteins, VmpA, RNAi

1 Introduction

Phytoplasmas are cell wall-less bacteria characterized by their ability to colonize two hosts belonging to two different kingdoms, their plants host and their insect vector (Lee et al., 2000; Gross et al., 2022). Phytoplasmas are responsible for severe diseases in a large number of cultivated and ornamental plants and are transmitted by leafhoppers, planthoppers, and psyllids (Weintraub and Beanland, 2006). The control of phytoplasma-associated diseases relies on prophylactic measures based on disease surveillance, elimination of infected plants in both production fields and nurseries, and insecticide treatments against the vector insects when recommended (Weintraub and Wilson, 2009; Jeger et al., 2016; Oliveira et al., 2019; European Food Safety Authority (EFSA) et al., 2020). Phytoplasmas perform a persistent propagative cycle into their insect vectors where they must invade and cross two main barriers, the midgut epithelium and salivary gland cells (Maillet and Gouranton, 1971). Thus, after their ingestion with infected sap, adhesion of phytoplasmas to the apical surface of vector intestinal cells constitutes an initial and critical step in insect invasion. Once this first barrier is crossed, the adhesion of phytoplasmas to salivary gland cells is as well critical for transmission to the plant achieved upon injection of infected saliva. A given phytoplasma has one or few insect vectors depending on the level of specificity of the interaction. Insights into the ecology and populations genetic of the flavescence dorée phytoplasmas (FDp) have revealed the correlation between vector specificity of phytoplasma strains and positively selected variant sequences of phytoplasma variable membrane proteins VmpA and VmpB (Malembic-Maher et al., 2020). It is now known that VmpA is acting as an adhesin that specifically interacts with glycoconjugates at the surface of insect vector cells (Arricau-Bouvery et al., 2018; Arricau-Bouvery et al., 2021). VmpA receptors on the surface of host cells are essential for phytoplasma colonization of insect cells, and variation in insect glycoproteins might be responsible for insect vector specificity. Once attached to insect cells, FD phytoplasmas enter cells by clathrin-mediated endocytosis, a process important for colonization of its insect vector (Arricau-Bouvery et al., 2023). Identifying VmpA receptors could provide new insight in the mechanism of entry of the FD phytoplasma into insect cells. Moreover, in a context of pesticide reduction, this knowledge could help in developing new strategies of disease control by blocking the phytoplasma–insect cell interaction as it could be achieved for the phloem-sap pest "*Candidatus* Liberibacter asiaticus" (Merfa et al., 2022; Guo et al., 2023).

Reducing the expression of VmpA receptors in the leafhopper cells in culture should be correlated with a decrease in their ability to bind VmpA. Knockdown gene expression is a powerful tool to elucidate gene function and can be achieved by long double-stranded RNA (dsRNA) introduced into the organism or the cells (Baum et al., 2007; Mondal et al., 2020). In RNA interference (RNAi), the long dsRNAs are processed in small interfering RNAs (siRNAs) that trigger degradation of the complementary target mRNA. RNAi in mammal cells is performed using siRNA, whereas in insects it is generally performed using long double-stranded RNA (Jackson et al., 2003). This approach had been used for instance to inactivate genes in several *Drosophila* cells in culture (Clemens et al., 2000; Echeverri and Perrimon, 2006). RNAi was also used with success in leafhoppers and whiteflies *via* injection or ingestion of dsRNAs (Abbà et al., 2019; Jain et al., 2022).

The objective of this study was to design a strategy to identify VmpA receptors. We first identified by mass spectrometry proteins present at the surface of *Euscelidius variegatus* cell line Euva-11 that potentially interact with the adhesin VmpA by purification on affinity column and far-western blot assays. Once these receptor candidates were identified, we intended to screen the candidates by measuring the effect of a decrease of their expression by *E. variegatus* cells in culture on their ability to bind VmpA-coated latex beads. We optimized RNAi to knockdown simultaneously up to 13 genes coding these candidates in the *E. variegatus* cell line Euva-11.

2 Materials and methods

2.1 Insect rearing, cell lines, and phytoplasma isolate

Healthy *E. variegatus* leafhoppers were originally collected in Villenave d'Ornon, France. They were reared in cages on broad beans *Vicia faba* var. aquadulce and oats *Avena sativa* from seeds purchased from Castros Gerand and Jardiland, respectively, at 25°C in a greenhouse under a 16-h light/8-h dark photoperiod. To obtain infected *E. variegatus*, L4–L5 nymphs were transferred by groups of 100 on FDp-infected broad bean for phytoplasma acquisition. Seven days later, *E. variegatus* were placed in cages on healthy broad bean for a latency period of 3–4 weeks. This study complies with relevant institutional, national, and international guidelines and legislation.

The *E. variegatus* Euva-11 cell line was established from embryos of *E. variegatus* (Arricau-Bouvery et al., 2018). In brief, the eggs were sterilized with bleach solution and then with 70% ethanol. After rinsing, the eggs were ground in culture medium made of 350 mL Schneider's Drosophila medium (Invitrogen), 100 mL Grace's insect cell culture medium (Invitrogen), 50 mL heat-inactivated fetal bovine serum (Eurobio), and 2 mL G-5 supplement (Invitrogen). The Euva-11 cells were cultivated at 25°C. After the first colonies developed and the cell line was established, the cells were passed using trypsinization every week with an additional change in modified culture medium made of 350 mL Schneider's Drosophila medium, 100 mL Grace's insect cell culture medium, and 50 mL heat-inactivated fetal bovine serum during the week.

The phytoplasma strain FD92 was originally transmitted to broad bean by infected *Scaphoideus titanus* sampled in FD-diseased vineyards in southwest France (Caudwell et al., 1970; Angelini et al., 2001). FDp was then continuously maintained in broad beans by *E. variegatus* transmission according to a published protocol (Caudwell et al., 1972).

2.2 Identification of candidate insect proteins

2.2.1 Purification of VmpA–*E. variegatus* protein complexes on affinity column

Three 75-cm² flasks of *E. variegatus* Euva cells were trypsinized. The cellular pellet obtained from 54 mL of culture was washed once with PBS 1× and then resuspended in 100 µL in Rx buffer [0.1% Triton X-100, 100 mM KCl, 3 mM NaCl, 3.5 mM $MgCl_2$, 1.25 mM EGTA, 10 mM Hepes, pH 7.3 (Suzuki et al., 2006; Galetto et al., 2011)]. The sample was vortexed, incubated at room temperature for 5 min, and centrifuged for 3 min at 14,000 g. The supernatant of Euva proteins was then recovered, and the concentration of proteins was measured using the Bradford assay (Bio-Rad). Resuspended proteins (1.3 mg) were incubated overnight at 4°C with 1 mg of the recombinant protein VmpA-His_6 of the FD92 phytoplasma (see Section 2.5) and protease inhibitor cocktail (Sigma-Aldrich). Then, the mixture was purified on an affinity nickel column using the ÄKTA™ system (GE Healthcare, US). As a negative control, a purification on the affinity nickel column was performed using 1.3 mg of Euva cell supernatant proteins in the absence of VmpA.

2.2.2 Protein separation by SDS-PAGE electrophoresis and far-western blot analysis

The pellet of trypsinized Euva cells resulting from the extraction with Rx buffer described previously was resuspended in Rx-T-DOC buffer (1% Triton X-100, 0.5% DOC, 100 mM KCl, 3 mM NaCl, 3.5 mM $MgCl_2$, 1.25 mM EGTA, 10 mM Hepes, pH 7.3), vortexed, and then incubated at 4°C on an orbital shaker for 1 h to solubilize membrane proteins. A centrifugation of 3 min was performed at a speed of 14,000 g at a temperature of 4°C. The supernatant containing an extract enriched in membrane proteins was then recovered and the pellet directly mixed with Laemmli buffer. In summary, the proteins were separated into three fractions, the proteins soluble in Rx fraction, the Rx-T-DOC soluble fraction, and the insoluble fraction, *i.e.*, pellet suspended directly in Laemmli buffer. An amount of 30 µg of proteins present in the Rx supernatant fraction and the equivalent in volume of supernatant recovered with Rx-T-DOC were suspended in Laemmli buffer to a final volume of 26 µL. Samples were boiled just before being separated by SDS-PAGE electrophoresis on two equivalent 10% acrylamide gels. Proteins from the first gel were then transferred on a nitrocellulose membrane for 1.25 h at 70 V and then stained with red Ponceau solution to assess the quality of protein transfer. The membrane was washed with purified water and then saturated with a blocking buffer consisting of a solution of PBS containing 5% of skimmed milk for 4 h at room temperature. After saturation, the membrane was incubated overnight at 4°C on an orbital shaker with the protease inhibitor cocktail (1/1,000) (Sigma-Aldrich) and the recombinant protein VmpA-His_6 at a concentration of 45 µg mL^{-1}. The membrane was then washed in PBS then in PBS + 0.2% Tween 20 prior to incubation with a primary anti-VmpA monospecific polyclonal antibody diluted 1:7,000 (Covalab). After incubation, the membrane was washed with PBS then with PBS + 0.2% Tween 20 and incubated with the secondary antibody anti-IgG rabbit-HRP (Sigma-Aldrich). After washing with PBS, the membrane was incubated with HRP substrate and visualized through the ChemiDoc Imaging System (Bio-Rad).

The second gel was stained with Coomassie blue. The bands corresponding to the signals observed on the far-western blot anti-VmpA were excised and digested with trypsin as previously described (Killiny 2006 Identification of a *Spiroplasma citri* hydrophilic protein associated with insect transmissibility. Microbiol. Read. Engl. 152, 1221–1230). The resulting digestion was analyzed by liquid chromatography tandem mass spectrometry (LC-MS/MS) as routinely performed on the proteomics platform of the University of Bordeaux, France, and sent to a Bordeaux proteomic platform to perform a mass spectrometry analysis.

2.2.3 Mass spectrometry analysis (nLC-MS/MS)

Search parameters were as follows: mass accuracy of the monoisotopic peptide precursor and peptide fragments was set to 10 ppm and 0.02 Da, respectively. Only b- and y-ions were considered for mass calculation. Oxidation of methionines (+16 Da), methionine loss (−131 Da), methionine loss with acetylation (−89 Da), and protein N-terminal acetylation (+42 Da) were considered as variable modifications, whereas carbamidomethylation of cysteines (+57 Da) was considered as fixed modification. Two missed trypsin cleavages were allowed. Peptide validation was performed using the Percolator algorithm (Käll et al., 2007), and only "high confidence" peptides were retained corresponding to a 1% false positive rate at the peptide level. Spectra from peptides higher than 5,000 Da or lower than 350 Da were rejected. The precursor detector node was included.

2.2.4 Database search and results processing

Data were searched by SEQUEST through Proteome Discoverer 2.5 (Thermo Fisher Scientific Inc.) against a SwissProt protein database (version 2022-01; 478,954 entries) and a collection of peptide sequences originating from the conceptual translation of RNA-seq data from *E. variegatus*. The dataset analyzed during the current study are available in the Transcriptome Shotgun Assembly database on NCBI: *E. variegatus*, transcriptome shotgun assembly repository, GenBank accession: GFTU00000000.1.

For the proteins selected after chromatography affinity and identified through mass spectrometry analysis, a first selection step consisted in the determination of VmpA specific retention ratio using the following equation:

$$(\text{« VmpA column » abundance} - \text{« control column » abundance}) * 100 = \text{« VmpA column » abundance}$$

The proteins were classified based on this value. A threshold of 90% of VmpA-specific retention was set in order to eliminate the proteins showing an affinity for the column itself. A gene ontology search was then performed in order to categorize the proteins based on their biological role.

Proteins identified by mass spectrometry analysis performed on excised bands were first selected restraining the results to peptides specifically matching sequences of the *E. variegatus in silico* predicted proteome. A second selection based on the molecular

weight of the proteins followed, according to the signal observed in the far-western blot comparing the positions of bands to the ladder. As the signal observed on the far-western blot was common to the soluble and insoluble fractions, the analysis of bands G and H was restricted to proteins identified in both bands.

The parameters considered to further select the VmpA putative targets were the presence of potential N-glycosylation sites predicted by the prediction tool Glycomine (glycomine.erc.monash.edu.) and the prediction of NxS/T pattern, and the presence of predicted transmembrane domains using TMHMM v2.0 software (Krogh et al., 2001) in the amino acidic sequence.

2.3 Knockdown gene approach to validate interaction between VmpA and insect proteins

2.3.1 Cloning of *E. variegatus* CDS

RNAs were extracted using TRIzol reagent (Thermo Fisher Scientific) under manufacturer instructions including a DNAse treatment for 1 h at 37°C. Reverse transcription was performed on 1 µg of *E. variegatus* RNA as template using SuperScript IV (Thermo Fisher) and random hexamer primers (Thermo Fisher) according to the manufacturer's instruction. The inserts were amplified by PCR and cloned into pGEM®-T Easy vector (Promega) or pMINI-T2 (NEB) using primers listed in Table S1. Plasmids were propagated in competent *E. coli* DH10b cells. The presence of the insert was checked through sequencing by Sanger technology (GENEWIZ, Azenta) using the primers matching flanking region on the plasmid. The sequence analysis and alignment onto reference sequences (TSA *Euscelidius variegatus* taxid:13064*)* were performed using ApE v3.1.3 (Davis and Jorgensen, 2022).

2.3.2 RNA interference on Euva-11 cells, RNA extraction, and mRNA analysis

The putative VmpA targets and GFP sequences were amplified by PCR from *E. variegatus* cDNA as a template using sequence-specific primers 5′ extended with 20 bp of T7 RNA polymerase promoter (Table S1). The HiScribe™ T7 High Yield RNA Synthesis Kit (New England Biolabs) was used on the PCR products to obtain the dsRNAs. dsRNAs were ethanol precipitated in the presence of sodium acetate 0.3 M and were resuspended in 20 µL of RNAse-free water. The purity and integrity of dsRNAs were determined through migration on agarose gel electrophoresis of 1/10 and 1/100 dilutions of the transcription products.

Euva cells were cultivated in 24-well plates (Falcon) to nearly 80% confluence and transfected with 1 µg dsRNA using FuGENE HD Transfection Reagent (Promega). At the end of incubation time of 3 or 7 days, the transfected Euva cells were collected using TRIzol Reagent (Thermo Fisher Scientific) and then stored at −20°C until extraction which was performed according to the manufacturer's instructions. cDNAs of the samples were obtained using SuperScript™ III Reverse Transcriptase (Thermo Fisher Scientific) and 2.5 µM random hexamer primers (Invitrogen). Real-time PCR was performed on the LightCycler 480 Real-Time PCR system (Roche Diagnostics Corp) using sequence-specific primers (Table S1) and N′,N′-dimethyl-N-[4-[(E)-(3-methyl-1,3-benzothiazol-2-ylidene)methyl]-1-phenylquinolin-1-ium-2-yl]-N-propylpropane-1,3-diamine (SYBR Green, Roche). The cycling programs for all amplifications was 95°C for 15 min, followed by 40 cycles of 95°C for 30 s, 60°C for 30 s, and 72°C for 30 s. The two housekeeping genes glutathione S-transferase (GST) and tubulin b (tubb) served as reference genes for mRNA quantification. The relative fold change in gene expression was calculated using the 2^{-DDCt} method (Livak and Schmittgen, 2001).

2.3.3 Adhesion assays of VmpA-His_6-coated beads to Euva cells

The recombinant VmpA-His_6 proteins were obtained as previously described (Arricau-Bouvery et al., 2018). In brief, the proteins were expressed in *E. coli* BL21 Star (DE3) cells containing the plasmid pET28-VmpA-His_6 and purified on a His-select nickel affinity gel packed column (Sigma) according to the manufacturer's protocol. Red fluorescent latex beads exposing ammine at their surface (4×10^9 beads at 1 µm, Sigma-Aldrich) have been coated with the recombinant VmpA-His_6. The beads were washed with MES buffer 50 mM pH 6.1 and then incubated with recombinant proteins at a final concentration of 9 µM of VmpA-His_6 + 1 µM BSA. EDAC 16 mM was added to activate the reaction. The beads were then incubated for 2 h in the dark on an orbital shaker. After a 3-min centrifugation, the coated beads have been washed once with MES buffer 50 mM pH 6.1 and then resuspended in 200 µL of the same buffer. The coated beads were stored in the dark at 4°C up to 7 days. Coating of the beads was verified for each experiment performing a dot blot using a rabbit antibody anti-VmpA.

Three days post transfection with dsRNA, to allow the turnover of the target proteins (Clemens et al., 2000), Euva cells on coverslip in 24-well plates were washed twice with Schneider's medium (Gibco). VmpA-His_6-coated beads were diluted in Schneider's medium (1/100), and 100 µL was dispensed on the cells. The cells were then incubated at 25°C for 1 h.

2.3.4 Immunofluorescent staining and microscopic observations

After incubation, cells were washed twice with Schneider medium and then twice with PBS 1× (Eurobio Scientific). The cells were then fixed using paraformaldehyde at a final concentration of 4% (Electron Microscopy Sciences) during 15 min. The fixed cells were washed for three times with PBS 1× then in distilled water and stained with DAPI 1 mg mL^{-1} during 5 min. The cells were then washed in water and mounted in ProLong Gold Antifade reagent (Invitrogen). Then, the cells were imaged using a Zeiss Axio Imager epifluorescence microscope with an objective with a numerical aperture of 1.4. The filters used for excitations and emissions were BP 377/50 and BP 447/60 for DAPI and BP 562/40 and LP 593 for red fluorescent beads. For Z-stack acquisition, images were acquired every 0.3 µm from the bottom to the top to Euva cells and Z-projections were performed before counting of adherent beads with the free software ImageJ (v. 1.53f)

(Schindelin et al., 2012). There were 20 random positions captured for each treatment.

The Euva cells cultivated in a 24-well plate were observed with the inverted microscope Eclipse TS100 (Nikon) at 3 days post transfection, prior to RNA extraction. Images were taken in random positions of the well at magnifications of 4, 10, and 20.

2.4 Assessment of uk1_LRR expression on *E. variegatus*

Non-infected *E. variegatus* young adults sampled from a synchronized rearing were dissected at the stereomicroscope. Male and female tissues were analyzed separately. Seven salivary glands from females and 7 from males, 7 midgut organs from females and 11 from males, and 6 ovaries with eggs were recovered, pooled to have a sufficient amount of biological material to analyze and kept in TRIzol. Total RNA extraction was performed as previously described, and relative quantification of *uk1_LRR* transcripts was assessed through real-time RT-PCR. Glutathione S-transferase (GST), tubulin b (tub b), and elongation factor 1 (EF1) were used as reference genes to normalize expression values.

A total of 240 nymphs of stages 4 and 5 were put on broad beans to obtain a synchronized rearing. After 10 days, half of young insects were transferred onto healthy broad beans while the other half were transferred onto broad beans infected with FDp for acquisition. After 7 days, eight insects were sampled for each condition and the remaining insects were transferred onto healthy broad beans for latency. Eight insects were sampled every 7 days up to 40 days after beginning of acquisition. The head and abdomen of each insect were analyzed separately. Total RNA was extracted as described previously. Relative quantification of *uk1_LRR* transcripts was assessed through real time RT-PCR as well as the expression of FDp tuf gene hereby used as a proxy of FDp titer and transcriptional activity. *E. variegatus* glutathione S-transferase (GST) was used as reference gene to normalize expression values.

3 Results

3.1 Selection of transmembrane Euva proteins interacting with VmpA retained in the affinity column

As VmpA interacted with proteins of the cell lines Euva established from *E. variegatus*, Euva proteins were purified using an affinity column consisting of VmpA-His_6 bound to nickel-resin and eluted proteins were identified by mass spectrometry (nLC-MS/MS). The control consisted of purification of the Euva proteins on the Ni-NTA column. Mass spectrometry analysis identified 1,422 proteins among proteins binding VmpA-His_6 retained by the column and 1,604 for the control condition (Euva proteins only). A cutoff of 90% was applied to the specific VmpA retention ratio which allowed the selection of 239 proteins (Figure 1A). They were classified based on the KEGG classification (Table 1). Proteins belonging to the transcriptional and translational machinery and proteins localized in the nucleus and mitochondria were removed from the pool of protein candidates that could interact with VmpA. The 148 remaining proteins were analyzed based on the presence of predicted glycosylation sites using Glycomine software that selected only the endoplasmin (endo) protein (one site with $p = 0.958$ and four sites with $p > 0.8$). We additionally searched the "NxS/T" glycosylation site patterns in the amino acidic sequence of the identified proteins and selected 125 candidates. Among them, the transmembrane segments were identified using TMHMM 2.0 software and only two membrane proteins were selected, the HERC4 E3 ubiquitin-protein ligase (HERC4) and the tumor necrosis factor receptor super family member wengen (wengen). Interestingly, five proteins that are known to be implicated in the turnover of the epidermal growth factor receptor (EGFR) were found among the pool of 148 proteins (Figure 1B). Despite the absence of the EGFR in this pool and because it is a 92kDa glycosylated protein present at the surface of almost all cells, we decided to additionally test EGFR as a fourth candidate. Indeed, it has been shown previously that VmpA-His_6 interacted essentially with Euva proteins with apparent masses of 90–95 kDa (Arricau-Bouvery et al., 2021). To test the effect of gene expression knockdown on the interaction between these four candidates and the protein VmpA, the production of these candidates within Euva cells was inhibited by RNA interference (RNAi) and VmpA adhesion assays were performed and are detailed below.

3.2 Selection of transmembrane Euva proteins interacting with VmpA using far-western assay

To better enrich protein fractions in transmembrane proteins, we increased the concentration of Triton X-100 and added sodium deoxycholate to the Rx buffer (Rx-T-DOC). The two cell lines Euva-11 and Euva-12 that showed different cell morphologies and therefore could express different proteins on their surface interacting with VmpA were used for the protein extraction process. The Euva-11 cell line was more homogenous and mostly contained cells that looked like epithelial cells. The Euva-12 cell line was more heterogenous but also contained epithelial-like cells. The different fractions of proteins extracted from Euva cells were submitted to far-western blot using VmpA-His_6 for interaction (Figure 2A). Even if the two cell lines did not fully look the same, no difference was observed between the VmpA-His_6 interaction patterns of Euva-11 proteins and Euva-12 proteins. The profile of proteins that interacted with VmpA-His_6 was quite similar between the different extracted fractions but for some bands the intensity of the signal observed was increased (Figure 2A, arrows). Seven main bands were visible in the fraction submitted to Rx-T-DOC extraction and eight in the insoluble fraction. Four bands were in

10.3389/fcimb.2023.1289100

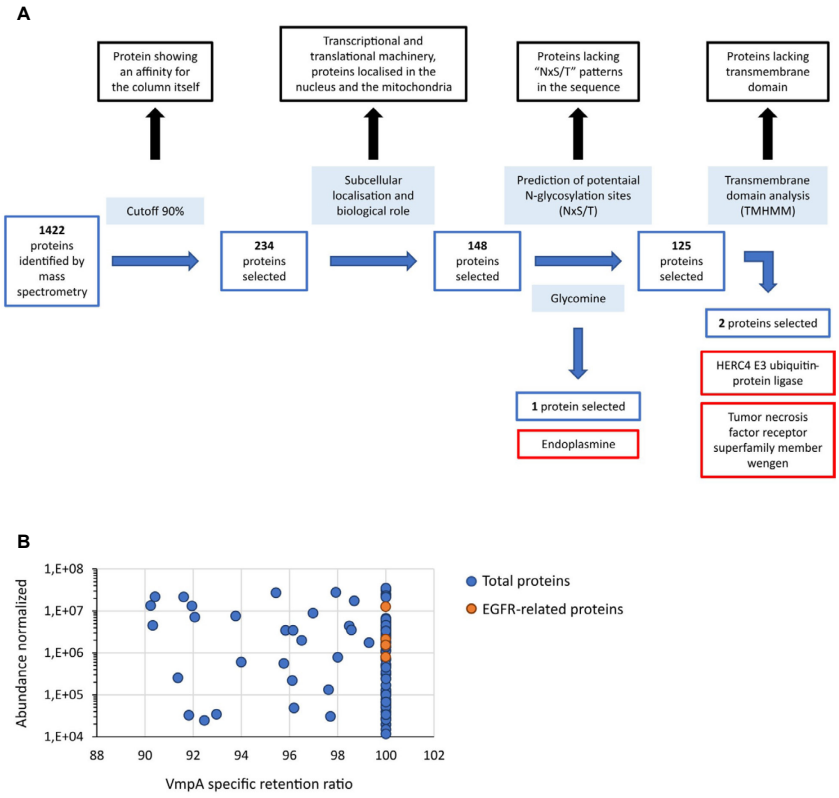

FIGURE 1
Proteins of Euva cells that interact with VmpA-His_6. (A) Process of selection of candidates that interact with VmpA-His_6. The different steps of the process are indicated inside light-blue boxes. The proteins without interest are indicated in boxes lined with black. The proteins selected at each step are indicated in boxes lined with blue, and the name of the three proteins finally selected are in boxes lined with red. (B) Abundance of the proteins interacting with VmpA-His_6 selected with a retention ratio superior to 90%. The five proteins interacting with EGFR and implicated in its recycling process are indicated in orange.

common between insoluble and soluble fractions, in detail bands of 32, 45, 90, and 110 kDa. In parallel of the far-western blot, Euva proteins with masses corresponding to those observed on far-western blot were excised from a Coomassie blue-stained gel and underwent nLC-MS/MS mass-spectrometry analysis. The bands of proteins that were removed from the SDS PAGE gel are indicated by square brackets, as shown in Figure 2B. A total of 205 proteins were selected because they both have TMHMM-predicted transmembrane segments and "NxS/T" pattern(s) (Table 2, details in Table S2). Among these proteins we selected nine proteins that were predicted to be mostly localized at the surface of the cell according to TMHMM prediction (Tables 2, 3).

TABLE 1 Repartition of the 239 Euva proteins that interacted with VmpA-His_6 in relation to their KEEG classification.

KEEG classification	Number of proteins
Global cellular processes	142
Cytoskeleton	18
Vesicular trafficking	17
Binding to membrane/to membrane receptor	9
Other	53

3.3 RNAi knockdown gene expression on Euva cells

RNA interference (RNAi) was used in the Euva cells to inhibit the production of the candidate proteins interacting with VmpA-His_6. Quantification of the mRNA of the four first candidates, *i.e.*, endo, EGFR, HERC4, and wengen, was performed 3 and 7 days after insect cell transfection with dsRNA. The dsRNA control corresponded to the GFP gene. Total RNAs were extracted, and real-time RT-PCR was used to quantify the effect of dsRNAs on the expression of these four genes. Three relative expression levels were calculated using the glutathione S-transferase (GST) and tubulin b (tubb) genes as references. A significant inhibition was observed 3 and 7 days post-transfection with dsRNA, irrespective of the gene considered (Figure 3). The reduction of specific transcripts varied between 3- and 68-fold depending on the gene and the time post transfection. No difference in inhibition rates was observed when we referred to the two reference genes, so only the GST reference gene was kept for the further experiments. No differences were observed between 3 and 7 days whatever the gene considered except for the wengen gene expression for which a slight decrease was observed at 7 days ($p = 0.03$ under the Kruskal–Wallis rank-sum test of the R commander package of R software version 4.0.3). Therefore, extraction of mRNAs and further experiments were

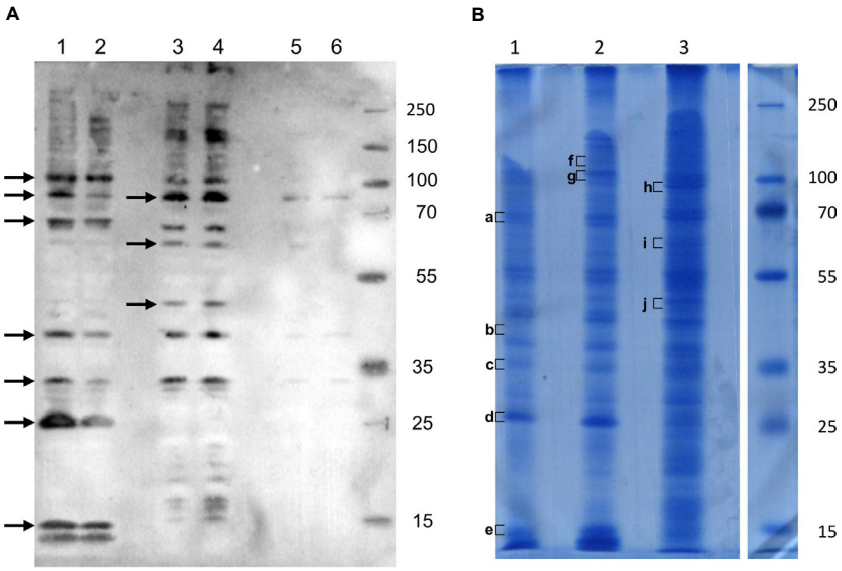

FIGURE 2
Interaction of VmpA-His$_6$ with Euva cell proteins *in vitro*. (A) Euva proteins separated on SDS PAGE and transferred to the nitrocellulose membrane were incubated with recombinant VmpA-His$_6$. Arrows indicated the insect proteins selected to be extracted from SDS PAGE gel indicated with square bracket in B (B) Euva proteins colored with Coomassie blue. Euva-12 (1) and Euva-11 (2) proteins present in the pellet (insoluble fraction). Euva-12 (3) and Euva-11 (4) proteins soluble in Rx-T-DOC buffer. Euva-12 (5) and Euva-11 (6) proteins soluble in the Rx buffer. a to j, bands of proteins that were analyzed with nLC-MS/MS.

performed 3 days post-transfection that should be adequate for turnover of the target protein as mentioned in Clemens et al. (Clemens et al., 2000).

When we tested the nine other genes, we found that the expression rate of the gene uk3 was too low for the RNAi assay to be performed (Ct values of 34–35). For the remaining eight genes, namely, integrin b, uk1_LRR, CD36-like, fasciclin, Na/Ca exchanger, cueball, uk2_TLR, and draper, a statistically significant inhibition of gene expression was achieved (Figure 4, black bars) with fold change values ranging from 2.03 for the fasciclin gene to 51.4 for the uk1_LRR gene.

3.4 Simultaneous multiplexing RNAi on Euva cells

The adhesin VmpA potentially interacts with several insect receptors, as multiple bands were observed after far-western blot with VmpA-His$_6$ (Figure 2). To maximize the chances to inhibit different VmpA receptor(s) at once, we performed assays in which several genes were inhibited simultaneously with dsRNA targeting the different genes selected. For all the 12 genes, significant differences were observed with the control condition, *i.e.*, GFP dsRNA, whatever the number of genes inhibited simultaneously including the targeted gene (Figure 4, gray bars). For the genes endo, wengen, integrin b, uk1_LRR, CD36-like, fasciclin, cueball, HERC4, uk2_TLR, and draper, no difference was observed between the inhibition with dsRNA targeting the gene studied alone and the inhibition induced with up to 13 several different dsRNA, including the targeted gene studied. The dsRNAs designed on uk3 sequences was also included in the multiplex silencing although its inhibition in transfected cells was not assessed. For the genes EGFR and Na/Ca exchanger, a lower gene expression inhibition efficiency was observed when 12 other genes were simultaneously inhibited with the gene studied compared to the single inhibition of the EGFR and Na/Ca exchanger genes.

We tested the effect of off target on the expression of four genes when two to six other genes were simultaneously inhibited. The results show that no significant difference was observed when dsRNA targeted genes other than the studied one compared to GFP dsRNA (Figure 5).

It must be noticed that the phenotype of transfected cells observed with light microscope and their ability to achieve confluence was not impacted by the silencing of any of the candidate genes nor when the 13 candidate genes were inhibited simultaneously (Supplementary Figures S1, S2).

3.5 Adhesion assays to Euva cells of VmpA-coated beads

The VmpA-His$_6$-bead adhesion assays were first performed 3 days after transfection using Euva-11 cells transfected with dsRNA targeting one gene. On average, 51 (± 5) Euva-11 cells and 200 (± 50) beads were observed per field. There were 20 fields photographed per condition, and three independent experiments were performed and pooled. The results show that, whatever the gene inhibited, no difference of bead adhesion was observed between the cells transfected with the dsRNA targeting candidate genes and GFP

10.3389/fcimb.2023.1289100

TABLE 2 Repartition of Euva proteins extracted with the buffer Rx Triton X-100 1% + DOC 0.5% and that interacted with VmpA-His_6.

Band	Property	Number of proteins	Number of proteins selected by				Protein selected for adhesion assays	Candidates abbreviation
			Weight (range of selection)		Transmembrane segment (TMHMM)	NxS/T pattern		
a	Insoluble	1,295	340	(60–80 kDa)	21 (6%)	21	Lysosome membrane protein 2 [Homalodisca vitripennis] Protein cueball isoform X1 [Homalodisca vitripennis]	CD36-like Cueball
b	Insoluble	1,446	333	(40–50 kDa)	23 (7%)	17		
c	Insoluble	950	280	(30–40 kDa)	17 (6%)	14		
d	Insoluble	886	240	(20–30 kDa)	17 (7%)	16		
e	Insoluble	322	19	(13–15 kDa)	1 (5%)	1		
f	Insoluble	1,077	153	(100–120 kDa)	13 (8%)	13	Transforming growth factor-beta-induced protein ig-h3-like [Homalodisca vitripennis] Protein draper isoform X1 [Zootermopsis nevadensis]	Fasciclin Draper
g+h	Insoluble + soluble	684	133	(85–110 kDa)	14 (11%)	14	Protein containing LRR domains (identification *via* InterPro) integrin b Sodium/calcium exchanger 3-like isoform X1 [Homalodisca vitripennis] Transforming growth factor-beta-induced protein ig-h3-like [Homalodisca vitripennis] Leucine-rich repeat-containing protein 15-like [Homalodisca vitripennis]	uk1_LRR Integrin b Na/Ca exchanger Fasciclin uk2_TLR
i	Soluble	1,441	421	(55–68 kDa)	58 (14%)	54	Protein cueball isoform X1 [Homalodisca vitripennis] Lysosome membrane protein 2 [Homalodisca vitripennis]	Cueball CD36-like
j	Soluble	1,222	462	(40–55 kDa)	63 (14%)	55	Uncharacterized protein LOC124356975 [Homalodisca vitripennis]	uk3

The proteins were selected sequentially by their weight, the presence of predicted transmembrane domain using TMHMM, and the presence of "NxS/T"-indicated potential site of glycosylation. The proteins selected for adhesion assays were indicated with their abbreviation.

dsRNA (Supplementary Figure S3A) except for the gene uk1_LRR (Figure 6A). For the gene uk1_LRR, the three repetitions were very homogeneous, *i.e.*, 0.89 ± 0.21, 0.87 ± 0.25, and 0.87 ± 0.28 of relative adhesion of beads with medians of 0.90, 0.82, and 0.75, respectively. At the same time as adhesion assays, the inhibition of the targeted genes was checked. Results show that for each gene, a significant decrease of the mRNA was measured (Figure 6B, Supplementary Figure S3B). The strongest inhibitions were observed for the genes uk1_LRR and wengen with 38.5-fold and 33-fold change of mRNA quantities respectively, and the weakest inhibition was observed for the gene fasciclin with twofold change.

As inhibition of the 13 genes simultaneously by RNAi did not show difference with the inhibition of a single gene, we thus inhibited the 13 genes simultaneously before to incubate the transfected cells with VmpA-His_6-coated beads. Unfortunately, no statistically difference in adhesion of VmpA-His_6-coated beads has been observed on cells where the expression of the 13 candidates was inhibited at once.

3.6 Characterization of the uk1_LRR gene

The uk1_LRR amino acidic and nucleotide sequences were investigated through a BLAST search, revealing several homologs in other organisms present in the databases (Table S3). Uk1_LRR was predicted by TMHMM2.0 to be a transmembrane protein anchored in the plasma membrane by a single 22–23-amino acids-long transmembrane segment located in the C-terminal part (Figures 7A, D). Most of the proteins were predicted to be exposed to the cell surface. The uk1_LRR protein contains four leucine-rich-repeat (LRR) domains of 219, 163, 80, and 146 aa

10.3389/fcimb.2023.1289100

TABLE 3 Characteristics of the Euva proteins selected for adhesion assays.

Band	TSA *Euscelidius variegatus* (NCBI)	Sequence (BLASTP)	Abbreviation	Predicted transmembrane segments (TMHMM)	NxS/T	MW (kDa) protein
a	ORF01214079_GFTU01004399.1_00136_01779_f1	Lysosome membrane protein 2 [Homalodisca vitripennis]	CD36-like	2	6	61
	ORF03010044_GFTU01011408.1_00185_01996_f2	Protein cueball isoform X1 [Homalodisca vitripennis]	Cueball	1	6	67
f	ORF02093016_GFTU01007852.1_00001_02736_f1	Transforming growth factor-beta-induced protein ig-h3-like [Homalodisca vitripennis]	Fasciclin	1	5	94
	ORF03898939_GFTU01016123.1_00223_03282_f1	Protein draper isoform X1 [Zootermopsis nevadensis]	Draper	1	11	109
g+h	ORF03757228_GFTU01015247.1_00222_02681_f3	Protein containing LRR domains (identification *via* InterPro)	uk1_LRR	1	14	87
	ORF03985247_GFTU01016611.1_00180_02645_f3	integrin beta	integrin b	1	7	91
	ORF03874906_GFTU01015965.1_00117_02747_f3	Sodium/calcium exchanger 3-like isoform X1 [Homalodisca vitripennis]	Na/Ca exchanger	12	6	95
	ORF02093016_GFTU01007852.1_00001_02736_f1	Transforming growth factor-beta-induced protein ig-h3-like [Homalodisca vitripennis]	Fasciclin	1	5	94
	ORF03639633_GFTU01014488.1_00117_02468_f3	Leucine-rich repeat-containing protein 15-like [Homalodisca vitripennis]	uk2_TLR	1	7	82
i	ORF03010044_GFTU01011408.1_00185_01996_f2	Protein cueball isoform X1 [Homalodisca vitripennis]	Cueball	1	6	67
	ORF01214079_GFTU01004399.1_00136_01779_f1	Lysosome membrane protein 2 [Homalodisca vitripennis]	CD36-like	2	6	61
j	ORF00560024_GFTU01001746.1_00401_01750_f2	Uncharacterized protein LOC124356975 [Homalodisca vitripennis]	uk3	1	2	48

(from N-ter to C-ter sequence) classified in the ribonuclease inhibitor-like group. Furthermore, consistent with sequence prediction indicating LRR domains, structural prediction (Robetta, Baker Lab) revealed a horseshoe-shaped molecule consisting of parallel b-strands on the inner concave side and helical elements on the outer convex sites (Figure 7B). There were 14 potential N-glycosylation sites (NxST motif) found in the uk1_LRR amino acid sequence and are localized on the protein predicted structure in Figure 7C.

No paralogous gene was found in the *E. variegatus* transcriptome. However, it has been possible to identify an ortholog gene in *S. titanus* (Transcriptome Shotgun Assembly ref. "Scaphoideus titanus taxid:376741"), the natural vector of flavescence doreéphytoplasmas, with an amino acid identity of 90.6% (Clustal 2.1). *E. variegatus* uk1_LRR consists of 781 amino acids while the *S. titanus* sequence is 779 amino acids long. Potential N-glycosylation sites were conserved between the two proteins, both in number (14) and in position, with a shift that reflects the difference in protein sequence length.

3.7 Assessment of uk1_LRR expression in *E. variegatus*

To assess uk1_LRR expression in the different organs of the insect vector, real-time RT-PCR was performed on salivary glands, digestive tubes, and ovaries with eggs dissected from healthy *E. variegatus*. The organ showing the highest uk1_LRR expression values was the digestive tube (Figure 8A). The gene was expressed 6 and 18 times less in the salivary glands and ovaries, respectively, when compared to digestive tubes.

uk1_LRR expression was then assessed on synchronized *E. variegatus* adults up to 40 days after feeding onto FD92

10.3389/fcimb.2023.1289100

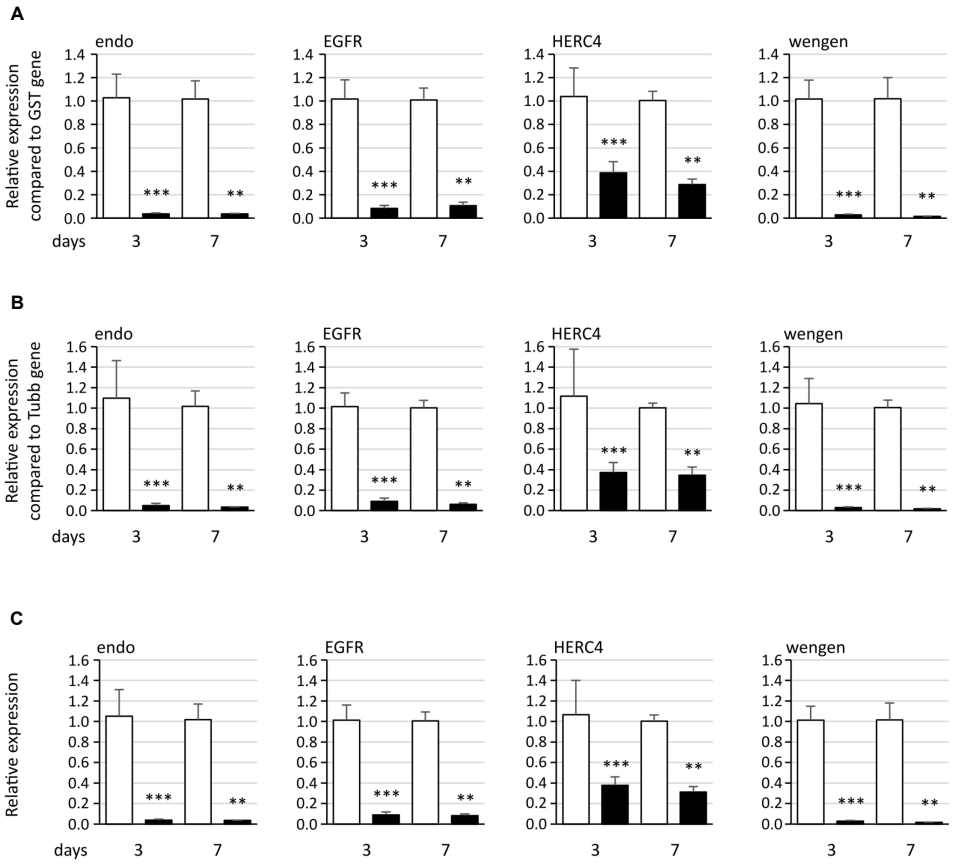

FIGURE 3
Expression of the four genes endoplasmin (endo), epidermal growth factor receptor (EGFR), HERC4 E3 ubiquitin-protein ligase (HERC4), and tumor necrosis factor receptor superfamily member wengen (wengen) in Euva cells with regard to the reference gene glutathione S-transferase (A), tubulin b (B), and both genes (C). White boxes correspond to Euva cells transfected with GFP dsRNA, and black boxes correspond to Euva cells transfected with dsRNA targeting the gene indicated above the graphs. ** indicates a significant difference with $p < 0.01$ and *** with $p < 0.001$ under the Kruskal–Wallis rank-sum test of the R commander package of R software version 4.0.3.

phytoplasma-infected broad beans or onto healthy plants as control, both in abdomens (Figure 8B) and in heads containing the salivary glands (Figure 8C). Even though no statistically significant differences were found in expression of uk1_LRR between healthy and FD92-infected insects, a trend is clearly visible. At 7 days post acquisition, the uk1_LRR gene was more expressed in FD92-infected insects, both in the heads and in the abdomens, than in non-infected insects. While the uk1_LRR gene expression remained stable in the insect that fed on non-infected plants, the uk1_LRR mRNA decreased over time in the insects fed on phytoplasma-infected plants. An increase in abdomens and heads was observed 28 days post acquisition, before uk1_LRR mRNA expression decreased.

As far as phytoplasma tuf mRNA relative quantities are concerned, both heads and abdomens were found to be positive to phytoplasma detection since the first sampling date, 7 days after the beginning of acquisition (Figure 8D). At 7 and 14 days, quantities of tuf mRNA in the abdomens were significantly higher than in the heads, then titers were significantly higher in the heads than in the abdomens. The quantities of tuf mRNA were nearly stable in the abdomens over the latency whereas they increased over time in the heads.

4 Discussion

Mechanisms driving the colonization of insect vector cells by phytoplasma are poorly deciphered. The first phytoplasma protein able to interact with protein of insect vector was the Antigenic Membrane Protein AMP. It was demonstrated that AMP of "*Candidatus* phytoplasma asteris" was able to interact with the cellular microfilament and more specifically with the actin of vectoring leafhopper species but not with actin of non-vectoring leafhopper species (Suzuki et al., 2006). In addition, the amp gene and its ortholog stamp in "*Ca.* P. solani" were shown to be submitted to heavy positive selection indicating a possible adaptation process acting on this gene (Kakizawa et al., 2006; Fabre et al., 2011). However, the interaction of AMP with actin is certainly involved in the intracellular trafficking of phytoplasmas once they are internalized into the insect vector cells. Prior to this step, phytoplasma must interact with the surface proteins of the insect cells. Our recent work demonstrated that VmpA and VmpB proteins of group 16SrV-C and V-D phytoplasmas are highly variable and that their variability correlates with the specific transmission of Vmp variants by leafhopper of the subfamily *Deltocephalinae* (Malembic-Maher et al., 2020). We could

10.3389/fcimb.2023.1289100

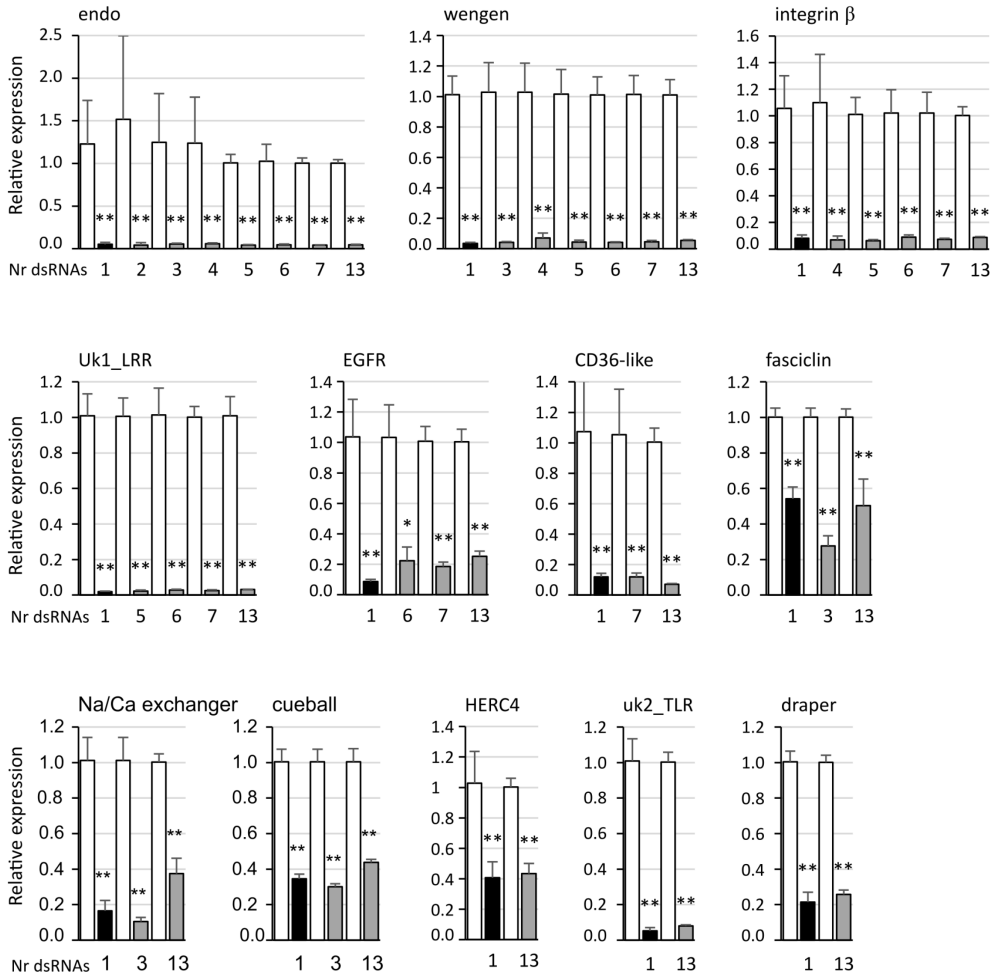

FIGURE 4
Expression of the candidate genes endoplasmin (endo), tumor necrosis factor receptor super family member wengen (wengen), integrin b protein containing LRR domains (uk1_LRR), epidermal growth factor receptor (EGFR), lysosome membrane protein 2 (CD36-like), transforming growth factor-beta-induced protein ig-h3-like (fasciclin), sodium/calcium exchanger 3-like isoform X1 (Na/Ca exchanger), protein cueball isoform X1 (cueball), HERC4 E3 ubiquitin-protein ligase (HERC4), leucine-rich repeat-containing protein 15-like (uk2_TLR), and protein draper isoform X1 (draper) in Euva cells with regard to the reference gene glutathione S-transferase. White boxes correspond to Euva cells transfected with GFP dsRNA, black boxes with dsRNA targeting the gene indicated above the graphs, and gray boxes with several dsRNA including the gene studied, the number of which is indicated under the graph. * indicates a significant difference with $p < 0.05$ and ** with $p < 0.01$ under the Kruskal–Wallis rank-sum test of the R commander package of R software version 4.0.3 with regard to the GFP dsRNA control.

previously demonstrate that VmpA acts as an adhesin able to bind cells of its insect vector in a lectin-like manner (Arricau-Bouvery et al., 2018; Arricau-Bouvery et al., 2021). After this initial step of adhesion, flavescence dorée phytoplasma enters insect cells by a clathrin-mediated endocytosis allowing infection of its insect vector (Arricau-Bouvery et al., 2023). We currently hypothesize that leafhopper species able to acquire FD phytoplasma have a glycoprotein set different to that of leafhopper species unable to achieve acquisition. Variations in the cortege of glycoproteins can lead to variations in the binding of lectins at the surface of hemipteran insect cells. For instance, an enhanced binding of the mannose-specific *Galanthus nivalis* lectin GNA to the gut glycoproteins of the rice planthopper *Nilaparvata lugens* by comparison to that of the rice leafhopper *Nephotettix cincticeps* is associated to a higher toxicity of GNA to *N. lugens* (Foissac et al., 2000). To identify the glycoprotein receptors for VmpA, we enrich Euva cell membrane protein fractions into proteins able to interact with VmpA. However, the number of proteins identified through mass spectrometry was large. We decided to focus our attention to the protein candidates predicted to be surface membrane proteins with a potential site for N-glycosylation. In order to validate their role in VmpA binding, we measured the binding of VmpA to Euva cells in which the expression of the corresponding gene was silenced.

RNAi is an efficient selective silencer of target genes, but it is not absolutely specific. Three main off-target effects due to siRNA delivery

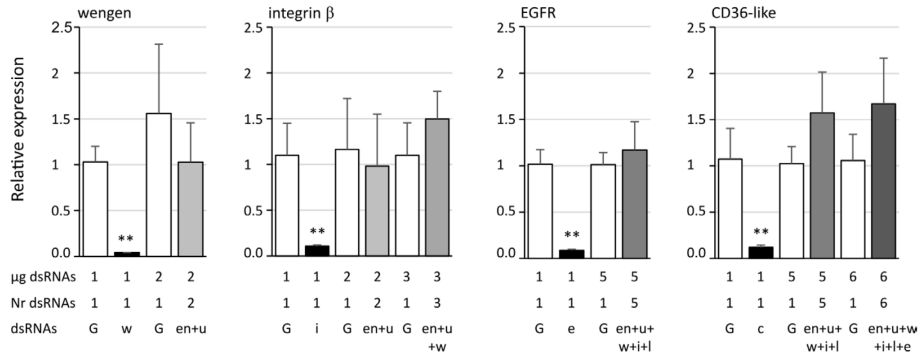

FIGURE 5
Expression of the candidate genes tumor necrosis factor receptor superfamily member wengen (wengen), integrin b, epidermal growth factor receptor (EGFR), and lysosome membrane protein 2 (CD36-like) in Euva cells with regard to the reference gene glutathione S-transferase. White boxes correspond to Euva cells transfected with GFP dsRNA (G) at the quantities indicated under the graph (µg dsRNA), black boxes with dsRNA targeting the gene studied and indicated above the graphs, and gray boxes with several dsRNA without dsRNA targeting the gene studied, the number of which is indicated under the graph (Nr dsRNA). dsRNAs indicates the targeted genes endoplasmin (en), uk3 (u), wengen (w), integrin b (i), unk1_LRR (l), CD36-like (c), and EGFR (e). ** indicates a significant difference with $p < 0.01$ under the Kruskal–Wallis rank-sum test of the R commander package of R software version 4.0.3 with regard to the GFP dsRNA control.

in an organism can be described and are reviewed by Jackson and Linsley (Jackson and Linsley, 2010). The first one, which is expected to not have influence in our study, is an inflammatory response against the siRNAs and/or the transfectant used to deliver dsRNAs in mammals. The second off-target effect is linked to the siRNA-induced sequence-dependent regulation of unintentional transcripts through partial sequence complementary to their 3′UTRs. Checking the effect on the other target genes showed that no off-target effect was observed in our case. However, even though no partial sequence homology was found in the *E. variegatus* transcriptome for the genes we tested, we cannot exclude that the expression of other genes could have been affected. A study showed that pooling 10 synthetic siRNAs targeting the same mRNA reduced the number and magnitude of off-target silencing compared to the use of a single siRNA (Kittler et al., 2007). In our case, we used long dsRNA instead of siRNA. The dsRNAs are taken by the RNAi machinery to produce several siRNAs targeting the same mRNA and could induce a reduction of off-target effects. The third off-target effect is due to a saturation of the endogenous RNAi machinery by exogenous siRNAs. In our case, when we compared the efficiency of the RNAi using one dsRNA (1 µg of dsRNAs) or up to 13 different dsRNA (13 µg of dsRNAs), we did not find any differences for 10 over 12 genes targeted suggesting that the quantity of dsRNAs used did not saturate the RNAi machinery. Usually, one gene at a time is knockdown by RNAi using either long dsRNA or multiple siRNAs targeting one gene and introduced by transfection into insect cells or vertebrate cells, respectively. We did not find examples of cultured cells transfected with multiple long dsRNA targeting several genes. However, an example of three genes silenced using Y-shaped siRNAs was described in a bone metastatic prostate cancer cell line (Kozuch et al., 2018). RNAi targeting several genes has been described in insects that were injected with or ingested dsRNA. For example, when two genes were targeted with two dsRNAs injected into the planthopper *N. lugens* or with two dsRNAs or a concatemer ingested by the whitefly *Bemisia tabaci*, knockdown of genes were similar to that observed with injection or ingestion of individual dsRNA. Use of concatemer showed an increase of gene knockdown when compared to mixed dsRNAs (Mao et al., 2021; Jain et al., 2022).

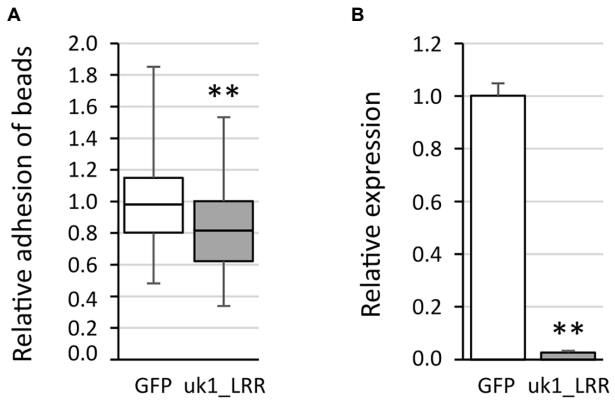

FIGURE 6
Adhesion of the VmpA-His_6-coated beads to the Euva-11 cells in the presence of dsRNA of the uk1_LRR gene and GFP as control. (A) Adhesion of VmpA-His_6-coated beads to Euva-11 cells 3 days after the cells were transfected with GFP dsRNA (white) or uk1_LRR dsRNA (gray). ** indicates a significant difference with $p = 0.003671$ for uk1_LRR under the Kruskal–Wallis rank-sum test. (B) Control of RNAi efficiency into Euva-11 cells transfected at the same time as cells incubated with beads in (A) The expression of the uk1_LRR gene was measured in Euva-11 cells with regard to the reference gene glutathione S-transferase. White box corresponds to Euva-11 cells transfected with GFP dsRNA and gray box with uk1_LRR dsRNA. ** indicates a significant difference with $p = 0.0004912$ under the Kruskal–Wallis rank-sum test of the R commander package of R software version 4.0.3 with regard to the GFP dsRNA control.

Using VmpA-coated beads instead of living phytoplasmas allowed us to avoid problems due to the concentration and the viability of phytoplasmas recovered from infected insects or infected plants. Moreover, this simplified system allows us to study the role of the sole VmpA in the interaction with the insect cells without the masking

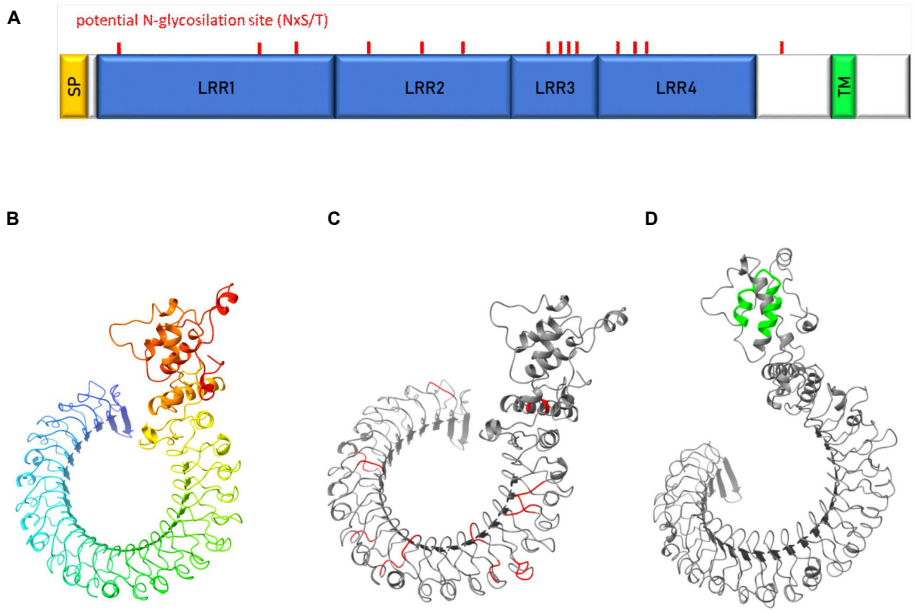

FIGURE 7
Characterization of uk1_LRR protein. (A) Schematic representation of uk1_LRR protein where the signal peptide (SP) predicted by InterPro and TMHMM is colored in yellow, the LRR domains predicted by InterPro in blue, and the transmembrane domain predicted by TMHMM (TM) in green. Predicted protein structures by Robetta (Baker Lab) were visualized with the software Chimera X (v.1.5) without signal peptide (B), with the potential N-glycosylation sites (aminoacidic motif « NxS/T ») highlighted in red (C) and the transmembrane domain highlighted in green (D).

effect of other Vmps or membrane factors. This strategy, applied to 12 candidates, revealed the possible implication of *E. variegatus* uk1_LRR protein in the adhesion to the vector cell mediated by phytoplasma strain FD92 VmpA. Indeed, the inhibition of the adhesion of VmpA-coated beads to Euva cells in culture was only partially achieved. The amount of uk1_LRR transcripts, as all of the gene candidates tested, was successfully decreased through RNAi but not completely knockout.

We have only few indications about the uk1_LRR function. Proteins with such LRR structures are frequently implicated in protein–protein interactions and have a variety of functions including immune response, apoptosis, autophagy, and neuronal development (Kobe and Kajava, 2001; Matsushima et al., 2019). The uk1_LRR protein of *E. variegatus* contains LRR domains classified in the ribonuclease inhibitor (RI)-like group. However, uk1_LRR does not show sequence homology with RI and is predicted to be exposed to the surface cell whereas the RI protein is cytosolic (Dickson et al., 2005). It is then highly probable that the uk1_LRR protein has a different function from RI. The other proteins sharing homologies with the uk1_LRR protein also contain the LRR domain classified in the RI-like group. However, the diversity of the proteins found, *i.e.*, artichoke-like protein, Toll pathway protein, or Toll-like receptor Tollo, as examples, only share their extracellular position and LRR domains. Several proteins matching amino acidic sequence of uk1_LRR in the homology search were annotated as carboxypeptidase N subunit-like.

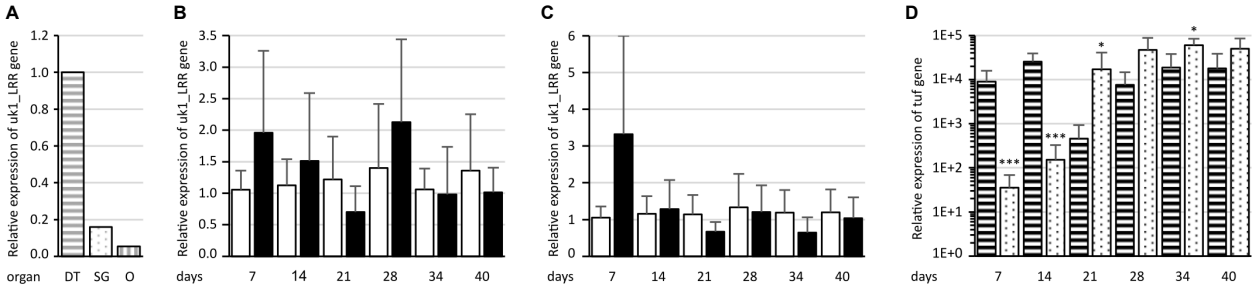

FIGURE 8
Assessment of uk1_LRR expression in *E. variegatus*. (A) Relative expression of uk1_LRR in the *E. variegatus* digestive tube (gray horizontal stripes) and salivary glands (gray dots) of male and female insects, and ovary and eggs (gray vertical stripes). (B) Relative expression of uk1_LRR of *E. variegatus* with regard to the reference gene glutathione S-transferase in abdomens or (C) in heads at different time points on non-infected plants (white bars) or on FD92 phytoplasma-infected plants (black bars). (D) Relative expression of the phytoplasma tuf gene at different time points in abdomens (horizontal stripes) and heads (dots) of *E. variegatus*. * indicates a significant difference with $p < 0.05$ and ***$p < 0.001$ (under the Kruskal–Wallis rank-sum test of the R commander package of R software version 4.0.3) in tuf expression between abdomens and heads at each time point.

However, the study of uk1_LRR sequence revealed the absence of carboxypeptidase domains. Therefore, the function of uk1_LRR remains to be identified.

We found that uk1_LRR was expressed in both phytoplasma-infected and uninfected insect vectors and was more or less stable over time during insect colonization by the phytoplasma. In the early stages of vector infection, right after ingestion of phytoplasma, the expression of uk1_LRR had a tendency to increase in infected insects when compared to same-age adults fed on healthy plants. Interestingly, a similar increase in expression was found in infected insect abdomens at 28 days of latency, when insects acquire again phytoplasmas from the faba beans that became systemically infected. Indeed, at this timepoint, the phytoplasma titer measured in insect abdomens increased, suggesting that the expression level of uk1_LRR follows the *de novo* ingestion of phytoplasmas. Furthermore, the evaluation of uk1_LRR expression in different insect tissues revealed that the digestive tubes were characterized by the highest level of transcripts when compared to salivary glands and ovaries and eggs. Taking consideration of these altogether, uk1_LRR could be implicated in the binding with VmpA in the early stages of insect infection following phytoplasma ingestion, *i.e.*, at the surface of intestine epithelial cells.

Data availability statement

The mass spectrometry proteomics data have been deposited to the ProteomeXchange Consortium via the PRIDE [1] partner repository with the dataset identifier PXD046447.

Ethics statement

The manuscript presents research on animals that do not require ethical approval for their study.

Author contributions

FC: Conceptualization, Formal Analysis, Investigation, Methodology, Writing – original draft, Writing – review & editing. SD: Conceptualization, Formal Analysis, Investigation, Methodology, Writing – review & editing. M-PD: Conceptualization, Formal Analysis, Investigation, Methodology, Writing – review & editing. SC: Formal Analysis, Investigation, Writing – review & editing. SM-M: Writing – review & editing. XF: Conceptualization, Formal Analysis, Funding acquisition, Investigation, Project administration, Supervision, Writing – original draft, Writing – review & editing. NA-B: Conceptualization, Formal Analysis, Funding acquisition, Investigation, Methodology, Project administration, Supervision, Writing – original draft, Writing – review & editing.

Funding

The author(s) declare financial support was received for the research, authorship, and/or publication of this article. FC was supported by a Ph.D. fellowship from INRAE-SPE and the Regional Council of Nouvelle-Aquitaine (Grant AAPR2020A-2019-8404510/810). This research was funded by the Plan National contre le Dépérissement du Vignoble (projects RISCA and RISCA II coordinated by Audrey Petit of French Wine and Vine Institute).

Acknowledgments

We acknowledge the "Pôle Imagerie du Végétal" of Bordeaux Imaging Center (BIC, UAR 3420, France-BioImaging infrastructure) for the use of the platform facilities and the invaluable support accorded to us during microscopic imaging. Thanks to Laure Béven for the support in the implementation of the protein extraction buffer (Rx-T-DOC) and in the far-western blot analysis. Thanks are given to Christophe Garcion for the *in silico* translation of the *E. variegatus* transcriptome. We acknowledge Denis Lacaze, Jean-Saïd Bey, Marielle Levillain, and Thierry Lusseau for plant and insect production and maintenance.

Conflict of interest

The authors declare that the research was conducted in the absence of any commercial or financial relationships that could be construed as a potential conflict of interest.

Publisher's note

Supplementary material

The Supplementary Material for this article can be found online at: https://www.frontiersin.org/articles/10.3389/fcimb.2023.1289100/full#supplementary-material

References

Abbà, S., Galetto, L., Ripamonti, M., Rossi, M., and Marzachì, C. (2019). RNA interference of muscle actin and ATP synthase beta increases mortality of the phytoplasma vector *Euscelidius variegatus*. *Pest Manag Sci.* 75, 1425–1434. doi: 10.1002/ps.5263

Angelini, E., Clair, D., Borgo, M., Bertaccini, A., and Boudon-Padieu, E. (2001). Flavescence doree in France and Italy - Occurrence of closely related phytoplasma isolates and their near relationships to Palatinate grapevine yellows and an alder yellows phytoplasma. *Vitis- J. Grapevine Res.* 40, 79–79. doi: 10.5073/vitis.2001.40.79-86

Arricau-Bouvery, N., Dubrana, M.-P., Canuto, F., Duret, S., Brocard, L., Claverol, S., et al. (2023). Flavescence dorée phytoplasma enters insect cells by a clathrin-mediated endocytosis allowing infection of its insect vector. *Sci. Rep.* 13, 2211. doi: 10.1038/s41598-023-29341-1

Arricau-Bouvery, N., Duret, S., Dubrana, M.-P., Batailler, B., Desqué, D., Béven, L., et al. (2018). Variable membrane protein A of flavescence doréephytoplasma binds the midgut perimicrovillar membrane of *euscelidius variegatus* and promotes adhesion to its epithelial cells. *Appl. Environ. Microbiol.* 84, e02487–e02417. doi: 10.1128/AEM.02487-17

Arricau-Bouvery, N., Duret, S., Dubrana, M.-P., Desqué, D., Eveillard, S., Brocard, L., et al. (2021). Interactions between the flavescence dorée phytoplasma and its insect vector indicate lectin-type adhesion mediated by the adhesin VmpA. *Sci. Rep.* 11, 11222. doi: 10.1038/s41598-021-90809-z

Baum, J. A., Bogaert, T., Clinton, W., Heck, G. R., Feldmann, P., Ilagan, O., et al. (2007). Control of coleopteran insect pests through RNA interference. *Nat. Biotechnol.* 25, 1322–1326. doi: 10.1038/nbt1359

Caudwell, A., Kuszala, C., Bachelier, J. C., and Larrue, J. (1970). Transmission de la Flavescence doree de la vigne aux plantes herbacees par l'allongement du temps d'utilisation de la cicadelle *Scaphoideus littoralis* Ball et l'etude de sa survie sur en grand nombre d'especes vegetales. *Ann. Phytopathol.* 1572, 415–428.

Caudwell, A., Kuszala, C., Larrue, J., and Bachelier, J. C. (1972). Transmission de la Flavescence dorée de la fève à la fève par des cicadelles des genres *Euscelis* et *Euscelidius*. *Ann. Phytopathol.* 1572, 181–189.

Clemens, J. C., Worby, C. A., Simonson-Leff, N., Muda, M., Maehama, T., Hemmings, B. A., et al. (2000). Use of double-stranded RNA interference in *Drosophila* cell lines to dissect signal transduction pathways. *Proc. Natl. Acad. Sci.* 97, 6499–6503. doi: 10.1073/pnas.110149597

Davis, M. W., and Jorgensen, E. M. (2022). ApE, A plasmid editor: A freely available DNA manipulation and visualization program. *Front. Bioinforma* 2. doi: 10.3389/fbinf.2022.818619

Dickson, K. A., Haigis, M. C., and Raines, R. T. (2005)Ribonuclease Inhibitor: Structure and Function. In: *Progress in Nucleic Acid Research and Molecular Biology* (Academic Press). Available at: https://www.sciencedirect.com/science/article/pii/S0079660305800091 (Accessed August 9, 2023).

Echeverri, C. J., and Perrimon, N. (2006). High-throughput RNAi screening in cultured cells: a user's guide. *Nat. Rev. Genet.* 7, 373–384. doi: 10.1038/nrg1836

European Food Safety Authority (EFSA), Tramontini, S., Delbianco, A., Vos, S. (2020). Pest survey card on flavescence dorée phytoplasma and its vector *Scaphoideus titanus*. *EFSA Support Publ* 17, 1909E. doi: 10.2903/sp.efsa.2020.EN-1909

Fabre, A., Danet, J.-L., and Foissac, X. (2011). The stolbur phytoplasma antigenic membrane protein gene stamp is submitted to diversifying positive selection. *Gene* 472, 37–41. doi: 10.1016/j.gene.2010.10.012

Foissac, X., Thi Loc, N., Christou, P., Gatehouse, A. M. R., and Gatehouse, J. A. (2000). Resistance to green leafhopper *(Nephotettix virescens)* and brown planthopper *(Nilaparvata lugens)* in transgenic rice expressing snowdrop lectin (*Galanthus nivalis agglutinin*; GNA). *J. Insect Physiol.* 46, 573–583. doi: 10.1016/S0022-1910(99)00143-2

Galetto, L., Bosco, D., Balestrini, R., Genre, A., Fletcher, J., and Marzachì, C. (2011). The major antigenic membrane protein of "*Candidatus* phytoplasma asteris" Selectively interacts with ATP synthase and actin of leafhopper vectors. *PloS One* 6, e22571. doi: 10.1371/journal.pone.0022571

Gross, J., Gallinger, J., and Görg, L. M. (2022). Interactions between phloem-restricted bacterial plant pathogens, their vector insects, host plants, and natural enemies, mediated by primary and secondary plant metabolites. *Entomol Gen.*, 42, 185–215. doi: 10.1127/entomologia/2021/1254

Guo, C.-F., Qiu, J.-H., Hu, Y.-W., Xu, P.-P., Deng, Y.-Q., Tian, L., et al. (2023). Silencing of V-ATPase-E gene causes midgut apoptosis of *Diaphorina citri* and affects its acquisition of Huanglongbing pathogen. *Insect Sci.* 30, 1022–1034. doi: 10.1111/1744-7917.13146

Jackson, A. L., Bartz, S. R., Schelter, J., Kobayashi, S. V., Burchard, J., Mao, M., et al. (2003). Expression profiling reveals off-target gene regulation by RNAi. *Nat. Biotechnol.* 21, 635–637. doi: 10.1038/nbt831

Jackson, A. L., and Linsley, P. S. (2010). Recognizing and avoiding siRNA off-target effects for target identification and therapeutic application. *Nat. Rev. Drug Discovery* 9, 57–67. doi: 10.1038/nrd3010

Jain, R. G., Fletcher, S. J., Manzie, N., Robinson, K. E., Li, P., Lu, E., et al. (2022). Foliar application of clay-delivered RNA interference for whitefly control. *Nat. Plants* 8, 535–548. doi: 10.1038/s41477-022-01152-8

Jeger, M., Bragard, C., Caffier, D., Candresse, T., Chatzivassiliou, E., Dehnen-Schmutz, K., et al. (2016). Risk to plant health of Flavescence dorée for the EU territory. *EFSA J.* 14, e04603. doi: 10.2903/j.efsa.2016.4603

Kakizawa, S., Oshima, K., Jung, H.-Y., Suzuki, S., Nishigawa, H., Arashida, R., et al. (2006). Positive selection acting on a surface membrane protein of the plant-pathogenic phytoplasmas. *J. Bacteriol* 188, 3424–3428. doi: 10.1128/JB.188.9.3424-3428.2006

Käll, L., Canterbury, J. D., Weston, J., Noble, W. S., and MacCoss, M. J. (2007). Semi-supervised learning for peptide identification from shotgun proteomics datasets. *Nat. Methods* 4, 923–925. doi: 10.1038/nmeth1113

Kittler, R., Surendranath, V., Heninger, A.-K., Slabicki, M., Theis, M., Putz, G., et al. (2007). Genome-wide resources of endoribonuclease-prepared short interfering RNAs for specific loss-of-function studies. *Nat. Methods* 4, 337–344. doi: 10.1038/nmeth1025

Kobe, B., and Kajava, A. V. (2001). The leucine-rich repeat as a protein recognition motif. *Curr. Opin. Struct. Biol.* 11, 725–732. doi: 10.1016/S0959-440X(01)00266-4

Kozuch, S. D., Cultrara, C. N., Beck, A. E., Heller, C. J., Shah, S., Patel, M. R., et al. (2018). Enhanced cancer theranostics with self-assembled, multilabeled siRNAs. *ACS Omega* 3, 12975–12984. doi: 10.1021/acsomega.8b01999

Krogh, A., Larsson, B., von Heijne, G., and Sonnhammer, E. L. (2001). Predicting transmembrane protein topology with a hidden Markov model: application to complete genomes. *J. Mol. Biol.* 305, 567–580. doi: 10.1006/jmbi.2000.4315

Lee, I.-M., Davis, R. E., and Gundersen-Rindal, D. E. (2000). Phytoplasma: phytopathogenic mollicutes. *Annu. Rev. Microbiol.* 54, 221–255. doi: 10.1146/annurev.micro.54.1.221

Livak, K. J., and Schmittgen, T. D. (2001). Analysis of relative gene expression data using real-Time quantitative PCR and the 2−DDCT method. *Methods* 25, 402–408. doi: 10.1006/meth.2001.1262

Maillet, P. L., and Gouranton, J. (1971). Etude du cycle biologique du mycoplasme de la phyllodie du trèfle dans l'insecte vecteur, Euscelis lineolatus BrullÉHomoptera, Jassidae. *J. Microscopie* 11, 143–165.

Malembic-Maher, S., Desqué, D., Khalil, D., Salar, P., Bergey, B., Danet, J.-L., et al. (2020). When a Palearctic bacterium meets a Nearctic insect vector: Genetic and ecological insights into the emergence of the grapevine Flavescence dorée epidemics in Europe. *PloS Pathog.* 16, e1007967. doi: 10.1371/journal.ppat.1007967

Mao, K., Ren, Z., Li, W., Cai, T., Qin, X., Wan, H., et al. (2021). Carboxylesterase genes in nitenpyram-resistant brown planthoppers, *Nilaparvata lugens*. *Insect Sci.* 28, 1049–1060. doi: 10.1111/1744-7917.12829

Matsushima, N., Takatsuka, S., Miyashita, H., and Kretsinger, R. H. (2019). Leucine rich repeat proteins: sequences, mutations, structures and diseases. *Protein Pept. Lett.* 26, 108–131. doi: 10.2174/0929866526666181208170027

Merfa, M. V., Fischer, E. R., Souza E Silva, M., Francisco, C. S., Della Coletta-Filho, H., and de Souza, A. A. (2022). Probing the Application of OmpA-Derived Peptides to Disrupt the Acquisition of "*Candidatus* Liberibacter asiaticus" by *Diaphorina citri*. *Phytopathology* 112, 163–172. doi: 10.1094/PHYTO-06-21-0252-FI

Mondal, M., Brown, J. K., and Flynt, A. (2020). Exploiting somatic piRNAs in *Bemisia tabaci* enables novel gene silencing through RNA feeding. *Life Sci. Alliance* 3. doi: 10.26508/lsa.202000731

Oliveira, M. J. R. A., Roriz, M., Vasconcelos, M. W., Bertaccini, A., and Carvalho, S. M. P. (2019). Conventional and novel approaches for managing "flavescence doreé" in grapevine: knowledge gaps and future prospects. *Plant Pathol.* 68, 3–17. doi: 10.1111/ppa.12938

Schindelin, J., Arganda-Carreras, I., Frise, E., Kaynig, V., Longair, M., Pietzsch, T., et al. (2012). Fiji - an Open Source platform for biological image analysis. *Nat. Methods* 9, 676–682. doi: 10.1038/nmeth.2019

Suzuki, S., Oshima, K., Kakizawa, S., Arashida, R., Jung, H.-Y., Yamaji, Y., et al. (2006). Interaction between the membrane protein of a pathogen and insect microfilament complex determines insect-vector specificity. *Proc. Natl. Acad. Sci.* 103, 4252–4257. doi: 10.1073/pnas.0508668103

Weintraub, P. G., and Beanland, L. (2006). Insect vectors of phytoplasmas. *Annu. Rev. Entomol* 51, 91–111. doi: 10.1146/annurev.ento.51.110104.151039

Weintraub, P. G., and Wilson, M. R. (2009). Control of phytoplasma diseases and vectors. *Phytoplasmas Genomes Plant Hosts Vectors*, 233–249. doi: 10.1079/9781845935306.0233

Décryptage de l'adhésion du phytoplasme de la flavescence dorée aux cellules de son insecte vecteur

La flavescence dorée (FD) est une maladie de la vigne provoquée par un phytoplasme transmis par la cicadelle ampélophage *Scaphoideus titanus*. Elle affecte désormais de nombreuses régions viticoles en Europe du sud où elle provoque d'importantes pertes de rendement et des coûts de gestion élevés pour l'industrie viticole. En raison de son potentiel épidémique, le phytoplasme de la flavescence dorée est un organisme de quarantaine en Europe et fait donc l'objet d'une réglementation spéciale visant à limiter sa propagation. Cette réglementation impose la mise en oeuvre des seuls outils de lutte que sont la surveillance, l'arrachage des vignes infectées, le traitement à l'eau chaude des plants de pépinière et les traitements insecticides contre les populations de l'insecte vecteur.

Le mode de transmission des phytoplasmes par leurs insectes vecteurs est de type circulant et multipliant. Les phytoplasmes ingérés avec la sève d'une plante infectée arrivent dans la lumière de l'intestin moyen de la cicadelle et adhèrent à son épithélium. Une fois internalisés dans ces cellules intestinales, les phytoplasmes s'y multiplient et doivent traverser la membrane basale de l'épithélium de l'intestin moyen, circuler dans l'hémolymphe pour coloniser l'insecte et atteindre les glandes salivaires dont ils colonisent une partie des cellules. Ils sont alors transmis à une nouvelle plante lors de la prise alimentaire de l'insecte vecteur dont la salive contient les phytoplasmes. Ce cycle implique plusieurs interactions spécifiques entre les phytoplasmes et les protéines de l'insecte, qui reflète un degré de spécialisation des phytoplasmes pour une ou plusieurs espèces d'insectes vecteurs. Mieux comprendre l'interaction phytoplasme-insecte vecteur pourrait aider au développement de techniques innovantes pour contrôler les épidémies de FD. Le mécanisme moléculaire de colonisation des tissus de l'insecte vecteur par le phytoplasme n'a pas encore été décrypté mais il a été démontré que la protéine de surface VmpA du phytoplasme FD est une adhésine qui intervient dans les étapes précoces d'adhésion aux cellules de la cicadelle vectrice. La protéine VmpA interagit avec les résidus N-acetyl-glucosamine et mannose portés par les glycoprotéines membranaires de l'insecte vecteur. De plus, une étude européenne de génétique des populations des phytoplasmes FD couplée à des essais de transmissions par différentes

cicadelles vectrices dans les vignobles et leurs environnements a montré que seules certainesvariations de séquence de l'adhésine VmpA sont corrélées à la capacité de vection par la cicadelle *S. titanus*.

Dans ce contexte, l'objectif de mon projet de thèse était d'identifier les protéines d'insecte interagissant avec la VmpA. Pour tester l'interaction de la VmpA avec ses cibles potentielles chez l'insecte vecteur, j'ai opté pour des approches *in vitro* et *in vivo.*

L'approche *in vitro* a consisté à capturer sur une colonne d'affinité au nickel les complexes formés *in vitro* entre la large partie hydrophile de la VmpA marquée en C-terminal par six résidus histidine (VmpA-His_6) et les glycoprotéines des cellules de l'insecte vecteur *Euscelidius variegatus* en culture (cellules Euva). Les protéines ainsi capturées ont été caractérisées par leur profil en spectrométrie de masse nLC-MS/MS. Ces profils peptidiques ont été comparés aux profils des bases de données protéiques mais aussi à ceux du protéome d'*E. variegatus* prédit à partir de son transcriptome. Pour sélectionner les candidats parmi les nombreuses protéines capturées, les protéines candidates ont été triées en fonction de leur spécificité d'interaction avec la VmpA, de la présence dans leur séquence de sites potentiels de N-glycosylation et de segments transmembranaires compatibles avec leur localisation à la surface des cellules de l'insecte. L'endoplasmine, le récepteur au facteur de croissance EGF, une protéine E3 ubiquitin ligase HERC4-like et le Tumor Necrosis Factor wengen ont été ainsi sélectionnés.

Au vu du faible nombre de protéines membranaires représentées dans les fractions éluées de la colonne d'affinité, nous avons extrait les protéines membranaires des cellules d'*E. variegatus* en culture avec des tampons enrichis en détergents. Les fractions protéiques solubilisées et insoluble ont été séparées par électrophorèse dénaturantes en gel de polyacrylamide (SDS-PAGE), transférées sur membrane puis soumises à des essais d'interaction *in vitro* avec la protéine VmpA-His_6. Les bandes correspondant aux signaux d'interactions ont été excisées du gel de polyacrylamide et les protéines éluées ont été analysées par spectrométrie de masse nLC-MS/MS à la Plateforme Protéome de l'Université de Bordeaux. Les protéines candidates dont la masse molaire correspondait à celle des signaux d'interaction, dont la séquence présentait des sites potentiels de N-glycosylation et des segments transmembranaires, ont été sélectionnées. Il s'agit de l'integrin β, d'un récepteur CD36-like, d'un récepteur draper-like, d'une protéine LDL-like cueball, de la fasciclin, d'un

échangeur sodium-calcium, deux protéines de fonction inconnue caractérisées par des domaines leucine rich repeat (LRR) répétés (uk1_LRR, uk2_TLR) et une protéine inconnue (uk3).

Dans nos expériences, nous avons exploité un modèle *ex vivo* composé de cellules Euva et de billes de latex fluorescentes recouvertes de protéine VmpA-His_6 pour "imiter" le phytoplasme. Bien entendu, ce système est une simplification des conditions naturelles beaucoup plus complexes dans lesquelles se produit l'infection de l'insecte vecteur par le phytoplasme. Les résultats doivent donc être interprétés avec les précautions qui s'imposent. Cependant, ce système nous a permis de cribler rapidement les protéines candidates interagissant avec VmpA. L'utilisation de billes recouvertes de VmpA au lieu d'un phytoplasme vivant nous a permis d'éviter les problèmes liés à la concentration et à la viabilité des phytoplasmes FD préparés à partir d' insectes ou de plantes infectés. En effet, les phytoplasmes ne pouvant pas être cultivés *in vitro* à ce jour, l'obtention du matériel infectieux et la récupération des bactéries nécessite la production d'un très grand nombre de plantes et d'insecte infectées en serre de confinement. De plus, ce système simplifié nous permet d'étudier le rôle de la seule VmpA dans l'interaction avec les cellules d'insectes sans l'effet masquant d'autres adhésines ou facteurs membranaires du phytoplasme.

L'étape de validation de l'interaction avec la VmpA a alors consisté à mesurer l'effet de la baisse de l'expression des gènes candidats provoquée par interférence ARN (RNAi) sur l'adhésion aux cellules Euva de billes fluorescentes recouvertes de VmpA. Les treize gènes codant les protéines candidates retenues par l'approche *in vitro* ont été clonés à partir de l'ADNc d'*E. variegatus* pour la production de d'ARN double brin (ARNdb) employés dans les essais de RNAi. L'expression des gènes ciblés a été significativement réduite dans les cellules Euva transfectées par les ARNdb. Cette technique de RNAi a aussi été utilisée pour inhiber simultanément l'expression de douze gènes, tout en gardant un niveau d'inhibition comparable à celui obtenu dans le cadre de l'inhibition d'un seul gène. Cette inhibition multiple a été sans conséquence négative sur la capacité des cellules à se multiplier et à atteindre la confluence. L'adhésion des billes, comptées par observations au microscope à fluorescence, a été comparée avec l'adhésion des billes dans la condition témoin où les cellules étaient traitées avec de l'ARNdb ciblant un gène GFP inexistant chez *E. variegatus*. Nos

résultats ont montré que, lorsque l'expression de la protéine uk1_LRR était inhibée, les billes recouvertes de VmpA adhéraient significativement moins aux cellules Euva.

Cette protéine uk1_LRR est constituée de 4 domaines LRR (Leucine Rich Repeat) et les prédictions structurales indiquent qu'elle forme une structure en fer à cheval typique de protéines impliquées dans des interactions protéine-protéine. L'expression de uk1_LRR a été mesurée par PCR en temps réel chez des insectes *E. variegatus* infectés ou non-infectés par le phytoplasme FD. L'expression de uk1_LRR est restée stable chez les insectes non infectés tout au long de notre suivi de 40 jours alors que chez les insectes infectés, une augmentation de son expression a été constatée 7 jours après le début de l'acquisition de phytoplasmes sur plante infectée ainsi qu'à 28 jours, qui correspond probablement à une nouvelle phase d'acquisition par ingestion *de novo* du phytoplasme transmis à la fève durant la latence. Des insectes sains ont été disséqués pour évaluer l'expression de la protéine uk1_LRR par PCR en temps réel dans les intestins, les glandes salivaires et les ovaires. Le gène uk1_LRR était 6 fois plus exprimé dans les intestins par rapport aux glandes salivaires et 18 fois plus par rapport aux ovaires. Ces résultats sont compatibles avec une possible implication de la protéine uk1_LRR dans les étapes précoces de l'interaction entre le phytoplasme FD et son insecte vecteur, notamment, dans les phases suivant l'ingestion de la sève infectée.

Pour l'approche *in vivo*, la technique du double hybride chez la levure *Saccharomyces cerevisiae* a été utilisée pour visualiser d'éventuelles interactions entre la VmpA et l'ensemble des protéines de l'insecte vecteur *E. variegatus*. Aucun résultat positif d'interaction n'a été obtenu indiquant la faible propension de la VmpA aux interactions de type «protéine-protéine».

En conclusion, les travaux effectués dans le cadre de ma thèse ont amené à l'identification d'une protéine contenant des domaines LRR impliquée dans l'adhésion de la VmpA du phytoplasme de la flavescence dorée aux cellules en culture de l'insecte vecteur *E. variegatus*. Le rôle de cette protéine dans la transmission du phytoplasme aux plantes et dans la spécificité de vection restent à confirmer.

Si les essais de transmission et de spécificité du vecteur révèlent un rôle important de l'uk1_LRR dans la perturbation de la transmission du phytoplasme FD aux plantes, nous pourrions imaginer le développement de nouvelles stratégies pour gérer les épidémies. Si

l'inhibition du récepteur par les ARNdb s'avère efficace chez l'insecte, la technologie de l'inhibition génique induite par pulvérisation des ARNdb pourrait être exploitée et adaptée à l'application dans les vignobles. Le récepteur uk1_LRR devra être mieux caractérisé sur le plan structurel et fonctionnel. Cela pourrait contribuer au développement d'approches visant à perturber la transmission par compétition médiée par les insectes, comme cela a été développé, à titre d'exemple, pour la bactérie phytopathogène *Xylella fastidiosa* transmise par des cicadelles xylémophages. Ces outils pourraient aider à la mise en place de nouvelles stratégies de gestion des épidémies de FD dans les vignobles, dans le but de réduire l'apport d'insecticides pour le contrôle des populations de vecteurs.

De plus, le dispositif expérimental utilisé pour réaliser nos expériences s'est avéré adapté à l'étude des interactions entre les protéines des pathogènes et les protéines de leurs insectes vecteurs. Il pourrait donc être exploité pour étudier, moyennant des adaptations appropriées, d'autres pathosystèmes d'intérêt pour aider à mieux comprendre les mécanismes sous-jacents à ce type d'interactions.

Introduction générale

- ## Découverte, caractérisation, propriétés cellulaires et moléculaires des phytoplasmes

  - ### Découverte et caractérisation initiale des phytoplasmes

Avant la découverte des phytoplasmes, on pensait que les agents responsables de nombreuses jaunisses végétales étaient des virus. En effet, il n'était pas possible de cultiver les pathogènes associés à la maladie et, comme certains virus végétaux, ils pouvaient être transmis par des insectes hémiptères suceurs de sève tels que les cicadelles. De plus, les extraits de plantes malades passés à travers des filtres de 0,45 µm conservaient leur infectivité puisqu'ils pouvaient être réinjectés aux insectes vecteurs pour être transmis aux plantes.

Des phytoplasmes ont été observés pour la première fois par microscopie électronique en 1967 dans les tubes criblés de plantes affectées par le jaunissement, le nanisme ou les proliférations de tiges (Doi *et al.*, 1967). À l'époque, les phytoplasmes étaient appelés organismes de type mycoplasme (mycoplasma-like organism, MLO) en raison de leur ressemblance morphologique avec les mycoplasmes humains et animaux. Leurs caractéristiques phénotypiques observées dans des coupes ultrafines du phloème de plantes infectées consistent en des corps pléiomorphes de 100 à 800 nm entourés d'une membrane unitaire dépourvue de paroi cellulaire rigide. Dans leur publication, Doi et ses collègues mentionnent également un rapport récent qui décrit la disparition des symptômes de la plante et des corps pléiomorphes lors du traitement des plantes malades avec des tétracyclines.

En 1969, Hirumi et Maramorosch ont confirmé la présence de MLO dans les glandes salivaires d'insectes vecteurs de l'agent de la jaunisse de l'aster (Hirumi et Maramorosch, 1969).

En 1989, la comparaison des séquences et l'analyse phylogénétique du gène de l'ARNr 16S d'un MLO de l'Aster Yellows (AY) ont révélé que les MLO de l'AY devraient être provisoirement placés dans la classe des *Mollicutes* avec les mycoplasmes, les uréaplasmes, les spiroplasmes et

les acholeplasmes et qu'ils pourraient être plus étroitement apparentés aux acholeplasmes (Lim et Sears, 1989). Lim et Sears ont confirmé la parenté évolutive des MLO avec les acholeplasmes en déterminant que le MLO AY :

- utilise UGA comme codon stop, comme les acholeplasmes mais contrairement aux mycoplasmes et aux spiroplasmes, comme le montre la séquence de ses gènes de protéines ribosomiques *rplB*, *rpsS*, *rplV* et rpsC (Lim et Sears, 1991).
- est plus proche des acholeplasmes que des mycoplasmes selon l'analyse phylogénétique de ses gènes de protéines ribosomiques *rplV* et rpsC (Lim et Sears, 1992).
- ressemble aux acholeplasmes cultivés en l'absence de stérols car ils résistent à la digitonine qui solubilise les membranes et précipite le cholestérol, et sont sensibles aux solutions salines hypotoniques. L'AY MLO a cependant pu être différencié des acholeplasmes cultivés sans stérols par sa plus grande résistance à la lyse dans des solutions hypotoniques de saccharose (Lim *et al.*, 1992).

Par conséquent, le terme « phytoplasme » a été adopté en 1994 par l'équipe de travail sur les phytoplasmes lors du congrès 10th de l'Organisation internationale de mycoplasmologie, qui s'est tenu à Bordeaux, en France. Depuis leur découverte, les phytoplasmes ont été associés à des milliers de maladies végétales différentes avec une répartition mondiale (Rao *et al.*, 2018). Contrairement à la plupart des mycoplasmes animaux et humains, les phytoplasmes sont restés jusqu'à présent incultivables *in vitro*. Cela a limité leur caractérisation, leur identification et leur classification, ainsi que leur diagnostic, jusqu'à l'apparition des techniques moléculaires dans les années 1980-1990.

- Classification des phytoplasmes

Selon la taxonomie officielle les phytoplasmes sont classés dans l'embranchement bactérien *Mycoplasmatota* (anciennement *Tenericutes*), dans la classe *Mollicutes*, ordre *Acholeplasmatales*, famille *Acholeplasmataceae,* genre « *Candidatus* Phytoplasma » bien que le

manuel de Bergey pour la bactériologie déterminative place ce genre dans une famille sans nom et *incertae sedis* (Gasparich *et al.*, 2020).

Les premières tentatives de classification des phytoplasmes en groupes étaient basées sur la réactivité croisée d'anticorps monoclonaux et polyclonaux et sur l'hybridation croisée de sondes constituées d'ADN spécifique de phytoplasmes clonés (Lee *et al.*, 2000). Ensuite, l'avènement de la réaction en chaîne par polymérase (PCR) a stimulé la conception d'amorces universelles et spécifiques à un groupe, basées sur des régions hautement conservées des séquences du gène ribosomique 16S, pour le diagnostic et l'identification des phytoplasmes. Une classification plus précise a été possible en utilisant la technique RFLP (Restriction fragment length polymorphism) et les analyses phylogénétiques, (Lee, 1993 ; Schneider *et al.*, 1993). Actuellement, la classification des phytoplasmes comprend un total de 37 groupes. Outre la description en tant que groupe, il est possible de déclarer des espèces « *Candidatus* Phytoplasma species » (**tableau 1**). Les règles de description d'une nouvelle espèce ont été proposées par l'IRPCM Phytoplasma/Spiroplasma Working Team-Phytoplasma Taxonomy Group en 2004 (The Irpcm Phytoplasma/Spiroplasma Working Team-Phytoplasma Taxonomy Group, 2004). Ces règles ont été récemment mises à jour par de nouvelles lignes directrices (Bertaccini *et al.*, 2022). Celles-ci consistent en :

- une longueur minimale de la séquence d'ARNr 16S de 1500 pb
- la nouvelle espèce de phytoplasme doit partager moins de 98,65 % d'identité sur la séquence de l'ARNr 16S avec les espèces précédemment établies

ou

- si l'identité de l'ARNr 16S est supérieure à 98,65 %, au moins deux gènes de ménage conservés tels que *groEL*, *tuf, rp, secA, secY* doivent être utilisés pour délimiter la nouvelle espèce (approche MLSA).

Une séquence du génome entier couplée à la méthode de l'identité nucléotidique moyenne (ANI) a également été proposée pour la délimitation des espèces de « *Ca*. Phytoplasma ».

- Transmission et lutte prophylactique contre les maladies à phytoplasmes

Les phytoplasmes se limitent à la sève du phloème de la plante et sont transmis par les cicadelles (Cicadellidae), les fulgores (Fulgoroidea) et les psylles (Psyllidae) (Weintraub et Beanland, 2006). Ils effectuent un cycle de propagation persistant dans leurs insectes vecteurs où ils doivent envahir et traverser deux barrières principales, l'épithélium de l'intestin moyen et les cellules des glandes salivaires dans lesquelles ils se multiplient (Maillet et Gouranton, 1971). Ainsi, après leur ingestion de sève infectée, l'adhésion des phytoplasmes à la surface apicale des cellules intestinales du vecteur constitue une étape initiale et critique dans l'invasion des insectes. Une fois cette première barrière franchie, l'adhésion des phytoplasmes aux cellules des glandes salivaires est également critique pour la transmission à la plante qui se fait par injection de salive infectée. Un phytoplasme donné a un ou plusieurs insectes vecteurs en fonction du niveau de spécificité de l'interaction.

Les maladies à phytoplasme peuvent également être propagées par greffage et multiplication végétative par la production de boutures à partir de matériel végétal infecté par le phytoplasme dans les pépinières, par des tubercules de stockage, des rhizomes ou des bulbes (Lee *et al.*, 2000). Les mêmes auteurs signalent qu'il n'y a pas de preuves substantielles de la transmission des phytoplasmes par les semences. Cette voie de transmission semble peu probable en raison de l'absence de connexions vasculaires directes entre les plantes et leurs graines et aussi parce que les plantes infectées par des phytoplasmes ne produisent généralement pas de semences viables.

Comme il n'existe pas de méthode curative contre les phytoplasmes, la lutte contre les maladies associées aux phytoplasmes repose sur des mesures prophylactiques basées sur la surveillance des maladies, l'élimination des plantes infectées dans les champs de production et les pépinières, et les traitements insecticides contre les insectes vecteurs (Weintraub et Wilson, 2009).

- Caractéristiques du génome des phytoplasmes

La taille du génome des phytoplasmes varie de 530 à 1350 kbp, selon l'électrophorèse sur gel en champ pulsé (Marcone *et al.*, 1999). Il est constitué d'une molécule d'ADN chromosomique circulaire à double brin, sauf pour « *Ca.* P. mali », « *Ca.* P. pruni » et « *Ca.* P. prunorum » qui possèdent un chromosome linéaire (Kube *et al.*, 2008). Chez certaines espèces comme « *Ca.* P. asteris », « *Ca.* P. australiense », « *Ca.* P. pruni », « *Ca.* P. trifolii » et « *Ca.* P. aurantifolia », de petits plasmides circulaires extrachromosomiques de 3 à 5 kbp ont été décrits, dont certains pourraient avoir une origine virale en raison de la similitude de leur réplicase avec les réplicases des Geminivirus (Rekab *et al.*, 1999 ; Nishigawa *et al.*, 2001 ; Oshima *et al.*, 2001). D'après leurs séquences, les génomes des phytoplasmes sont caractérisés par une faible teneur en GC allant de 21 à 28 %, possèdent 2 opérons ribosomiques et 31 à 35 ARNt (Kube *et al.*, 2012). Le nombre de gènes codant pour des protéines varie de 481 pour « *Ca*. P. mali » à 1126 pour la souche « *Ca.* P. australiense » souche OY-M (Kube *et al.*, 2012 ; Andersen *et al.*, 2013).

Par rapport à d'autres mollicutes, la réduction du génome des phytoplasmes a entraîné une plus grande perte de gènes métaboliques. Les phytoplasmes sont dépourvus de gènes pour les ATP synthases F1F0, les enzymes de la voie des pentoses phosphates, les systèmes PTS pour l'importation des sucres, les enzymes pour la synthèse des nucléotides et pour la maturation post-traductionnelle des lipoprotéines (Oshima *et al.*, 2004). De manière surprenante, « *Ca.* P. mali » ne possède pas d'enzymes pour la partie de la glycolyse productrice d'ATP, qui s'arrête à donc à l'étape du glycérol-3-P et pourrait servir à la synthèse des phospholipides membranaires (Kube *et al.*, 2008). En contrepartie, les génomes des phytoplasmes codent pour diverses ATP synthases de type P et des transporteurs ABC, ce qui suggère leur forte dépendance au métabolisme de l'hôte et leur adaptation à une vie intracellulaire dans un environnement riche en nutriments. Des gènes codant pour des protéines impliquées dans la réplication de l'ADN, la transcription, la traduction et la translocation des protéines sont présents, ainsi qu'un système de sécrétion complet (Sec) qui permet l'insertion de protéines transmembranaires dans la membrane cellulaire ainsi que la libération d'effecteurs, des protéines ayant un impact sur le développement et la santé de l'hôte. « *Ca.* P. mali » et le phytoplasme de la flavescence dorée possèdent un

ensemble étendu de gènes pour la recombinaison homologue, tandis que « *Ca*. P. asteris » et « *Ca*. P. australiense » sont dépourvus de *recA*, *recG*, *recU*, *ruvA*, *ruvB* et d'un gène pour « holliday junction resolvase » (Kube *et al.*, 2008 ; Debonneville *et al.*, 2022).

Malgré la taille limitée des génomes de phytoplasmes, des séquences répétées sont présentes, une caractéristique partagée avec d'autres Mollicutes mais avec une organisation particulière. Dans les phytoplasmes, les gènes multicopies et les éléments de type transposon sont organisés en unités mobiles potentielles (PMU) (Bai *et al.*, 2006) et certaines de ces PMU semblent dégénérées (Jomantiene *et al.*, 2007 ; Wei *et al.*, 2008). Ces régions, bordées par des répétitions inversées de 330 pb, contiennent des gènes de réplication et de recombinaison ainsi que des gènes codant pour des facteurs de transcription, des protéines membranaires et des effecteurs sécrétés (Bai *et al.*, 2006). En effet, des données basées sur des génomes bactériens séquencés ont révélé que les gènes impliqués dans la pathogénicité/virulence sont probablement issus de l'intégration dans le génome bactérien de transposons ou de phages et sont donc localisés dans des îlots génomiques spécifiques appelés îlots de pathogénicité (PAIs) (Gal-Mor et Finlay, 2006). Une analyse comparative des génomes de deux souches de « *Ca.* P. asteris » a révélé la présence de PMU représentant 14 à 23% du chromosome (Bai *et al.*, 2006) et il a été estimé qu'en général, leur abondance explique près de 80 % de la variance de la taille du génome des phytoplasmes (Huang *et al.*, 2022). Ces régions répétées, contenant également des gènes codant pour des effecteurs, pourraient avoir un rôle dans l'adaptation des phytoplasmes aux différents environnements cellulaires et hôtes qu'ils colonisent. En effet, dans l'AY-WB, les gènes PMU1 sont plus fortement exprimés pendant la colonisation des insectes par rapport aux plantes (Toruño *et al.*, 2010). À plus grande échelle, il est suggéré que la régulation de l'expression des PMUs pourrait être une stratégie d'adaptation à différents environnements et que leur réarrangement pourrait augmenter les chances de changement d'hôte et d'occupation de nouvelles niches (Bai *et al.*, 2006) même si la gamme d'hôtes végétaux est principalement limitée par le comportement alimentaire des vecteurs compétents pour le phytoplasme. En outre, il existe des preuves solides que les composants des PMU ont été échangés au cours de l'évolution des phytoplasmes (Chung *et al.*, 2013). À l'appui de ce scénario, il a été montré que la souche

Witches' Broom (AY-WB) de l'Aster Yellows phytoplasma peut s'exciser des chromosomes sous une forme circulaire extrachromosomique (Toruño *et al.*, 2010).

Le génome complet d'une souche de phytoplasme de la flavescence dorée (FDp) isolée en Suisse a été publié en 2022 (Debonneville *et al.*, 2022) et des publications partielles complètes de la carte génétique des chromosomes et du génome de la souche FD92 (Malembic-Maher *et al.*, 2008 ; Carle *et al.*, 2011). La souche FDp CH possède un chromosome circulaire de 654 223 pb avec une teneur en G/C de 21,7 %. Parmi les principales caractéristiques métaboliques, le génome de CH code pour une voie complète de glycolyse et d'oxydation du pyruvate, une enzyme malolactique, une lactate déshydrogénase, une voie incomplète de biosynthèse des acides gras et aminés, des transporteurs ABC, un système complet de sécrétion des protéines, un faible nombre d'effecteurs sécrétés putatifs, des métalloprotéases à zinc ATP-dépendantes, un ensemble de gènes permettant la recombinaison homologue ainsi que six gènes ayant une fonction d'endonucléase. Aucune région semblable aux PMU n'a été identifiée, mais des gènes caractéristiques de ces structures ont été trouvés en copie unique et dispersés sur le génome circulaire.

Le séquençage récent de la souche FD92 de FDp longue de 647 kbp a mis en évidence un nombre inhabituel de gènes codant pour des zinc-protéases FtsH dépendantes de l'ATP, qui ont été précédemment associés à des variations dans la virulence des souches de « *Ca.* P. mali » (Seemüller *et al.*, 2013). Huit gènes *ftsH* complets ont été identifiés dans le génome de FD92 (Carle *et al.*, 2011 ; Jollard *et al.*, 2020). En plus de *ftsH6*, qui semble être l'orthologue bactérien original, les sept autres copies de gènes étaient regroupées sur une branche phylogénétique commune et distincte, ce qui suggère une duplication intra-génome des gènes *ftsH* plutôt que l'acquisition de copies multiples par transfert horizontal de gènes. L'expression des gènes *ftsH* semble être modulée en fonction de l'hôte. Le logiciel Phobius a prédit que deux des huit queues C de FtsH étaient extracellulaires et donc en contact direct avec le contenu cellulaire de l'hôte. Comme les phytoplasmes ne peuvent pas synthétiser d'acides aminés, ces données suggèrent que la FtsH du phytoplasme pourrait potentiellement améliorer le recyclage des protéines cellulaires du phytoplasme et promouvoir la dégradation des protéines de l'hôte (Jollard *et al.*, 2020).

- Flavescence dorée

  - Symptomatologie

La Flavescence Dorée (FD) est une maladie épidémique de la vigne classée dans la catégorie des jaunisses de la vigne (GY). La FD a été signalée pour la première fois en France en 1954 (Caudwell, 1957) et s'est depuis répandue dans les zones viticoles de quatorze pays européens (**Figure 2**), où elle provoque d'importantes pertes de rendement et de lourds coûts de gestion pour l'industrie viticole (Jeger *et al.*, 2016). Les GY sont associés à des phytoplasmes appartenant aux différents sous-groupes taxonomiques 16SrI, III, V, VII, XII qui induisent les mêmes symptômes : décoloration telle que le rougissement chez les cultivars rouges et le jaunissement chez les cultivars blancs, enroulement des feuilles vers le bas, lignification incomplète ou inexistante des sarments, flétrissure et dessèchement des raisins et des vrilles (**Figure 1)** (Boudon-Padieu, 2005 ; Constable, 2009). La vigne malade et infectée par la FDp peut se rétablir, bien que la capacité de rétablissement dépende des cultivars (Caudwell, 1961 ; Osler *et al.*, 2004).

La FD est associée à des phytoplasmes appartenant au groupe 16rS V sous-groupes C et D (FDp) (Caudwell *et al.*, 1971 ; Davis et Dally, 2001). Les phytoplasmes des deux sous-groupes sont transmis d'un plant de vigne à l'autre par la cicadelle vectrice *Scaphoideus titanus* (Schvester *et al.*, 1961 ; Mori *et al.*, 2002).

Les variétés de *vigne se* caractérisent par une sensibilité variable à la FD, et montrent une différence par rapport à l'incidence de la maladie et à la gravité des symptômes. À titre d'exemple, le cultivar italien Barbera s'est révélé très sensible à la FD, présentant de graves symptômes corrélés à des titres élevés de phytoplasme dans les plantes symptomatiques, tandis que le cultivar Nebbiolo ne présentait presque aucun symptôme et que les plantes étaient caractérisées par un titre plus faible de phytoplasme. (Roggia *et al.*, 2014). De même, dans la région viticole de Bordeaux, le Cabernet Sauvignon (CS) est classé comme un cultivar très sensible, tandis que le Merlot présente beaucoup moins de symptômes lorsqu'il est infecté par le FDp. Il a été démontré que les phytoplasmes dans le Merlot sont confinés à une zone limitée de la plante, près du site

d'alimentation de l'insecte, et que les charges de phytoplasmes étaient significativement plus faibles par rapport au CS, où les phytoplasmes ont été trouvés de manière systémique dans toute la plante (Eveillard *et al.*, 2016). De plus, la sensibilité variable de ces deux cultivars reflète la sensibilité de leurs parents, la Magdeleine noire des Charentes moins sensible pour le Merlot et le Sauvignon très sensible pour le CS. Le parent commun du Merlot et du CS, le Cabernet franc, a montré un degré de sensibilité intermédiaire, suggérant l'héritabilité génétique des traits de sensibilité au phytoplasme de la flavescence dorée dans les cultivars de *Vitis. Les* variétés moins sensibles ont également été associées à une survie plus faible du vecteur sur les plantes (Ripamonti *et al*, 2022a).

Les résultats des inoculations en serre de 28 variétés différentes de *Vitis* ont révélé un degré de sensibilité différent entre les accessions. Toutes les variétés ont développé des symptômes de FD et leur sévérité a été corrélée au titre de phytoplasme dans les plantes mesuré par PCR quantitative en temps réel (Eveillard *et al.*, 2016). Une autre étude menée sur 14 cultivars de vigne typiques de la région du Piémont (Italie) a révélé un degré variable de sensibilité entre les variétés, ce qui se traduit par une moindre sensibilité des cultivars Moscato, Brachetto, Freisa et confirme la faible sensibilité du Merlot aux symptômes de la FD. (Ripamonti *et al.*, 2021). Le Moscato et le Brachetto sont considérés comme des variétés aromatiques en raison de la présence accrue de composés aromatiques dans leurs feuilles et leurs baies, qui pourraient agir directement sur la colonisation de la plante par le phytoplasme ou indirectement en diminuant la survie des vecteurs sur la plante. L'efficacité de l'acquisition des vecteurs dépend à la fois des variétés de vigne et de la charge en phytoplasme, bien que ces deux paramètres ne soient pas toujours strictement corrélés (Galetto *et al.*, 2016). En effet, dans l'étude citée, un pourcentage plus élevé de *S. titanus* exposés a acquis le phytoplasme sur des variétés sensibles comme l'Arneis, même lorsque le titre de phytoplasme caractérisant les plantes était significativement inférieur à celui des cultivars moins sensibles, ce qui suggère que l'efficacité de l'acquisition par le vecteur détermine la propagation de la maladie, au moins à l'échelle du vignoble. Il est intéressant de noter qu'un profilage transcriptomique précoce comparatif sur des vignes exposées à des *S. titanus* infectés et non infectés a suggéré que l'infection par le FDp réprime les réponses de

défense induites par l'alimentation de l'insecte sur le cultivar de vigne Chardonnay (Bertazzon *et al.*, 2019).

Les *Vitis* sauvages et les porte-greffes tels que *V. rupestris*, *V. berlandieri* et *V. riparia,* principales espèces utilisées pour la sélection des porte-greffes, se caractérisent par une large gamme de titres de phytoplasmes tout en étant dépourvus de symptômes (Eveillard *et al.*, 2016). L'absence de symptômes constitue une difficulté pour la surveillance de la FD, car ces réservoirs de phytoplasmes constituent une source d'inoculum pour les foyers de FD dans les vignobles voisins (Lessio *et al.*, 2014).

- Surveillance et contrôle

En raison de son potentiel épidémique, la FDp est un organisme de quarantaine en Europe (liste A2 de l'OEPP, directive UE 2016/2031, règlement d'exécution de la Commission 2019/2072 et 2022/1630) et fait donc l'objet d'une réglementation spéciale, notamment

- plantation de matériel indemne de maladie
- surveillance annuelle des plantes symptomatiques dans les vignobles
- arrachage obligatoire des plants infectés dans les vignobles et les pépinières
- des traitements insecticides obligatoires dans des zones préconisées afin de réduire les populations de vecteurs.

La principale difficulté dans la gestion de la FD est la détection de la FDp dans les pépinières, car les porte-greffes de la vigne sont des porteurs sans symptômes qui transmettent la FDp aux cultivars sensibles greffés (Caudwell *et al.*, 1994). Les symptômes typiques de la FD apparaissent au cours de l'été de l'année qui suit l'inoculation des plantes, constituant une source d'inoculum pour *S. titanus* à la fin du printemps et au début de l'été avant leur détection au cours de la surveillance des vignobles en août-septembre. De plus, la coexistence de la FD avec le Bois noir, une autre maladie GY associée à « *Ca.* P. solani » et présentant la même symptomatologie peut retarder la détection des cas de FD.

La PCR multiplex en temps réel est couramment utilisée pour distinguer FDp d'autres phytoplasmes associés à GY tels que l'agent du Bois noir (Hren *et al.*, 2007 ; Angelini *et al.*, 2007 ; Pelletier *et al.*, 2009). Une fois confirmée par l'analyse moléculaire, les pieds infectés par le FDp sont arrachés et les parcelles de vignes présentant plus de 20 % d'infection sont entièrement éliminées.

Le traitement à l'eau chaude à 50°C pendant 45 minutes élimine le FDp de la vigne pour la plantation (Caudwell *et al.*, 1997). L'augmentation de l'utilisation de ce traitement dans le matériel de pépinière, combinée à une élimination accrue des vignobles abandonnés et des *Vitis* sauvages, devrait permettre de mieux limiter la propagation et l'impact de la FD (Jeger *et al.*, 2016).

- Épidémiologie, écologie et diversité génétique des phytoplasmes de la flavescence dorée

S. titanus, le vecteur naturel de la FDp dans les vignobles, est une cicadelle ampélophage, univoltine, allochtone, introduite au début du 20ème siècle en Europe depuis l'Amérique du Nord lors de l'importation de variétés américaines de *Vitis* destinées à être utilisées comme porte-greffe dans les vignobles européens pour surmonter la crise du phylloxéra. Le premier signalement de sa présence en Europe date de 1958 dans le sud-ouest de la France et, à partir de là, il se dissémine rapidement à travers le continent (Bonfils et Schvester, 1960 ; Chuche et Thiéry, 2014). Les populations européennes de *S. titanus* se sont avérées avoir une diversité limitée et, par conséquent, les introductions en provenance d'Amérique du Nord ont certainement été peu nombreuses (Papura *et al.*, 2012). *S. titanus* est désormais présent du Portugal à la Roumanie et du sud de l'Italie au nord-est de la France et de la Hongrie (**Figure 3**).

Le cycle de vie de *S. titanus*, représenté dans la **figure 4**, est entièrement accompli sur *Vitis* et a été décrit par Chuche et Thiéry (2014). Comme déjà mentionné, *S. titanus* est une espèce univoltine, ce qui signifie qu'elle se caractérise par une seule génération par an. Les œufs sont pondus d'août à septembre à l'intérieur de l'écorce des vignes à bois et hivernent pendant 6 à 8 mois. L'éclosion commence à la fin du printemps et dépend de la latitude, de l'altitude et de

l'année du vignoble ainsi que de la température, qui affecte le début, la dynamique et la durée de la période d'éclosion. Les adultes émergent au début de l'été après 5 à 8 semaines du premier stade nymphal. Les femelles deviennent matures 6 jours après l'émergence et ne s'accouplent qu'une seule fois, tandis que les mâles peuvent s'accoupler plusieurs fois.

Le phytoplasme de la FD s'acquiert en se nourrissant d'une vigne infectée dès le premier stade larvaire, même si les derniers stades nymphaux acquièrent le phytoplasme de manière plus efficace. Les phytoplasmes se multiplient d'abord dans les cellules épithéliales de la chambre de filtration, de l'intestin antérieur et de l'intestin moyen, puis atteignent l'hémolymphe d'où ils colonisent tous les organes sauf les tubes de Malpighi, les ovaires et les testicules, comme cela a été décrit pour *Euscelidius variegatus*, le vecteur expérimental du FDp (Lefol *et al.*, 1994). Une fois les glandes salivaires colonisées, généralement après plusieurs semaines, l'insecte reste infectieux tout au long de sa vie.

Les connaissances écologiques et génétiques sur l'épidémiologie de la FD ont révélé l'origine européenne du FDp (Malembic-Maher *et al.*, 2020). Alors que l'on pensait que la vigne était la seule plante hôte de la FDp, des phytoplasmes génétiquement apparentés au FDp ont été détectés au cours des années 2000 sur des aulnes (*Alnus glutinosa*) et des clématites (*Clematis vitalba*) (Angelini *et al.*, 2001 ; Arnaud *et al.*, 2007 ; Filippin *et al.*, 2009).

Pour mieux caractériser ces phytoplasmes, déchiffrer leurs cycles épidémiologiques et leur capacité à déclencher des foyers de FD, des aulnes, des clématites et des cicadelles ont été collectés en France, en Italie, en Allemagne, en Serbie et en Hongrie de 1995 à 2011 dans et autour de vignobles affectés ou non par des foyers de FD, ainsi que dans des zones non-viticoles. Plus de 80 % des aulnes collectés ont été trouvés infectés par des phytoplasmes du groupe 16SrV-C dans toutes les zones étudiées et la plupart d'entre eux étaient non symptomatiques. Les résultats ont également révélé une grande diversité génétique chez les aulnes avec 127 génotypes *map*, dont certains ont également été détectés dans les foyers de FD. Dans les foyers de FD, seuls 11 génotypes *map* ont été regroupés en trois groupes génétiques, map-FD1, FD2 et FD3, comme cela a été rapporté précédemment (Arnaud *et al.*, 2007). Ces données montrent l'existence d'un fort goulot d'étranglement entre les aulnes et la vigne. Les essais de transmission à la féverole

avec les cicadelles collectées sur les aulnes ont indiqué que les génotypes de phytoplasmes transmis par la cicadelle autochtone Macropsinae de l'aulne *Oncopsis alni* ne pouvaient pas être acquis et transmis par la cicadelle Deltocephalinae *S. titanus*. Au contraire, les génotypes de phytoplasmes transmis par les cicadelles Deltocephalinae *Allygus* sp. autochtones et *Orientus ishidae*, une cicadelle Deltocephalinae originaire d'Asie, ont pu être acquis et transmis par *S.* titanus (Malembic-Maher *et al.*, 2020).

Il est intéressant de noter que la variabilité des gènes de type adhésine *vmpA* et *vmpB* a permis de distinguer clairement trois groupes génétiques (**figure 5**). Le groupe Vmp-I regroupe les génotypes transmis uniquement par *O. alni*, tandis que les groupes Vmp-II et -III regroupent les génotypes transmis par les cicadelles Deltocephalinae et qui sont épidémiques dans les vignobles. Les analyses phylogénétiques des domaines répétés de VmpA et VmpB ont montré qu'ils ont évolué indépendamment dans le groupe Vmp-I, tandis que dans les groupes Vmp-II et-III, ils résultent de duplications récentes. Des billes de latex recouvertes de différents ratios de VmpA des groupes II et I ont montré que les VmpA du groupe II favorisaient une meilleure adhésion aux cellules épithéliales de l'espèce *Deltocephalinae Euscelidius variegatus* et étaient mieux retenus dans les intestins moyens d'*E. variegatus* et de *S. titanus* (Malembic-Maher *et al.*, 2020). Les auteurs ont donc conclu que les FDp étaient originaires des aulnes européens et que leur émergence en tant que pathogènes épidémiques de la vigne semblait limitée à certains variants génétiques possédant des adhésines Vmp compatibles avec les cicadelles Deltocephalinae telles que *S. titanus*. Le cycle écologique du FDp est résumé dans la **figure 6**. Une fois introduits dans le vignoble par l'alimentation occasionnelle des cicadelles de l'aulne Deltocephalinae, ces génotypes de phytoplasmes, compatibles avec la transmission par *S. titanus* et classés comme vectotypes II et III d'après leurs séquences de gènes vmp du groupe vmpII et III, ont acquis un potentiel épidémique élevé dans les vignobles en raison de l'abondance du vecteur et de sa nature ampélophage. Les phytoplasmes du vectotype I peuvent occasionnellement être détectés dans la vigne, mais ils ne déclenchent pas de foyers de FD (Malembic-Maher *et al.*, 2020). Ces génotypes non épidémiques sont classés comme isolats de la jaunisse de la vigne du Palatinat (PGY) car ils ont été initialement trouvés dans le sud-ouest de l'Allemagne avec *O. alni* comme vecteur de transfert (Maixner *et al.*, 2000). Un tiers de *C. vitalba* a été trouvé infecté dans des

zones viticoles et non viticoles en Italie, en Hongrie ou en Serbie, et en France en Bourgogne avec trois génotypes *map*, correspondant tous à des génotypes associés à des foyers de FD (Malembic-Maher *et al.*, 2020). Le seul vecteur signalé jusqu'à présent pour transmettre la FDp chez *C. vitalba* est la cicadelle *Dictyophara europaea* qui peut la transmettre expérimentalement à la vigne (Filippin *et al.*, 2009).

En France, 85 % des cas de FD sont associés au génotype M54, 15 % au génotype M50, avec très peu de cas de M38 et de variants de polymorphisme nucléotidique (SNP) de M50. (Malembic-Maher *et al.*, 2020). Dans les Balkans, M51 et M50 étaient prédominants jusqu'à ce que M54 apparaisse et augmente en fréquence (Plavec *et al.*, 2019 ; Krstić *et al.*, 2022). En Italie, M54, M3, M6, M12 et M50 ont été signalés jusqu'à présent (Arnaud *et al.*, 2007 ; Rossi *et al.*, 2019a ; Malembic-Maher *et al.*, 2020) mais un rapport récent n'a détecté que le génotype M54 (Rigamonti *et al.*, 2023). En Vénétie, les premiers foyers ont été associés à deux souches des sous-groupes taxonomiques 16SrV-C (FD-C, M3) et 16SrV-D (FD-D, M54), bien que seule la souche 16SrV-D ait pu être détectée chez *S. titanus* (Martini *et al.*, 1999). Des essais de transmission avec *S. titanus* ont en outre confirmé une efficacité de transmission plus élevée pour cette souche FD-D (M54) (Mori *et al.*, 2002). Cependant, lorsqu'elle est en compétition dans la pervenche de Madagascar ou en condition d'acquisition alimentaire mixte par la cicadelle vectrice expérimentale *E. variegatus*, la souche FD-C (M12) prend le dessus sur la souche FD-D (M54) (Rossi *et al.*, 2020 ; Rossi *et al.*, 2023).

Des études de modélisation (modèles spatiaux bayésiens) ont permis de mieux comprendre l'épidémiologie et la dispersion de la FD à l'échelle du paysage (Adrakey *et al.*, 2022). La probabilité d'infection par la FD dépend à la fois de l'environnement des vignobles et de la composition des cépages de la région. La probabilité d'infection par la FD augmente avec les proportions de forêts, de terrains urbains et d'agriculture biologique, tandis qu'elle diminue avec la proportion de vignobles. Les habitats semi-naturels peuvent en effet abriter des réservoirs de phytoplasmes de la FD tels que la *vigne* sauvage. La proportion de cultivars sensibles dans la zone augmente également de manière significative la probabilité d'infection par la FD.

La capacité de dispersion des adultes de *S. titanus* est assez faible, 25-30 mètres en dehors du vignoble (Lessio et Alma, 2004), mais les individus provenant de populations hébergées par des *Vitis* sauvages peuvent migrer dans un vignoble contigu jusqu'à 330 mètres, bien que 80% d'entre eux ne volent pas au-delà de 30 mètres (Lessio *et al.*, 2014). Par conséquent, la dispersion interrégionale des vecteurs est probablement liée à des activités humaines telles que le commerce des boutures de vigne. Néanmoins, certains rapports faisant état d'une longue dispersion de *S. titanus* et de cas de FD probablement dus à l'effet du vent ont été suggérés (Steffek *et al.*, 2007).

Le dernier rapport de l'EFSA inclut une perspective de propagation de la FD. D'après l'étude de modélisation CLIMEX de *S. titanus*, les régions viticoles de l'est, du centre et du nord de l'Europe exemptes de *S. titanus* jusqu'à ce jour, offriront dans les années à venir de bonnes conditions climatiques pour son établissement. Cependant, la poursuite de l'établissement de *S. titanus* dans les régions septentrionales sera limitée par l'absence de production extensive de vignes et donc par la distribution des plantes hôtes (Jeger *et al.*, 2016). Il faut tenir compte du fait que les zones géographiques propices à la culture de la vigne sont susceptibles de changer en raison de la perte de conditions climatiques adaptées liée au changement climatique (examiné dans Droulia et Charalampopoulos, 2021). Des températures plus chaudes et un déficit hydrique pendant la saison de culture de la vigne dans les zones viticoles du sud de l'Europe (*c'est-à-dire* le sud de la France, le sud de l'Italie, l'Espagne, le Portugal et la Grèce) entraîneront une redistribution des vignobles vers les zones qui sont aujourd'hui considérées comme trop froides pour y cultiver la vigne.

- ## Interaction du phytoplasme avec les hôtes

Les phytoplasmes sont des parasites obligatoires capables de coloniser à la fois le phloème des plantes et les insectes vecteurs. Les phytoplasmes modifient l'expression de leurs gènes lors du changement d'hôte. Une analyse menée sur « *Ca.* P. asteris » OY-M prélevée sur des plantes et des insectes infectés dans des conditions contrôlées, a révélé que 246 gènes (près de 33 % du nombre total de gènes) codant pour des transporteurs, des effecteurs et des gènes glycolytiques

étaient exprimés de manière différentielle dans les deux hôtes, peut-être sous la régulation de deux facteurs de transcription sigma différents trouvés dans le génome du phytoplasme (Oshima *et al.*, 2011).

Chez les plantes et les insectes hôtes, les phytoplasmes sont intracellulaires et toutes les protéines sécrétées sont donc directement en contact avec la machinerie de la cellule hôte. Les protéines sécrétées par les phytoplasmes dont il a été démontré qu'elles agissent comme effecteurs sont TENGU, SAP11, SAP54 et SAP05 pour « *Ca.* P. *asteris* » (Hoshi *et al.*, 2009 ; Sugio *et al.*, 2011a ; MacLean *et al.*, 2014 ; Huang *et al.*, 2021) et PM19_00185, pour « *Ca*. P. mali » (Strohmayer *et al.*, 2019). Jusqu'à présent, seuls SAP11 et SAP54 se sont révélés avoir un effet direct ou indirect sur les populations d'insectes vecteurs (Sugio *et al.*, 2011a ; MacLean *et al.*, 2014 ; Orlovskis et Hogenhout, 2016).

- Interaction entre le phytoplasme et la plante hôte

Les phytoplasmes habitent les tubes criblés du système vasculaire phloémien de la plante. Les cellules criblées sont reliées entre elles par des plaques criblées caractérisées par de petits pores permettant le transport des nutriments et, dans le cas d'une plante infectée, des phytoplasmes qui se propagent ainsi de manière systémique à travers la plante. (Christensen *et al.*, 2004). L'infection par le phytoplasme affecte gravement la fonction du phloème, entraînant l'effondrement des éléments criblés suite au dépôt de callose et à la nécrose. En outre, l'infection par le phytoplasme affecte gravement le transport des sucres dans la plante et provoque l'accumulation anormale de saccharose et d'amidon dans les feuilles sources matures (Lepka *et al.*, 1999).

Les phytoplasmes altèrent l'équilibre hormonal et le développement des plantes hôtes, provoquant une variété de symptômes. Les symptômes les plus courants des maladies à phytoplasmes se traduisent par un développement anormal des tissus et des organes, notamment la virescence (présence anormale de chlorophylle dans les organes floraux qui restent verts), la phyllodie (développement des parties florales en structures feuillues), le balais de

sorcière (prolifération de pousses auxiliaires et axillaires), l'allongement anormal des entrenœuds, le rabougrissement (entrenœuds anormalement courts et organes petits), la stérilité florale, la décoloration des feuilles et des pousses, l'enroulement des feuilles et la prolifération des feuilles à l'extrémité des tiges (**figure 7 ;** Marcone, 2014). Ces caractères acquis pourraient également avoir un rôle attractif pour les insectes vecteurs, qui préfèrent généralement les tissus jeunes et verts ou jaunissants pour se nourrir et pondre des œufs, ce qui entraîne une augmentation de la propagation des phytoplasmes parmi les populations de plantes hôtes (Hogenhout *et al.*, 2008). En outre, la stérilité induite des fleurs ou la conversion des fleurs en parties végétatives (phyllodie) pourrait retarder le passage à la reproduction et la mort, augmentant ainsi la phase de croissance végétative de la plante et permettant au phytoplasme de vivre plus longtemps dans sa plante hôte.

L'effecteur TENGU, une petite protéine de 38 acides aminés, identifiée pour la première fois dans le phytoplasme de l'« onion yellow » (OY), induit des entre-nœuds courts (nanisme) et le balai de sorcière lors d'une transfection transitoire chez *Nicotiana* benthamiana (Hoshi *et al.*, 2009). Les plantes transgéniques d'Arabidopsis exprimant TENGU présentaient les mêmes symptômes ainsi que des défauts de phyllotaxie et de stérilité florale. Les plantes transgéniques ont été caractérisées par une régulation négative significative des gènes répondant à l'auxine, ce qui explique le phénotype observé. L'analyse immuno-histochimique a révélé que TENGU était transporté du phloème, où les phytoplasmes étaient retenus, jusqu'aux bourgeons apicaux. De plus, il a été montré que TENGU induit la stérilité florale chez *Arabidopsis thaliana* en dérégulant les facteurs de réponse à l'auxine 6 et 8 (ARF6, ARF8) qui sont significativement régulés à la baisse à la fois dans les plantes transgéniques et dans les plantes infectées par le phytoplasme (Minato *et al.*, 2014). Cette dérégulation a entraîné une diminution de l'acide jasmonique et de l'auxine dans les bourgeons transgéniques, ce qui a nui à la signalisation hormonale et, par conséquent, au développement des fleurs. Il a également été démontré que TENGU supprime la mort cellulaire induite (Wang *et al.*, 2018a) et les protéases de l'hôte (Sugawara *et al.*, 2013).

L'effecteur SAP11 a un impact sur le développement de la plante hôte et renforce sa capacité à soutenir la reproduction de l'insecte vecteur par la modulation de la voie du jasmonate (Sugio *et al.*, 2011a). Il a été constaté que SAP11 et ses homologues interagissent avec des

facteurs de transcription spécifiques de l'hôte (Sugio *et al.*, 2011a ; Janik *et al.*, 2017 ; Wang *et al.*, 2018b ; Chang *et al.*, 2018 ; Pecher *et al.*, 2019). D'autres rapports ont indiqué que SAP11 était également impliqué dans l'interférence avec le système immunitaire et les réponses métaboliques de la plante hôte (Lu *et al.*, 2014 ; Tan *et al.*, 2016). Il est important de noter que des expériences d'immunolocalisation ont montré que TENGU et SAP11 se trouvaient dans des tissus végétaux autres que les tubes criblés du phloème où les phytoplasmes sont confinés, ce qui confirme que ces effecteurs sont sécrétés par les phytoplasmes et ensuite absorbés par les tissus puits de l'hôte (Bai *et al.*, 2009 ; Hoshi *et al.*, 2009).

L'effecteur SAP54, également connu sous le nom de PHYLLOGEN ou PHYL1, induit des transformations spectaculaires des parties florales en organes foliaires par la déstabilisation des facteurs de transcription MADS-box de l'hôte (MacLean *et al.*, 2011 ; MacLean *et al.*, 2014 ; Maejima *et al.*, 2014 ; Maejima *et al.*, 2015 ; Kitazawa *et al.*, 2017). SAP54 assure la médiation de la dégradation du facteur de transcription à domaine MADS (MTF) en interagissant avec les protéines de la famille RADIATION SENSITIVE23 (RAD23), des protéines eucaryotes qui font la navette entre les substrats et le protéasome. Les mutants *rad23* d'Arabidopsis ne présentent pas de conversion des fleurs en tissus semblables à des feuilles en présence de SAP54 et lors d'une infection par un phytoplasme, ce qui souligne l'importance de RAD23 pour l'activité de SAP54. Il est remarquable que les plantes avec des fleurs en forme de feuilles induites par SAP54 soient plus attrayantes pour la colonisation par les cicadelles vectrices du phytoplasme et que cette préférence de colonisation soit dépendante de RAD23 (MacLean *et al.*, 2014 ; Orlovskis et Hogenhout, 2016).

L'effecteur SAP05 de « *Ca.* P. asteris » se lie aux facteurs de transcription SPL et GATA des plantes ainsi qu'au récepteur d'ubiquitine RPN10 des plantes. Grâce à cette interaction, SAP05 assure la dégradation des SPL et des GATA par le biais d'un processus qui détourne RPN10, indépendamment de l'ubiquitination du substrat. En conséquence, SAP05 découple les transitions développementales des plantes et induit les symptômes du balai de sorcière (Huang et al., 2021).

- Interaction des phytoplasmes avec l'insecte hôte

Les phytoplasmes sont transmis par les cicadelles (Cicadellidae), les fulgores (Fulgoroidea) et les psylles (Psyllidae) (Weintraub et Beanland, 2006) de manière persistante et propagative (**Figure 8**). Les phytoplasmes sont acquis passivement par l'insecte lors de l'ingestion de tamis d'une plante infectée et se multiplient dans les tissus de l'insecte lors de la colonisation de l'hôte. En effet, l'injection de thymidine tritiée dans des abdomens d'*Euscelis lineolatus* infectés par des phytoplasmes, suivie de l'observation de coupes ultrafines des organes des insectes, a révélé que la multiplication des phytoplasmes se produit aussi bien au niveau extracellulaire (dans l'hémolymphe), que lorsque les phytoplasmes se trouvent à l'intérieur des cellules (dans le tube digestif et les glandes salivaires) (Gouranton et Maillet, 1973). La durée d'alimentation permettant d'acquérir une charge suffisante de phytoplasme est appelée « acquisition access period » (AAP) et sa durée dépend de l'association insecte-phytoplasme considérée. Après l'ingestion de sève infectée, l'adhésion des phytoplasmes à la surface apicale des cellules intestinales du vecteur constitue une étape initiale et critique dans l'invasion des insectes. Les phytoplasmes doivent ensuite franchir une première barrière constituée par l'épithélium de l'intestin moyen. Pendant une période de latence (LP) de quelques semaines, les phytoplasmes entrent dans le système circulatoire de l'hémolymphe et atteignent finalement les glandes salivaires, la deuxième barrière qu'ils doivent franchir. Une fois que les cellules des glandes salivaires sont colonisées, l'insecte devient infectieux tout au long de sa vie. La transmission aux plantes saines (« inoculation access period », PAI) est réalisée par l'injection de salive infectée pendant que l'insecte se nourrit dans les éléments criblés. En ce qui concerne l'association FDp-*S. titanus*, des essais de transmission réalisés en conditions contrôlées avec des adultes nouvellement émergés ont révélé qu'une AAP de 7 jours suivie d'une LP de 7 jours est suffisante pour assurer la transmission de la FDp aux fèves, même si l'efficacité de la transmission atteint son maximum après 14 jours de LP (Alma *et al.*, 2018). De plus, les charges en phytoplasmes mesurées dans l'insecte augmentent avec l'allongement de la durée de la LP, confirmant la multiplication des phytoplasmes au sein de l'insecte hôte. L'étude de la dynamique spatio-temporelle du phytoplasme OY dans son vecteur *Macrosteles striifrons* a révélé que les bactéries pénètrent dans l'épithélium de l'intestin moyen 7 jours après le début de la AAP (Koinuma *et al.*,

2020). Ensuite, après 7 à 14 jours de LP, les phytoplasmes se déplacent vers les muscles viscéraux entourant l'intestin moyen et vers l'hémocoele. Après 14-21 jours de LP, les phytoplasmes pénètrent dans les cellules de type III des glandes salivaires avant de coloniser le cerveau de l'insecte, où des preuves de leur présence ont été observées après 34 jours de LP.

- *Effet de la colonisation par le phytoplasme sur les insectes vecteurs*

L'impact de l'infection par le phytoplasme sur les insectes vecteurs varie en fonction de l'association considérée. La cicadelle *Macrosteles quadrilineatus* est le vecteur de l'aster yellow phytoplasma (AYp). Il a été constaté que les femelles élevées sur des plantes infectées par deux souches différentes d'AYp vivaient significativement plus longtemps et pondaient deux fois plus d'œufs que les femelles exposées à des plantes non infectées (Beanland *et al.*, 2000). *Dalbulus maidis* infectés par le phytoplasme du maïs ont survécu plus longtemps que les cicadelles non exposées et l'augmentation la plus remarquable de la survie a été observée pour la population d'insectes exposée simultanément à deux souches de phytoplasme (Ebbert et Nault, 2001). Au contraire, *Scaphoideus titanus* exposé au FDp a vécu significativement moins longtemps et a produit moins de descendants que les insectes nourris avec des fèves non infectées (Bressan *et al.*, 2005). L'évaluation de la fécondité des femelles de *S. titanus* a révélé que les insectes infectés par le FDp avaient un nombre réduit d'œufs de taille normale par rapport aux femelles non infectées. En outre, les œufs présentaient un retard significatif dans l'éclosion et le nombre de nymphes émergeant des œufs pondus par les femelles infectées était significativement inférieur à celui des femelles non exposées (Bressan *et al.*, 2005).

L'impact sur le *fitness* des vecteurs pourrait être direct ou indirect par la manipulation de la physiologie de la plante opérée par les effecteurs du phytoplasme. Nous avons déjà mentionné l'amélioration de la survie et de la fécondité de *M. quadrilineatus* élevé sur des plantes infectées par l'AY-WB. Il a été démontré que les mêmes effets sur la condition physique des insectes pouvaient être obtenus en élevant les insectes sur des plantes transgéniques exprimant l'effecteur SAP11. Cette augmentation a été corrélée à une diminution de la production de jasmonate par la plante, une phytohormone impliquée dans la réponse à l'herbivorie (Sugio *et al.*,

2011a). Il a également été démontré que SAP11 se lie aux facteurs de transcription TEOSINTE BRANCHED1, CYCLOIDEA, PROLIFERATING CELL FACTORS 1 et 2 (CIN-TCPs) liés à CINCINNATA, qui régulent physiologiquement le développement de la plante et favorisent indirectement la synthèse de jasmonate par la régulation de l'expression de la lipoxygénase LOX2, normalement régulée à la hausse lors de l'exposition aux insectes. Il est intéressant de noter que les insectes infectés par l'AY-WB ne sont pas les seuls à voir leur fécondité augmenter sur les plantes de l'AY-WB. Il a été constaté que même les insectes non infectés pondaient beaucoup plus d'œufs une fois transférés sur des plantes infectées par l'AY-WB, bien avant que le phytoplasme ne puisse infecter et achever son cycle dans l'insecte, ce qui démontre que l'augmentation de la fécondité provient de la manipulation de la plante et non de l'insecte.

Il a été démontré que les pommiers infectés par « *Ca.* P. mali » émettaient des quantités plus importantes de β-caryophyllène, une allomone sesquiterpénique qui attire les femelles nouvellement émergées du vecteur *Cacopsylla picta* (Mayer *et al.*, 2008a ; Mayer *et al.*, 2008b). Cette manipulation indirecte du comportement des insectes peut entraîner une augmentation du nombre de vecteurs transmetteurs parmi les populations d'insectes et pourrait contrebalancer le fait que *C. picta a* pondu beaucoup plus d'œufs sur les feuilles de plantes non infectées que sur les plantes infectées par « *Ca.* P. mali » (Mayer *et al.*, 2011 ; Görg *et al.*, 2021). En outre, il a été démontré que l'infection du pommier par « *Ca.* P. mali » a entraîné une diminution de la taille des descendants et une augmentation de la mortalité de *C. picta* (Mayer *et al.*, 2011). Les impacts directs de « *Ca.* P. mali » sur les insectes ont également été démontrés. Des analyses comparatives du transcriptome de *Cacopsylla melanoneura* infecté et non infecté par « *Ca.* P. mali » ont révélé que l'infection par le phytoplasme était corrélée à une augmentation des gènes impliqués dans la signalisation et la neurogenèse, la réponse à la lumière, l'horloge moléculaire et le rythme circadien (Weil *et al.*, 2020). En particulier, l'infection par le phytoplasme peut avoir un impact sur la défense de l'insecte médiée par le facteur de transcription NF-kB, ce qui entraîne une régulation à la baisse de la réponse immunitaire et de la signalisation du stress qui pourrait se traduire par une augmentation de la survie du vecteur. En outre, l'infection par le phytoplasme pourrait avoir des effets majeurs sur le comportement de vol des insectes. Les résultats suggèrent

une augmentation des mouvements des insectes infectés, comme cela a déjà été observé chez *E. variegatus* infecté par CYp (Galetto *et al.*, 2018).

- *Structure de l'intestin moyen de l'insecte*

Le tube digestif des hémiptères est caractérisé par la présence d'une membrane périmicrovillaire (PMM), une membrane recouvrant la membrane microvillaire dans la lumière intestinale. Cette structure est considérée comme une spécialisation typique des insectes ayant un régime alimentaire très dilué, tels que les phytophages se nourrissant de xylème et de phloème (revue dans Gutiérrez-Cabrera *et al.*, 2016). En effet, en termes d'absorption de nutriments, surtout lorsqu'elle est présente à très faible concentration, la PMMs est plus efficace en termes d'échanges que la membrane péritrophique (PM) classique contenant de la chitine et caractérisant la majorité des ordres d'insectes. La PMM transporte activement les ions potassium de l'espace périmicrovillaire vers les cellules de l'intestin moyen, générant un gradient qui permet l'absorption des nutriments comme les acides aminés et les sucres de la sève dans la lumière intestinale vers l'espace périmicrovillaire à travers les transporteurs présents au niveau de la PMM puis au niveau de la membrane microvillaire (MM). Cette spécialisation, associée à la présence d'une chambre de filtration liée à la PMM au niveau de l'intestin moyen, est importante pour faire face aux régimes dilués et pour éviter la dilution extrême de l'hémolymphe. La composition de la PMM est similaire à celle de la MM, car toutes deux sont riches en stérols, en Mg^{2+} et Na^{+} K^{+} ATPases, en molécules de liaison aux carbohydrates et en glycoconjugués, particulièrement riches en résidus de mannose (Gutiérrez-Cabrera *et al.*, 2016).

La glycosylation est une modification post-traductionnelle qui consiste à attacher une chaîne d'oligosaccharides au squelette du peptide. Elle se divise en deux catégories en fonction des acides aminés sur lesquels la chaîne d'oligosaccharides est liée. La N-glycosylation est liée aux résidus d'asparagine et la O-glycosylation aux résidus de sérine ou de thréonine. La N-glycosylation est la glycosylation la plus abondante chez les insectes et le type de N-glycane paucimannose, caractérisé par un nombre réduit de résidus mannose, s'est avéré être la glycosylation protéique la plus abondante chez *Drosophila melanogaster* (Schachter, 2009). La N-

glycosylation se produit au niveau du réticulum endoplasmique et de l'appareil de Golgi pendant la maturation des protéines. La voie de traitement initiale des N-glycosylations a lieu dans le réticulum endoplasmique et est assez similaire pour tous les eucaryotes (**figure 9**). Plusieurs enzymes de traitement de la N-glycosylation liée à l'asparagine (ALG) génèrent un oligosaccharide lié aux lipides qui est ensuite transféré sur le squelette du polypeptide par une oligosacharyl transférase (OST). La modification du polypeptide se produit au niveau d'un résidu asparagine (N), suivi dans la séquence aminoacide de la protéine par n'importe quel acide aminé sauf la proline (P), puis par une sérine (S) ou une thréonine (T) (séquence NxS/T). Le processus se poursuit dans l'appareil de Golgi, où les modifications divergent considérablement d'une espèce à l'autre. Chez les insectes, la mannosidase et la N-acétylglucosaminidase coupent les résidus mannose et N-acétylglucosamine (GlcNAc), ce qui entraîne la formation de glycanes paucimannosidiques (Man_{1-3} $GlcNAc_2$) ou oligomannosidiques (Man_{5-9} $GlcNAc_2$). Une autre caractéristique de la N-glycosylation typique des insectes est la présence de deux résidus fucose sur le GlcNAc le plus interne.

Une étude comparative a permis de décrire le glycoprotéome de cinq espèces d'insectes appartenant à cinq ordres différents et a révélé une grande diversité dans les profils de glycosylation (Vandenborre *et al.*, 2011). Dans cette étude, les glycoprotéines d'insectes ont été purifiées à l'aide d'une colonne d'affinité couplée à la lectine Galanthus Nivalis (GNA), qui se lie spécifiquement au mannose, et les protéines retenues ont été identifiées par spectrométrie de masse. Les cinq espèces ne partagent que 1,5 % des protéines glycosylées communes. Le pourcentage de protéines glycosylées classées en fonction de leur rôle biologique varie selon les ordres. Parmi les glycoprotéines identifiées dans l'ensemble global, les auteurs ont trouvé des protéines membranaires typiques telles que la laminine, la cadhérine, la contactine, la chaoptine, les lectines de type C, les protéines de transport, les protéines liées aux processus métaboliques et de nombreuses protéines transmembranaires contenant des répétitions riches en leucine (LRR). Le nombre de protéines LRR identifiées dans les différents ordres reflète la diversité des profils du glycoprotéome. Par exemple, 14 protéines LRR glycosylées ont été trouvées chez *Acyrthosiphon pisum* (Hemiptera) alors que seulement 4 LRR ont été identifiées chez *Tribolium castaneum* (Coleoptera) et une seule chez *Drosophila melanogaster* (Diptera). Les protéines LRR

glycosylées n'ont pas été trouvées chez *Bombyx mori* (Lépidoptère) ni chez *Apis mellifera* (Hyménoptère). Les profils de glycosylation peuvent changer au sein d'une même espèce en fonction des stades de reproduction et de développement (Vandenborre *et al.*, 2011).

- Adhésion des bactéries aux cellules eucaryotes et entrée dans celles-ci

Les bactéries ont développé une pléthore de mécanismes pour interagir avec leurs cellules hôtes, mais nous pouvons résumer les premières étapes de cette interaction en deux stratégies principales, le mécanisme de la « zipper » et celui du « trigger » (Swanson et Baer, 1995). Ces deux mécanismes entraînent une réorganisation du cytosquelette des cellules hôtes, qui aboutit à l'internalisation des bactéries. Le mécanisme de « zipper » commence par la liaison des bactéries aux récepteurs présents à la surface de leur cellule hôte par l'intermédiaire d'adhésines. Par exemple, les protéines de surface InlA et InlB de *Listeria monocytogenes* interagissent respectivement avec la E-cadhérine et le récepteur du facteur de croissance des hépatocytes, deux protéines exposées à la surface des cellules épithéliales. Cette interaction déclenche une cascade de signaux qui implique également la machinerie d'endocytose médiée par la chlatrine (revue dans Ribet et Cossart, 2015). Le mécanisme de « trigger » implique la sécrétion d'effecteurs bactériens qui, une fois injectés dans le cytosol de la cellule hôte, permettent un réarrangement important du cytosquelette formant des protubérances membranaires, appelées « ruffles », qui finissent par englober la cellule bactérienne. Ce processus fait intervenir le système de sécrétion bactérien de type III (T3SS), un complexe de protéines en forme d'aiguille appelé injectisome, qui permet l'injection d'effecteurs solubles sécrétés dans les cellules hôtes. *Salmonella typhimurium* l'exploite pour délivrer dans le cytosol des cellules hôtes un mélange d'effecteurs activant les Rho GTPases stimulant les réarrangements de l'actine et permettant le remaniement de la membrane (Hardt *et al.*, 1998).

Une stratégie de « trigger » très particulière impliquant des adhésines a été décrite chez les *E. coli* entéropathogènes et entérotoxigènes. Ces souches d'*E. coli* sont caractérisées par une région génomique appelée « *locus* of entorocyte effacement » (LEE) qui code pour un T3SS, des chaperons et des effecteurs qui seront transloqués à travers la paroi cellulaire bactérienne et la

membrane de la cellule hôte dans le cytosol de l'hôte via l'injectisome du T3SS. L'un de ces effecteurs, appelé « translocated intimin receptor » (Tir), sera intégré dans la membrane de la cellule hôte et servira de récepteur pour une adhésine codée par LEE, l'intimin (Kenny *et al.*, 1997). En d'autres termes, l'agent pathogène ne code pas seulement pour son adhésine mais aussi pour son récepteur qui est délivré par l'injectisome et intégré à la surface de la cellule hôte. L'interaction Tir-intimin déclenche une cascade de signaux conduisant à des réarrangements du cytosquelette permettant la formation d'une structure en forme de piédestal pour l'attachement des bactéries aux cellules épithéliales intestinales de l'hôte (revue dans Pizarro-Cerdá et Cossart, 2006).

En ce qui concerne les phytoplasmes, seul le système de sécrétion protéique Sec-dépendant a été trouvé codé dans leurs génomes (Kube *et al.*, 2012). Comme ce système n'a pas été rapporté comme supportant l'injection de protéines bactériennes dans la cellule-hôte à partir de bactéries extracellulaires, nous illustrerons donc des exemples de mécanismes « zipper » d'interaction entre les pathogènes et leurs hôtes. Même si les stratégies et les structures utilisées pour réaliser l'adhésion peuvent être très différentes, nous verrons à l'aide d'exemples comment elles partagent des caractéristiques communes telles que la liaison de l'adhésine bactérienne aux protéines glycosylées de l'hôte eucaryote.

Streptococcus suis est un agent zoonotique qui provoque des méningites chez les porcs et les humains et constitue un modèle pour l'étude des infections streptococciques. Il a été démontré que l'adhésion de *S. suis* à l'épithélium pharyngien du porc implique la liaison de son adhésine SadP à des glyconcojugués contenant du Galα1-4Gal- (galabiose). SadP est ancrée dans la paroi cellulaire et présente dans sa partie C-terminale sept répétitions en tandem de 57 acides aminés riches en glutamate et en proline (Kouki *et al.*, 2011). *Streptococcus pyogenes,* responsable d'infections cutanéo-muqueuses chez l'homme, est caractérisé par une variété d'adhésines. Le processus d'adhésion aux cellules commence par l'adhésion aux protéines de la matrice extracellulaire de l'hôte, en particulier les fibronectines et le collagène, avec plus d'une douzaine d'adhésines différentes. La liaison avec la fibronectine de la matrice extracellulaire crée une sorte de pont permettant l'internalisation des bactéries dans la cellule hôte par l'intermédiaire de l'intégrine (Kreikemeyer *et al.*, 2004). Il est intéressant de noter que la même

stratégie d'adhésion et d'internalisation a évolué chez *Staphylococcus* aureus, une bactérie phylogénétiquement éloignée (Massey *et al.*, 2001).

Des structures bactériennes particulières, les fimbrias, sont des pili bactériens qui jouent un rôle dans l'adhésion à une surface. Ils sont ancrés à la membrane externe de la bactérie et se caractérisent par la présence d'une adhésine conférant une spécificité de liaison à l'extrémité de leur échafaudage. Les souches d'*E. coli* uropathogènes présentent des « pyelonephritis-associated pili » (P-pili) et des pili de type I. Le premier type assure la liaison avec la membrane extérieure de la bactérie. Le premier type se lie aux groupements Galα-(1-4)-Gal de différents glycolipides présents sur les cellules des voies urinaires par l'intermédiaire de l'adhésine PapG. Il a été démontré que l'expression différentielle des variantes de PapG détermine la spécificité du tissu et de l'hôte (Hultgren *et al.*, 1991). L'adhésine caractéristique des pili de type I est appelée FimH. Elle reconnaît les résidus de mannose sur les glycoprotéines des cellules hôtes avec une affinité différente selon la virulence de la souche. En fait, la FimH des bactéries commensales présente une affinité plus élevée pour les résidus trimannose, tandis que les souches uropathogènes FimH se caractérisent par une affinité plus élevée pour les résidus monomannose qui sont particulièrement enrichis sur les cellules des voies urinaires. La liaison de la FimH aux résidus manomannose de l'uroplakine 1a présente sur les cellules de la vessie déclenche une cascade de signalisation conduisant à l'absorption des bactéries (revue dans Pizarro-Cerdá et Cossart, 2006).

Le rôle des adhésines dans les premiers stades de l'infection de l'hôte est également important pour les pathogènes végétaux à transmission vectorielle. Par exemple, *Xylella fastidiosa* est capable d'infecter une variété d'espèces de plantes hôtes. Le cycle de *X. fastidiosa* dans le vecteur est multiplicatif mais non circulatif et, après la mue, le vecteur perd son infectivité en raison de l'élimination de l'intestin antérieur, qui est la partie de l'exosquelette colonisée par cette bactérie, au niveau du precibarium et du cibarium (Purcell et Finlay, 1979 ; Almeida et Purcell, 2006). Dans la plante, *X. fastidiosa* colonise les vaisseaux du xylème et ne peut être acquise par ses insectes vecteurs que lorsque sa population cellulaire atteint une densité critique dans les vaisseaux de la plante, passant d'un phénotype de colonisation de la plante à un phénotype de colonisation des insectes (Newman *et al.*, 2004 ; Almeida *et al.*, 2005). La

dégradation de la pectine végétale par *X. fastidiosa* au cours de la colonisation des vaisseaux du xylème induit un changement important dans son phénotype et son expression génétique, ce qui permet l'acquisition de la bactérie par le vecteur. En fait, un élément constitutif de la pectine, le Na-galuctoronate, libéré par sa dégradation, est responsable d'une hausse dans la régulation de plusieurs gènes de *X. fastidiosa* impliqués dans sa pathogénicité et sa capacité à adhérer aux surfaces. Cela inclut les adhésines afimbriales HxfA et HxfB qui sont impliquées dans la colonisation initiale des pièces buccales du vecteur (Killiny et Almeida, 2009b ; Killiny et Almeida, 2014). Des essais de compétition pour l'adhésion réalisés sur des extraits d'intestin antérieur de cicadelles vectrices ont révélé que HxfA et HxfB ont une affinité pour le mannose et une affinité plus forte pour la N-acétylglucosamine, la fraction monomérique de la chitine. La présence de N-acétylglucosamine perturbe complètement l'adhésion bactérienne aux extraits de protéines de l'intestin antérieur (Killiny et Almeida, 2009a). Les essais de transmission ont indiqué que HxfA et HxfB étaient principalement importants pour l'adhésion précoce aux vecteurs, tandis que l'adhésine fimbriale FimA était nécessaire à la fois pour l'adhésion et la rétention à l'intestin antérieur de l'insecte vecteur (Killiny et Almeida, 2014).

Le mollicule *Spiroplasma citri* est une bactérie hélicoïdale et mobile sans paroi cellulaire qui peut être cultivée *in vitro*. *S. citri*, comme les phytoplasmes, est transmise aux plantes par des cicadelles telles que *Circulifer haematoceps* de manière persistante et propagative. Deux adhésines du spiroplasme se sont révélées essentielles à son adhésion aux cellules vectrices et à l'infection des insectes. Des essais d'interaction *in vitro* ont démontré que la spiraline, la lipoprotéine membranaire la plus abondante de *S. citri*, se lie aux glycoprotéines de l'insecte vecteur (Killiny *et al.*, 2005). Des observations par microscopie à balayage laser ont permis de démontrer que la spiraline se relocalise dans la partie de la surface membranaire de *S. citri* en contact avec les cellules du vecteur, que la capacité des mutants dépourvus de spiraline à adhérer aux cellules de l'insecte est altérée et que des billes de latex recouvertes de spiraline recombinante sont capables d'adhérer aux cellules du vecteur. En outre, des essais de compétition avec des lectines ont indiqué que la spiraline avait des propriétés de type lectine similaires à celles de la lectine *Vicia villosa* agglutininin (VVA) (Duret *et al.*, 2014). Les plasmides pSci1 à pSci5 présents dans les souches de *S. citri* transmissibles par les insectes contiennent huit

gènes codant pour des protéines liées à l'adhésion de *S. citri* (ScARP) (Yu *et al.*, 2000 ; Berg *et al.*, 2001 ; Saillard *et al.*, 2008). Les ScARP partagent une structure commune composée d'un peptide signal N-terminal, d'un domaine composé de 6 à 8 séquences répétées de 39 à 42 acides aminés, d'une hélice transmembranaire C-terminale suivie d'une portion conservée d'acides aminés chargés. Il a été démontré que le domaine ScARP (Rep3d) de ScARP3d est impliqué dans la liaison de *S. citri* aux cellules de *C. haematoceps* en culture mais aussi dans l'internalisation de billes de latex recouvertes de Rep3d déclenchant un mécanisme impliquant la polymérisation de l'actine des cellules d'insectes (Béven *et al.*, 2012).

- Protéines membranaires des phytoplasmes et interaction avec les insectes vecteurs

Les phytoplasmes sont des bactéries sans paroi cellulaire et leurs protéines membranaires jouent donc un rôle important dans l'interaction avec les cellules hôtes, puisqu'elles se trouvent à l'interface entre les deux organismes. Les protéines membranaires de phytoplasmes les plus étudiées sont les protéines membranaires immunodominantes (IDP), à savoir la protéine membranaire immunodominante (Imp), la protéine membranaire immunodominante A (IdpA) et la protéine membranaire antigénique (Amp) (Kakizawa *et al.*, 2006b). Les IDP se caractérisent par une grande variabilité des séquences d'acides aminés entre des souches de phytoplasmes étroitement apparentées. La forte proportion de mutations non synonymes trouvées dans les gènes *amp* et *imp* des souches de phytoplasmes indique que ces gènes ont été soumis à une forte pression de sélection positive diversifiante et suggère donc leur rôle dans l'adaptation (Kakizawa *et al.*, 2006a ; Fabre *et al.*, 2011 ; Siampour *et al.*, 2013).

La protéine Amp de la souche OY de « *Ca.* P. asteris » (OYp) colocalise avec les microfilaments du muscle lisse viscéral entourant l'intestin de son insecte vecteur *Macrosteles striifrons*. Des essais d'interaction *in vitro* ont confirmé que l'Amp se lie à l'actine, aux chaînes légères et lourdes de myosine (Suzuki *et al.*, 2006). De plus, il a été démontré que les complexes Amp-microfilament (complexe AM) jouent un rôle dans la spécificité du vecteur. En effet, des colonnes d'affinité exposant l'Amp du OYp ont permis de retenir l'actine de trois espèces de cicadelles vectrices mais pas l'actine de deux espèces de cicadelles non vectrices. Dans une autre

étude, l'amplification de la souche « *Ca.* P. asteris » du chrysantemum yellow phytoplasma (CYp) s'est avéré interagir avec l'actine et les sous-unités α et β de l'ATP synthase du vecteur *E. variegatus* (Galetto *et al.*, 2011). *Bien que l'*ATP synthase soit connue pour être une protéine mitochondriale, l'observation par microscopie confocale et les essais d'interaction *in vitro* ont également révélé sa localisation ectopique à la surface externe des cellules de l'intestin moyen et des glandes salivaires de l'insecte, suggérant son rôle de récepteur pour la protéine Amp. Le rôle de la protéine CYp Amp dans la compétence des insectes vecteurs *Macrosteles quadripunctulatus* et *E. variegatus* a été confirmé *in vivo* en démontrant que l'alimentation préalable des insectes avec un anticorps anti-Amp diminuait à la fois l'efficacité d'acquisition du phytoplasme et l'inoculation aux plantes (Galetto *et al.*, 2011 ; Rashidi *et al.*, 2015).

Il a été démontré que la protéine Imp du phytoplasme FD se lie à l'extrait de protéine membranaire d'espèces vectrices telles que *E. variegatus* et *S. titanus*, mais pas à l'extrait d'espèces non vectrices, ce qui suggère son rôle dans la spécificité du vecteur (Trivellone *et al.*, 2019). La protéine Imp du phytoplasme Wheat Blue Dwarf (WBD) interagit avec l'α-tubuline de son vecteur, la cicadelle *Psammotettix striatus* (Ding *et al.*, 2022). *L'*inhibition de l'expression de l'α-tubuline chez les insectes vivants grâce à la technologie ARNi a entraîné une diminution significative de l'efficacité de la transmission du phytoplasme aux plantules de blé par rapport aux insectes témoins.

Les Vmps sont exposées à la face externe de la cellule du phytoplasme et se caractérisent par une organisation commune. Elles possèdent un peptide signal à leur extrémité N-terminale, un nombre variable de grands domaines répétés de 78 à 82 acides aminés et un domaine transmembranaire hydrophobe C-terminal qui ancre la protéine dans la membrane cellulaire. La variabilité de *vmp1* parmi douze isolats différents de « *Ca.* P. solani » (anciennement connu sous le nom de phytoplasme de Stolbur) a révélé des différences dans la taille des protéines dues à des variations dans le nombre de domaines répétés ainsi qu'à des mutations ponctuelles, essentiellement non synonymes. Vmp1 est apparu beaucoup plus variable que les gènes de ménage pris comme référence (Cimerman *et al.*, 2009).

Deux gènes, *vmpA* et *vmpB*, codant pour des protéines sans homologie entre elles ou avec Vmp1 mais présentant une organisation similaire avec des domaines répétés de 78 acides aminés ont été trouvés dans le chromosome de la souche FDp FD92. Comme nous l'avons expliqué plus haut, les protéines *vmpA* et *vmpB* se sont avérées variables en taille et en séquence. Les VmpA et VmpB de la souche FD92 (génotype M54, cluster map-FD2) possèdent trois domaines répétés, tandis que les VmpA et VmpB de la souche FD-CAM05 (génotype M50, cluster map-FD1) possèdent respectivement quatre et deux domaines répétés. La variation de VmpA et VmpB dans un ensemble d'isolats européens a révélé que leurs séquences se regroupaient en trois groupes phylogénétiques correspondant à la spécificité de transmission par différentes espèces de cicadelles : seuls les groupes II et III pouvaient être transmis par les cicadelles Deltocephalinae, y compris *S. titanus* (Malembic-Maher *et al.*, 2020). D'après leur structure, VmpA et VmpB sont ancrés par leur domaine hydrophobe transmembranaire C-terminal à la membrane FDp. La grande partie centrale hydrophile des protéines contenant les domaines répétés est donc exposée à la surface du FDp. Des anticorps dirigés contre leurs parties centrales hydrophiles répétitives ont permis de détecter VmpA et VmpB dans *Vicia faba* et *E. variegatus* infectés par FDp, ce qui indique que les deux gènes sont exprimés au cours de la colonisation des plantes et des insectes vecteurs (Malembic-Maher *et al.*, 2020).

Il a été démontré que VmpA médiait la liaison avec les cellules de l'épithélium de l'intestin moyen de l'insecte vecteur *E.* variegatus (Arricau-Bouvery *et al.*, 2018). Les billes recouvertes de la protéine recombinante VmpA-His_6, ont montré une adhésion accrue aux cellules *E. variegatus* en culture par rapport aux billes de contrôle recouvertes de GFP. De plus, les essais de compétition ont révélé une forte diminution de l'adhésion des billes recouvertes de VmpA aux cellules après incubation des billes avec des anticorps anti-His_6 -VmpA. Le rôle important de VmpA dans l'adhésion aux cellules d'insectes a été démontré en utilisant un *S. citri* recombinant déficient pour l'adhésion et exprimant la protéine VmpA à sa surface (Renaudin *et al.*, 2015). Les spiroplasmes exprimant VmpA ont montré une augmentation statistiquement significative de l'adhésion aux cellules d'*E. variegatus par* rapport aux spiroplasmes de contrôle. L'ingestion de billes fluorescentes recouvertes de VmpA par *E. variegatus* a permis d'observer la présence de ces billes dans les intestins disséqués et la chambre filtrante à 1, 2 et 4 jours après l'acquisition

de l'alimentation. L'observation par microscopie électronique à transmission sur des tubes digestifs disséqués a confirmé l'observation faite par microscopie à fluorescence et a révélé la présence de billes enchâssées dans les membranes périmicrovillaires recouvrant la surface apicale des cellules épithéliales de l'intestin moyen (Arricau-Bouvery *et al.*, 2018).

Les tubes digestifs et les glandes salivaires d'*E. variegatus* et de *S. titanus* infectés ont été colorés avec différentes lectines fluorescentes et observés par microscopie à balayage laser, révélant des taches de phytoplasme localisées à proximité d'agrégats de GNA, de lectine de *Lens Culinaris* (LCA) et de lectine de *Lycopersicon Esculentum* (LEL) (Arricau-Bouvery *et al.*, 2021). De telles structures n'ont pas été observées dans les organes d'insectes témoins non infectés, ce qui suggère que les phytoplasmes induisent la formation de glycoprotéines qui peuvent être liées par ces types de lectines. La protéine recombinante VmpA-His_6 a ensuite été incubé avec les différents sucres reconnus par GNA (mannose), LCA (glucose et mannose), et LEL (N-acétylglucosamine) à différentes concentrations. Ensuite, le taux d'adhésion de la VmpA recombinante aux cellules a été estimé. Lorsque la VmpA est préincubée avec du mannose, elle montre une augmentation de l'adhésion aux cellules de manière dose-dépendante, tandis que la préincubation avec de la N-acétylglucosamine entraîne une diminution de l'adhésion de la VmpA aux cellules. Dans les essais de compétition, une diminution statistiquement significative de l'adhésion des billes fluorescentes recouvertes de VmpA-His_6 aux cellules Euva a été observée lorsque les cellules étaient pré-incubées avec les lectines LCA, GNA et LEL, ce qui suggère que la VmpA partage les mêmes substrats, i.*e.* des glycoprotéines exposant des résidus mannose et N-acétylglucosamine (Arricau-Bouvery *et al.*, 2021). L'analyse de far-western blot a révélé deux caractéristiques intéressantes de l'interaction de VmpA avec les protéines des cellules Euva : i) la pré-incubation de VmpA avec de la N-acétylglucosamine a totalement inhibé l'interaction de VmpA avec les protéines Euva supérieures à 40 kDa et ii) la pré-incubation de VmpA avec du mannose a entraîné une interaction plus forte avec les protéines de poids moléculaire élevé, en accord avec l'adhésion accrue de la VmpA-His_6 aux cellules Euva en présence de mannose. De plus, les billes recouvertes de VmpA pré-incubées avec du mannose et observées au microscope à fluorescence ont tendance à former des agrégats par rapport aux billes recouvertes de VmpA non traitées. L'ensemble de ces résultats suggère que VmpA se lie au mannose et que cette liaison

entraîne la formation de multimères de VmpA qui peuvent augmenter l'affinité de cette adhésine pour les protéines glycosylées avec des résidus de N-acétylglucosamine.

Des essais de pull down utilisant des billes recouvertes de VmpA-His_6 et des protéines extraites des glandes salivaires d'*E. variegatus* montrent que VmpA interagit, au moins *in vitro*, avec AP-2, une protéine adaptatrice impliquée dans l'endocytose dépendante de la clathrine. (Arricau-Bouvery *et al.*, 2023). L'internalisation du FDp par les cellules S2 de la *drosophile* en présence de drogues inhibant l'endocytose dépendante de la clathrine, comme la chlorpromazine, a été réduite par rapport à l'entrée du FDp dans les cellules non traitées. L'inhibition génique par ARNi ciblant la chaîne lourde de la clathrine des cellules S2 a montré une inhibition similaire de l'internalisation du FDp. Cependant, l'entrée du phytoplasme n'a pas été complètement bloqué, ce qui suggère soit une internalisation résiduelle due à une expression résiduelle de la clathrine, soit une autre voie d'entrée dans les cellules. Cette dernière hypothèse est étayée par la plus forte inhibition de l'entrée du phytoplasme dans les cellules S2 traitées à la cytochalasine D, un inhibiteur de la polymérisation de l'actine impliqué dans d'autres processus d'endocytose. Des observations par microscopie à balayage laser sur des cellules S2 infectées par FDp et exprimant une chaîne lourde de clathrine recombinante couplée à la GFP ont révélé une colocalisation des phytoplasmes colorés par un anticorps anti-VmpA et de la chaîne lourde de clathrine à la surface des cellules. Des expériences d'ARNi *in vivo* réalisées sur *E. variegatus* par ingestion d'ARNdb ciblant la chaîne lourde de clathrine ont révélé une quantité significativement plus faible de transcrits du facteur d'élongation du phytoplasme (*Tuf) à la* fois dans les têtes et les abdomens par rapport aux insectes témoins non infectés (Arricau-Bouvery *et al.*, 2023).

En résumé, VmpA est impliqué dans l'interaction entre FDp et les cellules d'insectes dès les premiers stades de l'infection des insectes, en particulier dans l'adhésion aux cellules et dans l'internalisation ultérieure des bactéries.

- L'interface pathogène-hôte comme cible pour lutter contre les maladies à transmission vectorielle

La définition des pesticides de la FAO est la suivante : « substance ou mélange de substances utilisées pour contrôler, prévenir ou détruire tout ravageur, vecteur de maladie animale ou humaine, plante indésirable ou espèce animale affectant la production, la gestion, la vente, le stockage et le transport des denrées alimentaires ». En 2019, la quantité mondiale de pesticides appliquée était d'environ 4,19 millions de tonnes métriques, et les insecticides représentaient 29,5 % du total (revue dans Pathak *et al.*, 2022). De nos jours, l'impact délétère des insecticides sur l'environnement et la santé humaine a été largement rapporté par les chercheurs. La menace concernant l'environnement comprend la persistance des pesticides, leur dégradation et leur migration en dehors de leur zone d'application par des processus de transfert tels que l'adsorption, la lixiviation, la volatilisation, la dérive de pulvérisation et le ruissellement (revue dans Tudi *et al.*, 2021) ainsi que leur bioaccumulation dans des espèces non ciblées, ce qui a des effets néfastes sur la biodiversité. L'impact sur la santé humaine peut virtuellement toucher tous les consommateurs, bien que les catégories les plus concernées soient les travailleurs agricoles qui appliquent directement les produits dans leur champ et les habitants des zones rurales entourant les champs cultivés, en particulier dans les pays qui emploient encore des polluants organiques persistants tels que le dichlorodiphényltrichloroéthane (DDT) (Pathak *et al.*, 2022).

Les principales mesures visant à limiter la propagation des maladies à transmission vectorielle comprennent l'application de traitements insecticides, mais des résultats préliminaires prometteurs suggèrent que d'autres approches, visant à réduire la transmission au lieu de la population de vecteurs, pourraient être possibles. La perturbation de l'interaction entre un agent pathogène et son vecteur pourrait faire appel à deux approches différentes, ciblant la protéine de l'agent pathogène ou le site de liaison du récepteur de l'insecte. Dans le domaine de la santé humaine, les adhésines bactériennes sont des cibles prometteuses pour de nouveaux médicaments antimicrobiens afin de surmonter les problèmes liés à l'utilisation des antibiotiques. Diverses stratégies agissant au niveau de l'adhésion des cellules bactériennes ont été mises en œuvre pour le traitement des maladies (Asadi *et al.*, 2019). L'utilisation de composés imitant le

ligand naturel de l'adhésine a rendu moins probable le développement d'une résistance des bactéries aux médicaments qu'avec les composés bactéricides (Ofek *et al.*, 2003). De même, de nouvelles stratégies de gestion des maladies à transmission vectorielle pourraient être développées en ciblant les protéines impliquées dans les premiers stades de l'infection des insectes vecteurs en raison de leur rôle central dans la transmission des agents pathogènes. Les approches qui donnent des résultats préliminaires prometteurs sont l'utilisation de molécules, de protéines ou de peptides recombinants pour surpasser la liaison de l'adhésine bactérienne aux protéines du vecteur. Dans le cas de *X. fastidiosa* HxfsA et HxfsB, il a été démontré que l'administration de sucres particuliers ou de lectines à des insectes réduisait l'efficacité de la transmission du pathogène aux plantes (Killiny *et al.*, 2012). En effet, l'ajout de lectines liant des résidus de N-acétylglucosamine dans le régime alimentaire artificiel de la cicadelle vectrice *Graphocephala atropunctata*, a partiellement entravé la transmission de *X. fastidiosa* aux plantes en raison de la saturation des sites de liaison des récepteurs. De même, l'ajout de carbohydrates contenant de la N-acétylglucosamine se liant aux lectines de la surface cellulaire de la bactérie a entraîné une réduction du taux de transmission réussie (Killiny *et al.*, 2012). Cependant, la transmission n'a pas été complètement bloquée, ce qui suggère la complexité de la formation du biofilm permettant la colonisation du vecteur. Des résultats prometteurs ont été obtenus par la synthèse de peptides recombinants conçus sur des protéines de liaison à la chitine de *X. fastidiosa*. Les peptides recombinants délivrés *via* un système d'alimentation artificielle ont supplanté l'adhésion bactérienne aux cellules des pièces buccales des insectes, réduisant ou bloquant complètement l'efficacité de la transmission du vecteur aux plantes jusqu'à 10 jours après l'acquisition dans des conditions contrôlées (Labroussaa *et al.*, 2016).

De même, un peptide (GBP 3.1) se liant à l'intestin moyen et à l'intestin postérieur du puceron *Acyrthosiphon pisum a* été identifié et testé quant à son rôle dans l'infection par le virus du « Pea Enation Mosaic Virus » (PEMV). Les pucerons nourris avec un régime artificiel contenant du GBP 3.1 avant l'acquisition du PEMV à partir de plantes infectées ont montré une absorption réduite des virions de l'intestin vers l'hémocoele du vecteur, restreignant la transmission virale persistante nécessitant l'accumulation de virions dans l'hémocoele de l'insecte (Liu *et al.*, 2010). Une autre étude a démontré que le riz transgénique exprimant la protéine spike du « Rice Ragged

Stunt Oryzavirus » (RRSV) présentait une bonne résistance à l'infection virale. En outre, la cicadelle vectrice du RRSV *Nilaparvata lugens* nourrie de plantes transgéniques était bien protégée contre l'infection par le RRSV une fois transférée sur des plantes infectées par le RRSV (Chaogang *et al.*, 2003).

Les travaux préliminaires axés sur l'approche de la résistance médiée par les planticorps ont prouvé, au moins sur le plan conceptuel, qu'ils méritaient d'être étudiés comme moyen de faire face à l'infection par le phytoplasme. Dans le cadre de cette stratégie, les adhésines du phytoplasme pourraient être des cibles intéressantes pour la production d'anticorps par des plantes hôtes transgéniques. Cela pourrait diminuer le taux d'infection de l'insecte vecteur grâce au masquage de l'adhésine, comme cela a été démontré *in vitro/ex vivo* pour le phytoplasme CY (Rossi *et al.*, 2019b).

L'inhibition médié par l'ARNdb a donné des résultats prometteurs à la fois sur le vecteur expérimental et naturel de la FDp dans des conditions de laboratoire. L'administration d'ARNdb ciblant les filaments d'actine et l'ATP synthase β par micro-injection conduit à une inhibition presque complet de l'expression de deux gènes qui dure jusqu'à 14 jours, entraînant une diminution significative de la survie des insectes (Abbà *et al.*, 2019). En outre, la microinjection d'*E. variegatus* avec un ARNdb ciblant l'ATP synthase β induit une stérilité presque complète chez les femelles (Galetto *et al.*, 2021b) ainsi qu'une diminution significative de la multiplication du phytoplasme dans les vecteurs (Galetto *et al.*, 2021a). L'impact a également été évalué sur les femelles de *S. titanus*, révélant une altération de la morphologie des œufs en développement dans les ovaires (Ripamonti *et al.*, 2022b). L'ARNdb ciblant la chaîne lourde de la clathrine et administré par alimentation artificielle à *E. variegatus* a efficacement diminué l'expression du gène dans la tête et l'abdomen des insectes et a entraîné une diminution de la colonisation par le phytoplasme de l'intestin moyen et des glandes salivaires (Arricau-Bouvery *et al.*, 2023).

Des efforts sont faits pour mieux comprendre le potentiel et les limites de l'administration d'ARNdb dans des conditions de terrain. L'inhibition génique induite par l'hôte (HIGS) repose sur l'expression d'ARNdb ou d'ARNsi par la plante hôte. Une fois que l'insecte, dans notre cas, se nourrit de la plante, il acquiert les molécules d'ARN qui déclencheront sa réponse ARNi. La

première plante commerciale de maïs transgénique exprimant un ARNdb ciblant un gène essentiel de la chrysomèle occidentale des racines du maïs a récemment reçu l'autorisation de commercialisation en Chine et aux États-Unis (SmartStax® Pro, Bayer CropScience). L'inhibition génique induite par un virus (VIGS) exploite des virus recombinants pour l'administration spécifique d'ARNdb (examiné dans Kolliopoulou *et al.*, 2017). L'un des principaux avantages de cette technique est que le virus peut être très spécifique à l'hôte, et donc ne pas avoir d'impact sur les organismes non ciblés. En outre, la production d'ARNdb aurait lieu directement dans les cellules de l'insecte, surmontant ainsi la difficulté d'absorption des ARNdb dans l'environnement qui pourrait expliquer la faible réponse à l'ARNi caractérisant certaines espèces d'insectes. D'autres technologies de type VIGS exploitent divers micro-organismes modifiés tels que des bactéries, des levures et des insectes symbiotes (Whitten *et al.*, 2016 ; Zhang *et al.*, 2019 ; Mysore *et al.*, 2021). Cependant, la dissémination de virus recombinants et d'organismes modifiés dans l'environnement soulève de sérieuses questions quant aux implications écologiques de ces traitements*, i.e.* effets sur les espèces non visées et l'élargissement éventuel de la gamme d'hôtes. En outre, la possibilité d'utiliser des OGM pour des applications agricoles est toujours controversée en Europe. Néanmoins, d'autres méthodes n'impliquant pas d'organismes transgéniques peuvent être exploitées pour déclencher une réponse ARNi chez les insectes sur le terrain. Le Spray Induced Gene Silencing (SIGS) consiste en l'application de solutions contenant des ARNdb sur les surfaces de la plante hôte et délivrées à l'insecte lorsqu'il se nourrit des tissus de la plante. Des efforts pour adapter l'administration de molécules d'ARN aux conditions de terrain ont récemment été déployés afin de surmonter les limites du SIGS, telles que la courte persistance de l'ARNdb « nu » dans l'environnement. La modification chimique des ARNdb nus, l'utilisation de nanocarriers tels que les lyposomes, les polymères (Jain *et al.*, 2022) et des peptides (Numata *et al.*, 2014) ainsi que l'administration dans la plante par injection dans le tronc ou absorption dans le pétiole (Dalakouras *et al.*, 2018) ont montré qu'elles augmentaient la stabilité des ARNdb dans l'environnement, ce qui accroît l'efficacité des stratégies ARNi pour lutter contre les ravageurs dans les champs (revue dans Christiaens *et al.*, 2020).

- Objectif du travail et schéma expérimental

La gestion de la propagation de la FD passe par le contrôle de la taille de la population de vecteurs au moyen de traitements insecticides. Dans un contexte de réduction des pesticides, d'autres approches et outils doivent être développés pour contrôler les maladies vectorielles liées aux cultures. Pour atteindre cet objectif, nous devons obtenir autant d'informations que possible sur les interactions entre le pathogène et ses vecteurs, afin d'identifier les principaux facteurs impliqués dans l'infection du vecteur, la compétence vectorielle et la transmission à la plante hôte.

Comme nous l'avons mentionné dans la section précédente, les séquences VmpA et VmpB du phytoplasme FD sont corrélées à la capacité de *Scaphoideus titanus* à transmettre le pathogène et, par conséquent, au potentiel épidémique de la souche du phytoplasme. (Malembic-Maher *et al.*, 2020). VmpA est une adhésine de phytoplasme impliquée dans la liaison à l'intestin moyen des insectes vecteurs *S. titanus* et *E. variegatus* (Arricau-Bouvery *et al.*, 2018 ; Malembic-Maher *et al.*, 2020). VmpA présente des propriétés de lectine, avec une liaison spécifique aux résidus N-acétylglucosamine et mannose sur les cellules d'insectes (Arricau-Bouvery *et al.*, 2021). L'identification des protéines interagissant avec VmpA dans les cellules d'insectes pourrait non seulement permettre de mieux comprendre les premiers stades de l'infection par les insectes et de la colonisation des cellules, mais aussi contribuer au développement de nouvelles stratégies de contrôle de la propagation de la FD, en perturbant l'infection par les insectes et, par conséquent, la transmission du pathogène au sein du vignoble. En outre, le décryptage des facteurs responsables de la compétence vectorielle dans les souches épidémiques du phytoplasme de la FD pourrait permettre de prédire de nouveaux insectes vecteurs potentiels parmi les espèces allochtones émergentes qui pourraient se répandre dans de nouvelles zones de distribution dans le contexte du changement climatique.

Nous avons commencé à rechercher des protéines de vecteurs d'insectes susceptibles d'interagir avec la protéine VmpA du FDp en utilisant deux approches différentes. D'une part, nous avons utilisé une approche ciblée, en mettant l'accent sur les protéines transmembranaires des vecteurs d'insectes présentant un potentiel de glycosylation. Pour ce faire, nous avons réalisé

deux essais d'interaction *in vitro* différents, afin d'enrichir et d'identifier par spectrométrie de masse les protéines d'*E. variegatus* interagissant expérimentalement avec VmpA. Parmi les protéines identifiées, les candidats les plus intéressants ont été criblés pour leur rôle de récepteur dans un système modèle simplifié composé de cellules cultivées d'*E. variegatus* (l'interface du vecteur) et de billes fluorescentes en latex recouvertes d'un VmpA recombinant de la souche FDp FD92 (« imitant » le phytoplasme). Cela nous a permis d'évaluer l'efficacité de la réponse ARNi médiée par l'ARNdb des cellules en culture d'*E. variegatus*, jusqu'à ce jour démontrée uniquement chez les insectes *E. variegatus* par l'alimentation ou la micro-injection (Abbà *et al.*, 2019 ; Galetto et *al.*, 2021a ; Galetto *et al.*, 2021b ; Ripamonti *et al.*, 2022b ; Arricau-Bouvery *et al.*, 2023). Afin d'évaluer le rôle de l'interaction protéique avec VmpA dans la compétence vectorielle, nous avons tenté de comparer dans nos essais VmpA d'une souche transmissible et non transmissible de *S. titanus* de phytoplasmes appartenant au groupe V de 16Sr, les souches FD92 et PGYA, respectivement. Cette approche et les résultats obtenus sont décrits dans le chapitre 1.

D'autre part, nous avons essayé d'étudier les interactions protéine-protéine susceptibles de se produire entre VmpA et les protéines de l'insecte vecteur. Dans le chapitre 2, nous présenterons la mise en place d'un test classique de double hybride de levure pour évaluer si les protéines d'*E. variegatus* interagissent avec VmpA de la souche transmissible FD92 de *S. titanus* dans un système d'expression hétérologue constitué de cellules *Saccharomyces cerevisiae.*

Conclusions et perspectives

Les protéines membranaires du FDp constituent le premier point de contact avec les cellules des insectes vecteurs et jouent donc un rôle crucial dans les premiers stades de l'infection par le vecteur. Cependant, les mécanismes qui sous-tendent l'adhésion des FDp aux cellules, l'internalisation et le trafic intracellulaire doivent encore être clarifiés. Dans la **figure 39**, nous avons résumé l'état des connaissances sur les interactions entre les protéines membranaires du FDp et les cellules de ses insectes vecteurs, ainsi que les questions qui restent sans réponse.

VmpA agit comme une lectine et assure la liaison entre le phytoplasme et l'épithélium intestinal de l'insecte vecteur. Son récepteur est une protéine transmembranaire glycosylée en N-acétylglucosamine (Arricau-Bouvery *et al.*, 2021). VmpB a une organisation similaire avec des domaines répétés rappelant les protéines de surface bactériennes impliquées dans la colonisation des cellules eucaryotes, et est donc supposé être une adhésine de type lectine similaire à VmpA. Le FDp ne possède pas d'orthologue Amp mais possède une protéine Imp. Il a été démontré que la protéine Imp de FDp interagit sélectivement *in vitro* avec des espèces d'insectes vecteurs (Trivellone *et al.*, 2019), mais ses cibles chez les insectes doivent encore être identifiées. Il a été démontré que l'Imp du phytoplasme du « wheat blue dwarf » interagit avec l'α tubuline de son insecte vecteur et que l'inhibition de l'α tubuline par ARNi diminue l'efficacité de la transmission du phytoplasme (Ding *et al.*, 2022). On a constaté que l'Imp of lime witches broom phytoplasma se liait *in vitro* à trois protéines inconnues de sa cicadelle vectrice *Hishimonus phycitis* et à l'ATP synthase, à l'actine et à la myosine de *S. titanus* (Siampour *et al.*, 2011). L'inhibition par ARNi de l'ATP synthase chez *E. variegatus* a un impact négatif sur la multiplication du FDp chez l'insecte (Galetto *et al.*, 2021b). En outre, l'expression ectotopique de l'ATP synthase dans la membrane plasmique de l'intestin moyen et des glandes salivaires d'*E. variegatus* a été démontrée (Galetto *et al.*, 2011). La FDp-Imp et l'ATP synthase du vecteur interagissent-ils, et si oui, leur interaction est-elle importante pour la colonisation des cellules d'insectes ?

Après leur adhésion initiale aux cellules hôtes, les phytoplasmes de la FD sont internalisés par endocytose médiée par la clathrine (Arricau-Bouvery *et al.*, 2023) mais leur trafic intracellulaire doit encore être étudié. Les FDp s'échappent-ils ou non de la vésicule endosomale ? Les FDp bloquent-ils la fusion des vésicules endosomales et lysosomales pour échapper à la dégradation comme le fait *Shigella flexneri* (Sun *et al.*, 2021)? Des observations en microscopie électronique suggèrent que la multiplication des FDp a lieu dans le cytosol des cellules épithéliales de l'intestin moyen et des cellules des glandes salivaires (Gouranton et Maillet, 1973), soutenant le fait que les FDp échappent aux vésicules d'endocytose.

Lorsque les phytoplasmes sortent des cellules épithéliales, ils doivent traverser la lame basale pour accéder à l'hémocoele. Le FDp est-il capable de perturber la structure de la lame basale ou profite-t-il de son renouvellement pour la traverser ? Lorsqu'il pénètre dans l'hémocoele, le FDp colonise tous les organes vecteurs des insectes, à l'exception des tubes de Malpighi, des ovaires et des testicules (Lefol *et al.*, 1994). Les FDp se fixent sur les glandes salivaires à travers lesquelles ils n'infectent que certaines cellules (Arricau-Bouvery *et al.*, 2018) et en particulier les acini III, IV et V (Lefol *et al.*, 1993). Les mécanismes d'infection de ces cellules restent à identifier. Les adhésines Vmp jouent-elles un rôle dans l'invasion des cellules des glandes salivaires ou d'autres protéines membranaires sont-elles impliquées ? Des essais d'adhésion de billes de latex enduites de Vmps sur des glandes salivaires disséquées devraient être réalisés pour tester cette hypothèse.

Le dispositif expérimental utilisé pour réaliser nos expériences s'est avéré adapté à l'étude des interactions entre les protéines du pathogène et les cellules de son vecteur, ce qui nous a permis d'obtenir des informations préliminaires sur le rôle d'un récepteur VmpA putatif dans l'adhésion de la FDp aux cellules d'*E. variegatus*. Il pourrait donc être exploité pour étudier au moins certains des points critiques mentionnés plus haut concernant l'interaction de la FDp avec les cellules hôtes. En outre, ce système pourrait, moyennant des adaptations appropriées, être appliquée à d'autres pathosystèmes d'intérêt pour aider à mieux comprendre les mécanismes sous-jacents à ce type d'interactions.

Nous avons réussi à mettre en œuvre notre protocole ARNi afin d'inhiber l'expression de 12 gènes dans les cellules d'Euva, sans affecter négativement leur capacité à croître et à se multiplier. Cela pourrait ouvrir de nouvelles possibilités dans l'inhibition des réseaux de gènes dans les cellules et fournir un outil utile pour clarifier les interactions moléculaires entre les phytoplasmes et leurs insectes vecteurs. L'inhibition de cibles multiples par les ARNdb devrait également être évaluée *in vivo* par injection et ingestion*,* ainsi que l'impact du traitement sur les gènes hors cible et sur la survie et le développement des insectes chez *E. variegatus* et *S. titanus*.

D'après les analyses de far-western blot, VmpA interagit avec plus d'une protéine d'*E.* variegatus (Arricau-Bouvery *et al.*, 2021, chapitre 1 **section 2.2**). Le protocole ARNi multiplex sera utile pour tester d'autres protéines identifiées par l'analyse par spectrométrie de masse. Une fois que d'autres protéines candidates dont la diminution de l'expression est corrélée à une diminution de l'adhésion des billes recouvertes de VmpA aux cellules d'*E. variegatus* en culture auront été sélectionnées, il sera possible de délivrer des combinaisons d'ARNdb pour évaluer l'effet additif de la diminution de leur expression sur l'adhésion des billes recouvertes de VmpA aux cellules d'insecte.

Les expériences réalisées dans le cadre de ce projet ont mis en évidence l'implication d'une protéine LRR de l'insecte dans l'adhésion de VmpA aux cellules de son vecteur. Cependant, l'implication de cette protéine dans la transmission aux plantes et dans la spécificité du vecteur reste à démontrer. Afin d'évaluer l'impact de la protéine dans la survie de l'insecte et dans la transmissibilité du phytoplasme aux plantes, l'ARNi *in vivo* ciblant uk1_LRR chez *E. variegatus* et *S. titanus* devrait être effectué avant les essais d'acquisition et de transmission. Plusieurs travaux ont montré l'efficacité avec laquelle l'ARNi médié par l'ARNdb parvient à diminuer l'expression de l'ARNm cible à la fois chez *E. variegatus* et *S. titanus* (Abbà *et al.*, 2019 ; Ripamonti *et al.*, 2022b ; Arricau-Bouvery *et al.*, 2023). Nous avons démontré que le niveau de transcription uk1_LRR dans les cellules Euva diminue jusqu'à 58 fois par rapport à la condition de contrôle. Nous ne pouvons pas tenir pour acquis qu'une telle efficacité sera la même lorsque le traitement ARNi sera imposé à des insectes vivants, mais cette stratégie mérite d'être explorée.

Afin de valider davantage l'interaction uk1_LRR-VmpA, l'expression de l'uk1_LRR d'*E. variegatus* dans un système d'expression hétérologue comme les cellules S2 de *drosophile* serait nécessaire afin de produire une protéine avec un profil de glycosylation similaire à celui des cellules de cicadelle qui pourrait alors être utilisée pour effectuer des tests d'interaction *in vitro*. Si nos résultats sont confirmés, il s'agirait du premier rapport d'un récepteur pour la protéine VmpA chez l'insecte vecteur du phytoplasme FD. D'autre part, l'interaction de uk1_LRR avec VmpA de génotypes de phytoplasmes non transmissibles par *E. variegatus* et *S. titanus* tels que PGYA devra être mesurée avec des tests optimisés, afin d'évaluer l'impact de l'interaction uk1_LRR-VmpA dans la spécificité de la transmission. Inversement, les orthologues uk1_LRR d'espèces de cicadelles non vectrices telles qu'*Oncopsis alni* devront être exprimés et leur capacité à interagir ou non avec la VmpA de la souche FD92 devra être vérifiée.

Si les essais de transmission et de spécificité du vecteur révèlent un rôle important de l'uk1_LRR dans la perturbation de la transmission du phytoplasme FD aux plantes, nous pourrions imaginer le développement de nouvelles stratégies pour gérer les épidémies. Si l'inhibition du récepteur par les ARNdb s'avère efficace chez l'insecte, la technologie de l'inhibition génique induite par pulvérisation pourrait être exploitée et adaptée à l'application dans les vignobles. Le récepteur uk1_LRR devra être mieux caractérisé sur le plan structurel et fonctionnel. Cela pourrait contribuer au développement d'approches visant à perturber la transmission médiée par les insectes par compétition, comme cela a été développé pour *Xylella fastidiosa* (Killiny et al., 2011, Labroussaa et al., 2016). Ces outils pourraient aider à mettre en place de nouvelles stratégies de gestion des épidémies de FD dans les vignobles, dans le but de réduire l'apport d'insecticides pour le contrôle des populations de vecteurs.